

STATE OF ALASKA  
DEPARTMENT OF NATURAL RESOURCES  
DIVISION OF GEOLOGICAL & GEOPHYSICAL SURVEYS

Tony Knowles, *Governor*

John T. Shively, *Commissioner*

Milton A. Wiltse, *Acting Director and State Geologist*

1996

This DGGS Report of Investigations is a final report of scientific research. It has received technical review and may be cited as an agency publication.

Report of Investigations 95-6  
CATALOG AND INITIAL ANALYSES OF  
GEOLOGIC DATA RELATED TO MIDDLE TO LATE  
QUATERNARY DEPOSITS, COOK INLET REGION,  
ALASKA

by  
Richard D. Reger, DeAnne S. Pinney,  
Raymond M. Burke, and Milton A. Wiltse



STATE OF ALASKA  
Tony Knowles, *Governor*

DEPARTMENT OF NATURAL RESOURCES  
John T. Shively, *Commissioner*

DIVISION OF GEOLOGICAL & GEOPHYSICAL SURVEYS  
Milton A. Wiltse, *Acting Director and State Geologist*

Division of Geological & Geophysical Surveys publications can be inspected at the following locations. Address mail orders to the Fairbanks office.

Alaska Division of Geological  
& Geophysical Surveys  
794 University Avenue, Suite 200  
Fairbanks, Alaska 99709-3645

University of Alaska Anchorage Library  
3211 Providence Drive  
Anchorage, Alaska 99508

Elmer E. Rasmuson Library  
University of Alaska Fairbanks  
Fairbanks, Alaska 99775-1005

Alaska Resource Library  
222 W. 7th Avenue  
Anchorage, Alaska 99513-7589

Alaska State Library  
State Office Building, 8th Floor  
333 Willoughby Avenue  
Juneau, Alaska 99811-0571

This publication released by the Division of Geological & Geophysical Surveys, was produced and printed in Fairbanks, Alaska by Date Line Copies, at a cost of \$22 per copy. Publication is required by Alaska Statute 41, "to determine the potential of Alaskan land for production of metals, minerals, fuels, and geothermal resources; the location and supplies of groundwater and construction materials; the potential geologic hazards to buildings, roads, bridges, and other installations and structures; and shall conduct such other surveys and investigations as will advance knowledge of the geology of Alaska."

**Cover:** *View southeast of Homer Spit, a submarine moraine complex formed by grounding of the tidal glacier that occupied Kachemak Bay during the Skilak stade of the Naptowne glaciation. Photograph 137-9 taken June 25, 1990, by R.D. Reger.*

## CONTENTS

	Page
Introduction .....	1
Data presentation .....	1
Radiocarbon dates .....	1
Tephra studies .....	1
Methodology .....	1
Geochemical results .....	25
Correlation, distribution, and age .....	25
Late Quaternary tephras .....	25
Lethe tephra .....	25
Crooked Creek tephra .....	36
Funny River tephra .....	36
Tephra 1A .....	36
Tephra 1B .....	41
Tephra 1C .....	41
Tephra 2? .....	41
Tephra 3 .....	41
Tephra 4 .....	45
Tephra 5 .....	47
Tephra 7? .....	47
Tephra 8? .....	49
Tephra 12? .....	49
Tephra 13 .....	49
Middle Quaternary tephras .....	49
Goose Bay tephra .....	49
Stampede tephra .....	51
Fossils .....	52
Middle inlet collections .....	52
Upper inlet collections .....	53
Soil profiles .....	54
Sterling profiles .....	54
Kachemak Bay profiles .....	55
Turnagain Arm profiles .....	55
Discussion .....	57
Till-source study .....	57
Methodology .....	58
Initial results and analysis .....	58
Results of multivariate analysis .....	63
Implications .....	68
Conclusions .....	70
Acknowledgments .....	70
References cited .....	72
Appendix A: Stratigraphic sections and soil profiles .....	77
Appendix B: Multivariate analysis of magnetic susceptibility and pebble compositions of till samples .....	171

## FIGURES

Figure	1. Graph showing distribution of 104 radiocarbon dates older than 6,000 <sup>14</sup> C yr B.P. in the Cook Inlet region .....	24
	2. Map showing distribution of Lethe tephra samples (n = 29) in Kenai Lowland relative to former limits of the Naptowne glaciation .....	33

**FIGURES** (continued)

3. Graph showing tentative relative ages of late Quaternary tephras, based on stratigraphic relations in Kenai Lowland .....	37
4-12. Maps:	
4. Distribution of Crooked Creek tephra samples (n = 11) in Kenai Lowland relative to former limits of the Naptowne glaciation .....	38
5. Distribution of Funny River tephra samples (n = 5) in Kenai Lowland relative to former limits of the Naptowne glaciation .....	39
6. Distribution of tephra 1A samples (n = 6) in Kenai Lowland relative to former limits of the Naptowne glaciation .....	40
7. Distribution of tephra 1B samples (n = 6) in Kenai Lowland relative to former limits of the Naptowne glaciation .....	42
8. Distribution of tephra 1C samples (n = 4) in Kenai Lowland relative to former limits of the Naptowne glaciation .....	43
9. Distribution of tephra 3 samples (n = 3) in Kenai Lowland relative to former limits of the Naptowne glaciation .....	44
10. Distribution of tephra 4 samples (n = 3) in Kenai Lowland relative to former limits of the Naptowne glaciation .....	46
11. Distribution of tephra 5 samples (n = 4) in Kenai Lowland relative to former limits of the Naptowne glaciation .....	48
12. Distribution of tephra 13 samples (n = 3) in Kenai Lowland relative to former limits of the Naptowne glaciation .....	50
13. Profiles comparing soils developed on type Moosehorn, Killely, and Skilak moraines .....	56
14. Graph showing mean magnetic susceptibility of six size fractions in 68 till samples from six known source areas in the Cook Inlet region .....	59
15. Graph showing standard deviation of mean magnetic susceptibility of six size fractions in 68 till samples from six known source areas in the Cook Inlet region .....	64
16-19. Maps:	
16. Distribution of CHAID predictions at the 99-percent confidence level and till sources predicted by the glaciation model in the Cook Inlet region .....	66
17. Comparison of CHAID predictions at the 95-percent confidence level and till sources predicted by the glaciation model in the Cook Inlet region .....	67
18. Comparison of till sources predicted by multiple discriminant analysis and sources predicted by the glaciation model in the Cook Inlet region .....	69
19. Map showing revised model of Naptowne glaciation in the Cook Inlet region .....	71
A1-A33. Stratigraphic sections:	
A1. Section 1, Anchorage D-8 SW Quadrangle (ANC-1, sheet 1) .....	87
A2. Section 2, Anchorage C-7 NE Quadrangle (ANC-9, sheet 1) .....	88
A3. Section 3, Anchorage B-8 NW Quadrangle (ANC-22, sheet 1) .....	Pocket
A4. Section 4, Anchorage B-8 SW Quadrangle (ANC-36, sheet 1) .....	89
A5. Section 5, Anchorage A-8 NW Quadrangle (ANC-39, sheet 1) .....	90
A6. Section 6, Kenai D-1 NW Quadrangle (KEN-1, sheet 2) .....	91
A7. Section 7, Kenai D-1 NW Quadrangle (KEN-2, sheet 2) .....	92
A8. Section 8, Kenai D-3 SW Quadrangle (KEN-6, sheet 2) .....	93
A9. Section 9, Kenai D-3 SE Quadrangle (KEN-14, sheet 2) .....	94
A10. Section 10, Kenai C-4 NE Quadrangle (KEN-15, sheet 2) .....	95
A11. Section 11, Kenai C-4 NE Quadrangle (KEN-18, sheet 2) .....	96
A12. Section 12, Kenai C-3 NE Quadrangle (KEN-27, sheet 2) .....	97
A13. Section 13, Kenai C-4 NW Quadrangle (KEN-36, sheet 2) .....	98
A14. Section 14, Kenai C-3 NE Quadrangle (KEN-38, sheet 2) .....	99
A15. Section 15, Kenai C-3 NW Quadrangle (KEN-40, sheet 2) .....	100
A16. Section 16, Kenai C-4 NW Quadrangle (KEN-41, sheet 2) .....	101
A17. Section 17, Kenai C-4 SE Quadrangle (KEN-44, sheet 2) .....	102
A18. Section 18, Kenai C-4 SE Quadrangle (KEN-46, sheet 2) .....	103

**FIGURES** (continued)

A19. Section 19, Kenai C-4 SE Quadrangle (KEN-50, sheet 2) .....	104
A20. Section 20, Kenai C-4 SE Quadrangle (KEN-53, sheet 2) .....	105
A21. Section 21, Kenai C-3 SW Quadrangle (KEN-56, sheet 2) .....	106
A22. Section 22, Kenai C-3 SE Quadrangle (KEN-58, sheet 2) .....	107
A23. Section 23, Kenai C-4 SE Quadrangle (KEN-60, sheet 2) .....	108
A24. Section 24, Kenai C-3 SE Quadrangle (KEN-62, sheet 2) .....	109
A25. Section 25, Kenai C-3 SE Quadrangle (KEN-64, sheet 2) .....	110
A26. Section 26, Kenai C-2 SW Quadrangle (KEN-65, sheet 2) .....	111
A27. Section 27, Kenai C-2 SW Quadrangle (KEN-66, sheet 2) .....	112
A28. Section 28, Kenai C-3 SE Quadrangle (KEN-68, sheet 2) .....	113
A29. Section 29, Kenai C-2 SW Quadrangle (KEN-71, sheet 2) .....	114
A30. Section 30A, Kenai C-4 SE Quadrangle (KEN-78, sheet 2) .....	115
A31. Section 30B, Kenai C-4 SE Quadrangle (KEN-78, sheet 2) .....	115
A32. Section 30C, Kenai C-4 SE Quadrangle (KEN-78, sheet 2) .....	116
A33. Section 31 on type Killey moraine, Kenai C-2 SW Quadrangle (KEN-79, sheet 2) .....	117
A34. Soil profile showing distribution of silt and clay (calculated as percent of <2-mm fraction) with depth, profile S1 on flat crest of type Killey moraine, Kenai C-2 SW Quadrangle (KEN-79, sheet 2) .....	118
A35. Stratigraphic section 32 on type Moosehorn moraine, Kenai C-2 SW Quadrangle (KEN-80, sheet 2) .....	119
A36. Soil profile showing distribution of silt and clay (calculated as percent of <2-mm fraction) with depth, profile S2 on flat crest of type Moosehorn moraine, Kenai C-2 SW Quadrangle (KEN-80, sheet 2) .....	120
A37-A48. Stratigraphic sections:	
A37. Section 33, Kenai C-2 SW Quadrangle (KEN-81, sheet 2) .....	121
A38. Section 34, Kenai C-3 SE Quadrangle (KEN-82, sheet 2) .....	122
A39. Section 35, Kenai C-3 SE Quadrangle (KEN-83, sheet 2) .....	123
A40. Section 36, Kenai C-3 SE Quadrangle (KEN-85, sheet 2) .....	124
A41. Section 37, Kenai C-2 SW Quadrangle (KEN-86, sheet 2) .....	125
A42. Section 38, Kenai C-2 SW Quadrangle (KEN-87, sheet 2) .....	126
A43. Section 39, Kenai C-4 SE Quadrangle (KEN-88, sheet 2) .....	127
A44. Section 40, Kenai C-2 SW Quadrangle (KEN-90, sheet 2) .....	128
A45. Section 41, Kenai B-4 NE Quadrangle (KEN-96, sheet 2) .....	129
A46. Section 42, Kenai B-3 NW Quadrangle (KEN-97, sheet 2) .....	130
A47. Section 43, Kenai B-3 NW Quadrangle (KEN-100, sheet 2) .....	131
A48. Section 44 on type Skilak moraine, Kenai B-2 NE Quadrangle (KEN-101, sheet 2) .....	132
A49. Soil profile showing distribution of silt and clay (calculated as percent of <2-mm fraction) with depth, profile S3 on flat crest of type Skilak moraine, Kenai B-2 NE Quadrangle (KEN-101, sheet 2) .....	133
A50-A77. Stratigraphic sections:	
A50. Section 45, Kenai B-4 NE Quadrangle (KEN-103, sheet 2) .....	134
A51. Section 46, Kenai B-3 NW Quadrangle (KEN-105, sheet 2) .....	135
A52. Section 47, Kenai B-3 NW Quadrangle (KEN-107, sheet 2) .....	136
A53. Section 48, Kenai B-3 NW Quadrangle (KEN-110, sheet 2) .....	137
A54. Section 49, Kenai B-4 NE Quadrangle (KEN-113, sheet 2) .....	138
A55. Section 50, Kenai B-4 NE Quadrangle (KEN-115, sheet 2) .....	139
A56. Section 51, Kenai B-4 NW Quadrangle (KEN-116, sheet 2) .....	140
A57. Section 52, Kenai B-4 SE Quadrangle (KEN-117, sheet 2) .....	141
A58. Section 53, Kenai B-4 SE Quadrangle (KEN-118, sheet 2) .....	142
A59. Section 54, Kenai B-4 SE Quadrangle (KEN-119, sheet 2) .....	143
A60. Section 55, Kenai B-4 SE Quadrangle (KEN-120, sheet 2) .....	143
A61. Section 56, Kenai B-4 SE Quadrangle (KEN-122, sheet 2) .....	144
A62. Section 57, Kenai B-4 SE Quadrangle (KEN-123, sheet 2) .....	145

## FIGURES (continued)

A63.	Section 58, Kenai B-4 SE Quadrangle (KEN-124, sheet 2).....	146
A64.	Section 59, Kenai B-4 SE Quadrangle (KEN-126, sheet 2).....	147
A65.	Section 60, Kenai B-4 SW Quadrangle (KEN-128, sheet 2).....	148
A66.	Section 61, Kenai B-4 SW Quadrangle (KEN-129, sheet 2).....	149
A67.	Section 62, Kenai B-4 SE Quadrangle (KEN-130, sheet 2).....	150
A68.	Section 63, Kenai B-4 SE Quadrangle (KEN-132, sheet 2).....	151
A69.	Section 64, Kenai B-4 SE Quadrangle (KEN-139, sheet 2).....	152
A70.	Section 65, Kenai A-4 NW Quadrangle (KEN-140, sheet 2).....	153
A71.	Section 66, Kenai A-5 SE Quadrangle (KEN-141, sheet 2).....	154
A72.	Section 67, Seldovia D-5 SW Quadrangle (SEL-2, sheet 3).....	155
A73.	Section 68, Seldovia D-5 SW Quadrangle (SEL-3, sheet 3).....	156
A74.	Section 69, Seldovia C-5 NW Quadrangle (SEL-4, sheet 3).....	157
A75.	Section 70, Seldovia D-5 SW Quadrangle (SEL-5, sheet 3).....	157
A76.	Section 71, Seldovia C-5 NW Quadrangle (SEL-6, sheet 3).....	158
A77.	Section 72, Seldovia C-5 NW Quadrangle (SEL-7, sheet 3).....	159
A78.	Soil profile showing distribution of silt and clay (calculated as percent of <2-mm fraction) with depth, profile S4 on flat crest of Moosehorn-age moraine of Kachemak Bay lobe, Seldovia C-5 NW Quadrangle (SEL-7, sheet 3).....	160
A79.	Stratigraphic section 73, Seldovia C-5 NE Quadrangle (SEL-13, sheet 3).....	161
A80.	Soil profile showing distribution of silt and clay (calculated as percent of <2-mm fraction) with depth, profile S5 on flat crest of Moosehorn-age moraine of Kachemak Bay lobe, Seldovia C-5 NE Quadrangle (SEL-13, sheet 3).....	162
A81.	Stratigraphic section 74, Seldovia C-5 NE Quadrangle (SEL-14, sheet 3).....	163
A82.	Stratigraphic section 75, Seward D-8 Quadrangle (SEW-4, sheet 4).....	164
A83.	Soil profile showing distribution of silt and clay (calculated as percent of <2-mm fraction) with depth, profile S6 on flat crest of Elmendorf-age Bird Creek moraine in Turnagain Arm, Seward D-7 NW Quadrangle (SEW-2, sheet 4).....	165
A84.	Soil profile showing distribution of silt and clay (calculated as percent of <2-mm fraction) with depth, profile S7 on crest of 9,900-yr-old latest-Naptowne moraine in Turnagain Pass, southwestern quarter of Seward D-6 Quadrangle (SEW-12, sheet 4).....	166
A85.	Stratigraphic section 76, Tyonek A-1 NE Quadrangle (TYO-8, sheet 5).....	167
A86.	Stratigraphic section 77, Tyonek A-1 NE Quadrangle (TYO-9, sheet 5).....	168
A87.	Stratigraphic section 78, Tyonek A-1 NE Quadrangle (TYO-10, sheet 5).....	169
B1.	Ternary diagram of metasediment, quartz, and plutonic percentages in 85 pebble collections from tills in the Cook Inlet region.....	182

## TABLES

Table	1. Relation of map index numbers (sheets 1–5) to field site numbers, stratigraphic sections, radiocarbon samples, tephra samples, magnetic-susceptibility samples, pebble collections, fossil collections, and soil profiles in the Cook Inlet region.....	2
	2. Summary of radiocarbon dates associated with middle to late Quaternary deposits in Cook Inlet trough and vicinity.....	10
	3. Average glass compositions of middle and late Quaternary tephra samples collected at 58 localities in Kenai Lowland and vicinity.....	26
	4. Similarity-coefficient matrix for Lethe tephra samples collected in Kenai Lowland.....	34
	5. Similarity-coefficient matrix for samples of Crooked Creek tephra collected in Kenai Lowland.....	37
	6. Similarity-coefficient matrix for samples of Funny River tephra collected in Kenai Lowland ..	41
	7. Similarity-coefficient matrix for samples of tephra 1A collected in Kenai Lowland.....	45
	8. Similarity-coefficient matrices for samples of tephtras 1B and 1C collected in Kenai Lowland ..	45
	9. Similarity-coefficient matrices for samples of tephtras 3 and 4 collected in Kenai Lowland .....	47
	10. Similarity-coefficient matrices for samples of tephtras 5 and 13 collected in Kenai Lowland ....	47

TABLES (continued)

11. Similarity-coefficient matrices for samples of Goose Bay tephra and Stampede tephra collected from the type section of the Goose Bay peat, locality ANC-22 (sheet 1) .....	51
12. Abundances of glass-coated ferromagnesian grains in three tephra samples from the lower Goose Bay peat, locality ANC-22 (sheet 1) .....	51
13. Composition of macrofossil collections from the Bootlegger Cove Formation in the middle and upper Cook inlet region .....	52
14. Radiocarbon ages of macrofossil collections from the Bootlegger Cove Formation in the middle and upper Cook Inlet region .....	53
15. Standardized mean magnetic susceptibility of six size fractions in 109 till samples collected in the Cook Inlet region .....	60
16. Composition of pebbles collected from tills at 92 sites in the Cook Inlet region .....	62
17a. Mean magnetic susceptibility of six size fractions in groups of Naptowne-age till samples derived from six known sources and from four areas where till source is uncertain in the Cook Inlet region .....	65
17b. Mean standard deviations of magnetic susceptibility in six size fractions in groups of Naptowne-age till samples derived from six known sources and from four areas where till source is uncertain in the Cook Inlet region .....	65
18a. Mean pebble compositions in groups of Naptowne-age tills derived from six known sources and from three areas where till source is uncertain in the Cook Inlet region .....	68
18b. Mean standard deviations of pebble compositions in groups of Naptowne-age tills derived from six known sources and from three areas where till source is uncertain in the Cook Inlet region .....	68
A1. Symbols and terminology used in stratigraphic sections .....	78
A2. Definitions of symbols in summary soil descriptions .....	79
A3. Summary field description of soil profile S1 on flat crest of type Killey moraine, Kenai C-2 SW Quadrangle (KEN-79, sheet 2) .....	80
A4. Summary field description of soil profile S2 on flat crest of type Moosehorn moraine, Kenai C-2 SW Quadrangle (KEN-80, sheet 2) .....	81
A5. Summary field description of soil profile S3 on flat crest of type Skilak moraine, Kenai B-2 NE Quadrangle (KEN-101, sheet 2) .....	82
A6. Summary field description of soil profile S4 on flat crest of Moosehorn-age moraine of Kachemak Bay lobe, Seldovia C-5 NW Quadrangle (SEL-7, sheet 3) .....	83
A7. Summary field description of soil profile S5 on flat crest of Moosehorn-age moraine of Kachemak Bay lobe, Seldovia C-5 NW Quadrangle (SEL-13, sheet 3) .....	84
A8. Summary field description of soil profile S6 on flat crest of Elmendorf-age Bird Creek moraine, Turnagain Arm, Seward D-7 NW Quadrangle (SEW-2, sheet 4) .....	85
A9. Summary field description of soil profile S7 on flat crest of 9,900-yr-old latest-Naptowne moraine in Turnagain Pass, southwestern quarter of Seward D-6 Quadrangle (SEW-12, sheet 4) .....	86
B1. Composition of CHAID training subset of samples representing known till sources predicted by the proposed glaciation model in the Cook Inlet region .....	172
B2. Partitioning rules for predicting till sources in the Cook Inlet region at the 99- and 95-percent confidence levels, based on CHAID analysis of a subset (n = 27) of samples assigned by the proposed glaciation model to various source areas .....	173
B3. Comparison of till sources predicted by the proposed glaciation model and sources predicted by CHAID, based on magnetic-susceptibility measurements of 0- $\Phi$ and 4- $\Phi$ fractions and percent of metasediment and plutonic pebbles .....	174
B4. Matching of model sources and CHAID predictions of till sources in the Cook Inlet region at the 99-percent confidence level in three data subsets .....	176
B5. Matching of model sources and CHAID predictions of till sources in the Cook Inlet region at the 95-percent confidence level in three data subsets .....	177
B6. Distribution of mismatches of till sources predicted by the proposed glaciation model in the Cook Inlet region and sources predicted by CHAID at the 99-percent confidence level in two data subsets .....	179

**TABLES (continued)**

B7.	Distribution of mismatches of till sources predicted by the proposed glaciation model in the Cook Inlet region and sources predicted by CHAID at the 95-percent confidence level in two data subsets .....	180
B8.	Number of pebble collections in two subsets related to till sources predicted by the proposed glaciation model in the Cook Inlet region .....	181
B9.	Linear discriminant functions produced by multiple discriminant analysis of 92 pebble collections to predict till sources in the Cook Inlet region .....	181
B10.	Comparison of till sources predicted by the proposed glaciation model and sources predicted by multiple discriminant analysis, based on percent of metasediment, plutonic, and quartz pebbles .....	183
B11.	Matching of till sources predicted by the proposed glaciation model in the Cook Inlet region and sources predicted by multiple discriminant analysis of 92 pebble collections in two subsets .....	184
B12.	Distribution of mismatches of till sources predicted by the proposed glaciation model in the Cook Inlet region and sources predicted by multiple discriminant analysis of 92 pebble collections in two subsets .....	185
B13.	Composition of the pebble-count subset analyzed by CHAID .....	186
B14.	Partitioning rules developed by CHAID from pebble-count subset (n = 85) to predict till sources in the Cook Inlet region at the 99-percent confidence level .....	186
B15.	Comparison of till sources predicted by the proposed glaciation model in the Cook Inlet region and sources predicted by CHAID at the 99-percent confidence level, based on percent of metasediment till pebbles .....	187
B16.	Matching of till sources predicted by the proposed glaciation model in the Cook Inlet region and sources predicted by CHAID at the 99-percent confidence level in two data subsets, based on the metasediment-pebble content of 85 pebble collections .....	188

**SHEETS**

Sheet	1. Sample localities in the Anchorage Quadrangle, Alaska .....	Pocket
	2. Sample localities in the Kenai Quadrangle, Alaska .....	Pocket
	3. Sample localities in the Seldovia Quadrangle, Alaska .....	Pocket
	4. Sample localities in the Seward Quadrangle, Alaska .....	Pocket
	5. Sample localities in the Tyonek Quadrangle, Alaska .....	Pocket

# CATALOG AND INITIAL ANALYSES OF GEOLOGIC DATA RELATED TO MIDDLE TO LATE QUATERNARY DEPOSITS, COOK INLET REGION, ALASKA

by

Richard D. Reger,<sup>1</sup> DeAnne S. Pinney,<sup>2</sup> Raymond M. Burke,<sup>3</sup> and Milton A. Wiltse<sup>2</sup>

## INTRODUCTION

This Report of Investigations catalogs geologic field and laboratory data accumulated during Alaska Division of Geological & Geophysical Surveys (DGGs) studies of middle to late Quaternary sediments in the Cook Inlet region and presents initial interpretations of these data. This information and the associated geologic mapping (Reger, 1977, 1978a,b and 1981a-d; Reger and Carver, 1977 and 1978a,b; Daniels, 1981a,b; Cameron and others, 1981; Updike and Ulery, 1983a,b and 1986; Rawlinson, 1986; Combellick and Reger, 1988; Reger and Petrik, 1993; and Reger and others, 1994a-d) are the foundations for summaries of the glacial history of the Cook Inlet region by Reger and Updike (1983a,b), Reger (1985), Reger and others (1995), and Reger and Pinney (1996).

## DATA PRESENTATION

Sample sites of DGGs and others are tied by index numbers to base maps of the Anchorage, Kenai, Seldovia, Seward, and Tyonek Quadrangles (sheets 1-5) in table 1, which provides latitude and longitude locations for each sample site. Seventy-eight stratigraphic sections and seven soil profiles are illustrated and briefly described in appendix A.

## RADIOCARBON DATES

Stratigraphic context and temporal significance of 104 radiocarbon dates in the Cook Inlet region are summarized in table 2; these dates are from both published and unpublished sources. In some instances, we offer interpretations of dates that differ from the interpretations of previous authors to reflect either advances in our knowledge of the glacial history or differences of opinion. Our set of radiocarbon dates is trimodal (fig. 1) and includes: (a) a subset of dates of terrestrial materials between 6,000 and 13,750 <sup>14</sup>C yr B.P. (n = 64); (b) a subset of dates of glaciomarine or glacioestuarine macrofossils between

13,500 and 16,500 <sup>14</sup>C yr B.P. (n = 19); and (c) a subset of infinite dates for reworked wood and lignite of Tertiary age or coal-contaminated organic silt in the Kenai Lowland (n = 8) and infinite dates for the Goose Bay peat or correlative peats in the Anchorage Lowland (n = 13).

Among the terrestrial samples, the oldest surface peat (collected by Karlstrom in the East Foreland area) dates 13,500 ± 400 <sup>14</sup>C yr B.P. (table 2, C64). The oldest finite date is 16,480 ± 170 <sup>14</sup>C yr B.P. for plates of *Balanus evermanni* collected at the mouth of Kenai River (table 2, C83).

Our repeated attempts to date the Goose Bay peat at its type locality on the west side of Knik Arm (Karlstrom, 1964) (table 1, locality ANC-22 and fig. A3) by the radiocarbon method merely duplicated the infinite dates previously published by Karlstrom (1964). However, with a radiocarbon-enrichment age of >73,400 <sup>14</sup>C yr B.P. (table 2, C104) we push the minimum age of the Goose Bay peat back in time 28,400 <sup>14</sup>C yr farther than the oldest date previously documented (Reger and Updike, 1983a, fig. 106).

## TEPHRA STUDIES

During our field investigations, volcanic-ash layers were encountered in nearly every excavation, and tephra were sampled at 59 localities (table 1). We did not sample the widespread, unnamed tephra complex in and just beneath the surface organic material primarily because it provides little chronological information for the glacial story and it is undoubtedly composed of the distal airfall products of several historic and prehistoric eruptions from a variety of volcanoes, including Mt. Katmai, Mt. Augustine, Mt. Redoubt, Mt. Spurr (Crater Peak), and Hayes volcano (Wilcox, 1959; Riehle, 1983, 1985, 1994; Riehle and others, 1981, 1990; Kienle and Nye, 1990; Begét and others, 1991, 1994; Begét, Reger, and others, 1991; Begét and Kienle, 1992; Begét and Nye, 1994; Combellick and Pinney, 1995).

## METHODOLOGY

The stratigraphic context of the various tephra was documented in the field (app. A), and the glass components of potentially significant volcanic ashes were cleaned and concentrated in the DGGs sediment laboratory using the methods described by Pinney (1991). (*Text cont'd. p. 25*)

<sup>1</sup>Present address: P.O. Box 638, La Grande, Oregon 97850.

<sup>2</sup>Alaska Division of Geological & Geophysical Surveys, 794 University Avenue, Suite 200, Fairbanks, Alaska 99709-3645.

<sup>3</sup>Department of Geology, Humboldt State University, Arcata, California 95521-4957.

**Table 1.** Relation of map index numbers (sheets 1–5) to field site numbers, stratigraphic sections, radiocarbon samples, tephra samples, magnetic-susceptibility samples, pebble collections, fossil collections, and soil profiles in the Cook Inlet region. Latitudes and longitudes were provided in original sources or determined by digitizing locations on 1:250,000-scale topographic maps and are estimated to be accurate to within 5 seconds. Microprobe geochemistry of tephra samples with asterisk(\*) numbers not reported because of great variation

Map index number	Latitude	Longitude	Field site number	Stratigraphic section	Radiocarbon sample	Tephra sample	Magnetic-susceptibility sample	Pebble collection	Macrofossil collection	Soil profile
ANC-1	61°50'05"N	149°58'39"W	81Re106	1	C51	---	---	---	---	---
ANC-2	61°47'58"N	147°47'48"W	---	---	C56, C62	---	---	---	---	---
ANC-3	61°46'26"N	149°48'33"W	90Re106	---	---	---	M55	P36	---	---
ANC-4	61°46'03"N	149°31'47"W	90Re105	---	---	---	M54	P35	---	---
ANC-5	61°45'57"N	149°31'34"W	---	---	C37	---	---	---	---	---
ANC-6	61°45'50"N	149°37'59"W	90Re104	---	---	---	M53	P34	---	---
ANC-7	61°44'26"N	149°43'17"W	---	---	C55	---	---	---	---	---
ANC-8	61°42'59"N	149°14'48"W	77JTK49	---	C24	---	---	---	---	---
ANC-9	61°41'44"N	149°15'05"W	88Re53	2	C23	---	---	---	---	---
ANC-10	61°39'02"N	149°52'58"W	90Re108	---	---	---	M57	P38	---	---
ANC-11	61°36'41"N	149°46'50"W	90Re109	---	---	---	M58	P39	---	---
ANC-12	61°34'27"N	149°23'25"W	90Re115	---	---	---	M64	P45	---	---
ANC-13	61°34'05"N	149°40'47"W	90Re110	---	---	---	M59	P40	---	---
ANC-14	61°33'22"N	149°31'32"W	90Re111	---	---	---	M60	P41	---	---
ANC-15	61°32'18"N	149°36'24"W	90Re112	---	---	---	M61	P42	---	---
ANC-16	61°31'24"N	149°15'32"W	KA6	---	C49	---	---	---	---	---
ANC-17	61°29'45"N	149°18'10"W	KA1	---	C22	---	---	---	---	---
ANC-18	61°28'33"N	149°42'52"W	90Re113	---	---	---	M62	P43	---	---
ANC-19	61°26'17"N	149°47'13"W	90Re114	---	---	---	M63	P44	---	---
ANC-20	61°25'42"N	149°25'03"W	90Re116	---	---	---	M65	P46	---	---
ANC-21	61°23'32"N	149°51'30"W	90Re103	---	---	---	M52	P33	---	---
ANC-22	61°23'32"N	149°51'18"W	85Re1, 88Re54, 92Re20, 93Re42	3	C89, C93, C96, C98, C99, C104	KL-025, KL-027, KL-081p1, KL-081p2, KL-082, KL-083	---	---	---	---
ANC-23	61°23'32"N	149°50'21"W	---	---	C97	---	---	---	---	---
ANC-24	61°23'26"N	149°53'06"W	KA4B	---	C26	---	---	---	---	---
ANC-25	61°22'12"N	149°31'37"W	---	---	C102	---	---	---	---	---
ANC-26	61°21'56"N	149°42'46"W	---	---	C103	---	---	---	---	---
ANC-27	61°21'16"N	149°33'01"W	---	---	C91	---	---	---	---	---
ANC-28	61°18'52"N	149°38'29"W	---	---	C95	---	---	---	---	---
ANC-29	61°18'35"N	149°34'46"W	---	---	C94	---	---	---	---	---
ANC-30	61°18'25"N	149°54'32"W	91Re43A	---	---	---	M97	P78	---	---
ANC-31	61°18'22"N	149°35'05"W	90Re118	---	---	---	M67	P48	---	---
ANC-32	61°17'26"N	149°50'06"W	---	---	C35	---	---	---	---	---

Table 1. (continued)

Map index number	Latitude	Longitude	Field site number	Stratigraphic section	Radiocarbon sample	Tephra sample	Magnetic-susceptibility sample	Pebble collection	Macrofossil collection	Soil profile
ANC-33	61°15'52"N	149°55'18"W	---	---	C68	---	---	---	F1	---
ANC-34	61°15'51"N	149°55'27"W	---	---	C53	---	---	---	---	---
ANC-35	61°15'45"N	149°52'14"W	---	---	C58	---	---	---	---	---
ANC-36	61°15'34"N	149°55'57"W	77Re22	4	C76	---	---	---	F2	---
ANC-37	61°14'45"N	149°58'17"W	---	---	C77	---	---	---	---	---
ANC-38	61°14'29"N	149°40'38"W	90Re117	---	---	---	M66	P47	---	---
ANC-39	61°14'17"N	149°58'57"W	82Re12	5	C72	---	---	---	F3	---
ANC-40	61°13'39"N	149°42'29"W	90Re119	---	---	---	M68	P49	---	---
ANC-41	61°11'59"N	149°59'25"W	---	---	C52	---	---	---	---	---
ANC-42	61°11'58"N	149°59'00"W	---	---	C79	---	---	---	---	---
ANC-43	61°11'56"N	149°58'52"W	---	---	C65	---	---	---	---	---
ANC-44	61°11'48"N	149°44'53"W	90Re120	---	---	---	M69	P50	---	---
ANC-45	61°11'18"N	149°48'12"W	90Re121	---	---	---	M70	P51	---	---
ANC-46	61°05'09"N	149°50'01"W	---	---	C13, C100	---	---	---	---	---
ANC-47	61°03'54"N	149°47'08"W	90Re122	---	---	---	M71	P52	---	---
KEN-1	60°58'48"N	150°18'11"W	92Re21	6	C47	KL-134*	---	---	---	---
KEN-2	60°58'02"N	150°17'20"W	90Re102	7	C54, C60	KL-111	---	---	---	---
KEN-3	60°48'27"N	151°01'05"W	90Re57	---	---	---	M37	P22	---	---
KEN-4	60°48'12"N	151°46'04"W	91Re48	---	---	---	---	P81	---	---
KEN-5	60°48'03"N	151°52'54"W	91Re47	---	---	---	---	P80	---	---
KEN-6	60°47'59"N	151°00'56"W	90Re58	8	---	KL-037*	---	---	---	---
KEN-7	60°47'27"N	150°50'25"W	91Re16	---	---	---	M78	P59	---	---
KEN-8	60°47'05"N	151°05'55"W	---	---	C87	---	---	---	---	---
KEN-9	60°47'00"N	151°04'28"W	90Re59	---	---	---	M40	P24	---	---
KEN-10	60°46'50"N	151°11'58"W	---	---	C20	---	---	---	---	---
KEN-11	60°46'25"N	150°50'31"W	91Re15	---	---	---	M77	P58	---	---
KEN-12	60°46'10"N	150°47'54"W	91Re17	---	---	---	M79	P60	---	---
KEN-13	60°45'17"N	150°30'15"W	91Re28	---	---	---	M87	P68	---	---
KEN-14	60°44'58"N	150°51'27"W	91Re18	9	---	KL-099	---	---	---	---
KEN-15	60°44'27"N	151°18'07"W	90Re61	10	---	KL-040	M44	P28	---	---
KEN-16	60°44'15"N	151°20'13"W	90Re60	---	---	---	M42	P26	---	---
KEN-17	60°44'04"N	151°37'45"W	91Re25	---	---	---	M85	P66	---	---
KEN-18	60°43'59"N	151°09'37"W	90Re62	11	---	KL-015p1, KL-015p2, KL-016	M46	P29	---	---
KEN-19	60°43'59"N	150°48'50"W	91Re22	---	---	---	M82	P63	---	---
KEN-20	60°43'53"N	151°21'12"W	90Re68	---	---	---	M48	P31	---	---
KEN-21	60°43'52"N	151°20'01"W	90Re63	---	---	---	M47	P30	---	---

Table 1. (continued)

Map index number	Latitude	Longitude	Field site number	Stratigraphic section	Radiocarbon sample	Tephra sample	Magnetic-susceptibility sample	Pebble collection	Macrofossil collection	Soil profile
KEN-22	60°43'49"N	150°46'03"W	91Re23	---	---	---	M83	P64	---	---
KEN-23	60°43'49"N	151°43'23"W	91Re24	---	---	---	M84	P65	---	---
KEN-24	60°43'44"N	151°21'26"W	90Re69	---	---	---	M49	P32	---	---
KEN-25	60°43'44"N	150°33'42"W	91Re27	---	---	---	M86	P67	---	---
KEN-26	60°43'36"N	150°52'23"W	91Re14	---	---	---	M76	P57	---	---
KEN-27	60°43'25"N	150°54'15"W	91Re19	12	---	KL-100	---	---	---	---
KEN-28	60°43'14"N	150°53'55"W	91Re20	---	---	---	M80	P61	---	---
KEN-29	60°42'57"N	151°44'16"W	91Re44	---	---	---	M98	P79	---	---
KEN-30	60°42'46"N	150°53'11"W	91Re21	---	---	---	M81	P62	---	---
KEN-31	60°42'37"N	150°48'32"W	90Re130	---	---	---	M75	P56	---	---
KEN-32	60°41'25"N	151°23'38"W	---	---	C101	---	---	---	---	---
KEN-33	60°40'54"N	151°23'17"W	---	---	C61	---	---	---	---	---
KEN-34	60°40'54"N	150°47'09"W	90Re129	---	---	---	M74	P55	---	---
KEN-35	60°40'37"N	151°23'01"W	---	---	C85	---	---	---	---	---
KEN-36	60°39'38"N	151°18'55"W	90Re67	13	---	KL-017, KL-018p1, KL-018p2	---	---	---	---
KEN-37	60°39'21"N	151°01'54"W	91Re38	---	---	---	M94	P75	---	---
KEN-38	60°38'58"N	150°49'21"W	91Re3	14	---	KL-096, KL-097*, KL-098*	---	---	---	---
KEN-39	60°38'25"N	151°21'06"W	---	---	C64	---	---	---	---	---
KEN-40	60°38'17"N	151°04'22"W	91Re37	15	---	KL-106	---	---	---	---
KEN-41	60°38'05"N	151°20'02"W	90Re65	16	---	KL-013p1, KL-013p2	---	---	---	---
KEN-42	60°37'47"N	150°48'12"W	90Re128	---	---	---	M73	---	---	---
KEN-43	60°37'36"N	151°06'41"W	91Re36	---	---	---	M93	P74	---	---
KEN-44	60°37'25"N	151°07'54"W	92Re5	17	---	KL-124	---	---	---	---
KEN-45	60°36'58"N	151°20'33"W	---	---	C92	---	---	---	---	---
KEN-46	60°35'47"N	151°12'49"W	92Re4	18	C4, C5	KL-121*, KL-122*, KL-123	---	---	---	---
KEN-47	60°35'47"N	150°48'03"W	90Re27	---	---	---	M25	P12	---	---
KEN-48	60°35'44"N	150°50'39"W	90Re28	---	---	---	---	P13	---	---
KEN-49	60°35'16"N	151°19'56"W	---	---	C86	---	---	---	---	---
KEN-50	60°34'24"N	151°13'46"W	92Re6	19	---	KL-125	---	---	---	---
KEN-51	60°33'38"N	150°37'59"W	90Re24, 90MW17	---	---	---	M23	P11	---	---

Table 1. (continued)

Map index number	Latitude	Longitude	Field site number	Stratigraphic section	Radiocarbon sample	Tephra sample	Magnetic-susceptibility sample	Pebble collection	Macrofossil collection	Soil profile
KEN-52	60°33'35"N	150°47'17"W	90Re32A	---	---	---	M27	---	---	---
KEN-53	60°33'07"N	151°14'17"W	91Re39	20	C83	---	---	---	F4	---
KEN-54	60°33'04"N	150°49'39"W	90Re125	---	---	---	---	P54	---	---
KEN-55	60°33'02"N	150°37'48"W	90Re23, 90MW16	---	---	---	M22	P10	---	---
KEN-56	60°32'58"N	150°59'25"W	91Re42	21	---	KL-110	---	---	---	---
KEN-57	60°32'53"N	150°58'15"W	91Re43	---	---	---	M96	P77	---	---
KEN-58	60°32'50"N	150°48'17"W	90Re127	22	---	KL-029, KL-032p1, KL-032p2, KL-032p3	---	---	---	---
KEN-59	60°32'37"N	150°44'28"W	90Re25	---	---	---	M24	---	---	---
KEN-60	60°32'28"N	151°10'42"W	91Re2, 91-30, 91-30R	23	C27, C30, C31, C48	---	---	---	---	---
KEN-61	60°32'27"N	150°45'49"W	90Re31, 90MW31	---	---	---	M26	P14	---	---
KEN-62	60°32'21"N	150°49'46"W	91MW25	24	---	KL-066	---	---	---	---
KEN-63	60°32'13"N	150°51'27"W	90Re32, 90MW26	---	---	---	---	P15	---	---
KEN-64	60°32'13"N	150°46'15"W	91Re64A	25	C10, C17	KL-112p1, KL-112p2, KL-112p3, KL-112p4, KL-113	---	---	---	---
KEN-65	60°32'05"N	150°44'54"W	90Re43	26	---	KL-050p1, KL-050p2, KL-051	---	---	---	---
KEN-66	60°32'04"N	150°43'53"W	90Re35, 90MW6	27	---	KL-062, KL-063	---	P16	---	---
KEN-67	60°32'02"N	150°28'00"W	90Re17	---	---	---	M16	P7	---	---
KEN-68	60°31'57"N	150°55'10"W	90Re126	28	---	KL-033	---	---	---	---
KEN-69	60°31'56"N	150°23'03"W	90Re16	---	---	---	M15	---	---	---
KEN-70	60°31'50"N	150°14'52"W	90Re14	---	---	---	M13	P6	---	---
KEN-71	60°31'49"N	150°44'01"W	90Re34	29	---	KL-057	---	---	---	---
KEN-72	60°31'47"N	150°43'38"W	90Re21	---	---	---	M20	P9	---	---
KEN-73	60°31'43"N	150°34'17"W	90Re19	---	---	---	M18	P8	---	---
KEN-74	60°31'38"N	150°32'32"W	90Re18	---	---	---	M17	---	---	---
KEN-75	60°31'37"N	150°38'14"W	90Re20	---	---	---	M19	---	---	---

Table 1. (continued)

Map index number	Latitude	Longitude	Field site number	Stratigraphic section	Radiocarbon sample	Tephra sample	Magnetic-susceptibility sample	Pebble collection	Macrofossil collection	Soil profile
KEN-76	60°31'37"N	150°37'56"W	90Re22	---	---	---	M21	---	---	---
KEN-77	60°31'31"N	150°16'25"W	90Re15	---	---	---	M14	---	---	---
KEN-78	60°31'30"N	151°12'31"W	91Re3, 91-16, KE1	30	C2, C3, C6, C14	---	---	---	---	---
KEN-79	60°31'25"N	150°37'42"W	90MW10	31	---	---	---	---	---	S1
KEN-80	60°31'23"N	150°42'34"W	90MW8	32	---	---	---	---	---	S2
KEN-81	60°31'23"N	150°40'38"W	90MW104	33	C12	---	---	---	---	---
KEN-82	60°31'13"N	150°53'13"W	90Re33	34	---	KL-072	---	---	---	---
KEN-83	60°31'06"N	150°47'45"W	90Re36	35	---	KL-060, KL-061	---	---	---	---
KEN-84	60°31'02"N	150°59'55"W	91Re41	---	---	---	M95	P76	---	---
KEN-85	60°30'58"N	150°45'30"W	90MW24	36	---	KL067, KL-068	---	---	---	---
KEN-86	60°30'57"N	150°38'48"W	91Re8	37	---	KL-088	---	---	---	---
KEN-87	60°30'55"N	150°40'51"W	90Re42	38	---	KL-052, KL-053	---	---	---	---
KEN-88	60°30'41"N	151°16'18"W	90Re71	39	---	KL-020, KL-021	---	---	---	---
KEN-89	60°30'41"N	150°10'15"W	90Re13	---	---	---	M12	---	---	---
KEN-90	60°30'11"N	150°36'42"W	92Re2	40	---	KL-117*	---	---	---	---
KEN-91	60°30'07"N	150°29'36"W	90Re2	---	---	---	M1	P1	---	---
KEN-92	60°29'43"N	151°02'51"W	90Re37	---	---	---	M28	---	---	---
KEN-93	60°29'42"N	150°27'31"W	90Re3, 90MW14	---	---	---	M2	P93	---	---
KEN-94	60°29'24"N	150°00'39"W	90Re10	---	---	---	M9	---	---	---
KEN-95	60°29'21"N	150°02'14"W	90Re11	---	---	---	M10	P5	---	---
KEN-96	60°29'20"N	151°11'59"W	91Re31	41	---	KL-102p1, KL-102p2, KL-102p3	---	---	---	---
KEN-97	60°29'17"N	151°03'07"W	91Re35	42	---	KL-105	---	---	---	---
KEN-98	60°29'16"N	150°04'12"W	90Re12	---	---	---	M11	---	---	---
KEN-99	60°29'11"N	150°16'51"W	HL-4-M	---	C67	---	---	---	---	---
KEN-100	60°28'47"N	151°03'22"W	90Re38	43	---	KL-065	---	---	---	---
KEN-101	60°28'45"N	150°27'24"W	90Re40A	44	---	KL-056	---	---	---	S3
KEN-102	60°28'37"N	150°27'46"W	90Re4	---	---	---	M3	---	---	---
KEN-103	60°28'29"N	151°16'38"W	90Re72, 90Re72A	45	C7, C80, C81, C82 <sup>a</sup>	---	---	---	F5	---
KEN-104	60°28'19"N	150°19'33"W	90Re7	---	---	---	M6	---	---	---
KEN-105	60°28'17"N	151°07'10"W	90Re70	46	---	KL-011, KL-012	---	---	---	---
KEN-106	60°28'16"N	150°22'05"W	90Re6	---	---	---	M5	P2	---	---
KEN-107	60°28'05"N	151°04'51"W	91Re66	47	---	KL-116*	---	---	---	---
KEN-108	60°28'01"N	151°04'19"W	91Re29	---	---	---	M88	P69	---	---
KEN-109	60°27'39"N	150°16'58"W	90Re8	---	---	---	M7	P3	---	---

Table 1. (continued)

Map index number	Latitude	Longitude	Field site number	Stratigraphic section	Radiocarbon sample	Tephra sample	Magnetic-susceptibility sample	Pebble collection	Macrofossil collection	Soil profile
KEN-110	60°27'37"N	150°57'48"W	91Re40	48	---	KL-109	---	---	---	---
KEN-111	60°27'34"N	151°09'01"W	91Re30	---	---	---	M89	P70	---	---
KEN-112	60°27'25"N	150°12'57"W	90Re9	---	---	---	M8	P4	---	---
KEN-113	60°27'00"N	151°14'14"W	92Re7	49	---	KL-126*	---	---	---	---
KEN-114	60°23'35"N	151°15'00"W	SK34	---	C29	---	---	---	---	---
KEN-115	60°23'00"N	151°16'54"W	KS1	50	C11, C44	---	---	---	---	---
KEN-116	60°22'37"N	151°18'57"W	92Re14	51	---	KL-130	---	---	---	---
KEN-117	60°22'18"N	151°17'59"W	91Re12	52	---	KL-095p1, KL-095p2, KL-095p3	---	---	---	---
KEN-118	60°22'11"N	151°11'40"W	90Re51	53	---	KL-044p1, KL-044p2	---	---	---	---
KEN-119	60°21'18"N	151°15'58"W	92Re8	54	---	KL-127	---	---	---	---
KEN-120	60°20'46"N	151°13'07"W	92Re10	55	---	KL-128, KL-129	---	---	---	---
KEN-121	60°20'22"N	151°14'07"W	90Re52	---	---	---	M34	---	---	---
KEN-122	60°20'21"N	151°13'39"W	91Re65	56	C1, C9, C43	KL-114*, KL-115	---	---	---	---
KEN-123	60°19'58"N	151°16'02"W	91Re10	57	---	KL-090, KL-091	---	---	---	---
KEN-124	60°18'25"N	151°15'33"W	91Re11	58	---	KL-092*, KL-093, KL-094p1, KL-094p2	---	---	---	---
KEN-125	60°18'12"N	151°22'40"W	91Re34	---	---	---	M92	P73	---	---
KEN-126	60°18'08"N	151°15'37"W	92Re18	59	C84	KL-135	---	---	---	---
KEN-127	60°17'58"N	151°00'11"W	---	---	C88	---	---	---	---	---
KEN-128	60°17'57"N	151°22'21"W	90Re39	60	C8	KL-075	---	---	---	---
KEN-129	60°17'56"N	151°22'53"W	77Re18	61	C34, C90	---	---	---	---	---
KEN-130	60°17'15"N	151°16'45"W	91Re32	62	---	KL-104	M90	P71	---	---
KEN-131	60°17'10"N	151°21'45"W	91Re33	---	---	---	M91	P72	---	---
KEN-132	60°17'02"N	151°14'33"W	90Re54	63	---	KL-022, KL-023	M35	P21	---	---
KEN-133	60°16'55"N	151°14'19"W	90Re61A	---	---	---	M45	---	---	---
KEN-134	60°16'43"N	151°14'22"W	90Re60A	---	---	---	M43	P27	---	---
KEN-135	60°16'19"N	151°14'19"W	90Re59A	---	---	---	M41	P25	---	---
KEN-136	60°16'02"N	151°14'42"W	90Re58A	---	---	---	M39	---	---	---
KEN-137	60°15'52"N	151°14'16"W	90Re57A	---	---	---	M38	P23	---	---
KEN-138	60°15'18"N	151°10'56"W	90Re55	---	---	---	M36	---	---	---
KEN-139	60°15'16"N	151°13'06"W	90Re56	64	---	KL-034	---	---	---	---
KEN-140	60°10'03"N	151°26'46"W	92Re16	65	---	KL-131*	---	---	---	---

Table 1. (continued)

Map index number	Latitude	Longitude	Field site number	Stratigraphic section	Radiocarbon sample	Tephra sample	Magnetic-susceptibility sample	Pebble collection	Macrofossil collection	Soil profile
KEN-141	60°08'21"N	151°31'18"W	91Re5	66	---	KL-085, KL-086p1, KL-086p2, KL-086p3	---	---	---	---
KEN-142	60°05'36"N	151°36'51"W	---	---	C33	---	---	---	---	---
SEL-1	59°48'04"N	151°09'27"W	---	---	C59	---	---	---	---	---
SEL-2	59°47'42"N	151°47'31"W	92Re30	67	C19, C21	---	---	---	---	---
SEL-3	59°47'15"N	151°51'20"W	92Re29	68	---	---	---	---	---	---
SEL-4	59°46'12"N	151°51'22"W	92Re24	69	---	KL-136	---	---	---	---
SEL-5	59°43'50"N	151°50'05"W	92Re27	70	---	KL-137	---	---	---	---
SEL-6	59°43'49"N	151°46'06"W	91Re6	71	---	KL-087	---	---	---	---
SEL-7	59°43'33"N	151°44'02"W	90Re44	72	---	KL-001, KL-002, KL-003, KL-004, KL-006*, KL-008	---	---	---	S4
SEL-8	59°43'25"N	151°44'02"W	90Re45	---	---	---	M29	P17	---	---
SEL-9	59°42'51"N	151°43'00"W	90Re50	---	---	---	M33	---	---	---
SEL-10	59°41'45"N	151°41'13"W	90Re49	---	---	---	M32	P20	---	---
SEL-11	59°40'20"N	151°40'29"W	90Re48	---	---	---	M31	P19	---	---
SEL-12	59°39'52"N	151°34'12"W	90Re46	---	---	---	M30	P18	---	---
SEL-13	59°39'49"N	151°32'13"W	90Re47	73	---	KL-048, KL-049p1, KL-049p2	---	---	---	S5
SEL-14	59°38'06"N	151°30'41"W	91Re1	74	C40	---	---	---	---	---
SEL-15	59°35'04"N	151°08'25"W	---	---	C18, C39	---	---	---	---	---
SEW-1	60°58'26"N	149°27'36"W	90Re124	---	---	---	M72	P53	---	---
SEW-2	60°58'07"N	149°26'39"W	90Re90	---	---	---	---	---	---	S6
SEW-3	60°57'23"N	149°24'36"W	82Re4	---	C69, C75	---	---	---	F6	---
SEW-4	60°57'14"N	149°42'16"W	82Re36	75	C66	---	---	---	F7	---
SEW-5	60°57'01"N	149°10'38"W	---	---	C38	---	---	---	---	---
SEW-6	60°56'46"N	149°10'42"W	TA1	---	C42	---	---	---	---	---
SEW-7	60°56'35"N	149°40'08"W	82Re6	---	C73	---	---	---	F8	---
SEW-8	60°55'54"N	149°39'35"W	82Re5	---	C74	---	---	---	F9	---
SEW-9	60°49'12"N	148°58'30"W	---	---	C15	---	---	---	---	---
SEW-10	60°49'02"N	148°57'35"W	TA8	---	C46	---	---	---	---	---
SEW-11	60°47'49"N	149°13'01"W	RC84-15	---	C36	---	---	---	---	---
SEW-12	60°47'39"N	149°13'12"W	90Re91	---	---	---	---	---	---	S7
TYO-1	60°43'49"N	150°02'20"W	90Re107	---	---	---	M56	P37	---	---

Table 1. (continued)

Map index number	Latitude	Longitude	Field site number	Stratigraphic section	Radiocarbon sample	Tephra sample	Magnetic-susceptibility sample	Pebble collection	Macrofossil collection	Soil profile
TYO-2	61°39'39"N	150°14'15"W	78Re34	---	C45	---	---	---	---	---
TYO-3	61°26'03"N	151°45'31"W	91Re59	---	---	---	---	P92	---	---
TYO-4	61°22'04"N	151°45'20"W	91Re58	---	---	---	M109	P91	---	---
TYO-5	61°18'13"N	151°45'48"W	91Re57	---	---	---	M108	P90	---	---
TYO-6	61°15'36"N	151°58'28"W	91Re56	---	---	---	M107	P89	---	---
TYO-7	61°15'02"N	150°58'20"W	---	---	C78	---	---	---	---	---
TYO-8	61°14'49"N	150°01'43"W	82Re17	76	C70	---	---	---	F10	---
TYO-9	61°14'36"N	150°00'25"W	82Re14	77	C63	---	---	---	F11	---
TYO-10	61°14'32"N	150°00'07"W	82Re20	78	C57, C71	---	---	---	F12	---
TYO-11	61°12'53"N	151°57'55"W	91Re55	---	---	---	M106	P88	---	---
TYO-12	61°10'09"N	150°13'19"W	82Re40	---	C50	---	---	---	---	---
TYO-13	61°08'47"N	150°10'52"W	---	---	C16	---	---	---	---	---
TYO-14	61°08'08"N	151°36'05"W	91Re51	---	---	---	M102	P84	---	---
TYO-15	61°07'29"N	150°15'24"W	---	---	C28	---	---	---	---	---
TYO-16	61°04'20"N	151°07'53"W	91Re50	---	---	---	M101	P83	---	---
TYO-17	61°03'36"N	152°08'08"W	91Re54	---	---	---	M105	P87	---	---
TYO-18	61°02'35"N	152°04'20"W	91Re53	---	---	---	M104	P86	---	---
TYO-19	61°01'49"N	150°21'07"W	90Re100	---	---	---	M50	---	---	---
TYO-20	61°01'34"N	150°20'38"W	---	---	C41	---	---	---	---	---
TYO-21	61°01'22"N	150°20'24"W	90Re101	---	---	---	M51	---	---	---
TYO-22	61°00'52"N	150°19'51"W	---	---	C25	---	---	---	---	---
TYO-23	61°00'40"N	151°57'26"W	91Re52	---	---	---	M103	P85	---	---
TYO-24	61°00'35"N	151°21'10"W	91Re49A	---	---	---	M100	---	---	---
TYO-25	61°00'34"N	151°21'43"W	91Re49	---	---	---	M99	P82	---	---
TYO-26	61°00'17"N	150°19'31"W	---	---	C32	---	---	---	---	---

\*Location of C82 is tentative because precise latitude and longitude were not provided by Schmoell and Yehle (1983; 1986, locality B7) or Schmoell and others (1984, locality B4). The site indicated is the only section along Kalifornsky beach where we found *Balanus* plates in Bootlegger Cove Formation.

**Table 2.** Summary of radiocarbon dates associated with middle to late Quaternary deposits in the Cook Inlet trough and vicinity. Interpretations of stratigraphic context and chronological significance may differ considerably from original sources because of re-evaluation of glacial history. Footnotes provided at end of table. BCF = Bootlegger Cove Formation

Sample <sup>a</sup> locality	Laboratory/field number	Material and stratigraphic context	Chronological significance	Radiocarbon age ( <sup>14</sup> C yr B.P.)	Source
C1	GX-18230 [91RE65 S-2C]	Sphagnum peat from depth of 234.5-237.5 cm in peat boring; beneath tephra KL-115	Maximum age for tephra KL-115 but dates reversed	6,020 ± 175 <sup>b</sup>	This study (section 56)
C2	Beta-47182 [91RE3 C-1]	Organic silt with some wood and fibrous peat from beneath 1.8-m-thick surface peat and underlying 0.7-m-thick clayey estuarine silt with trace pebbles and organic material (rhizomes)	Maximum age for upper 0.7 m of estuarine silt near mouth of Kenai River	6,120 ± 50 <sup>b</sup>	This study (section 30A)
C3	Beta-45211 [91-16 & 16B]	Basal sample of 2-m-thick surface peat overlying clayey estuarine silt on tread of 6-m terrace	Maximum age for surface peat on 6-m terrace near mouth of Kenai River	6,190 ± 80 <sup>b</sup>	Combellick and Reger (1994, locality 91-16) (section 30B)
C4	GX-18232 [92RE4 S-5]	Fibrous sphagnum peat and organic silt from depth of 101.5-103.5 cm in peat boring; 1.5 cm above tephra KL-123	Minimum age for tephra KL-123	6,360 ± 145 <sup>b</sup>	This study (section 18)
C5	GX-18225 <sup>c</sup> [92RE4 S-8]	Fibrous sphagnum peat and organic silt from depth of 105.5-113 cm in peat boring; beneath tephra KL-123	Maximum age for tephra KL-123	6,801 ± 55 <sup>b</sup>	This study (section 18)
C6	Beta-49103 [KE1]	Top of 0.2-m-thick peat from depth of 4.2 m at base of 2-m-thick clayey estuarine silt	Maximum age for upper 2 m of estuarine fill near mouth of Kenai River	7,170 ± 120 <sup>b</sup>	Combellick and Reger (1994, borehole KE1) (section 30C)
C7	GX-16520 [90RE72 C-1]	Peat overlying 12.4 m of nearshore sand and gravel above dropstone diamicton of lower marine terrace	Minimum age for emergence of nearshore granular sediments in Kalifornsky beach area	7,175 ± 115 <sup>b</sup>	This study (section 45)

Table 2. (continued)

Sample <sup>a</sup> locality	Laboratory/field number	Material and stratigraphic context	Chronological significance	Radiocarbon age ( <sup>14</sup> C yr B.P.)	Source
C8	GX-16519 [90RE39 C-5]	Organic silt beneath 1.4-m-thick section of eolian and paludal silts, tephra, and peat and above 53-cm-thick fluvial rhythmite in fill of channel cut into Mooschorn-age terminal moraine	Minimum age for recession of Mooschorn-age glacier from Cohoe area	7,560 ± 340 <sup>b</sup>	This study (section 60)
C9	GX-18229 [91RE65 S-2A]	Sphagnum peat from depth of 229-232.5 cm in peat boring; above tephra KL-115	Minimum age for tephra KL-115	7,605 ± 210 <sup>b</sup>	This study (section 56)
C10	GX-18227 [91RE64A S-3A]	Sphagnum peat from depth of 293-296 cm in peat boring; above tephra KL-113	Minimum age for tephra KL-113	7,725 ± 210 <sup>b</sup>	This study (section 25)
C11	Beta-49111 [KS1]	Top of 1.1-m-thick peat at depth of 6.3 m beneath 4.5 m of estuarine clayey silt fill in lower Kasilof River valley	Maximum age for flooding of lower Kasilof River valley by estuarine waters	7,740 ± 60 <sup>b</sup>	Combellick and Reger (1994, borehole KS1) (section 50)
C12	GX-16517 [90MW104]	Organic silt from depth of 55 cm at base of kettle fill in moraine of Mooschorn age	Minimum age for recession of Mooschorn-age glacier from Sterling area	7,835 ± 240 <sup>b</sup>	This study (section 33)
C13	W-2151	Peat in lower part of 1.2-m-thick sand underlain by 1.2 m of gravel and 12.7 m of interbedded sand and glacioestuarine diamicton	Minimum age for recession of Skilak-age glacier from Potter area (Potter Hill railroad cut)	7,890 ± 250	Sullivan and others (1970, p. 332)
C14	Beta-49104 [KE1]	Base of 0.2-m-thick peat from depth of 4.4 m beneath 2 m of clayey estuarine silt and above sand and gravel	Minimum age for gravel below depth of 4.4 m in 6-m terrace near mouth of Kenai River	8,080 ± 250 <sup>b</sup>	Combellick and Reger (1994, borehole KE1) (section 30C)
C15	---	Wood fragments from laminated silt near depth of 93 m in estuarine deposits	Minimum age for recession of Elmendorf-age glacier from Portage area	8,230 ± 100	Bartsch-Winkler and others (1983), Bartsch-Winkler and Schmolt (1984)
C16	W-2306	Basal peat overlying glaciodeltaic deposits	Minimum age for recession of Skilak-age glacier from Fire Island	8,290 ± 250	Schmolt and others (1981, locality 3)

Table 2. (continued)

Sample <sup>a</sup> locality	Laboratory/field number	Material and stratigraphic context	Chronological significance	Radiocarbon age ( <sup>14</sup> C yr B.P.)	Source
C17	GX-18228 [91RE64A S-3C]	Sphagnum peat from depth of 297.5–300 cm in peat boring; beneath tephra KL-113	Maximum age for tephra KL-113	8,375 ± 210 <sup>b</sup>	This study (section 25)
C18	BGS-1279	Transported <i>Alnus</i> branch in deltaic sand, silt, and gravel 0.8 m below upper outwash sand and gravel	Minimum age for recession of Elmendorf-age glacier from lower Kachemak Bay in Halibut Cove area	8,400 ± 100 <sup>b</sup>	Wiles (1992), Wiles and Calkin (1994)
C19	GX-18405 [92RE30 S-1]	Peaty organic silt from base of 2.6-m-thick peat in former drainage channel	Minimum age for fluvial activity in drainage channel northeast of Anchor Point	8,515 ± 235 <sup>b</sup>	Reger and Petrik (1993), this study (section 67)
C20	L-163B <sup>d</sup>	Wood and organic silt from near base of lower 1.2-m-thick peat unconformably overlying sequence of thinly laminated silt and clay with some sand and gravel	Minimum age for advance of Killey-age glacier from northwest Boulder Point area	8,650 ± 450	Olson and Broecker (1959, p. 6), Karlstrom (1964, pls. 4 and 6, locality E-1, table 3)
C21	GX-18404 [92RE30 F-1]	Wood from base of 2.6-m-thick peat in former drainage channel	Minimum age for fluvial activity in drainage channel northeast of Anchor Point	8,745 ± 100 <sup>b</sup>	Reger and Petrik (1993), this study (section 67)
C22	GX-15229 <sup>c</sup>	Organic silt from depth of 8.5 m in estuarine fjord filling	Minimum age for recession of Elmendorf-age glacier from upper Knik Arm	8,850 ± 120 <sup>b</sup>	Combellick (1990, 1991, borehole KA1)
C23	GX-14445 [88Re53 C-1]	Peaty organic silt from base of 1.5-m-thick wood-bearing paludal deposit above 20 cm of olive-gray paludal silt overlying outwash sand and gravel	Minimum age for retreat of Elmendorf-age glacier and deposition of outwash alluvium at mouth of canyon of upper Little Susitna River	9,120 ± 350 <sup>b</sup>	This study (section 2)
C24	GX-5019 [77JTK49 C-1]	Silty peat with scattered wood fragments from base of 0.9-m-thick layer underlying 1.2-m-thick silty alluvial-fan sand and overlying gravelly sand deposited in ice-marginal bedrock channel	Minimum age for thinning of Elmendorf-age glacier blocking mouth of Little Susitna River canyon north of Palmer	9,155 ± 215	Reger and Updike (1983a, locality C)

Table 2. (continued)

Sample <sup>a</sup> locality	Laboratory/field number	Material and stratigraphic context	Chronological significance	Radiocarbon age ( <sup>14</sup> C yr B.P.)	Source
C25	L-163D <sup>d</sup>	Organic silt underlying 9.1 m of Holocene eolian sand and silt and overlying loess capping till weathered to depths of 0.9 to 1.5 m	Minimum age for recession of Killey-age glacier from Point Possession area	9,200 ± 600	Broecker and others (1956, p. 156), Karlstrom (1964, pls. 4 and 6, locality D-2, table 3)
C26	GX-15294	Organic silt from depth of 3.8 m in estuarine deposits	Minimum age for recession of Elmendorf-age glacier from Goose Bay area	9,255 ± 420 <sup>b</sup>	Combellick (1990, 1991, borehole KA4B)
C27	Beta-59790 {91RE2,91-30, & 91-30R}	Coarsely fibrous woody sedge peat from base of 2.3-m-thick surface peat on 11-m terrace	Maximum age for surface peat and minimum age for underlying sand in 11-m terrace near mouth of Kenai River	9,260 ± 100 <sup>b</sup>	Combellick and Reger (1994, locality 91-30, 30R) (section 23)
C28	W-536	Peat from base of 1.5-m-thick bed overlying pond deposits on top of diamicton thought to overlie and interfinger with extensive deltaic deposits that interfinger with BCF	Minimum age for recession of Skitak-age glacier from Fire Island and retreat of estuarine waters in which BCF was deposited	9,300 ± 250	Müller and Dobrovolny (1959, p. 32), Rubin and Alexander (1960, p. 165), Karlstrom (1964, pl. 6, locality C-2, table 3)
C29	GX-10782	Peat from depth of 3.6 m in paludal deposits capping upper marine terrace between Kenai and Kasilof Rivers	Minimum age for marine deposits on upper terrace in Kasilof area	9,410 ± 225	Rawlinson (1986, core SK34)
C30	Beta-59789 {91RE2,91-30, & 91-30R}	Wood from middle of 10-cm-thick sand underlying 2.3-m-thick surface peat on 11-m terrace	Age of sand beneath surface peat on 11-m terrace near mouth of Kenai River	9,440 ± 90 <sup>b</sup>	Combellick and Reger (1994, locality 91-30, 30R) (section 23)
C31	Beta-59791 {91RE2, 91-30, & 91-30R}	Peat and organic silt from just beneath sharp lower contact 10-cm-thick sand on 11-m terrace	Maximum age of sand beneath surface peat on 11-m terrace near mouth of Kenai River	9,470 ± 90 <sup>b</sup>	Combellick and Reger (1994, locality 91-30, 30R) (section 23)
C32	L-137C <sup>d</sup>	Compressed and deformed peat beneath 4.6 m of Holocene eolian sand and silt and overlying organic silt (loess) capping Killey-age diamicton	Minimum age for recession of Killey-age glacier from Point Possession area	9,500 ± 650	Broecker and others (1956, p. 156), Karlstrom (1964, pls. 4 and 6, locality D-3, table 3)

Table 2. (continued)

Sample <sup>a</sup> locality	Laboratory/field number	Material and stratigraphic context	Chronological significance	Radiocarbon age ( <sup>14</sup> C yr B.P.)	Source
C33	L-137L <sup>d</sup>	Wood from base of 3-m-thick peat overlying 6 m of channel sand and gravel resting on pre-Naptowne till	Minimum age for alluvium in former channel near Ninitchik	9,600 ± 650	Broecker and others (1956, p. 156), Karlstrom (1964, pl. 4, locality I, table 3)
C34	GX-5209 [77RE18 C-2]	Woody fibrous sedge peat from lowest 3 cm of 36-cm-thick peat overlying 10-cm-thick organic silt above 5- to 10-cm-thick flowtill overlying 140-cm-thick channel gravel cut into till of Moosehorn age	Minimum age for channel postdating Moosehorn-age advance from northwest in Coho area	9,665 ± 230	This study (section 61)
C35	W-2936	Peat from base of paludal deposit overlying postglacial alluvium	Minimum age for recession of glacier from type Elmendorf moraine in lower Knik Arm	9,760 ± 350	Yehle and others (1990, locality 3)
C36	GX-10649 (RC84-15-1C)	Peat from depth of 1.8 m in organic sediments ponded behind outer end moraine	Minimum age for readvance of glaciers in Tincan and Lyons Creek valleys after recession of late Elmendorf-age glacier from upper Turnagain Arm	9,850 ± 390	Reger and others (1995, locality AC)
C37	W-336	Twigs and wood fragments from base of 2.1-2.4-m-thick organic kettle filling in terminal moraine of Elmendorf age	Minimum age for recession of Elmendorf-age glacier from terminal moraine in Willow Creek valley	9,870 ± 250	Rubin and Alexander (1958, p. 1483)
C38	W-2302	Compressed wood and peat from beneath diamicton and estuarine silt and clay and overlying bedded deltaic gravel	Minimum age for recession of Elmendorf-age glacier from Girdwood area and deposition of BCF in upper Turnagain Arm	10,180 ± 350	Bartsch-Winkler and Schmoll (1984)
C39	Beta-33348	Aquatic plant material from base of 2-m-thick lacustrine silt-clay rhythmite	Minimum age for recession of Elmendorf-age glacier from lower Kachemak Bay in Halibut Creek area	10,240 ± 70 <sup>h</sup>	Wiles (1992), Wiles and Calkin (1994)

Table 2. (continued)

Sample <sup>a</sup> locality	Laboratory/field number	Material and stratigraphic context	Chronological significance	Radiocarbon age ( <sup>14</sup> C yr B.P.)	Source
C40	Beta-47180 [91RE1 C-1]	Sphagnum peat from base of 2-m-thick postglacial peat overlying 6.8 m of clayey gravel till of Killey age	Minimum age for retreat of Killey-age glacier in Homer area	10,310 ± 70 <sup>b</sup>	This study (section 74)
C41	W-474	Organic silt from near base of bog deposit buried beneath eolian sand and overlying diamicton	Minimum age for recession of Killey-age glacier from Point Possession area	10,370 ± 350	Rubin and Alexander (1958, p. 1479), Karlstrom (1964, pls. 4 and 6, locality D-1, table 3)
C42	GX-15215	Organic silt from depth of 16.8 m in estuarine deposits	Minimum age for recession of Elmendorf-age glacier from Girdwood area	10,375 ± 310	Combellick (1990, 1991, borehole TA1)
C43	GX-18231 [91RE65 S-4]	Sphagnum peat from depth of 305-310 cm in peat boring; base of thawed kettle fill over permafrost	Minimum age for base of kettle fill in Moosehorn-age moraine in Kasilof area	10,380 ± 285 <sup>b</sup>	This study (section 56)
C44	Beta-49112 [KS1]	Base of 1.1-m-thick peat at depth of 7.4 m beneath 4.5 m of estuarine clayey silt and above at least 0.5 m of silt and fine sand with numerous pebbles	Minimum age for incision of lower valley of Kasilof River	10,450 ± 110 <sup>b</sup>	Combellick and Reger (1994, borehole KS1) (section 50)
C45	GX-6041 [78RE34-4]	Organic silt 0.1 to 0.2 m below top of 1-m-thick silty and sandy peat underlying 0.6-m-thick woody sphagnum peat and overlying 0.4-m-thick organic silt on top of sandy gravel at base of scarp cut into pitted outwash of Elmendorf age	Minimum age for outwash from Elmendorf-age moraine to east and cutting of scarp in the Red Shirt Lake area by estuarine waters in which BCF was deposited	10,720 ± 460	Reger and Updike (1983a, locality 1)
C46	GX-15224	Organic silt from depth of 15.4 m in estuarine deposits	Minimum age for recession of Elmendorf-age glacier from Portage area	10,730 ± 525	Combellick (1990, 1991, borehole TA8)
C47	GX-18234 [92RE21 S-1]	Organic silt from base of 7.7-m-thick peat with scattered wood overlying glacier-deformed diamicton of Killey age	Minimum age for recession of Killey-age glacier from Point Possession area	10,895 ± 120 <sup>b</sup>	Combellick and Reger (1994), this study (section 6)

Table 2. (continued)

Sample <sup>a</sup> locality	Laboratory/field number	Material and stratigraphic context	Chronological significance	Radiocarbon age ( <sup>14</sup> C yr B.P.)	Source
C48	Beta-47181 [91RE2 C-1]	Interbedded organic silt and inorganic fine sand and silt beneath 2.3 m of surface peat and 0.3 m of fluvial sand on 11-m terrace of lower Kenai River	Minimum age for 11-m terrace of lower Kenai River	11,280 ± 150 <sup>b</sup>	Combellick and Reger (1994, locality 91-30, 30R) (section 23)
C49	GX-15241	Organic silt from depth of 7.7 m in estuarine deposits	Minimum age for recession of Elmendorf-age glacier from upper Knik Arm	11,400 ± 720 <sup>c</sup>	Combellick (1990, 1991, borehole KA6)
C50	Beta-5581 [82RE40 C-1]	Peat from base of 1.8-m-thick bed overlying BCF	Minimum age for recession of Skilak-age glacier from Fire Island and emergence from estuarine waters in which BCF was deposited	11,450 ± 150	Reger and Updike (1983a, p. 202)
C51	GX-10785 [81RE106 C-4]	Organic fine silty sand from base of 0.3-m-thick paludal organic fine sand and silt underlying 4.5-m-thick surface peat and overlying channelled outwash gravel of Skilak age <sup>f</sup>	Minimum age for Skilak-age outwash in Little Willow Creek area	11,540 ± 450	This study (section 1)
C52	W-540	Peat from base of 2.4-m-thick bed overlying 3 m of sand that overlies 1.8 to 3 m of BCF	Minimum age for emergence from glacioestuarine waters in which BCF was deposited in Point Woronzof area	11,600 ± 300	Rubin and Alexander (1960, p. 165), Miller and Dobrovolny (1959, p. 68, pl. 9), Schmoll and others (1972, locality E)
C53	W-2375	Peat from beneath colluvium overlying till of type Elmendorf moraine	Minimum age for Elmendorf advance in lower Knik Arm	11,690 ± 300	Schmoll and others (1972, locality F), Spiker and others (1977, p. 346)
C54	GX-16521 [90RE102 C-1]	Compressed wood from depth of 70 cm in 94-cm-thick unit of interbedded thin peat, organic silt, pond clay, and tephra filling kettle in Killey-age terminal moraine	Minimum age for recession of Killey-age glacier from Point Possession area	11,905 ± 180 <sup>b</sup>	This study (section 7)

Table 2. (continued)

Sample <sup>a</sup> locality	Laboratory/field number	Material and stratigraphic context	Chronological significance	Radiocarbon age ( <sup>14</sup> C yr B.P.)	Source
C55	W-360	Basal organic pond silt in depression on Skilak-age moraine	Minimum age for recession of Skilak-age glacier in Deception Creek area <sup>g</sup>	11,930 ± 250	Rubin and Alexander (1958, p. 1483), Karlstrom (1964, pl. 1, locality T, table 3)
C56	Beta-11174	Basal peaty silt in pond sediments and peat filling depression on late Naptowne moraine	Minimum age for recession of Matanuska Glacier	12,210 ± 120	Williams (1986)
C57	Beta-5580 [82RE20 C-1]	Organic silt from beneath 1.8-m-thick peat overlying 3-m-thick fan-delta sand above BCF	Minimum age for recession of Skilak-age glacier from Point MacKenzie and retreat of estuarine waters in which BCF was deposited	12,250 ± 140	Reger and Updike (1983a, p. 202), this study (section 78)
C58	W-2589	Basal organic swamp deposit overlying till of type Elmendorf moraine	Minimum age for recession of glacier from type Elmendorf moraine in lower Knik Arm	12,350 ± 350	Yehle and others (1990, 1991, locality 4)
C59	W-5518	Pebbly organic silt from depth of 4.38 to 4.57 m in Circle Lake core	Minimum age for recession of Moosehorn-age glacier from upper Kachemak Bay	12,800 ± 300	Ager and Shaw (1986), Ager (written commun., 1992)
C60	GX-16522 [90RE102 C-2]	Organic clayey silt from depth of 80 cm in 94-cm-thick unit of interbedded thin peat, organic silt, pond clay, and tephra filling kettle in Killey-age terminal moraine	Minimum age for recession of Killey-age glacier from Point Possession area	12,860 ± 195 <sup>b</sup>	This study (section 7)
C61	W-416	Peat from base of 0.9- to 1.5-m-thick section of lacustrine organic clay, silt, and sand overlying deformed glaciofluvial gravel and sand graded to Killey-age ice limit at East Foreland	Minimum age for deposition of Killey-age outwash and melting of underlying stagnant glacial ice of Killey age in Nikiski area <sup>h</sup>	12,900 ± 300	Rubin and Alexander (1958, p. 1479), Karlstrom (1964, pls. 4 and 6, locality F-2, table 3)
C62	USGS-2175	Basal peaty silt in pond sediments and peat filling depression on late Naptowne moraine	Minimum age for recession of Matanuska Glacier	13,100 ± 60	Williams (1986)
C63	AA-2227 <sup>c</sup> [82RE14]	<i>Mya truncata</i> shells from silty-clay facies of BCF 1 m above contact with ice-stagnation deposits of Skilak stage	Dates BCF at mouth of Knik Arm	13,470 ± 120	Reger and others (1995, locality N), this study (section 77)

Table 2. (continued)

Sample <sup>a</sup> locality	Laboratory/field number	Material and stratigraphic context	Chronological significance	Radiocarbon age ( <sup>14</sup> C yr B.P.)	Source
C64	W-748	Silty peat with twigs from base of organic lake sediments overlying deformed outwash gravel graded to Killey-age ice limit at East Foreland	Minimum age for deposition of Killey-age outwash and melting of underlying stagnant glacial ice of Killey age in Nikiski area <sup>b</sup>	13,500 ± 400	Rubin and Alexander (1958, p. 1479), Karlstrom (1964, pls. 4 and 6, locality G-1, table 3)
C65	W-2151	Mollusk shells from macrofossil-rich zone of BCF	Dates middle or upper sublittoral glacioestuarine environment in which BCF was deposited in Point Woronzof area	13,690 ± 400	Sullivan and others (1970, p. 333), Schmoll and others (1972, locality A)
C66	GX-20129 <sup>c</sup> [82Re36]	<i>Macoma balthica</i> shells from 3-m-thick dropstone-rich, thin-bedded sand in upper BCF overlain by 3 m of colluvium	Dates upper BCF west of Hope just beyond Elmendorf maximum in Turnagain Arm	13,718 ± 160 <sup>b</sup>	Reger and others (1995, locality U), this study (section 75)
C67	W-4827	Organic mud from depth of 250–260 cm beneath bottom of Hidden Lake	Minimum age for retreat of Skilak-age glacier from Hidden Lake basin	13,730 ± 110	Rymer and Sims (1982, core HL-4-M), Sims (written commun., 1992)
C68	W-2389 [82Re11]	Mollusk shells from macrofossil-rich zone of BCF	Dates middle or upper sublittoral glacioestuarine environment in which BCF was deposited in lower Knik Arm	13,750 ± 500	Schmoll and others (1972, locality D), Spiker and others (1977, p. 346)
C69	W-2919	Mollusk shells of BCF incorporated into till of Elmendorf-age advance <sup>1</sup>	Dates BCF and maximum age for Elmendorf-age advance in upper Turnagain Arm	13,900 ± 400	Schmoll and Yehle (1983, locality A; 1986, locality B4), Bartsch-Winkler and Schmoll (1984)
C70	GX-20127 <sup>c</sup> [82Re17]	<i>Mya truncata</i> shells from interbedded medium sand and silt layers up to 20 cm thick 6 m below top of BCF	Dates upper BCF west of Point MacKenzie	13,994 ± 90 <sup>b</sup>	Reger and others (1995, locality P), this study (section 76)
C71	GX-20128 [82Re20]	<i>Mya truncata</i> shells from dropstone-rich diamicton 3 m below top of BCF	Dates BCF west of Point MacKenzie	14,078 ± 214	Reger and others (1995, locality M), this study (section 78)

Table 2. (continued)

Sample <sup>a</sup> locality	Laboratory/field number	Material and stratigraphic context	Chronological significance	Radiocarbon age ( <sup>14</sup> C yr B.P.)	Source
C72	GX-19989 <sup>c</sup> {82Re12}	<i>Balanus</i> plates from 1- to 2-cm-thick sand layers interbedded with clayey silt in upper BCF overlain by up to 5 m of fan-delta sand	Dates upper BCF at Point MacKenzie	14,100 ± 90 <sup>b</sup>	Reger and others (1995, locality K), this study (section 5)
C73	GX-16529 <sup>c</sup> {82RE6}	<i>Hiatella arctica</i> and <i>Macoma balthica</i> shells from colluvium derived from BCF <sup>d</sup>	Dates BCF and nearby Elmendorf-equivalent advance in Hope area	14,160 ± 140 <sup>b</sup>	Reger and others (1995, locality V)
C74	GX-17133 <sup>c</sup> {82RE5}	<i>Hiatella arctica</i> shells from colluvium derived from BCF	Dates BCF and nearby Elmendorf-equivalent advance in Hope area	14,200 ± 100 <sup>b</sup>	Reger and others (1995, locality W)
C75	GX-16524 <sup>c</sup> {82RE4}	<i>Macoma balthica</i> shells from BCF incorporated into till of Elmendorf-age advance <sup>d</sup>	Dates BCF and maximum age for Elmendorf-age advance in upper Turnagain Arm	14,290 ± 140 <sup>b</sup>	Reger and others (1995, locality X), Schmoll and Yehle (1986, locality B4)
C76	AA-2226 <sup>c</sup> {77RE22F}	<i>Hiatella arctica</i> shells from 6 m below top of BCF and 0.3 m above Skitak-age diamicton	Dates BCF in lower Knik Arm and minimum age for recession of Skitak-age glacier from lower Knik Arm	14,300 ± 140	Reger and others (1995, locality J), this study (section 4)
C77	W-2367	Mollusk shells from macrofossil-rich zone of BCF	Dates middle or upper sublittoral glacioestuarine environment in which BCF was deposited in Point MacKenzie area	14,300 ± 350	Schmoll and others (1972, locality C), Spiker and others (1977, p. 346)
C78	W-4292	Shells in glacioestuarine silt and clay of BCF	Dates BCF in lower Beluga River area	14,350 ± 200	Schmoll and Yehle (1983, locality B; 1986, locality B5), Schmoll and others (1984, locality B5)
C79	W-2369	Mollusk shells from macrofossil-rich zone of BCF	Dates middle or upper sublittoral glacioestuarine environment in which BCF was deposited in Point Woronzof area	14,900 ± 350	Schmoll and others (1972, locality B), Spiker and others (1977, p. 346)

Table 2. (continued)

Sample <sup>a</sup> locality	Laboratory/field number	Material and stratigraphic context	Chronological significance	Radiocarbon age ( <sup>14</sup> C yr B.P.)	Source
C80	GX-16528 <sup>c</sup> [90RE72 C-2]	Calcareous <i>Balanus</i> plates from 0.6 m below top of platy, dense, pebbly dropstone diamicton of BCF	Dates BCF in upper marine terrace along Kalifornsky beach	16,000 ± 150 <sup>b</sup>	This study (section 45)
C81	GX-16527 <sup>c</sup> [90RE72 C-1]	Calcareous <i>Balanus</i> plates from 0.5 m above base of 3-m-thick, massive dropstone diamicton of BCF	Dates BCF in upper marine terrace along Kalifornsky beach	16,090 ± 160 <sup>b</sup>	This study (section 45)
C82	W-4937	Calcareous <i>Balanus</i> plates in glaciomarine silt and clay assigned to BCF	Dates BCF in upper marine terrace along Kalifornsky beach	16,340 ± 140	Schmoll and Yehle (1983; 1986, locality B7), Schmoll and others (1984, locality B7)
C83	WSU-4304 [91RE39 F-1]	Calcareous <i>Balanus</i> plates from 1 m below top of deformed glaciomarine fine sand and silt assigned to BCF	Dates BCF and close maximum age for fluctuating tidewater glacier in vicinity of Kenai	16,480 ± 170 <sup>b</sup>	This study (section 20)
C84	GX-18233 [92RE18 S-1]	Organic silt at base of 10-cm-thick sand layer in upper fan-delta gravel of Killey age in Kasilof area	Probably contaminated by finely divided clastic Tertiary coal	26,240 ± 2,100 <sup>b</sup>	This study (section 59)
C85	L-163A <sup>d</sup>	Residual after removal of humic acid from iron-oxide-stained lignitized log in silt, sand, and gravel of Killey-age outwash graded to ice limit at East Forceland	Probably reworked material without significance for dating enclosing sediments in Nikiski area <sup>1</sup>	39,000 ± 2,600 <sup>k</sup> (39,000 ± 2,000 for humic-acid fraction)	Olson and Broecker (1959, p. 5-6), Karlstrom (1964, pls. 4 and 6, locality 5, table 3)
C86	L-137D <sup>d</sup>	Lignitized log from base of 15-m-thick iron-oxide-stained and flexured gravel overlying glaciolacustrine or glacioestuarine deposits	Probably reworked material without significance for dating enclosing sediments in Kenai area	>24,000	Broecker and others (1956, p. 156), Karlstrom (1964, pls. 4 and 6, locality 7, table 3)
C87	L-117M <sup>d</sup>	Log from basal outwash of Killey age	Probably reworked material without significance for dating enclosing sediments in Boulder Point area	>25,000	Broecker and others (1956, p. 156), Karlstrom (1964, pls. 4 and 6, locality 3, table 3)
C88	W-76	Partly lignitized wood from outwash sand	Probably reworked material without significance for dating enclosing sediments in Tustumena Lake area	>32,000 <sup>1</sup>	Suess (1954, p. 471), Karlstrom (1964, pl. 4, locality 8, table 3)

Table 2. (continued)

Sample <sup>a</sup> locality	Laboratory/field number	Material and stratigraphic context	Chronological significance	Radiocarbon age ( <sup>14</sup> C yr B.P.)	Source
C89	W-77	Wood from Goose Bay peat beneath till of type Elmendorf moraine	Maximum age for Elmendorf stage and minimum age for former interglaciation in Goose Bay area	>32,000 <sup>m</sup>	Suess (1954, p. 471), Karlstrom (1964, pls. 1 and 6, locality 1, table 3) (section 3)
C90	GX-5208 [77RE18 C-1]	Abraded, lignitized wood in friable fan-delta sand beneath drift of Moosehorn-age advance	Probably reworked material without significance for dating enclosing sediments in Coho area	>37,000	This study (section 61)
C91	W-2913	Organic clayey pond silt with occasional freshwater gastropods overlain by drift of Elmendorf advance and underlain by drift of pre-Naptowne age	Maximum age for type Elmendorf advance and minimum age for former interglaciation in Eagle River area	>37,000	Yehle and Schmoll (1989, locality 2)
C92	W-294	Woody material near base of 0.6- to 0.9-m-thick contorted organic silt overlain by 3.9 m of uncontorted lacustrine organic silt and peat and underlain by 0.3- to 0.6-m-thick contorted sand and silt resting on contorted gravel	Possibly reworked material without significance for dating enclosing sediments in Kenai area <sup>n</sup>	>37,000	Rubin and Suess (1956, p. 444), Karlstrom (1964, pls. 4 and 6, locality 6, table 3)
C93	W-174	Wood from upper 15 cm of Goose Bay peat at type locality	Maximum age for type Elmendorf advance and minimum age for former interglaciation in Goose Bay area	>38,000	Rubin and Suess (1956, p. 486), Karlstrom (1964, pls. 1 and 6, locality 1, table 3) (section 3)
C94	W-1806	Woody fragments in silt overlain by gravel presumably of Elmendorf age	Maximum age for overlying Elmendorf outwash and minimum age for former interglaciation in Eagle River area	>38,000	Marsters and others (1969, p. 221), Yehle and Schmoll (1989, locality 3)
C95	W-535	Very thin peat beneath Elmendorf-age till and outwash	Maximum age for Elmendorf advance and minimum age for former interglaciation in Eagle River area	>38,000 <sup>n</sup>	Rubin and Alexander (1960, p. 164-165), Miller and Dobrovoly (1959, p. 16, pl. 9)

Table 2. (continued)

Sample <sup>a</sup> locality	Laboratory/field number	Material and stratigraphic context	Chronological significance	Radiocarbon age ( <sup>14</sup> C yr B.P.)	Source
C96	W-644	Wood from base of advance outwash of type Elmendorf advance overlying compressed Goose Bay peat that overlies pre-Naptowne glacial deposits	Probably reworked material without significance for dating enclosing sediments in Goose Bay area	>40,000	Rubin and Alexander (1960, p. 169), Karlstrom (1964, pls. 1 and 6, locality 1, table 3) (section 3)
C97	W-2366	Organic fragments in 5-cm-thick brown sand beneath BCF	Maximum age for BCF in Point MacKenzie area	>40,000	Spiker and others (1977, p. 346)
C98	I-11,949 [78RE24 C-1]	Wood from upper 10 cm of 0.9- to 1.8-m-thick highly compressed Goose Bay peat that overlies 3 m of outwash gravel of pre-Naptowne glaciation and underlies 4.6 to 8.5 m of advance outwash sand that in turn underlies 6.1 to 7.6 m of till of type Elmendorf moraine	Maximum age for type Elmendorf advance and minimum age for former interglaciation in Goose Bay area	>40,000	Reger and Updike (1983a, locality R), this study (section 3)
C99	I-11,950 [78RE24 C-2]	Compressed peat from middle of 0.9- to 1.8-m-thick bed overlying 3 m of outwash gravel of pre-Naptowne glaciation and underlying 4.6 to 8.5 m of advance outwash sand and gravel that in turn underlie 6.1 to 7.6 m of till of type Elmendorf moraine	Maximum age for type Elmendorf advance and minimum age for former interglaciation in Goose Bay area	>40,000	Reger and Updike (1983a, locality R), this study (section 3)
C100	I-12,029	Wood fragments from peaty zone at base of upper glacioestuarine diamicton of Skilak-age advance	Maximum age for Skilak age advance in Potter area	>40,000 <sup>g</sup>	Schmoll and Yehle (1983, p. 77), Bartsch-Winkler and Schmoll (1984, p. 8)
C101	L-117L <sup>d</sup>	Abraded, lignitized log from lowest 0.3 m of Holocene lacustrine organic silt unconformably overlying stratified sand and gravel graded to Killey-age ice limit at East Foreland	Probably reworked material without significance for dating enclosing sediments in Nikiski area	>44,000 <sup>f</sup>	Olson and Broecker (1959, p. 5), Karlstrom (1964, pls. 4 and 6, locality 4, table 3)
C102	W-2154	Peat overlain by 2.7 m of fluvial gravel of Elmendorf advance and underlain by 0.6 m of gray silty clay till(?) of pre-Naptowne glaciation	Maximum age for type Elmendorf advance and minimum age for former interglaciation in Chugiak area	>45,000	Sullivan and others (1970, p. 328), Yehle and Schmoll (1989, locality 1)

Table 2. (continued)

Sample <sup>a</sup> locality	Laboratory/field number	Material and stratigraphic context	Chronological significance	Radiocarbon age ( <sup>14</sup> C yr B.P.)	Source
C103	W-2911	Piece of wood from gravel beneath 5 m of BCF overlain by 30 m of advance outwash gravel and till of type Elmendorf moraine	Probably reworked material without significance for dating enclosing sediments in Eagle Bay area	>45,000	Yehle and others (1990, locality 2)
C104	QL-1736 {88RE 54 S-2}	16-cm-thick organic silt from middle of 1-m-thick Goose Bay peat overlain by 6 m of advance outwash gravel and 6 m of till of type Elmendorf moraine	Minimum age for Goose Bay peat and maximum age for type Elmendorf advance in Goose Bay area	>73,400 <sup>b</sup>	This study (section 3)

<sup>a</sup>To locate sample sites and nearby geographic features, see table 1 and sheets 1-5.

<sup>b</sup>Sample corrected for natural isotopic fractionation based on <sup>13</sup>C content.

<sup>c</sup>Atomic mass spectrometer (AMS) date.

<sup>d</sup>Karlstrom (1964, p. 59) accepted as generally valid all solid-carbon dates from Lamont Observatory younger than 14,000 yr B.P. because they are consistent with results obtained by the gas-proportional technique during reruns of the same samples. Reruns of samples initially dated between 14,000 and 22,000 yr B.P. by the black-carbon method produced infinite dates by the gas-counting method (Olson and Broecker, 1959, p. 5).

<sup>e</sup>Because disseminated organic material, which could include very fine grained detrital coal, was dated, this age could be spuriously old (Reger and others, 1995, locality C).

<sup>f</sup>Dated sample from near bottom of section G-G' at station 21 (Cameron and others, 1981, sheet 1).

<sup>g</sup>These moraines were attributed to the Eklutna glaciation by Karlstrom (1964, pl. 1) and to the Knik glaciation by Reger and Updike (1983a, pl. 1).

<sup>h</sup>Karlstrom (1964, p. 24) interpreted deformation in this and other sections in the East Foreland-Lower Salmatof Lake area to be the result of glaciotectionic stresses generated during repeated eastward advances by the Trading Bay lobe. We interpret the deformation there to be the result of both glaciotectionic stresses generated by grounding of partially floating tidewater glaciers and the melting of stagnant glacial ice on which outwash alluvium was deposited.

<sup>i</sup>Schmoll and Yehle (1986, p. 205) interpreted sediments enclosing 13,900-yr-old mollusk shells in the roadcut near Mile 99 of Seward Highway to be colluvial bedrock rubble incorporating reworked sediments of the Bootlegger Cove Formation and, based on an extrapolated age of 14,000 yr for basal sediments in a 93-m core at Portage (Bartsch-Winkler and others, 1983), concluded that Turnagain Arm was ice free about 14,000 yr ago. We interpret the exposure to be BCF deposits overridden by a rapid westward advance of the Elmendorf-age glacier into estuarine waters of upper Turnagain Arm. We believe that crushed shells in the exposure, were preserved in till in a leeward pressure shadow provided by the bedrock outcrop along the east side of the exposure, perhaps because the overriding glacier was at least partially floating.

<sup>j</sup>Karlstrom (1964, p. 24, table 3) interpreted sample W-163A, a transported log, as dating an early Naptowne (Pro-Naptowne) advance from the west side of Cook Inlet.

<sup>k</sup>Gas-counting rerun of sample 163A, which was initially dated at 22,000 ± 2,000 yr B.P. by the black-carbon method (Olson and Broecker, 1959, p. 6). More recently, this sample was redated older than the maximum limit of radiocarbon dating (Meyer Rubin, in Schmoll and others, 1984, p. 27).

<sup>l</sup>Acetylene rerun of sample L-117J, which was previously dated by the solid-carbon technique at 15,800 ± 400 yr B.P. (Kulp and others, 1951, p. 568).

<sup>m</sup>Acetylene rerun of sample L-117A, which was previously dated by the solid-carbon method at 19,000 ± 900 yr B.P. (Kulp and others, 1952, p. 412-413).

<sup>n</sup>Karlstrom (in Rubin and Suess, 1956, p. 444) attributed the "highly weathered and contorted" gravel at the base of this section to the Eklutna glaciation and deformation of the overlying contorted silt to the maximum advance of the Knik or Naptowne glaciation, probably the latter.

<sup>o</sup>Reanalysis of sample L-101B, which was initially dated by the solid-carbon method at 14,300 ± 600 yr B.P. (Kulp and others, 1951, p. 568).

<sup>p</sup>Originally dated at 34,000 ± 2,000 yr B.P. (W-1804) by the solid-carbon method (Marsters and others, 1969, p. 220).

<sup>q</sup>Originally dated at 19,200 ± 1,000 yr B.P. (L-117L) by the solid-carbon method (Kulp and others, 1952, p. 412).

<sup>r</sup>Sample enriched 9.41 times by Minze Stuiver at University of Washington Quaternary Isotope Laboratory.

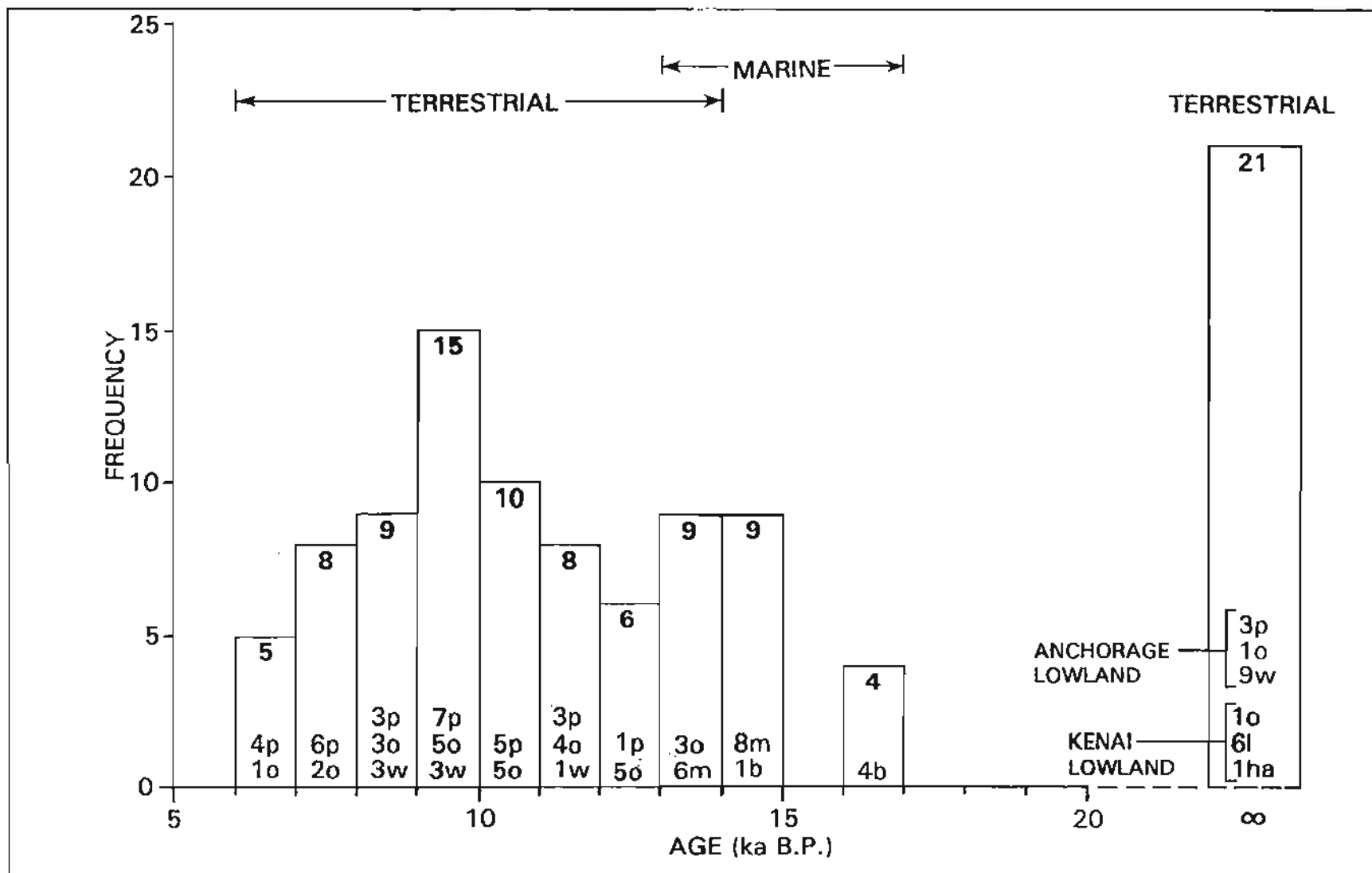


Figure 1. Distribution of 104 radiocarbon dates older than 6,000 <sup>14</sup>C yr B.P. in the Cook Inlet region. Symbols indicate materials analyzed: b = Balanus plate, ha = humic-acid extract, l = lignite or lignitized wood, m = mollusk shell, o = organic silt or sand, p = peat, w = wood or wood fragments.

The major-oxide geochemistry of the purified glass shards was analyzed with the Kevex Series 82 Electron Microprobe in the Department of Geology, Washington State University, using an 8- $\mu$ m-wide electron beam operated at 15 kV and 11.5 nA. This instrument was calibrated at least once daily, using standards CCNM-11 (obsidian), K-411 (National Bureau of Standards glass), and CV-A99 (basaltic glass) to ensure precise and accurate results. Individual glass shards were exposed to the electron beam for 10 seconds, and the resulting data were normalized to 100 percent (table 3). Glass concentrates and grain mounts are archived in the Alaska Tephrochronology Center (ATC) at the University of Alaska (Fairbanks).

### GEOCHEMICAL RESULTS

Among the 88 tephra samples analyzed, single tephtras are represented by 63 samples (71.6 percent) and mixed tephtras, which possibly include shards of up to four distinct chemical populations, are represented by 12 samples (13.6 percent). Although 13 samples (14.8 percent) were collected from volcanic-ash layers that appear to be composed of one tephtra in the field, their shard geochemistry is so variable that we could not isolate a meaningful population, and the results are not reported, except to show their stratigraphic positions (app. A). These samples are indicated by an asterisk after the sample number in table 1 and appendix A. In this study we recognize 16 chemically distinct tephtras (table 3).

### CORRELATION, DISTRIBUTION, AND AGE

Mean major-oxide compositions of shards in tephtra samples from Kenai Lowland and vicinity (table 3) were compared to microprobe geochemistry of tephtras from Hayes volcano (Riehle, 1985; Begét, Reger, and others, 1991; Campbell, unpub. data), Mt. Spurr (Riehle, 1985), Mt. Redoubt (Riehle, 1985), Mt. Iliamna (Riehle, 1985), Mt. Augustine (Riehle, 1985; Begét, unpub. data), cores from Skilak Lake (Stihler, 1991; Begét and others, 1994), Aniakchak caldera (Riehle and others, 1987), Kaguyak caldera (Swanson, unpub. data), the 1912 eruption of Mt. Katmai (Avery, unpub. data), the upper drainage of Susitna River (Dilley, 1988, unpub. data; ATC, unpub. data), and interior Alaska (Westgate and others, 1983, 1990; Westgate, 1988; Begét and Keskinen, 1991; Begét, Reger, and others, 1991).

In this study, correlations of tephtras at different field localities are primarily based on geochemical similarities as determined by electron microprobe and most are considered tentative. The exceptions are (a) the Lethe tephtra, which has a distinctive shard morphology and geochemistry and a consistent mineralogy, and (b) the Stampede tephtra, for which we developed mineralogical data and

stratigraphic information. A similarity coefficient (SC) (Borchardt and others, 1972) of 0.96 or greater indicates that a tephtra pair is either part of the same tephtrafall or that they are members of a tephtra set with a high degree of similarity (Riehle, 1985). Values of 0.94 or 0.95 indicate that the pair of tephtras was deposited during the same tephtrafall—in which concentrations of one or more elements are variable—or that they are members of the same tephtra set (where supported by stratigraphic or mineralogic evidence). Values of 0.90 to 0.93 indicate that the samples are members of the same tephtra set but not the same tephtrafall.

### LATE QUATERNARY TEPHTRAS

#### LETHE TEPHTRA

(MEAN  $\text{SiO}_2 = 72.78 \pm 0.27$  PERCENT)

The most widespread tephtra we document in Kenai Lowland is the Lethe tephtra. This light yellowish-brown to orange volcanic-ash layer is identified at 29 localities in a narrow band from just south of Anchor River northeastward to just north of Swanson River (table 3, fig. 2). Correlation within this set of samples is good to excellent ( $SC = 0.93\text{--}0.99$ ) (table 4), and they undoubtedly almost all represent the same tephtrafall. The geochemistry of Lethe shards is very consistent as indicated by the small standard deviations in all eight major-oxide contents (table 3). The single exception could be sample KL-050p1, which has lower similarity coefficients than the other 30 samples.

The distinctive yellowish-brown to orange color is due to variable thicknesses of iron oxides that formed on shard surfaces during weathering of this relatively iron-rich dacitic tephtra. Unweathered glass is light gray in transmitted light. Lethe shards are robust compared to other tephtras in the area, tend to be platy or blocky, and contain few to numerous vesicles that are commonly stretched. Triple junctions and bubble walls are commonly preserved. Petrographic studies by Pinney (1993) demonstrate that populations of iron-magnesian minerals are dominated by orthopyroxene and clinopyroxene in the Lethe tephtra. The former is generally three to four times more plentiful than the latter. Amphibole (green) content is low—generally 0 to 5 percent.

In samples from five sections, shards of Lethe tephtra are mixed with shards of other tephtras (table 3). This mixing could result from simultaneous or near-simultaneous initial deposition of these tephtras or from reworking of previously deposited tephtras. Lethe tephtra is clearly reworked in sections 13 and 66. In section 13 (fig. A13), a population of reworked Lethe shards (KL-018p1) is mixed with shards of Funny River tephtra (KL-018p2) in a layer that is stratigraphically above a layer of unmixed Lethe tephtra (KL-017). In section 66 (fig. A71), a population of redeposited Lethe shards (KL-086p3) (*Text cont'd. p. 36*)

**Table 3.** Average glass compositions of middle and late Quaternary tephra samples collected at 58 localities in Kenai Lowland and vicinity. Major oxides in glass separates given in normalized weight percent. One standard deviation in weight percent given below each oxide concentration. Discrete shard populations within multimodal samples indicated by letter "p" followed by population number. Number of analyses per sample = n. Sample localities shown in table 1 and sheets 1-3. Stratigraphic sections provided in appendix A

Sample	n	SiO <sub>2</sub>	Al <sub>2</sub> O <sub>3</sub>	NaO	CaO	FeO**	K <sub>2</sub> O	MgO	TiO <sub>2</sub>	Total	Section
Lethe tephra											
KL-011	9	73.23 0.45	13.59 0.16	4.25 0.11	2.45 0.15	2.83 0.22	2.43 0.08	0.63 0.07	0.59 0.04	100.00	46
KL-017	9	72.47 0.24	13.86 0.10	4.35 0.11	2.61 0.09	2.98 0.08	2.40 0.08	0.71 0.03	0.62 0.05	100.00	13
KL-018p1	7	72.69 0.36	13.75 0.12	4.27 0.15	2.61 0.13	3.02 0.12	2.35 0.05	0.71 0.05	0.62 0.03	100.02	13
KL-022	14	72.72 0.32	13.72 0.12	4.36 0.12	2.56 0.13	2.96 0.18	2.33 0.08	0.71 0.07	0.64 0.04	100.00	63
KL-029	11	72.55 0.47	13.91 0.17	4.24 0.13	2.54 0.14	3.05 0.15	2.39 0.08	0.69 0.07	0.63 0.04	100.00	22
KL-033	14	72.66 0.39	13.75 0.12	4.39 0.12	2.55 0.12	2.93 0.19	2.40 0.08	0.69 0.06	0.62 0.07	99.99	28
KL-034	8	73.32 0.49	13.56 0.21	4.35 0.07	2.37 0.18	2.76 0.15	2.40 0.02	0.63 0.05	0.62 0.04	100.01	64
KL-050p1	5	72.88 0.29	13.46 0.10	4.01 0.09	2.61 0.03	3.05 0.11	2.61 0.08	0.70 0.04	0.68 0.06	100.00	26
KL-052	10	72.76 0.36	13.77 0.12	4.30 0.14	2.58 0.12	2.89 0.08	2.38 0.07	0.68 0.04	0.63 0.03	99.99	38
KL-063	11	72.94 0.37	13.65 0.11	4.41 0.12	2.47 0.12	2.82 0.11	2.42 0.06	0.67 0.06	0.62 0.05	100.00	27
KL-068	8	73.06 0.47	13.80 0.15	4.22 0.11	2.43 0.17	2.89 0.21	2.42 0.09	0.64 0.05	0.53 0.15	99.99	36
KL-072	13	72.75 0.45	13.90 0.20	4.25 0.11	2.51 0.14	2.91 0.15	2.46 0.06	0.67 0.05	0.56 0.17	100.01	34
KL-085	10	72.77 0.33	13.87 0.13	4.35 0.09	2.46 0.12	2.89 0.15	2.36 0.06	0.70 0.07	0.59 0.05	99.99	66
KL-086p3	9	72.45 0.28	13.77 0.09	4.37 0.13	2.61 0.12	3.05 0.17	2.40 0.07	0.71 0.03	0.64 0.03	100.00	66
KL-087	14	72.73 0.47	13.70 0.20	4.32 0.35	2.52 0.20	3.00 0.20	2.42 0.10	0.69 0.08	0.63 0.07	100.01	71

Table 3. (continued)

Sample	n	SiO <sub>2</sub>	Al <sub>2</sub> O <sub>3</sub>	NaO	CaO	FeO*	K <sub>2</sub> O	MgO	TiO <sub>2</sub>	Total	Section
Lethe tephra (continued)											
KL-088	12	72.87 0.42	13.76 0.16	4.24 0.10	2.53 0.13	2.91 0.17	2.40 0.07	0.67 0.04	0.61 0.04	99.99	37
KL-095p1	4	73.50 0.36	13.35 0.19	4.13 0.13	2.28 0.01	2.83 0.12	2.60 0.05	0.68 0.05	0.62 0.04	99.99	52
KL-096	15	72.45 0.41	13.82 0.17	4.46 0.08	2.58 0.16	2.96 0.20	2.38 0.06	0.71 0.05	0.63 0.04	99.99	14
KL-099	10	72.35 0.24	13.97 0.09	4.28 0.11	2.73 0.09	2.94 0.17	2.38 0.05	0.71 0.03	0.63 0.04	99.99	9
KL-100	12	72.74 0.44	13.87 0.10	4.27 0.13	2.58 0.16	2.88 0.19	2.34 0.03	0.68 0.07	0.64 0.03	100.00	12
KL-102p3	7	73.01 0.47	13.64 0.16	4.41 0.09	2.44 0.12	2.83 0.24	2.37 0.10	0.67 0.07	0.62 0.05	99.99	41
KL-105	9	72.47 0.30	13.89 0.19	4.30 0.08	2.65 0.12	3.00 0.12	2.36 0.06	0.68 0.06	0.64 0.06	99.99	42
KL-106	10	72.51 0.30	13.95 0.11	4.28 0.13	2.63 0.10	2.94 0.09	2.34 0.06	0.71 0.04	0.64 0.06	100.00	15
KL-109	10	72.38 0.28	13.91 0.07	4.32 0.09	2.65 0.09	3.02 0.14	2.34 0.05	0.74 0.04	0.64 0.07	100.00	48
KL-110	17	72.77 0.47	13.77 0.16	4.46 0.12	2.49 0.16	2.86 0.17	2.35 0.06	0.68 0.06	0.63 0.05	100.01	21
KL-124	15	72.72 0.44	13.71 0.14	4.48 0.10	2.53 0.19	2.95 0.18	2.33 0.06	0.67 0.05	0.62 0.04	100.01	17
KL-125	15	72.72 0.49	13.74 0.16	4.45 0.13	2.52 0.13	2.90 0.15	2.39 0.07	0.69 0.08	0.60 0.06	100.01	19
KL-127	16	72.86 0.48	13.70 0.20	4.47 0.12	2.47 0.16	2.86 0.21	2.38 0.08	0.66 0.07	0.61 0.05	100.01	54
KL-128	15	72.61 0.44	13.85 0.14	4.41 0.20	2.57 0.17	2.90 0.12	2.33 0.07	0.70 0.07	0.64 0.04	100.01	55
KL-136	32	72.96 0.45	13.72 0.15	4.27 0.11	2.46 0.18	2.91 0.17	2.40 0.08	0.68 0.06	0.61 0.07	100.01	69
KL-137	32	73.13 0.49	13.65 0.18	4.28 0.15	2.42 0.09	2.84 0.14	2.40 0.19	0.65 0.08	0.61 0.08	99.98	70
Mean	31	72.78 0.27	13.75 0.14	4.32 0.10	2.52 0.09	2.92 0.08	2.39 0.06	0.68 0.02	0.62 0.03	99.98	---
Crooked Creek tephra											
KL-023	9	77.83 0.38	13.10 0.26	3.92 0.16	1.90 0.11	1.16 0.14	1.61 0.10	0.32 0.06	0.16 0.02	100.00	63

Table 3. (continued)

Sample	n	SiO <sub>2</sub>	Al <sub>2</sub> O <sub>3</sub>	NaO	CaO	FeO**	K <sub>2</sub> O	MgO	TiO <sub>2</sub>	Total	Section
Crooked Creek tephra (continued)											
KL-032p1	11	77.91 0.22	13.04 0.23	3.94 0.08	1.84 0.16	1.10 0.01	1.65 0.12	0.34 0.02	0.17 0.03	99.99	22
KL-056	9	77.97 0.29	12.95 0.11	3.96 0.17	1.85 0.10	1.10 0.10	1.68 0.10	0.33 0.04	0.16 0.03	100.00	44
KL-057	7	77.80 0.16	13.05 0.14	3.94 0.12	1.91 0.14	1.14 0.09	1.62 0.07	0.36 0.06	0.18 0.03	100.00	29
KL-061	8	77.86	13.00 0.17	3.95 0.12	1.88 0.10	1.14 0.10	1.65 0.05	0.34 0.09	0.17 0.04	99.99 0.03	35
KL-065	9	77.91	12.86 0.22	4.01 0.10	1.96 0.12	1.17 0.13	1.53 0.16	0.36 0.08	0.19 0.04	99.99 0.03	43
KL-066	8	77.80	13.05 0.16	3.96 0.05	1.89 0.09	1.11 0.06	1.68 0.10	0.35 0.06	0.16 0.03	100.00 0.02	24
KL-086p1	10	77.72	12.99 0.31	4.07 0.20	1.94 0.13	1.10 0.12	1.68 0.04	0.34 0.08	0.16 0.02	100.00 0.03	66
KL-113	15	77.71	13.02 0.32	4.04 0.24	1.97 0.33	1.14 0.13	1.63 0.14	0.34 0.06	0.16 0.05	100.01 0.03	25
KL-115	15	77.89	12.92 0.42	4.15 0.27	1.84 0.18	1.06 0.13	1.69 0.19	0.29 0.08	0.17 0.07	100.01 0.03	56
KL-130p1	15	77.64	13.09 0.39	4.14 0.31	1.92 0.14	1.08 0.10	1.64 0.14	0.33 0.08	0.17 0.08	100.01 0.08	51
Mean	11	77.82	13.00 0.10	4.01 0.07	1.90 0.08	1.12 0.04	1.64 0.03	0.34 0.04	0.17 0.02	100.00 0.06	---
Funny River tephra											
KL-012	5	62.10	16.01 0.45	4.59 0.25	5.08 0.19	6.91 0.24	1.87 0.21	2.18 0.11	1.25 0.12	99.99 0.05	46
KL-018p2	5	62.06	15.98 0.49	4.64 0.14	5.22 0.11	6.84 0.19	1.82 0.21	2.20 0.07	1.24 0.09	100.00 0.06	13
KL-067	6	62.01	16.17 0.28	4.53 0.30	5.22 0.23	6.86 0.16	1.68 0.20	2.29 0.15	1.24 0.19	100.00 0.08	36
KL-075	10	62.08	16.18 0.45	4.62 0.19	5.12 0.11	6.78 0.23	1.82 0.21	2.17 0.09	1.23 0.17	100.00 0.09	60
KL-135	10	62.17	15.99 0.34	4.84 0.14	5.19 0.35	6.70 0.12	1.77 0.24	2.16 0.12	1.17 0.21	99.99 0.06	59
Mean	5	62.09	16.07 0.06	4.65 0.10	5.17 0.12	6.82 0.06	1.79 0.08	2.20 0.07	1.22 0.05	100.01 0.03	---
Tephra 1A											
KL-001	7	78.19	12.54 0.29	3.66 0.19	1.95 0.10	1.42 0.14	1.72 0.16	0.32 0.16	0.21 0.09	100.01 0.10	72

Table 3. (continued)

Sample	n	SiO <sub>2</sub>	Al <sub>2</sub> O <sub>3</sub>	NaO	CaO	FeO**	K <sub>2</sub> O	MgO	TiO <sub>2</sub>	Total	Section
Tephra 1A (continued)											
KL-002	7	77.95	12.60 0.33	3.74 0.14	2.09 0.12	1.42 0.12	1.61 0.16	0.38 0.08	0.21 0.02	100.00 0.04	72
KL-003	10	77.80	12.66 0.25	3.80 0.11	2.11 0.13	1.41 0.10	1.60 0.14	0.38 0.04	0.25 0.03	100.01 0.03	72
KL-020	12	78.12	12.39 0.21	3.93 0.17	2.00 0.08	1.36 0.08	1.60 0.10	0.35 0.07	0.25 0.03	100.00 0.04	39
KL-040	9	77.87	12.37 0.32	3.93 0.18	2.05 0.09	1.44 0.10	1.74 0.09	0.35 0.05	0.26 0.02	100.01 0.03	10
KL-053	9	77.87	12.47 0.18	3.94 0.14	1.94 0.13	1.44 0.14	1.72 0.14	0.34 0.13	0.27 0.03	99.99 0.05	38
KL-090	10	77.47	12.62 0.46	4.03 0.27	1.98 0.09	1.46 0.15	1.82 0.15	0.37 0.39	0.26 0.03	100.01 0.07	57
KL-091	7	78.00	12.50 0.20	3.89 0.15	2.00 0.11	1.39 0.11	1.65 0.08	0.34 0.06	0.24 0.04	100.01 0.06	57
KL-093	7	77.93	12.44 0.21	3.92 0.09	1.97 0.11	1.41 0.09	1.73 0.07	0.37 0.05	0.22 0.03	99.99 0.10	58
KL-094p1	6	77.47	12.76 0.38	4.09 0.31	2.08 0.11	1.45 0.15	1.58 0.14	0.34 0.09	0.24 0.05	100.01 0.03	58
Mean	10	77.87	12.54 0.24	3.89 0.12	2.02 0.13	1.42 0.06	1.68 0.03	0.35 0.08	0.24 0.02	100.00 0.02	---
Tephra 1B											
KL-016	4	77.92	12.33 0.34	3.90 0.22	1.89 0.14	1.49 0.30	1.90 0.13	0.29 0.22	0.28 0.09	100.00 0.05	11
KL-044p1	6	77.75	12.43 0.23	4.01 0.11	1.71 0.11	1.50 0.13	2.01 0.11	0.32 0.13	0.28 0.02	100.01 0.05	53
KL-051	13	77.80	12.46 0.21	4.00 0.15	1.82 0.10	1.46 0.10	1.84 0.10	0.34 0.13	0.28 0.02	100.00 0.05	26
KL-060	6	77.79	12.42 0.17	3.99 0.08	1.79 0.06	1.47 0.04	1.91 0.05	0.31 0.04	0.31 0.04	99.99 0.06	35
KL-062	10	77.72	12.44 0.27	4.05 0.14	1.88 0.09	1.46 0.17	1.82 0.09	0.34 0.14	0.29 0.07	100.00 0.05	27
KL-104	7	77.97	12.36 0.37	3.94 0.17	1.78 0.06	1.49 0.06	1.86 0.11	0.32 0.10	0.29 0.04	100.01 0.04	62
Mean	6	77.83	12.41 0.09	3.98 0.05	1.81 0.05	1.48 0.06	1.89 0.02	0.32 0.06	0.29 0.02	100.00 0.01	---

Table 3. (continued)

Sample	n	SiO <sub>2</sub>	Al <sub>2</sub> O <sub>3</sub>	NaO	CaO	FeO <sup>*a</sup>	K <sub>2</sub> O	MgO	TiO <sub>2</sub>	Total	Section
<b>Tephra 1C</b>											
KL-004	8	77.80	12.90 0.21	3.80 0.15	2.11 0.08	1.27 0.13	1.53 0.09	0.39 0.09	0.19 0.05	99.99 0.03	72
KL-044p2	4	77.00	13.22 0.39	3.97 0.11	2.23 0.20	1.35 0.10	1.56 0.02	0.40 0.11	0.28 0.05	100.01 0.12	53
KL-049p1	7	77.28	13.14 0.41	3.82 0.22	2.26 0.09	1.38 0.12	1.53 0.18	0.41 0.05	0.20 0.09	100.02 0.13	73
KL-123	15	77.53	13.01 0.32	3.91 0.25	2.13 0.17	1.29 0.15	1.52 0.11	0.41 0.11	0.20 0.04	100.00 0.06	18
Mean	4	77.40	13.07 0.34	3.88 0.14	2.18 0.08	1.32 0.07	1.54 0.05	0.40 0.02	0.22 0.01	100.01 0.04	---
<b>Tephra 2?</b>											
KL-112p4	3	76.61	12.73 0.35	4.21 0.15	1.54 0.07	1.42 0.19	2.84 0.08	0.30 0.08	0.35 0.05	100.00 0.06	25
<b>Tephra 3</b>											
KL-013p1	8	75.37	13.39 0.39	4.13 0.17	1.99 0.10	1.86 0.11	2.47 0.16	0.44 0.10	0.36 0.04	100.01 0.07	16
KL-048	7	75.02	13.70 0.33	4.31 0.16	1.83 0.07	1.71 0.10	2.67 0.11	0.41 0.06	0.34 0.02	99.99 0.03	73
KL-049p2	6	74.98	13.56 0.38	4.22 0.13	1.88 0.14	1.91 0.14	2.68 0.16	0.42 0.12	0.35 0.07	100.00 0.04	73
KL-112p3	5	75.78	13.24 0.42	4.14 0.21	1.94 0.14	1.65 0.14	2.54 0.14	0.39 0.18	0.32 0.05	100.00 0.02	25
Mean	4	75.29	13.47 0.37	4.20 0.20	1.91 0.08	1.78 0.07	2.59 0.12	0.42 0.10	0.34 0.02	100.00 0.02	---
<b>Tephra 4</b>											
KL-021	10	75.53	13.70 0.41	3.85 0.20	2.04 0.12	1.53 0.15	2.64 0.22	0.49 0.11	0.22 0.10	100.00 0.04	39
KL-094p2	7	74.91	13.81 0.38	4.05 0.34	2.34 0.22	1.73 0.30	2.34 0.18	0.55 0.39	0.27 0.29	100.00 0.07	58
KL-111	11	75.18	13.73 0.48	3.90 0.31	2.26 0.30	1.63 0.18	2.60 0.28	0.46 0.37	0.24 0.08	100.00 0.04	7
Mean	3	75.21	13.75 0.31	3.93 0.06	2.21 0.10	1.63 0.16	2.53 0.10	0.50 0.16	0.24 0.05	100.00 0.03	---
<b>Tephra 5</b>											
KL-015p2	4	73.26	14.20 0.45	4.28 0.18	2.22 0.11	2.21 0.09	2.75 0.14	0.57 0.16	0.50 0.04	99.99 0.08	11

Table 3. (continued)

Sample	n	SiO <sub>2</sub>	Al <sub>2</sub> O <sub>3</sub>	NaO	CaO	FeO**	K <sub>2</sub> O	MgO	TiO <sub>2</sub>	Total	Section
<b>Tephra 5 (continued)</b>											
KL-086p2	6	74.10	13.34 0.50	4.39 0.30	2.13 0.17	2.55 0.17	2.48 0.40	0.47 0.14	0.54 0.09	100.00 0.07	66
KL-102p2	5	74.58	13.29 0.44	4.27 0.14	2.15 0.12	2.28 0.22	2.44 0.42	0.52 0.08	0.48 0.05	100.01 0.10	41
KL-129p1	7	73.57	13.91 0.44	4.35 0.33	2.22 0.15	2.38 0.17	2.47 0.44	0.64 0.11	0.46 0.15	100.00 0.11	55
Mean	4	73.88	13.69 0.58	4.32 0.44	2.18 0.06	2.36 0.05	2.54 0.15	0.55 0.14	0.50 0.07	100.00 0.03	---
<b>Tephra 7?</b>											
KL-013p2	4	73.13	14.04 0.41	4.22 0.08	2.62 0.12	2.56 0.07	2.24 0.25	0.70 0.09	0.50 0.06	100.01 0.04	16
<b>Tephra 8?</b>											
KL-112p2	5	71.24	14.48 0.45	4.51 0.37	2.77 0.20	2.86 0.25	2.58 0.15	0.93 0.15	0.62 0.31	99.99 0.07	25
<b>Tephra 12?</b>											
KL-129p2	3	68.92	15.36 0.24	4.82 0.21	3.71 0.20	3.51 0.13	1.98 0.13	1.13 0.04	0.58 0.15	100.01 0.06	55
<b>Tephra 13</b>											
KL-032p3	5	64.52	15.78 0.38	4.22 0.21	5.06 0.11	5.68 0.16	1.75 0.24	2.17 0.10	0.82 0.06	100.00 0.05	22
KL-050p2	6	65.38	15.54 0.47	4.31 0.15	4.95 0.15	5.27 0.14	1.81 0.22	1.92 0.09	0.82 0.17	100.00 0.14	26
KL-095p2	5	65.01	15.86 0.40	4.28 0.27	5.21 0.13	5.26 0.23	1.66 0.27	1.88 0.05	0.84 0.12	100.00 0.04	52
KL-095p3	4	63.83	15.91 0.22	4.19 0.33	5.67 0.10	5.72 0.07	1.57 0.19	2.29 0.07	0.83 0.08	100.01 0.03	52
Mean	4	64.69	15.77 0.67	4.25 0.16	5.22 0.05	5.48 0.32	1.70 0.25	2.07 0.10	0.83 0.20	100.00 0.01	---
<b>Goose Bay tephra</b>											
KL-027	15	65.51	16.27 0.50	4.27 0.26	4.46 0.17	4.57 0.25	2.57 0.38	1.48 0.11	0.87 0.14	100.00 0.10	3
KL-081p1	15	66.87	15.77 0.45	4.25 0.17	3.93 0.11	4.40 0.19	2.70 0.29	1.28 0.14	0.81 0.08	100.01 0.07	3
KL-081p2	7	64.85	16.68 0.24	4.32 0.80	4.76 0.11	4.56 0.34	2.41 0.46	1.55 0.25	0.88 0.24	100.01 0.12	3

Table 3. (continued)

Sample	n	SiO <sub>2</sub>	Al <sub>2</sub> O <sub>3</sub>	NaO	CaO	FeO**	K <sub>2</sub> O	MgO	TiO <sub>2</sub>	Total	Section
Goose Bay tephra (continued)											
Mean	3	65.74	16.24 1.03	4.28 0.46	4.38 0.04	4.51 0.42	2.56 0.10	1.44 0.15	0.85 0.14	100.01 0.04	---
Stampede tephra											
KL-025	15	77.24	13.30 0.38	4.40 0.26	1.71 0.13	1.32 0.12	1.47 0.14	0.35 0.04	0.22 0.08	100.01 0.03	3
KL-082	15	77.58	13.13 0.48	4.37 0.22	1.61 0.11	1.25 0.13	1.51 0.14	0.34 0.09	0.21 0.03	100.00 0.07	3
KL-083	15	77.68	13.10 0.47	4.35 0.20	1.61 0.09	1.24 0.16	1.46 0.13	0.34 0.04	0.22 0.05	100.00 0.05	3
Mean	3	77.50	13.18 0.23	4.37 0.11	1.64 0.03	1.27 0.06	1.48 0.04	0.34 0.03	0.22 0.01	100.00 0.01	---
Tephras of unknown affinity											
KL-008	7	75.72	13.56 0.49	3.77 0.08	2.18 0.07	1.64 0.13	2.50 0.19	0.47 0.10	0.16 0.03	100.00 0.10	72
KL-015p1	6	77.97	12.37 0.38	3.98 0.20	1.77 0.10	1.42 0.09	1.89 0.18	0.31 0.14	0.30 0.03	100.01 0.07	11
KL-032p2	4	69.96	14.36 0.50	4.12 0.24	3.40 0.17	4.07 0.13	2.28 0.28	1.09 0.03	0.70 0.07	99.98 0.03	22
KL-102p1	3	78.92	11.64 0.36	3.38 0.43	0.65 0.22	0.92 0.12	4.11 0.15	0.15 0.37	0.23 0.01	100.00 0.10	41
KL-112p1	8	74.69	13.64 0.23	4.28 0.17	2.08 0.07	1.92 0.14	2.52 0.21	0.44 0.18	0.43 0.08	100.00 0.08	25
KL-130p2	3	79.74	11.82 0.04	3.78 0.07	1.30 0.02	1.01 0.05	1.98 0.13	0.21 0.09	0.16 0.05	100.00 0.02	51

\*Total iron expressed as FeO\*.

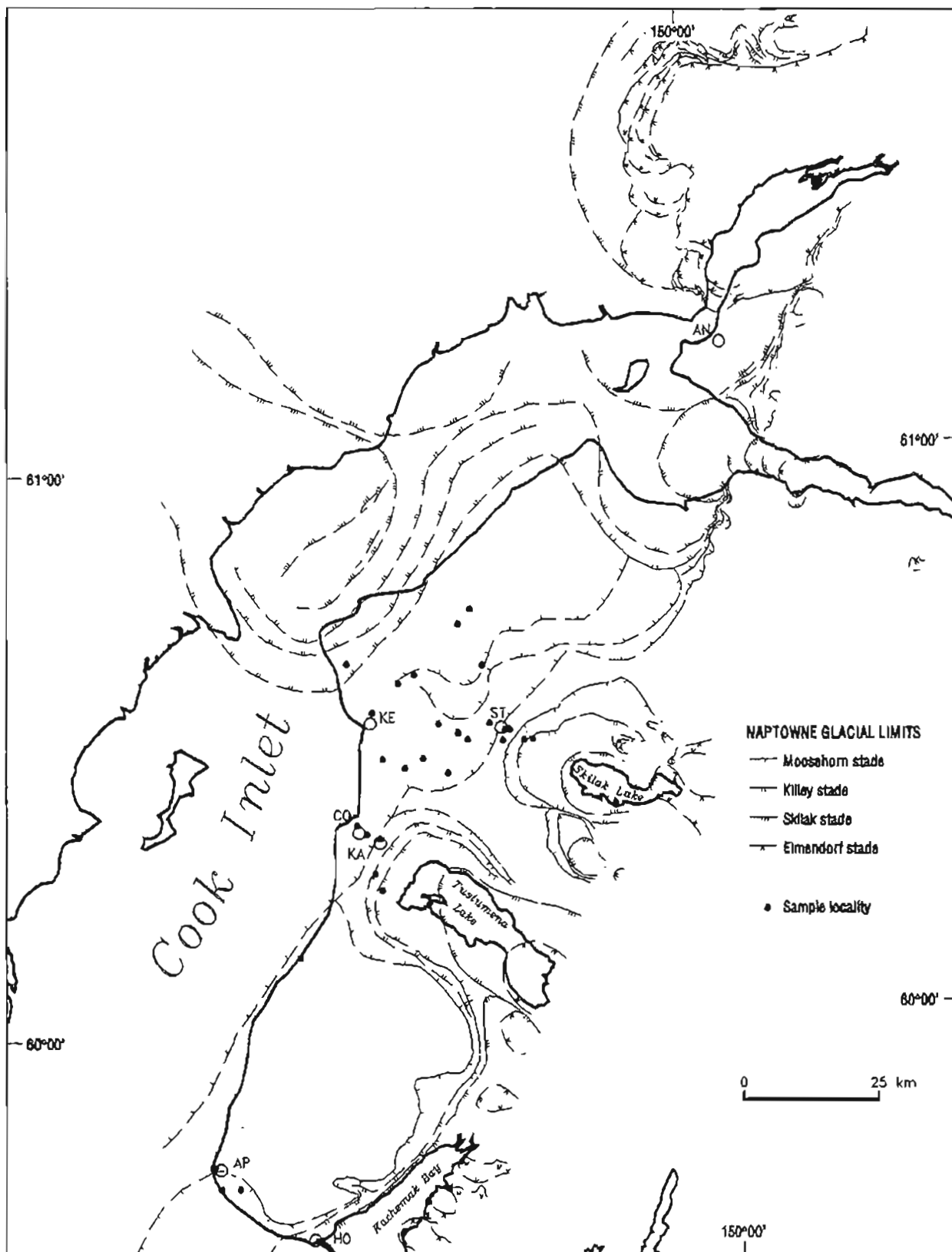


Figure 2. Distribution of *Letho* tephra samples ( $n = 29$ ) in Kenai Lowland relative to former limits of the Naptowne glaciation. Geographic localities: AN = Anchorage; AP = Anchor Point; CO = Cohoe; HO = Homer; KA = Kasilof; KE = Kenai; ST = Sterling.

Table 4. Similarity-coefficient matrix for *Lethe tephra* samples collected in Kenai Lowland

	KL-095p1	KL-034	KL-011	KL-137	KL-068	KL-102p3	KL-136	KL-063	KL-088	KL-127	KL-085	KL-110	KL-052	KL-072	KL-100	KL-087
KL-095p1	1.00															
KL-034	0.96	1.00														
KL-011	0.96	0.98	1.00													
KL-137	0.97	0.99	0.99	1.00												
KL-068	0.95	0.96	0.98	0.98	1.00											
KL-102p3	0.97	0.98	0.98	0.98	0.96	1.00										
KL-136	0.97	0.97	0.98	0.98	0.97	0.99	1.00									
KL-063	0.97	0.98	0.98	0.99	0.97	0.99	0.99	1.00								
KL-088	0.96	0.97	0.98	0.98	0.97	0.98	0.99	0.98	1.00							
KL-127	0.96	0.98	0.98	0.98	0.97	0.99	0.99	0.99	0.98	1.00						
KL-085	0.96	0.97	0.97	0.97	0.97	0.98	0.99	0.98	0.98	0.98	1.00					
KL-110	0.96	0.97	0.97	0.98	0.96	0.99	0.98	0.99	0.98	0.99	0.98	1.00				
KL-052	0.96	0.97	0.97	0.97	0.96	0.98	0.98	0.98	0.99	0.98	0.98	0.99	1.00			
KL-072	0.96	0.96	0.97	0.97	0.98	0.97	0.98	0.97	0.99	0.97	0.98	0.97	0.97	1.00		
KL-100	0.96	0.96	0.96	0.97	0.96	0.98	0.98	0.97	0.98	0.97	0.98	0.99	0.99	0.97	1.00	
KL-087	0.96	0.96	0.97	0.97	0.96	0.98	0.98	0.98	0.98	0.97	0.98	0.98	0.99	0.97	0.98	1.00
KL-050p1	0.95	0.93	0.94	0.94	0.93	0.94	0.95	0.94	0.95	0.94	0.95	0.94	0.96	0.94	0.96	0.96
KL-022	0.95	0.96	0.96	0.96	0.95	0.97	0.97	0.97	0.98	0.97	0.98	0.98	0.99	0.96	0.99	0.99
KL-125	0.96	0.97	0.97	0.97	0.96	0.98	0.99	0.98	0.99	0.99	0.99	0.99	0.99	0.98	0.98	0.98
KL-124	0.95	0.97	0.96	0.97	0.96	0.98	0.98	0.98	0.98	0.99	0.98	0.99	0.98	0.97	0.98	0.98
KL-018p1	0.95	0.96	0.96	0.97	0.95	0.97	0.98	0.97	0.98	0.97	0.98	0.97	0.98	0.97	0.98	0.98
KL-033	0.96	0.97	0.97	0.97	0.96	0.98	0.99	0.98	0.99	0.98	0.98	0.98	0.99	0.97	0.98	0.99
KL-128	0.95	0.96	0.96	0.96	0.95	0.98	0.97	0.97	0.98	0.97	0.98	0.99	0.99	0.97	0.99	0.98
KL-029	0.95	0.96	0.96	0.97	0.96	0.97	0.98	0.97	0.98	0.97	0.97	0.98	0.98	0.97	0.98	0.99
KL-106	0.94	0.95	0.95	0.96	0.95	0.97	0.97	0.96	0.97	0.96	0.97	0.97	0.98	0.96	0.99	0.98
KL-017	0.95	0.96	0.96	0.97	0.95	0.97	0.98	0.97	0.98	0.97	0.98	0.97	0.98	0.97	0.98	0.98
KL-096	0.94	0.96	0.95	0.96	0.95	0.97	0.97	0.97	0.97	0.97	0.98	0.98	0.99	0.96	0.98	0.98
KL-105	0.95	0.95	0.95	0.96	0.95	0.97	0.97	0.97	0.98	0.97	0.97	0.98	0.99	0.96	0.99	0.98
KL-086p3	0.94	0.95	0.95	0.96	0.95	0.97	0.97	0.97	0.97	0.96	0.97	0.97	0.98	0.96	0.98	0.99
KL-109	0.94	0.95	0.94	0.95	0.94	0.96	0.96	0.96	0.96	0.96	0.97	0.97	0.98	0.95	0.98	0.98
KL-099	0.94	0.95	0.95	0.96	0.95	0.97	0.97	0.96	0.97	0.96	0.97	0.97	0.98	0.96	0.98	0.98

Table 4. (continued)

	KL-050pl	KL-022	KL-125	KL-124	KL-018pl	KL-033	KL-128	KL-029	KL-106	KL-017	KL-096	KL-105	KL-086p3	KL-109	KL-099
KL-095pl															
KL-034															
KL-011															
KL-137															
KL-068															
KL-102p3															
KL-136															
KL-063															
KL-088															
KL-127															
KL-085															
KL-110															
KL-052															
KL-072															
KL-100															
KL-087															
KL-050pl	1.00														
KL-022	0.96	1.00													
KL-125	0.95	0.98	1.00												
KL-124	0.95	0.98	0.99	1.00											
KL-018pl	0.96	0.99	0.98	0.98	1.00										
KL-033	0.96	0.99	0.99	0.99	0.99	1.00									
KL-128	0.96	0.99	0.98	0.98	0.98	0.99	1.00								
KL-029	0.96	0.98	0.98	0.98	0.99	0.99	0.98	1.00							
KL-106	0.96	0.99	0.97	0.97	0.99	0.98	0.99	0.98	1.00						
KL-017	0.96	0.99	0.98	0.98	0.99	0.99	0.98	0.98	0.99	1.00					
KL-096	0.96	0.99	0.98	0.98	0.98	0.99	0.99	0.98	0.99	0.99	1.00				
KL-105	0.96	0.98	0.97	0.98	0.99	0.98	0.98	0.98	0.99	0.98	0.98	1.00			
KL-086p3	0.97	0.99	0.97	0.97	0.99	0.98	0.98	0.98	0.99	0.99	0.99	0.99	1.00		
KL-109	0.96	0.98	0.97	0.97	0.98	0.97	0.98	0.98	0.99	0.98	0.98	0.99	0.99	1.00	
KL-099	0.96	0.98	0.97	0.97	0.98	0.98	0.98	0.98	0.99	0.99	0.98	0.98	0.98	0.98	1.00

is mixed with shards of apparently reworked tephra 5 (KL-086p2) and shards of Crooked Creek tephra (KL-086p1) in a layer that is stratigraphically above a layer of unmixed Lethe tephra (KL-085). The degree of reworking is less obvious in sections 26, 41, and 52, where populations of Lethe shards are mixed with shard populations of tephra 5 and 13. Section 26 (fig. A26) was measured at Sterling on the second highest terrace of the Kenai River system. On the adjacent, highest terrace, Lethe tephra (KL-063) is unmixed in nearby section 27 (fig. A27). Because of these relations, we conclude that primary airfall Lethe tephra is redeposited in section 26 and, in the process, became mixed with tephra 13. Section 41 (fig. A45) was measured on the distal surface of the fan delta that was built by Kenai River onto the upper marine terrace between Kenai and Kasilof. Section 52 (fig. A57) was measured on the distal surface of the fan delta simultaneously built by Kasilof River onto the same marine terrace. There is a high likelihood that distal parts of both fan deltas were submerged later than medial and proximal surfaces on which we found unmixed Lethe tephra—for example, KL-124 in section 17 (fig. A17) on the fan delta at Kenai and KL-127 in section 54 (fig. A59) on the equivalent fan delta at Kasilof. Thus, reworking and mixing of Lethe and tephra 5 and 13 probably occurred at localities KEN-96 and KEN-117 (sheet 2). These arguments also lead us to tentatively conclude that deposition of tephra 5 and 13 probably slightly postdates deposition of Lethe tephra (fig. 3).

Lethe tephra is the distal airfall equivalent of the complex pyroclastic products of an explosive eruption of one of the volcanoes in the vicinity of Mt. Katmai about 260 km southwest of the southern Kenai Lowland (Pinney and Begét, 1991a,b; Pinney, 1993). On the basis of shard morphology, ferromagnesian mineral content, and microprobe geochemistry of glass shards, our Kenai Lowland samples strongly correlate with samples of Lethe tephra from the Windy Creek area (Pinney 1993) (SC = 0.96–0.99). Pinney and Begét (1991a,b) and Pinney (1993) provide a minimum age of  $12,640 \pm 100$  <sup>14</sup>C yr B.P. (Beta-33666) for Lethe volcanoclastics in the Windy Creek area, where they overlie drift of the Iliuk stade and underlie drift of the Ukak stade of the late-Wisconsin Brooks Lake glaciation. Primary airfall Lethe tephra discontinuously covers deposits of Moosehorn and Killey stades of the Naptowne glaciation in Kenai Lowland and is not present on deposits of the Skilak stade (Reger and Pinney, 1996). Stratigraphic evidence indicates that Lethe tephra was deposited across Kenai Lowland late in the Killey stade. Killey-age glaciomarine sediments in the upper marine terrace at Kalifornsky (sheet 2, locality KEN-103) date as young as  $16,000 \pm 150$  <sup>14</sup>C yr B.P. (table 2, C80) and stratigraphically underlie fan-delta sediments that are in turn overlain by Lethe-bearing loess at Kasilof (fig. A59). Thus, the known maximum age of Lethe tephra in Kenai Lowland is  $16,000$  <sup>14</sup>C yr B.P. (fig. 3).

#### CROOKED CREEK TEPHRA (MEAN SiO<sub>2</sub> = 77.82 ± 0.10 PERCENT)

One of several grayish brown-weathering Holocene tephra in Kenai Lowland that are the products of brief, small eruptions of Cook Inlet volcanoes—and not known to be widely distributed—is the Crooked Creek tephra, which is first recognized and informally named in this study. This tephra is identified in 11 stratigraphic sections (table 3) in a narrow belt from west of Tustumena Lake northeast to the vicinity of Sterling (fig. 4). Correlation within this set of samples is good to excellent (SC = 0.93–0.99) (table 5). We know of no correlative tephra in the region, but we speculate (from the distribution and high silica content) that Crooked Creek tephra could have been erupted from Mt. Augustine. The Crooked Creek tephra was deposited between  $7,725 \pm 210$  <sup>14</sup>C yr ago and  $8,375 \pm 210$  <sup>14</sup>C yr ago (fig. A25; table 2, C10 and C17). It could possibly be the distal equivalent of tephra layer G, which dates  $>1,830 \pm 80$  <sup>14</sup>C yr B.P. and  $<39,890$  <sup>14</sup>C yr B.P. on Augustine Island (Begét and Kienle, 1992).

#### FUNNY RIVER TEPHRA (MEAN SiO<sub>2</sub> = 62.09 ± 0.06 PERCENT)

Another of the dark-weathering Holocene tephra in Kenai Lowland is the Funny River tephra, first recognized at locality KEN-85 (table 1, sheet 2) and informally named in this study. Funny River tephra is identified at five localities that form an irregular triangle with corners at Kenai, Sterling, and Coho (fig. 5); it has a low silica content relative to other tephra in the area (table 3). Correlation within this small set of samples is outstanding (SC = 0.97–0.99) (table 6). We know of no tephra that correlate with Funny River tephra, which was deposited after the Crooked Creek tephra (fig. 3) and has a close maximum-limiting age of  $7,560 \pm 340$  <sup>14</sup>C yr B.P. (fig. A65; table 2, C8).

#### TEPHRA 1A (MEAN SiO<sub>2</sub> = 77.87 ± 0.24 PERCENT)

One of several geochemically very similar tephra in Kenai Lowland that are tentatively attributed to explosive eruptions of Mt. Augustine is tephra 1A. This volcanic ash is documented at six locations (fig. 6). Similarity coefficients within this set of samples range from 0.93 to 0.98 (table 7). Tephra layers attributed to tephra 1A are clearly redeposited in sections 57 (fig. A62), 58 (fig. A63), and 72 (fig. A77), but the other six samples are apparently undisturbed airfall samples. The stratigraphy in section 72 demonstrates that primary tephra 1A is younger than tephra 1C. Comparisons of shard geochemistry indicate that uncontaminated samples of tephra 1A correlate with Augustine ash sample H-88-2-5 collected by Begét (unpub. data) in the Homer area (SC = 0.95–0.97) and with sample 87A-9A collected by Begét (unpub. data) on Augustine Island (SC = 0.94–0.98). In section (*Text cont'd. p. 41*)

Radiocarbon age

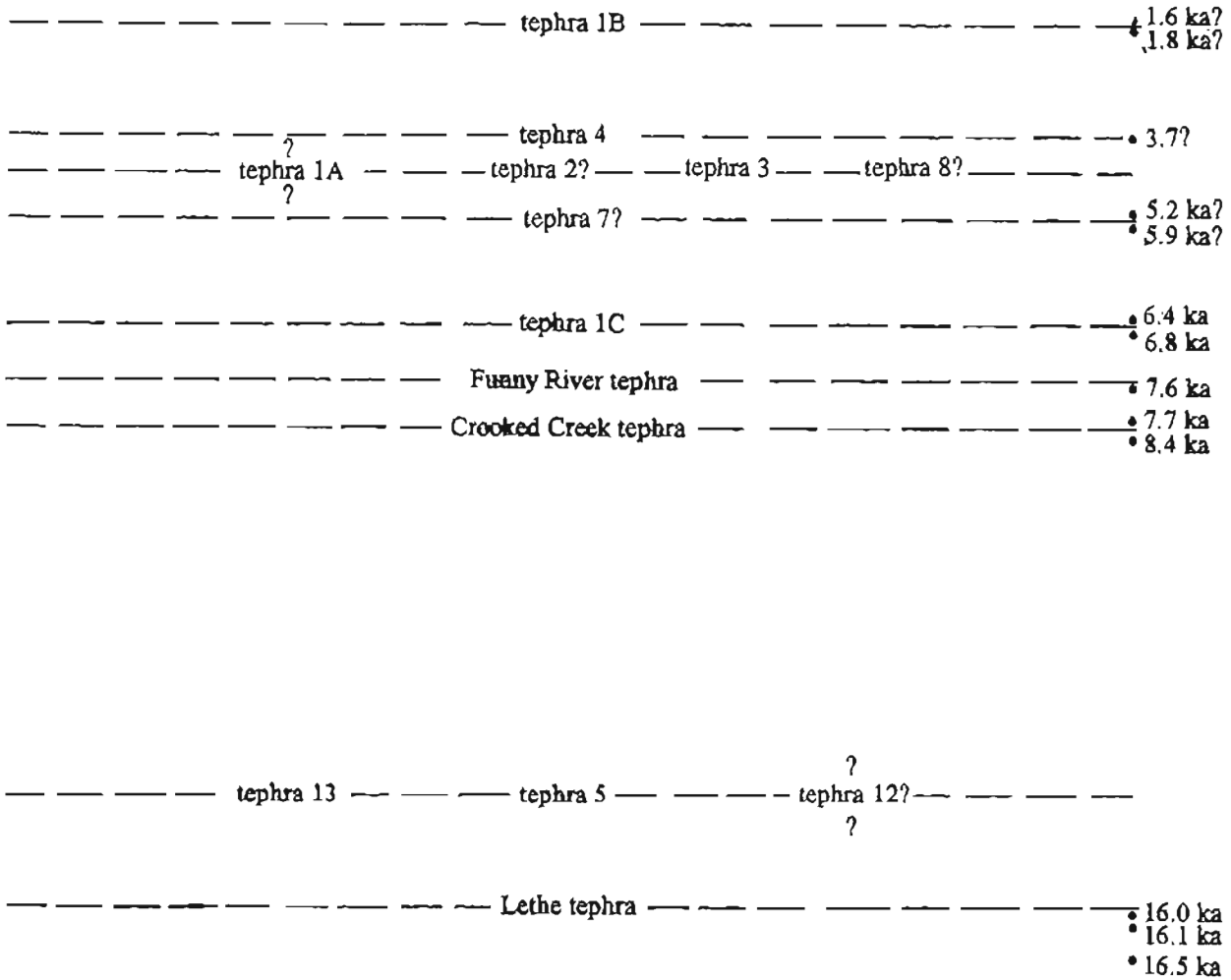


Figure 3. Tentative relative ages of late Quaternary tephra, based on stratigraphic relations in Kenai Lowland. Uncertain temporal placements are indicated by question marks above and below the pertinent tephra. Questionable tephra ages result from tentative correlations with tephra that are dated elsewhere.

Table 5. Similarity-coefficient matrix for samples of Crooked Creek tephra collected in Kenai Lowland

	<u>KL-115</u>	<u>KL-065</u>	<u>KL-056</u>	<u>KL-061</u>	<u>KL-023</u>	<u>KL-066</u>	<u>KL-057</u>	<u>KL-032pl</u>	<u>KL-113</u>	<u>KL-086pl</u>	<u>KL-130pl</u>
KL-115	1.00										
KL-065	0.93	1.00									
KL-056	0.97	0.94	1.00								
KL-061	0.96	0.96	0.98	1.00							
KL-023	0.95	0.95	0.98	0.97	1.00						
KL-066	0.96	0.95	0.99	0.98	0.97	1.00					
KL-057	0.94	0.97	0.96	0.99	0.97	0.97	1.00				
KL-032pl	0.96	0.95	0.99	0.99	0.97	0.98	0.97	1.00			
KL-113	0.95	0.96	0.98	0.98	0.98	0.98	0.97	0.98	1.00		
KL-086pl	0.96	0.95	0.98	0.98	0.97	0.98	0.97	0.98	0.98	1.00	
KL-130pl	0.97	0.95	0.97	0.98	0.97	0.97	0.97	0.98	0.97	0.98	1.00

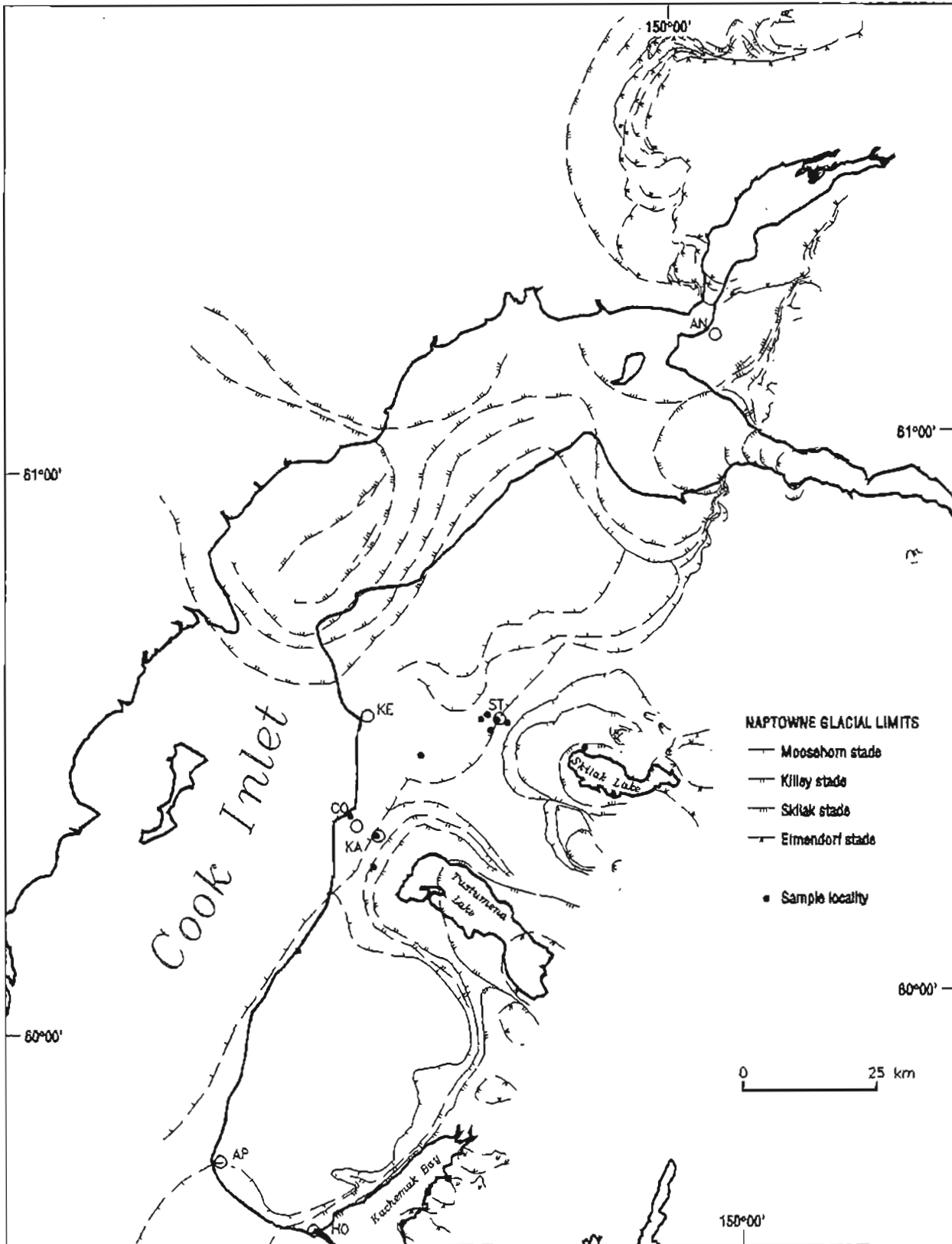


Figure 4. Distribution of Crooked Creek tephra samples ( $n = 11$ ) in Kenai Lowland relative to former limits of the Naptowne glaciation. Geographic localities: AN = Anchorage; AP = Anchor Point; CO = Cohoe; HO = Homer; KA = Kasilof; KE = Kenai; ST = Sterling.

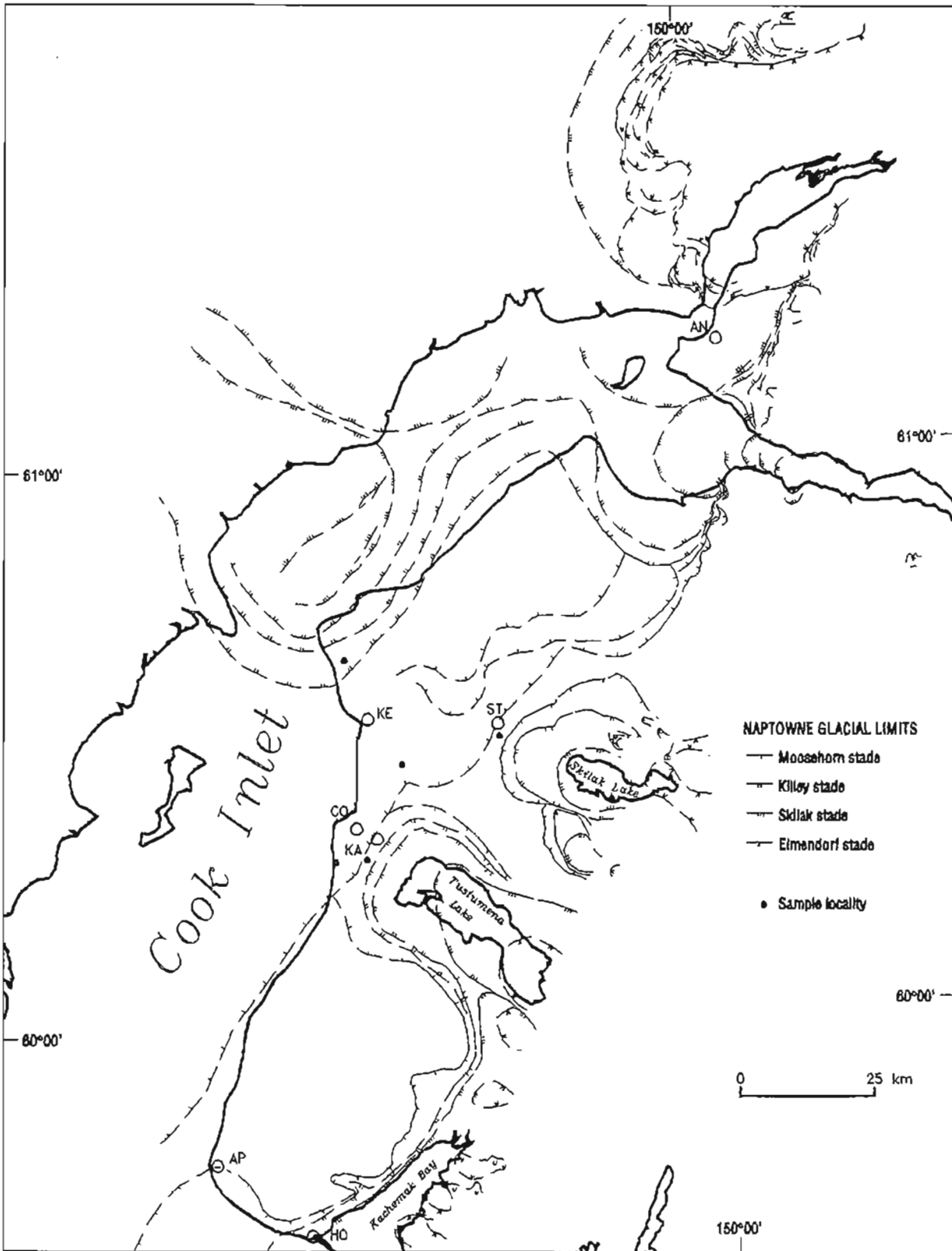


Figure 5. Distribution of Funny River tephra samples (n = 5) in Kenai Lowland relative to former limits of the Naptowne glaciation. Geographic localities: AN = Anchorage; AP = Anchor Point; CO = Cohoe; HO = Homer; KA = Kasilof; KE = Kenai; ST = Sterling.

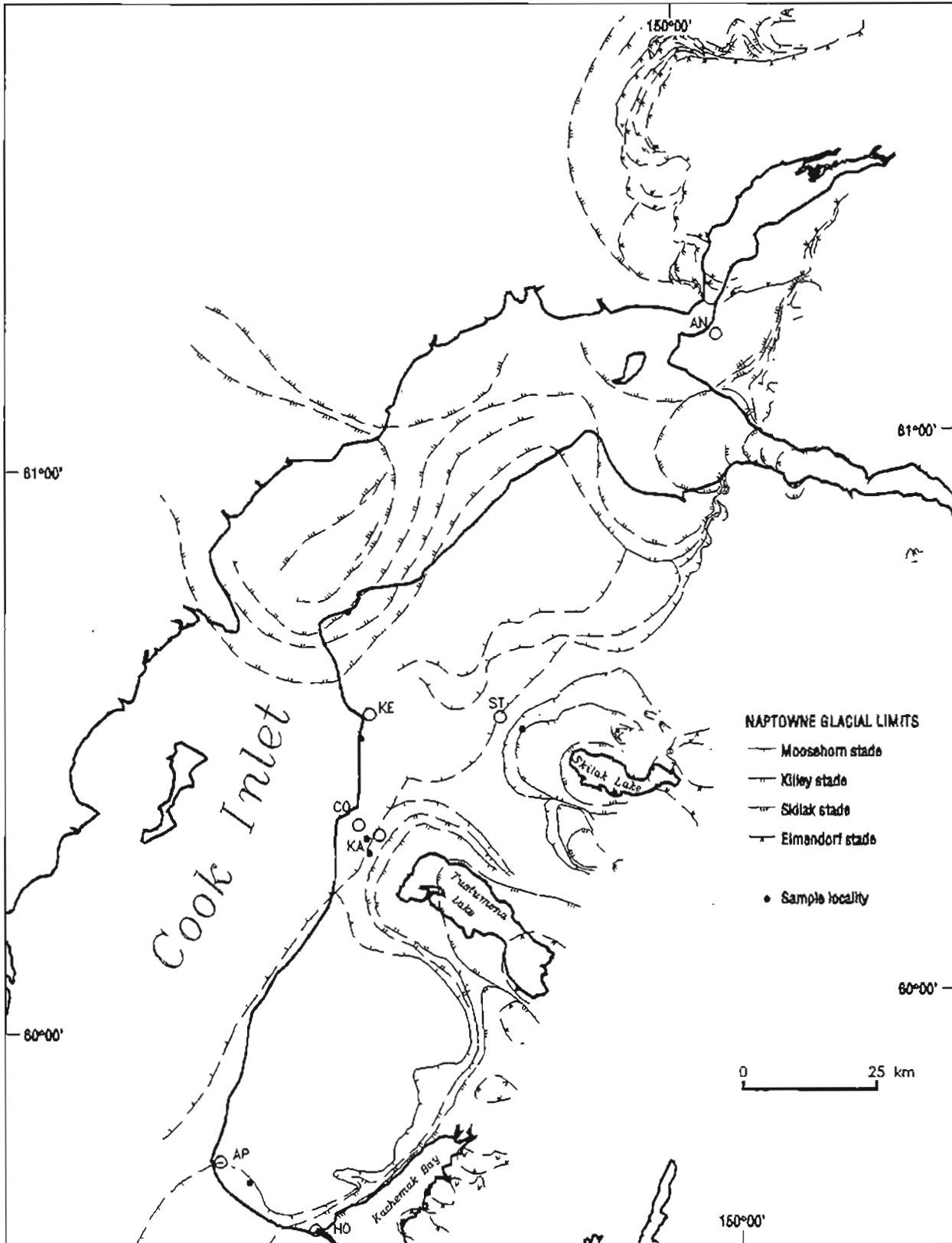


Figure 6. Distribution of tephra IA samples (n = 6) in Kenai Lowland relative to former limits of the Naptowne glaciation. Geographic localities: AN = Anchorage; AP = Anchor Point; CO = Cohoe; HO = Homer; KA = Kasilof; KE = Kenai; ST = Sterling.

**Table 6.** Similarity-coefficient matrix for samples of Funny River tephra collected in Kenai Lowland

	KL-135	KL-012	KL-075	KL-018p2	KL-067
KL-135	1.00				
KL-012	0.97	1.00			
KL-075	0.98	0.99	1.00		
KL-018p2	0.98	0.99	0.99	1.00	
KL-067	0.97	0.97	0.98	0.98	1.00

39 (fig. A43) and section 59 (fig. A63), tephra 1A underlies tephra 4, indicating that tephra 1A is older (fig. 3).

#### TEPHRA 1B

(MEAN SiO<sub>2</sub> = 77.83 ± 0.09 PERCENT)

Very similar to tephra 1A, tephra 1B is geochemically different enough to justify separating the two (table 3). Major-oxide contents within the set of tephra 1B samples are very consistent (SC = 0.96–0.98) (table 8A). Apparently undisturbed samples of tephra 1B are identified in five of six sections in the Kasilof-Kenai-Sterling area (table 3, fig. 7). Shards of tephra 1B (KL-044p1) are mixed with shards of tephra 1C (KL-044p2) in section 53 (fig. A58).

Stratigraphic superposition in section 35 (fig. A39) demonstrates that tephra 1B is younger than Crooked Creek tephra (fig. 3). Apparently uncontaminated samples of tephra 1B correlate moderately well with Augustine ash sample A88-11-5, which was collected by Begét (unpub. data) from proximal tephra layer "I" on Augustine Island (SC = 0.94–0.96), indicating that these samples could represent the same tephrafall. Our samples correlate slightly less positively with Begét (unpub. data) sample A88-7-5 from tephra layer "I" on Mt. Augustine (SC = 0.93–0.95). Both Begét samples correlate strongly (SC = 0.98). Begét and Kienle (1992) date proximal tephra layer "I" >1,610 ± 70 <sup>14</sup>C yr B.P. (ETH-3826) and <1,830 ± 80 <sup>14</sup>C yr B.P. (B-24775). Thus, tephra 1B could also conceivably be >1,610 ± 70 and <1,830 ± 80 <sup>14</sup>C yr old. There is good correlation between our five Kenai Lowland samples and the mean geochemistry of shards from layer "Y" in the Windy Creek area (SC = 0.95–0.97) (Pinney, 1993), indicating that these distant tephra layers record the same eruption of Mt. Augustine. Layer "Y" correlates well with Begét samples A88-11-5 and A88-7-5 (SC = 0.97 and 0.95, respectively).

#### TEPHRA 1C

(MEAN SiO<sub>2</sub> = 77.40 ± 0.34 PERCENT)

Tephra 1C is identified in four widely scattered sections in Kenai Lowland (fig. 8), and correlation within this small sample set is good to excellent (SC = 0.93–0.98) (table 8B). This volcanic ash has the high silica content that seems to typify tephra derived from Mt. Augustine (table 3).

Comparison of shard geochemistry of tephra 1C and Augustine samples collected by Begét (unpub. data) indicates that our four samples correlate best with Augustine sample A88-4-2 (SC = 0.95–0.97), slightly less well with sample 87A-16A (SC = 0.93–0.97), and are least compatible with sample A88-1-1 (SC = 0.91–0.95). In section 18 (fig. A18), tephra 1C (KL-123) is dated >6,360 ± 145 <sup>14</sup>C yr B.P. (GX-18232) and <6,801 ± 55 <sup>14</sup>C yr B.P. (GX-18225) (table 2, C4 and C5). These dates, the dating of tephra layer "I" on Augustine Island, and our apparent correlation of tephra 1B with layer "I" indicate that tephra 1C was probably deposited in Kenai Lowland before tephra 1B (fig. 3) and that the mixing of tephra 1B and 1C in section 53 (fig. A58) is most likely due to redeposition of tephra 1C.

#### TEPHRA 2?

(MEAN SiO<sub>2</sub> = 76.61 ± 0.35 PERCENT)

A layer consisting of shards of several tephra was sampled at a depth of 2.6 m in a core collected in a peat fen just west of Moose River along the Sterling Highway (sheet 2, locality KEN-64; fig. A25). From this layer, a very small (n = 3) population of shards (KL-112p4) was separated, and we very tentatively and informally identify this small collection as tephra 2? (table 3). Also present are a few shards that we attribute to tephra 3 (KL-112p3), possible tephra 8? (KL-112p2), and an unnamed tephra (KL-112p1). We believe that the tephra in this complex layer are close to the same age (fig. 3) because mixing is unlikely in this situation. A radiocarbon date for peat 0.3 m below this layer in the core demonstrates that the mixed layer is <7,725 ± 210 <sup>14</sup>C yr old (GX-18227) (table 2, C10). Because of their geochemical similarities (SC = 0.95), we speculate that tephra 2? could correlate with another population of glass shards (ATC-644Ap1) that is archived in the ATC, but we have no supportive mineralogic or stratigraphic evidence. The volcano that produced the ATC sample is not identified.

#### TEPHRA 3

(MEAN SiO<sub>2</sub> = 75.29 ± 0.37 PERCENT)

Tephra 3 is identified in three sections—two in the Kenai-Sterling area and one near Homer (fig. 9). Chemical correlations between samples are excellent (SC = 0.95–0.98) (table 9A). This ash is mixed with other fine-grained tephra in sections 16, 25, and 73. As previously discussed, the setting and stratigraphy of section 25 indicate that tephra 3 (KL-112p3) is one of several tephra, including tephra 2? and 8?, that were erupted at about the same time after 7,725 ± 210 <sup>14</sup>C yr ago (GX-18227) (fig. A25) (fig. 3). The lower mixed layer in section 73 (fig. A79) is probably the result of the sifting of shards of a younger tephra 3 (KL-049p2) downward into an older layer of tephra 1C (KL-049p1). From stratigraphic evidence in section 72 (fig. A77) and (*Text cont'd.* p. 45)

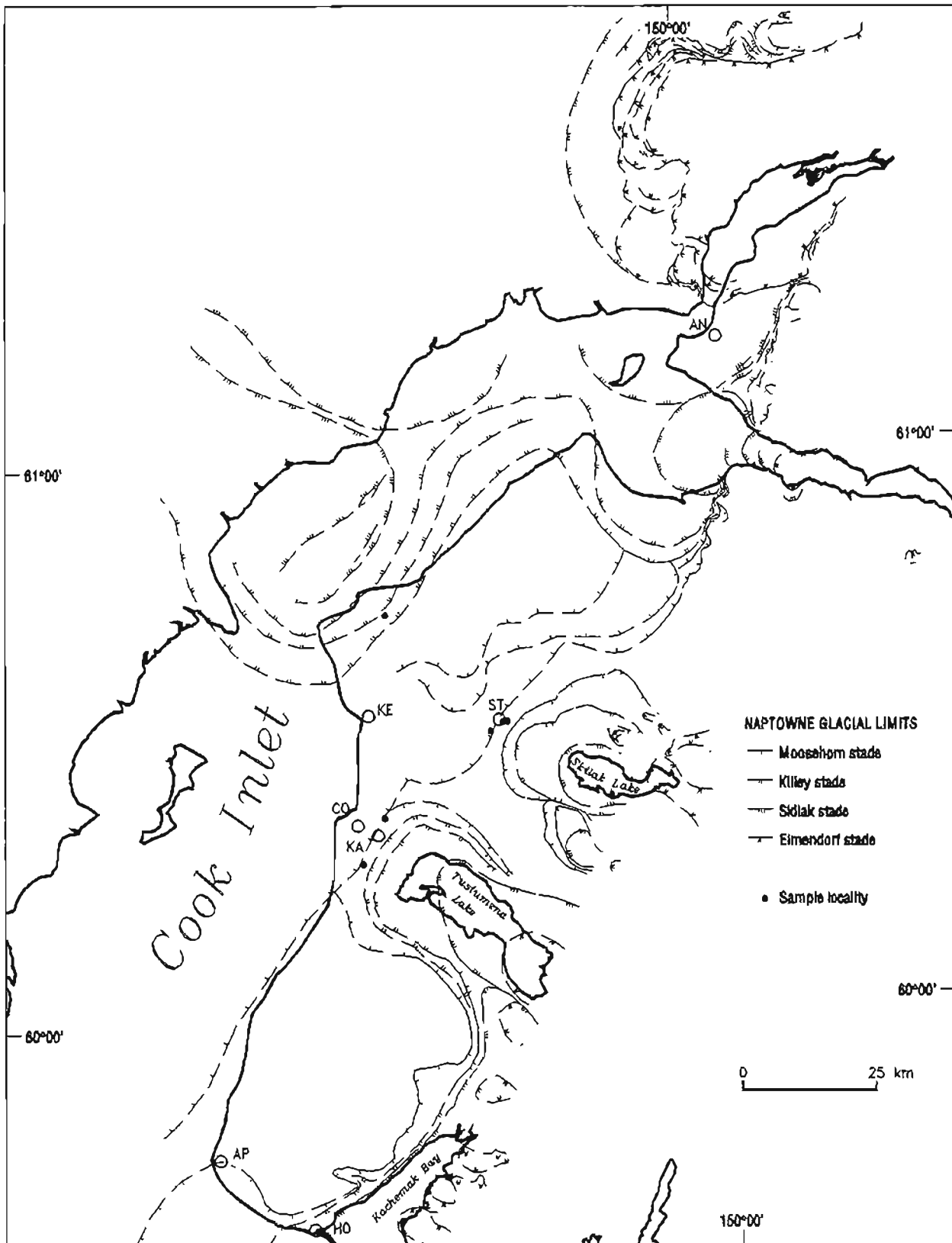


Figure 7. Distribution of tephra 1B samples (n = 6) in Kenai Lowland relative to former limits of the Naptowne glaciation. Geographic localities: AN = Anchorage; AP = Anchor Point; CO = Cohoe; HO = Homer; KA = Kasilof; KE = Kenai; ST = Sterling.

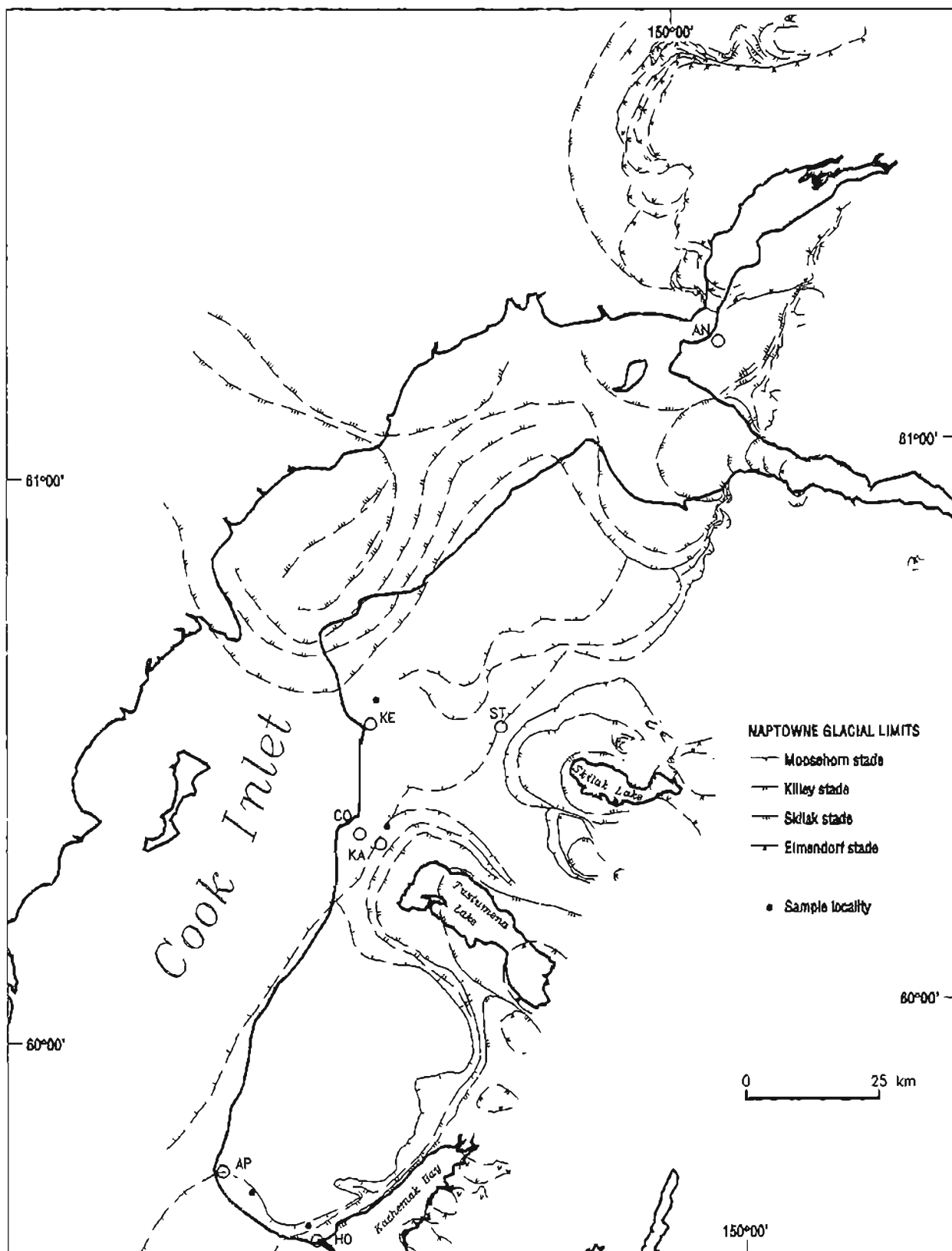


Figure 8. Distribution of tephra 1C samples (n = 4) in Kenai Lowland relative to former limits of the Naptowne glaciation. Geographic localities: AN = Anchorage; AP = Anchor Point; CO = Cohoe; HO = Homer; KA = Kasilof; KE = Kenai; ST = Sterling.

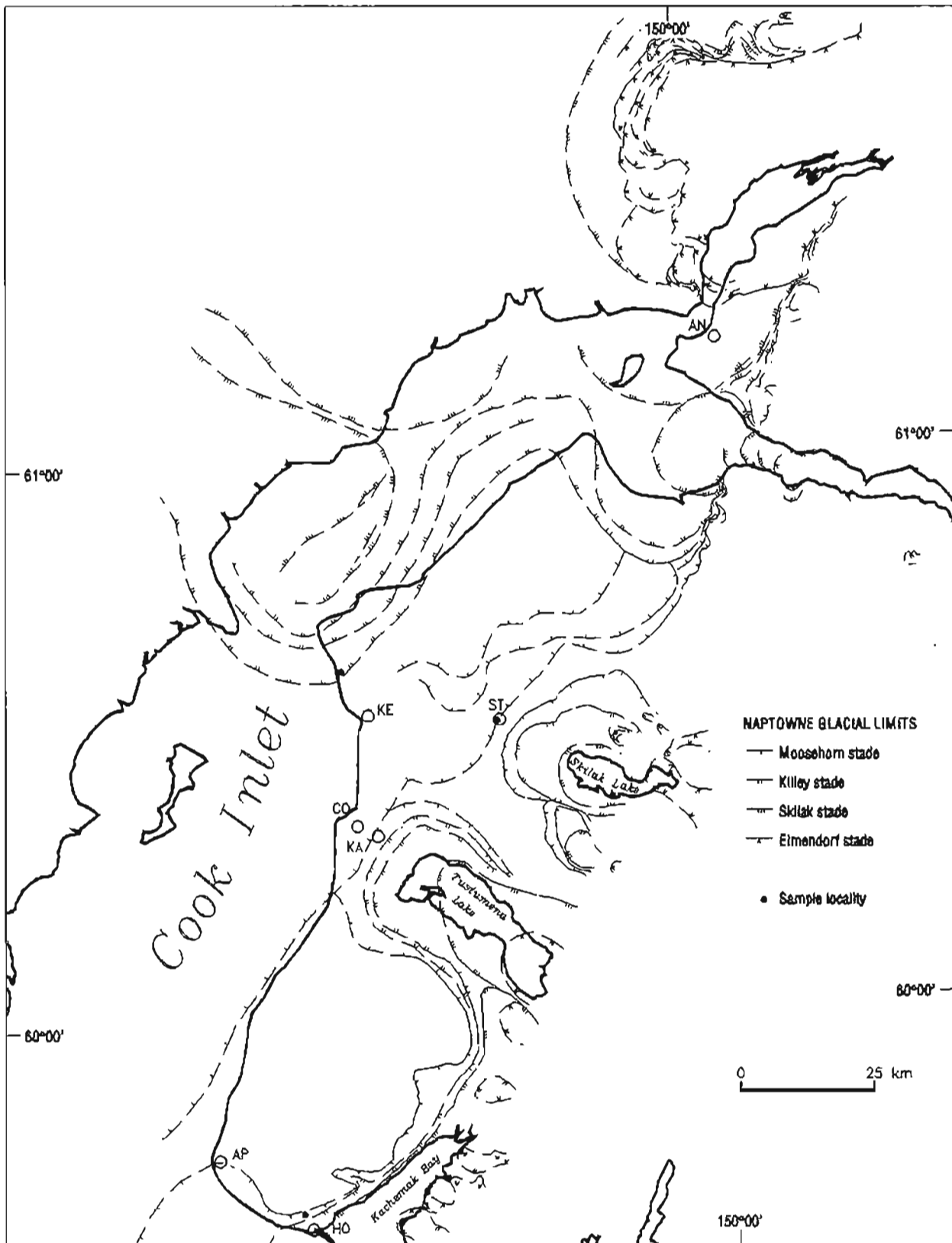


Figure 9. Distribution of tephra 3 samples ( $n = 3$ ) in Kenai Lowland relative to former limits of the Naptowne glaciation. Geographic localities: AN = Anchorage; AP = Anchor Point; CO = Cohoe; HO = Homer; KA = Kasilof; KE = Kenai; ST = Sterling.

Table 7. Similarity-coefficient matrix for samples of tephra 1A collected in Kenai Lowland

	<u>KL-001</u>	<u>KL-020</u>	<u>KL-091</u>	<u>KL-002</u>	<u>KL-093</u>	<u>KL-040</u>	<u>KL-053</u>	<u>KL-003</u>	<u>KL-094p1</u>	<u>KL-090</u>
KL-001	1.00									
KL-020	0.94	1.00								
KL-091	0.96	0.98	1.00							
KL-002	0.96	0.95	0.95	1.00						
KL-093	0.96	0.96	0.97	0.96	1.00					
KL-040	0.95	0.98	0.97	0.94	0.97	1.00				
KL-053	0.95	0.97	0.97	0.93	0.96	0.98	1.00			
KL-003	0.93	0.97	0.96	0.97	0.96	0.96	0.95	1.00		
KL-094p1	0.94	0.97	0.97	0.95	0.95	0.96	0.96	0.97	1.00	
KL-090	0.93	0.96	0.96	0.94	0.97	0.97	0.97	0.96	0.95	1.00

and section 73 (fig. A79), we are convinced that tephtras 1A and 3 are younger than tephtra 1C. However, we are uncertain about the temporal relation of tephtras 1A and 3 and about the relative ages of these two tephtras and tephtra 1B (fig. 3).

Among the tephtras surveyed, sample KL-013p1 of tephtra 3 correlates best with Augustine samples 87A-25A, A88-7-2, and A88-11-2 (Bégét, unpub. data) (SC = 0.95-0.96). Our samples KL-048, KL-049p2, and KL-112p3 could also relate to those proximal Augustine samples but are apparently not from the same tephtrafall (SC = 0.90-0.93).

#### TEPHTRA 4

(MEAN SiO<sub>2</sub> = 75.21 ± 0.31 PERCENT)

Tephtra 4 is identified with varying degrees of certainty in three sections in Kenai Lowland (table 3, fig. 10). Apparently unmixed shards of tephtra 4 (KL-021) were recovered from section 39 (fig. A43), and shards (KL-111) with apparently strong affinity (SC = 0.96) (table 9B) are present in section 7 (fig. A7). However, a radiocarbon date of 11,905 ± 180 yr B.P. (GX-16521) for organic silt just

below sample KL-111 in that kettle filling makes this correlation questionable because of stratigraphic relations in other sections and because of apparently firm correlations elsewhere (unless there is a significant unconformity between the dated organic silt and sample KL-111). The setting in the floor of a kettle indicates that a significant interval of nondeposition or erosion is unlikely. Our best example of tephtra 4 (sample KL-021) unquestionably overlies tephtra 1A in section 39 (fig. A43) and so must be younger than tephtra 1A (fig. 3). A small (n = 7) population of shards attributed to tephtra 4 (KL-094p2) is mixed with obviously redeposited shards of tephtra 1A (KL-094p1) in a layer that overlies apparently undisturbed tephtra 1A in section 58 (fig. A63). This stratigraphic relation also demonstrates that tephtra 4 is younger than tephtra 1A. However, the similarity of sample KL-094p2 and samples KL-021 and KL-111 is low (SC = 0.91 and 0.93, respectively) (table 9B), indicating that they could be part of the same tephtra set but are probably not from the same tephtrafall.

Table 8. Similarity-coefficient matrices for samples of tephtras 1B and 1C collected in Kenai Lowland

A. Tephtra 1B						
	<u>KL-104</u>	<u>KL-016</u>	<u>KL-051</u>	<u>KL-060</u>	<u>KL-044p1</u>	<u>KL-062</u>
KL-104	1.00					
KL-016	0.97	1.00				
KL-051	0.98	0.96	1.00			
KL-060	0.98	0.97	0.97	1.00		
KL-044p1	0.98	0.96	0.97	0.97	1.00	
KL-062	0.98	0.96	0.99	0.97	0.96	1.00
B. Tephtra 1C						
	<u>KL-004</u>	<u>KL-123</u>	<u>KL-049p1</u>	<u>KL-044p2</u>		
KL-004	1.00					
KL-123	0.98	1.00				
KL-049p1	0.97	0.98	1.00			
KL-044p2	0.93	0.94	0.95	1.00		

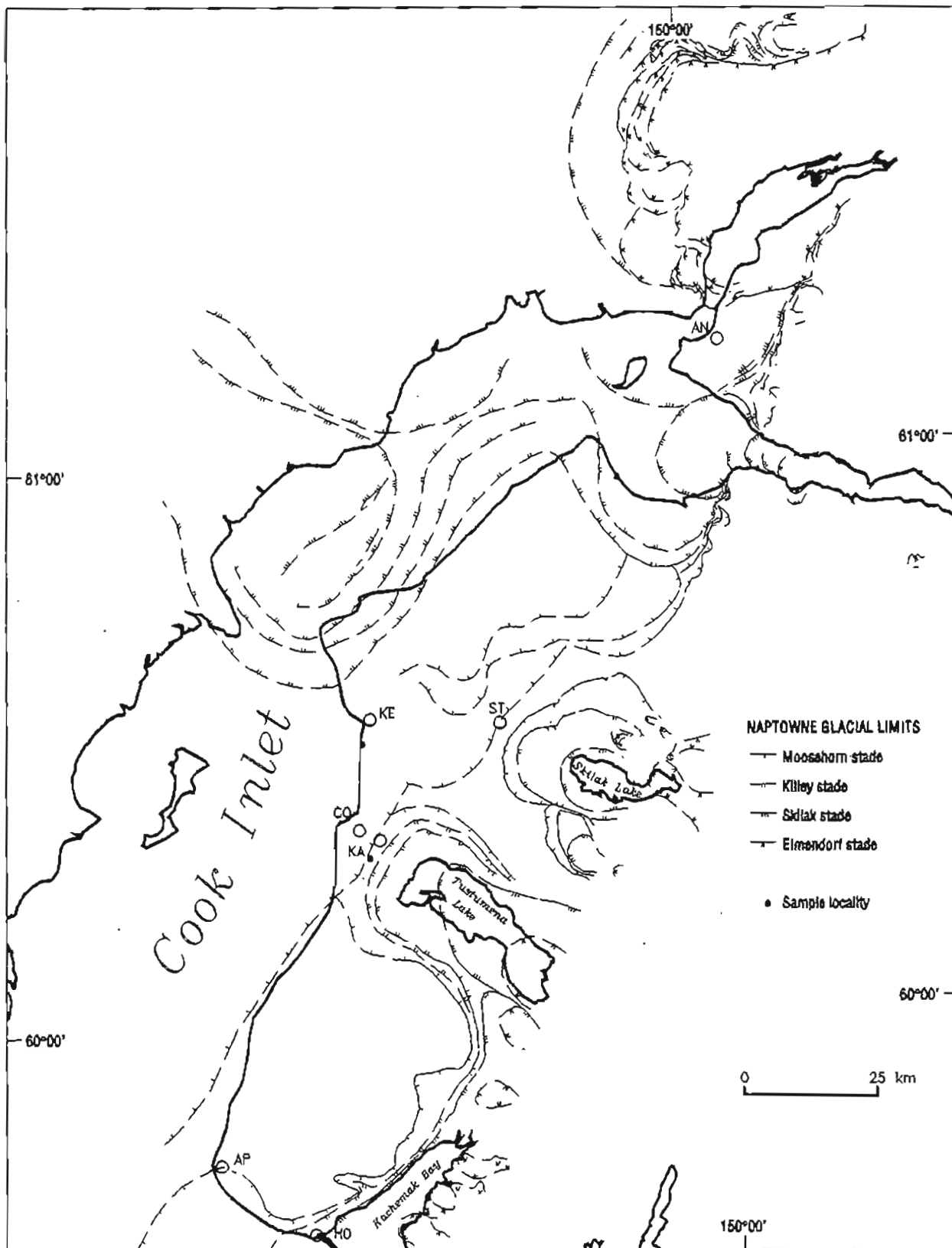


Figure 10. Distribution of tephra 4 samples ( $n = 3$ ) in Kenai Lowland relative to former limits of the Naptowne glaciation. Geographic localities: AN = Anchorage; AP = Anchor Point; CO = Cohoe; HO = Homer; KA = Kasilof; KE = Kenai; ST = Sterling.

Table 9. Similarity-coefficient matrices for samples of tephra 3 and 4 collected in Kenai Lowland

A. Tephra 3				
	<u>KL-112p3</u>	<u>KL-013p1</u>	<u>KL-048</u>	<u>KL-049p2</u>
KL-112p3	1.00			
KL-013p1	0.95	1.00		
KL-048	0.96	0.95	1.00	
KL-049p2	0.95	0.97	0.98	1.00
B. Tephra 4				
	<u>KL-021</u>	<u>KL-111</u>	<u>KL-094p2</u>	
KL-021	1.00			
KL-111	0.96	1.00		
KL-094p2	0.91	0.93	1.00	

Despite its apparently greater age, our sample KL-111 seems to correlate well with samples of the northeastern lobe of the Hayes tephra complex (ATC-636, ATC-637, and 88TL-CC of Begét, Reger, and others, 1991) from the upper drainage of Susitna River (SC = 0.95–0.96). Thus, there could be an unconformity below sample KL-111 (fig. A7). However, without supporting mineralogic evidence, we remain skeptical of this correlation. The northeastern lobe of the Hayes tephra complex has been firmly dated at close to 3,700 <sup>14</sup>C yr B.P. (Riehle, 1985, 1994; Riehle and others, 1990; Begét, Reger, and others, 1991). Sample KL-111 also seems to correlate with samples of both the rhyodacite Devil tephra (SC = 0.95), dated at >1,400 <sup>14</sup>C yr B.P. and <1,900 <sup>14</sup>C yr B.P. (Dilley, 1988), and the lower member of the Watana tephra set (SC = 0.96), dated >1,850 <sup>14</sup>C yr B.P. and <2,800 <sup>14</sup>C yr B.P. (Dilley, 1988). Mineralogical comparisons may resolve this dilemma. Samples KL-021 and KL-094p2 also seem to correlate with the samples from the upper Susitna River drainage (SC = 0.93–0.95), but without supporting mineralogic data, we remain unconvinced.

Another volcanic ash that is possibly correlative with tephra 4 is the ash layer represented by samples A-T1 and B-T1 from peats on low terraces of the Kasilof River and Kenai River, respectively (Combellick and Pinney, 1995). Their samples are geochemically most like Hayes proximal sample 23-A of Riehle (1985) (SC = 0.94–0.95) and could have been deposited as part of the same eastward-moving tephrafall. Combellick and Pinney (1995) dated samples A-T1 and B-T1 at an average age of 3,530 ± 70 <sup>14</sup>C yr B.P., which at 1 σ is identical to the average age of 3,650 ± 150 <sup>14</sup>C yr B.P. reported by Riehle (1985) for the Hayes tephra complex in the region. Comparisons of glass chemistry indicate that sample KL-111 most likely correlates with samples A-T1 and B-T1 (SC = 0.97 and 0.98, respectively); sample KL-021 probably does also (SC = 0.96). However, sample KL-094p2 is less likely to be closely correlative (SC = 0.92–0.93).

Our tephra 4 data leave us in a quandry about correlative tephra, but we tentatively believe that tephra 4 is part of the widespread tephra complex that was erupted from Hayes volcano about 3,700 <sup>14</sup>C yr ago (fig. 3).

#### TEPHRA 5

(MEAN SiO<sub>2</sub> = 73.88 ± 0.58 PERCENT)

We recovered populations of shards attributed to tephra 5 mixed with shards of other tephra in four sections distributed in a narrow, northeast-trending belt in Kenai Lowland (table 3, fig. 11). However, we are not confident that all of these populations represent the same tephrafall; instead they may be part of the same tephra set (SC = 0.92–0.95) (table 10A). As previously discussed, tephra 5 (KL-086p2) and Lethe tephra (KL-086p3) are redeposited and mixed with a younger Crooked Creek tephra (KL-086p1) in section 66 (fig. A71). The degree of redeposition of tephra 5 (if any) is uncertain in section 11 (fig. A11), section 41 (fig. A45), and section 55 (fig. A60), but we are inclined to think that tephra 5 is probably not significantly reworked there. On the basis of previously stated arguments (see Lethe tephra discussion) and stratigraphic relations in sections 41 and 55, we tentatively conclude that tephra 5 slightly postdates Lethe tephra in Kenai Lowland (fig. 3).

Among the tephra surveyed, our sample KL-015p2 correlates best with sample R-J (Riehle, 1985) from Mt. Redoubt (SC = 0.96). Our other three samples are less likely to have been erupted from that volcano (SC = 0.92–0.93).

#### TEPHRA 7?

(MEAN SiO<sub>2</sub> = 73.13 ± 0.41 PERCENT)

We isolated a single, small population of four shards (KL-013p2) from section 16 (fig. A16) that we very tentatively and informally call tephra 7? (table 3). These shards are mixed with a small population (n = 8) of shards that we attribute to tephra 3. Because the degree of redeposition of both tephra is uncertain in this section, we

Table 10. Similarity-coefficient matrices for samples of tephra 5 and 13 collected in Kenai Lowland

A. Tephra 5				
	<u>KL-102p2</u>	<u>KL-086p2</u>	<u>KL-129p1</u>	<u>KL-015p2</u>
KL-102p2	1.00			
KL-086p2	0.95	1.00		
KL-129p1	0.95	0.93	1.00	
KL-015p2	0.95	0.92	0.95	1.00
B. Tephra 13				
	<u>KL-050p2</u>	<u>KL-095p2</u>	<u>KL-032p3</u>	<u>KL-095p3</u>
KL-050p2	1.00			
KL-095p2	0.97	1.00		
KL-032p3	0.96	0.96	1.00	
KL-095p3	0.93	0.94	0.96	1.00

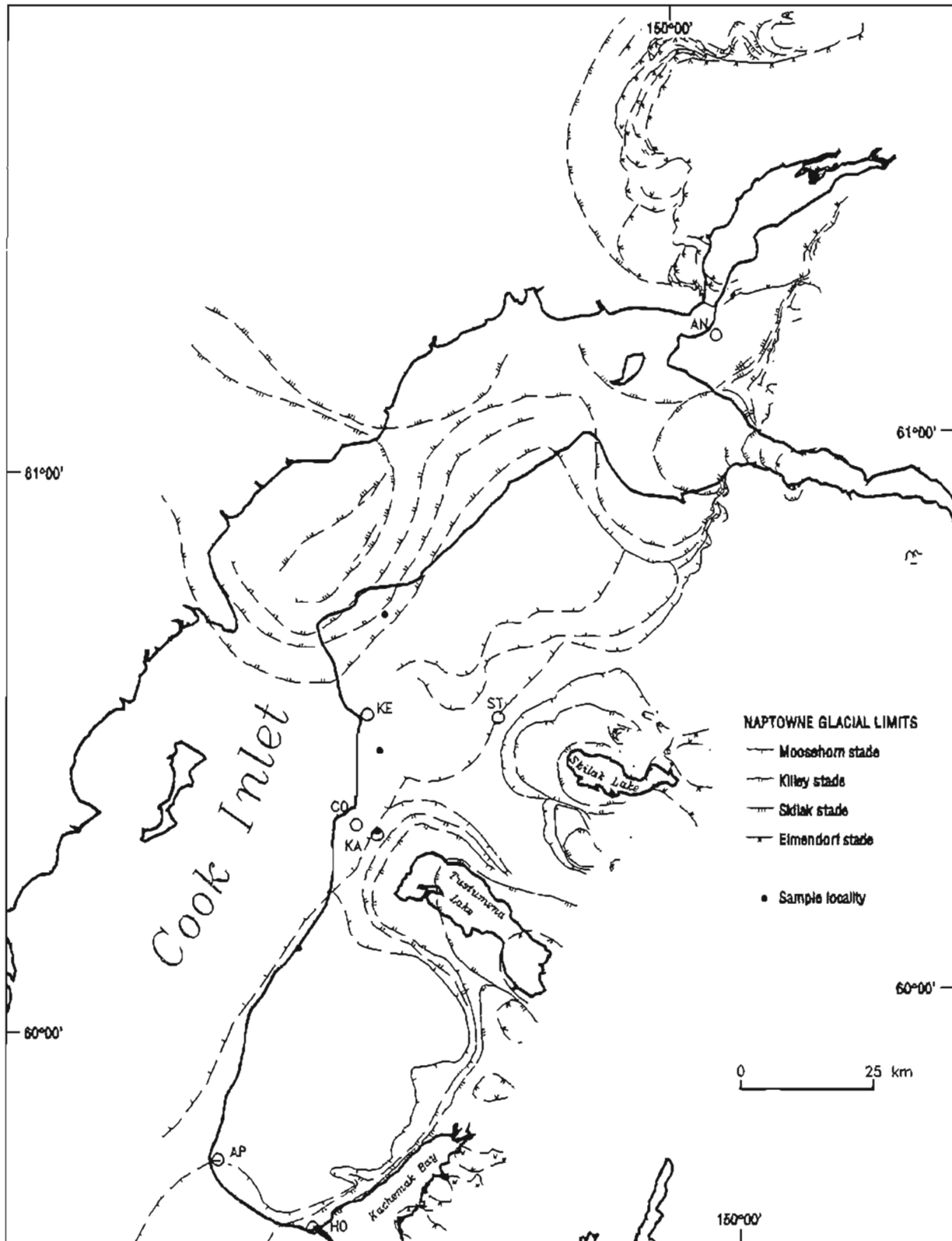


Figure 11. Distribution of tephra S samples ( $n = 4$ ) in Kenai Lowland relative to former limits of the Naptowne glaciation. Geographic localities: AN = Anchorage; AP = Anchor Point; CO = Cohoe; HO = Homer; KA = Kasilof; KE = Kenai; ST = Sterling.

cannot comment with certainty on their relative ages. However, if our few shards actually represent a legitimate tephra, their major-oxide content is comparable to the geochemistry of shards in samples R-EE and R-N (Riehle, 1985) and ATC sample ATC-644 (SC = 0.95–0.97). Our sample conceivably could also correlate with the Oshetna tephra (SC = 0.95), which dates >5,200 <sup>14</sup>C yr B.P. and <5,900 <sup>14</sup>C yr B.P. (Dilley, 1988) (fig. 3). The volcano that produced these samples is not identified.

#### TEPHRA 8?

(MEAN SiO<sub>2</sub> = 71.24 ± 0.45 PERCENT)

As previously discussed, from a depth of 2.6 m in a core (section 25, fig. A25) taken at locality KEN-64 (sheet 2) we isolated a small population (n = 5) of shards (KL-112p2) that we very tentatively and informally call tephra 8? (table 3). The layer of mixed tephra there was deposited after 7,725 ± 210 <sup>14</sup>C yr B.P. (GX-18227), but this is probably not a close maximum age. The setting of section 25 in a peat fen makes redeposition of tephra 8? unlikely. The mixing of this fine-grained volcanic ash with tephra 3 indicates that both are essentially coeval (fig. 3).

Assuming that the geochemistry of these few shards is representative of tephra 8?, we compared it with other tephra in the region. The best match (SC = 0.96) was achieved with sample R-5-E from Mt. Redoubt (Riehle, 1985).

#### TEPHRA 12?

(MEAN SiO<sub>2</sub> = 74.69 ± 0.23 PERCENT)

From section 55 (fig. A60), we collected a very small population (n = 3) of shards (KL-129p2) of a tephra that we very tentatively and informally call tephra 12? (table 3). These shards are mixed with a small population (n = 7) of shards that we attribute to tephra 5 (KL-129p1). Because the degree of reworking is uncertain in this sand-dune setting, we are uncertain of the relative ages of tephra 5 and 12? (fig. 3), but we are convinced that both are younger than the Lethe tephra (KL-128), which is stratigraphically lower in the section (fig. A60).

Our small population of tephra 12? shards compares geochemically with shards of a single sample (R-T) from Mt. Redoubt (Riehle, 1985) (SC = 0.95).

#### TEPHRA 13

(MEAN SiO<sub>2</sub> = 64.69 ± 0.22 PERCENT)

From four layers of mixed tephra in three sections in Kenai Lowland (fig. 12), we isolated four small populations of shards that we informally call tephra 13 (table 3). These shard populations are geochemically distinct and, except for sample KL-095p3, are chemically very similar (table 10B). We believe that samples KL-032p3, KL-050p2, and KL-095p2 represent a single tephra fall (SC = 0.96–0.97) and that sample KL-095p3 is probably part of

the same tephra set—if not part of the same tephra fall (SC = 0.93–0.96).

Although our samples apparently correlate with Oshetna 1 tephra in the upper Susitna River drainage (ATC, unpub. data) (SC = 0.95–0.97), stratigraphic relations cause us to be skeptical. The Oshetna tephra is dated at >5,200 <sup>14</sup>C yr B.P. and <5,900 <sup>14</sup>C yr B.P. (Dilley, 1988), considerably younger than the probable age of tephra 13 in the western Kenai Lowland (fig. 3). Stratigraphic relations in section 22 (fig. A22) indicate that tephra 13 is likely to be older than Crooked Creek tephra, which we date at >7,725 ± 210 <sup>14</sup>C yr B.P. and <8,375 ± 210 <sup>14</sup>C yr B.P. (fig. A25).

### MIDDLE QUATERNARY TEPHRAS

During our investigations of the Goose Bay peat at the type section (sheet 1, locality ANC-22), we encountered numerous thin, discontinuous layers of fine-grained volcanic ash that did not seem to be temporally significant (fig. A3). However, we documented two layers of tephra that are potentially useful for dating and correlation.

#### GOOSE BAY TEPHRA

(MEAN SiO<sub>2</sub> = 65.74 ± 1.03 PERCENT)

Just above the middle of the Goose Bay peat is a relatively thick, pinkish-gray tephra that has consistently cropped out of the bluff face during the past 10 years that we have watched the cliff recede in response to wave attack. This tephra was severely deformed by glacier overpressures during the Naptowne glaciation and probably during previous ice advances (Reger and others, 1995). We informally call this distinctive tephra layer the Goose Bay tephra (fig. A3). Of two samples that we collected from this fine-grained volcanic ash, KL-027 is apparently not significantly contaminated by shards from other tephra (table 3). However, KL-081 contains two populations of shards that are chemically distinct. KL-027 apparently correlates with KL-081p2 (SC = 0.97), indicating that both samples represent the same tephra (table 11A). KL-081p1 is chemically less similar to KL-027 (SC = 0.94) and is even less like KL-081p2 (SC = 0.92), perhaps as a result of multiple eruptions from the same volcano during conditions of changing magma chemistry. We know of no correlative tephra, including the widespread, 141-ka Old Crow tephra in interior Alaska (Westgate and others, 1983, 1990; Westgate, 1988; Begét, Edwards, and others, 1991).

<sup>40</sup>Ar/<sup>39</sup>Ar dating of the Goose Bay tephra by the laser method produced a three-sample (composite) isochron age of 378 ± 0.67 ka (Lager, 1994, written commun.). We believe that this age is the most reliable result of several attempts that we have made in the past to date the Goose Bay peat. A previous, questionable attempt to date the Goose Bay tephra by fission-track counts of 10,000 apatite grains produced a calculated mean age of 92.1 ka with a

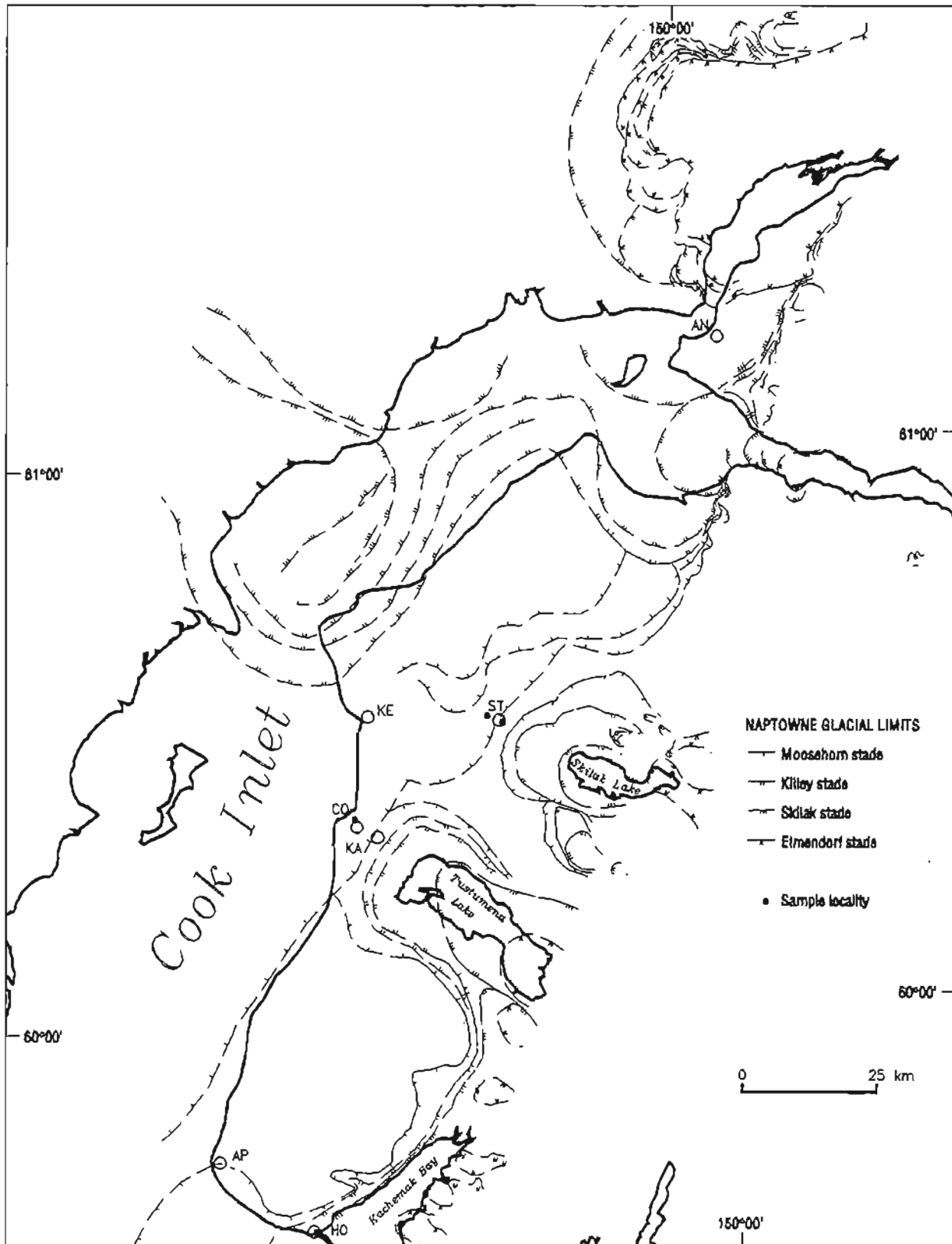


Figure 12. Distribution of tephra 13 samples ( $n = 3$ ) in Kenai Lowland relative to former limits of the Naptowne glaciation. Geographic localities: AN = Anchorage; AP = Anchor Point; CO = Cohoe; HO = Homer; KA = Kasilof; KE = Kenai; ST = Sterling.

**Table 11.** Similarity-coefficient matrices for samples of Goose Bay tephra and Stampede tephra collected from the type section of the Goose Bay peat, locality ANC-22 (sheet 1)

A. Goose Bay tephra			
	<u>KL-027</u>	<u>KL-081p1</u>	<u>KL-081p2</u>
KL-027	1.00		
KL-081p1	0.94	1.00	
KL-081p2	0.97	0.92	1.00
B. Stampede tephra			
	<u>KL-083</u>	<u>KL-082</u>	<u>KL-025</u>
KL-083	1.00		
KL-082	0.99	1.00	
KL-025	0.98	0.97	1.00

95-percent certainty that the actual age is less than 171.2 ka (Riehle, 1989, oral commun.; Zimmerman, 1990, written commun.). However, we could obtain few details on how this result was obtained, so we remain unconvinced that the calculated mean age is reliable. Thermoluminescence analyses of organic silts above and below the Goose Bay tephra in the section produced dates of  $181,300 \pm 18,500$  yr B.P. and  $175,100 \pm 11,500$  yr B.P., respectively (fig. A3), but we consider these results to be unreliable because of uncertainties in the amount of time that the local sediments were saturated. As previously discussed, radiocarbon dating was also unsuccessful because the peat is older than the maximum range of the method.

If the  $^{40}\text{Ar}/^{39}\text{Ar}$  date is reliable, the Goose Bay peat is

middle Pleistocene in age as are the underlying Knik till and associated deposits (fig. A3). This means that the Knik glaciation is much older than envisioned by previous workers (Karlstrom, 1957, 1964; Miller and Dobrovolsky, 1959). The Knik till and overlying lacustrine sediments are paleomagnetically normal, indicating that they are younger than 730,000 yr (fig. A3).

#### STAMPEDE TEPHRA

(MEAN  $\text{SiO}_2 = 77.50 \pm 0.23$  PERCENT)

Stratigraphically underlying the Goose Bay tephra in the lower part of the Goose Bay peat is a thin, light-colored, high-silica tephra couplet from which we collected samples KL-025, KL-082, and KL-083 (table 3, fig. A3). The presence of the two closely spaced layers that form the couplet indicates that two tephrafalls were likely involved, but the very consistent geochemistry among the three samples (SC = 0.97–0.99) indicates that they almost certainly came from the same source (table 11B).

Begét (1992, oral commun.) first correlated this tephra with his Stampede tephra in interior Alaska (Begét and Keskinen, 1991). Comparisons of the glass geochemistry of our samples with Stampede tephra samples ATC-669, ATC-670, and ATC-685 support this correlation (SC = 0.96–0.99). Counts of a small number of glass-coated ferromagnesian grains in our samples (table 12) also compare favorably with counts by Begét and Keskinen (1991, table 4), although they differ slightly. We document slightly less hornblende and did not find biotite or rutile. We believe that our high similarity-coefficient values and our very similar ferromagnesian counts are permissive if not conclusive evidence for the correlation suggested by Begét.

**Table 12.** Abundances of glass-coated ferromagnesian grains in three tephra samples from the lower Goose Bay peat, locality ANC-22 (sheet 1)

A. Actual grain counts					
Tephra sample	cpx	Number of grains counted <sup>a</sup>		Total	Frequency (%) cpx:opx:hbd
		opx	hbd		
KL-025	2	15	3	20	10:75:15
KL-082	5	15	12	32	16:47:37
KL-083	4	6	8	18	22:33:45
<b>TOTAL</b>	<b>11</b>	<b>36</b>	<b>23</b>	<b>70</b>	<b>—</b>
B. Relative-abundance classes <sup>b</sup>					
Sample	cpx	opx	hbd		
KL-025	S	A	S		
KL-082	S	C	C		
KL-083	S	C	C		

<sup>a</sup>Abbreviations: cpx = clinopyroxene; opx = orthopyroxene; hbd = hornblende.

<sup>b</sup>Classes indicate relative grain contents in the populations counted: A = abundant (>50 percent); C = common (30–50 percent); S = scarce (10–30 percent).

Assuming that the  $^{40}\text{Ar}/^{39}\text{Ar}$  age of the Goose Bay tephra is correct and that correlation of the lower tephra couplet with the Stampede tephra is valid, evidence in the Goose Bay section demonstrates that the Stampede tephra is slightly older than  $378 \pm 0.67$  ka but is middle Quaternary in age (fig. A3). Deformation of Stampede tephra during the Lignite Creek glaciation in Nenana River valley (Begét and Keskinen, 1991) had to occur later in middle Quaternary time in the type area of the Lignite Creek glaciation (Thorson, 1986).

## FOSSILS

We collected fossils from late Quaternary deposits in the eastern and northern Cook Inlet region with the intent of dating the sediments and gathering information on depositional conditions. A total of 12 macrofossil assemblages were collected from the Bootlegger Cove Formation (BCF) (table 13).

### MIDDLE INLET COLLECTIONS

BCF collections F4 and F5 from the Kenai-Kalifornsky area along the eastern shore of Cook Inlet are depauperate in species compared to collections from upper Cook Inlet. Generally, only scattered, broken, calcareous barnacle plates were found, although rare whelk shells were recovered at Kenai. Large barnacle plates are identified as *Balanus evermanni* in the Kenai section (fig. A20). This robust barnacle is typically found living in deep marine waters in Prince William Sound, where tidal currents are

strong (Foster, 1994, oral commun.). A sample of silty sand and one of pebbly diamicton from the Kenai section were submitted for microfossil analysis, including determination of their foraminiferal, ostracod, and diatom contents. The sand sample was barren, and in the diamicton a single *Diatoma* sp. was identified (Micropaleo Consultants, Inc., 1993, written commun.). We believe that this specimen is probably recycled from Tertiary rocks in the Cook Inlet Basin and has no Quaternary significance. The stratigraphy at Kenai indicates that *B. evermanni* lived on the surface of a sandy submarine fan in front of a tidewater glacier. This fan was overridden when the glacier advanced south-eastward, and the saturated fan sediments were folded and faulted (fig. A20) when the base of the tidal glacier came into contact with the inlet bottom. The tidal range is up to 9 m at Kenai, and we speculate that contact occurred during low tides. Dating of the *B. evermanni* plates demonstrates that the tidal glacier was at Kenai shortly after  $16,480 \pm 170$   $^{14}\text{C}$  yr B.P. (tables 2 and 14), during the Killey stage of the Naptowne glaciation (Reger and Pinney, 1996). This important section also demonstrates that a marine connection existed between middle Cook Inlet and the North Pacific Ocean as early as 16,500  $^{14}\text{C}$  yr ago.

The meager BCF macrofauna (F5) from the bluff at Kalifornsky consists of rare, broken barnacle plates (table 13), which we date at  $16,000 \pm 150$  and  $16,090 \pm 160$   $^{14}\text{C}$  yr B.P. (tables 2 and 14). Schmoll and Yehle (1983, 1986, loc. B5) and Schmoll and others (1984, loc. B7) reported a date of  $16,340 \pm 140$   $^{14}\text{C}$  yr B.P. (W-4937) for *Balanus* sp. plates from silt and clay assigned to BCF in the Kalifornsky beach bluff but did not provide specific

Table 13. Composition of macrofossil collections from the Bootlegger Cove Formation in the middle and upper Cook Inlet region

Species	Macrofossil collection <sup>a</sup>											
	F1 <sup>b</sup>	F2	F3	F4	F5	F6 <sup>c</sup>	F7	F8	F9	F10	F11	F12
Class Pelecypoda												
<i>Clinocardium ciliatum</i>	X	X	X	-	-	-	X	X	-	-	-	-
<i>Hiatella arctica</i>	X	X	X	-	-	-	X	X	X	X	X	X
<i>Macoma balthica</i>	X	X	X	-	-	X	X	X	X	X	X	X
<i>Macoma calcarea</i>	-	-	-	-	-	-	-	-	-	-	X	-
<i>Mya truncata</i>	X	-	X	-	-	X	-	X	X	X	X <sup>d</sup>	X
<i>Nuculana fossa</i>	-	X	X	-	-	-	-	X	-	-	-	-
Class Gastropoda												
<i>Buccinum cf. glaciale</i>	-	X	X	X	-	-	-	-	-	-	-	-
<i>Natica clausa</i>	-	X	-	-	-	-	-	-	-	-	-	-
Class Cirripedia												
<i>Balanus</i> sp.	X	X	X	-	X	-	-	-	-	-	-	-
<i>Balanus evermanni</i>	-	-	-	X	-	-	-	-	-	-	-	-

<sup>a</sup>See table 1 and sheets 1, 2, 4, and 5 for locations of sample sites.

<sup>b</sup>Locality D of Schmoll and others (1972).

<sup>c</sup>Mile 99.5 Seward Highway locality of Bartsch-Winkler and Schmoll (1984, p. 29)

<sup>d</sup>In growth position in marine clay with some silt and numerous dropstone pebbles.

**Table 14.** Radiocarbon ages of macrofossil collections from the Bootlegger Cove Formation in the middle and upper Cook Inlet region

Fossil collection <sup>a</sup>	Map index number <sup>a</sup>	Radiocarbon age ( <sup>14</sup> C yr B.P.)	Laboratory number	Source
F1	ANC-33	13,750 ± 500	W-2389	Schmoll and others (1972, loc. D)
F2	ANC-36	14,300 ± 140	AA-2226 <sup>b</sup>	Reger and others (1995, loc. I)
F3	ANC-39	14,100 ± 90	GX-19989 <sup>b,c</sup>	Reger and others (1995, loc. K)
F4	KEN-53	16,480 ± 170	WSU-4304 <sup>c</sup>	This study
F5	KEN-103	16,000 ± 150	GX-16528 <sup>b,c</sup>	This study
		16,090 ± 160	GX-16527 <sup>b,c</sup>	
F6	SEW-3	14,290 ± 140	GX-16524 <sup>b,c</sup>	Reger and others (1995, loc. X)
F7	SEW-4	13,718 ± 160	GX-20129 <sup>b,c</sup>	Reger and others (1995, loc. U)
F8	SEW-7	14,160 ± 140	GX-16529 <sup>b,c</sup>	Reger and others (1995, loc. V)
F9	SEW-8	14,200 ± 100	GX-17133 <sup>b,c</sup>	Reger and others (1995, loc. W)
F10	TYO-8	13,994 ± 90	GX-20127 <sup>b,c</sup>	Reger and others (1995, loc. P)
F11	TYO-9	13,470 ± 120	AA-2227 <sup>b</sup>	Reger and others (1995, loc. N)
F12	TYO-10	14,078 ± 214	GX-20128 <sup>b,c</sup>	Reger and others (1995, loc. M)

<sup>a</sup>See table 1 and sheets 1, 2, 4, and 5 for locations of sample sites.

<sup>b</sup>Atomic-mass-spectrometer (AMS) date.

<sup>c</sup>Sample corrected for natural isotopic fractionization based on <sup>13</sup>C content.

coordinates. We assume that their locality is the same as our section 45 (fig. A50) or close to it because this is the only BCF section in which we found barnacle plates along Kalifornsky beach. From section 45 we submitted five samples of sandy mud for analysis of their foraminifera, ostracod, and diatom contents in an effort to reconstruct conditions during BCF deposition. No ostracods or diatoms were found in any of the samples. Only one sample contained rare *Elphidium incertum* (three juveniles) and *Bucella cf. frigida* (two juveniles) (Micropaleo Consultants, Inc., 1991, written commun.). From this preliminary test we conclude that very cold glacioestuarine conditions of variable turbidity and salinity probably existed in middle Cook Inlet about 16,000 <sup>14</sup>C yr ago. The stratigraphy in section 45 (fig. A50) indicates that debris-laden icebergs probably floated at least as far south in Cook Inlet as the Kalifornsky area 16,000 <sup>14</sup>C yr ago and, as they melted, they rained silt, sand, and occasional dropstones onto the inlet floor, burying the barnacle plates. Like at Kenai, these plates were not found in growth positions but were probably swept along the bottom by strong tidal currents. Soft-sediment deformation of laminated clayey silts at the base of the bluff near the section indicates that the icebergs dragged their keels during low tides. Overturning of folds toward the southeast indicates that the icebergs were moving from the northwest at the time. However, this deformation does not necessarily reflect the ultimate source of the glacier ice; it could result from berg movement in response to tidal currents or wind, or both.

From the extensive exposure near the mouth of Kasilof River (sheet 2, loc. KEN-117), we submitted two samples of pebbly diamicton for microfossil analysis. Both samples

contained very rare to rare diatoms identified as *Tetracyclus cf. lacustris*, *Diatoma?* sp., *Pinnularis* sp., and *Melosira granulata* (Micropaleo Consultants, Inc., 1993, written commun.) (fig. A57). All are freshwater diatoms. Plafker (1956) found *Tetracyclus*, *Pinnularis*, and *Melosira* in diatomaceous earth of Holocene age north of Kenai, where *Melosira* is particularly abundant. We believe that the section at the mouth of Kasilof River was deposited in a very cold freshwater conditions and could slightly predate the section at Kalifornsky.

#### UPPER INLET COLLECTIONS

Macrofossils were collected from the BCF at 10 sites in the bluffs along Knik Arm and Turnagain Arm (table 13). These collections are dominated by up to six species of pelecypods, and minor elements include two species of gastropod and unidentified barnacle plates. With the exception of *Mya truncata* valves in collection F11 (table 13), which were collected in pairs in growth position in a silty clay with numerous pebble dropstones, we cannot verify that our macrofossils lived where they were found. Indeed, we postulate that, for a brief time after their deaths, most faunal remains would have been transported from their living sites on the bottom of upper Cook Inlet by strong tidal currents. Collections of unidentified mollusk shells from the macrofossil-rich zone in upper BCF in the Knik Arm and Turnagain Arm area are reported by Schmoll and others (1972), and a single collection of unidentified shells is reported from the thick BCF exposure near the mouth of Beluga River in western upper Cook Inlet (sheet 5, loc. TYO-7) (Schmoll and others, 1984; Schmoll and Yehle,

1986). Our BCF fauna from upper Cook Inlet is rich in species compared to the modern *Macoma balthica* fauna, which has probably existed in upper Cook Inlet for at least 6,000 <sup>14</sup>C yr (Bartsch-Winkler and others, 1983; Bartsch-Winkler and Schmoll, 1992; Combellick and Reger, 1994, loc. 92-20). With the exception of *M. balthica*, extant species of pelecypods represented in the BCF fauna are not known north of Kachemak Bay in lower Cook Inlet (Science Applications, Inc., 1977; Baxter, 1983; Foster, 1991; Kimker, 1994, oral commun.). There and in western lower Cook Inlet, they live in clear, locally turbulent marine waters. *Hiatella arctica*, *Macoma balthica*, *Macoma calcarea*, and *Mya truncata* persist in a variety of habitats from intertidal and sublittoral zones to depths of hundreds or even thousands of meters (Baxter, 1983; Foster, 1991). *Macoma balthica* has a great tolerance for both turbid waters and a broad range of salinities and is the only species of clam that tolerates the brackish, turbid conditions on tidal flats in upper Cook Inlet. *M. calcarea* also tolerates a broad range of salinities but lives in less turbid waters (Foster, 1994, oral commun.). Thus, the relatively complex macrofauna indicates that, at least during deposition of the macrofossil-rich zone of the upper BCF, waters in upper Cook Inlet were probably less turbid and more saline than the estuarine waters there today, even though the widespread presence of dropstone-rich facies indicates the presence of tidewater glaciers (Reger and others, 1995). We speculate that conditions in upper Cook Inlet then were similar to present conditions in some of the fjords along the coast of southcentral and southeastern Alaska, except that the waters were more tide dominated.

Schmidt (1963) first reported marine foraminifera and ostracods from the shell-rich zone on the south side of Knik Arm near locality ANC-43 (sheet 1). Freshwater microfossils are reported from several BCF zones in the Anchorage area (Schmoll and Yehle, 1986). Most workers agree that the microfauna in various parts of the BCF indicate widely variable conditions of salinity, but no systematic, intensive study of the distribution of BCF microfossils has been published.

Dating of the BCF proper in upper Cook Inlet is restricted to the shell-rich zone in the upper part of the formation. Shells of marine mollusks from this zone range in age from a minimum of 13,470 ± 120 <sup>14</sup>C yr B.P. (table 14, F11) to 14,900 ± 400 <sup>14</sup>C yr B.P. (table 2, C79). Schmoll and Yehle (1986) reported an age of 14,350 ± 200 <sup>14</sup>C yr B.P. for marine mollusk shells from BCF near the mouth of Beluga River (table 2, C78). Organic silt at the base of freshwater peat overlying BCF on Fire Island is 12,250 ± 140 <sup>14</sup>C yr old (table 2, C57), providing a firm minimum age for BCF in the upper Cook Inlet region.

## SOIL PROFILES

Soil development was considered important evidence

for assigning ages to moraines in the Cook Inlet region by Miller and Dobrovolsky (1959) and Karlstrom (1964). To evaluate the validity of their faith in this relative-age parameter, we briefly examined soil profiles on Naptowne moraines in three different parts of the region. The ages of these moraines were determined by physiographic and stratigraphic evidence other than soils. To minimize variations in rates of soil development due to different topographic position (Birkeland and others, 1991a; Berry, 1994), we measured profiles on flat summits of large moraines, except for the rounded crest of the small 9,900-yr-old moraine in Turnagain Pass (table A9).

The soils that are developed on the moraines in the areas we studied are spodosols. During profile formation (podzolization), leaching by organic acids results in development of a subsurface spodic (B) horizon by the down-profile translocation of a complex of iron, aluminum, manganese, clays, and organic matter (Rieger, 1983; Birkeland, 1984). This horizon is enriched in clays and iron sesquioxides or humic iron sesquioxides that initially result in a yellowing of the B horizon and later in reddening and brightening as more and more of these compounds accumulate as grain coatings, bridges, and cements. Where leaching is advanced in the upper part of the spodosol profile, removal of iron and aluminum by fulvic and other humic acids produces a very light colored albic (E) horizon just beneath the mat of surface vegetation.

## STERLING PROFILES

Our objective in documenting soil profiles in the type area of the Naptowne glaciation (Karlstrom, 1964) was, if possible, to establish a Naptowne chronosequence that we could relate to the entire Kenai Lowland.

The youngest profile, S3, was measured in a pit close to section 44 (fig. A48) at 89 m elevation on the flat crest of the type Skilak moraine (sheet 2, loc. KEN-101). The section exposed 54 cm of loess overlying 8 cm of sandy pebble-gravel till of Skilak age. There is some local frost disturbance in the loess, and pebbles are thinly capped with silt and clay, demonstrating some minor downward migration of silt and clay through the profile. The E horizon is as thick as 6 cm (fig. A49, table A5). Depth to the bottom of the B horizon is 17 cm. The moist field color of the Bs subhorizon is a light olive brown, and there is a slight increase in the content of silt and clay over subhorizon Bw<sub>2</sub> (fig. A49). Both silt and clay gradually decrease downward through the profile.

The intermediate profile, S1, was measured at 101 m elevation on the flat crest of the type Killey moraine (sheet 2, loc. KEN-79). Our soil pit was dug about 10 m south of section 31 (fig. A33), and the eolian sand layer is missing. Instead, 28 cm of loess overlies a sandy and pebbly till of Killey age. In this profile, silt-clay caps are weakly developed on pebbles through the entire section,

demonstrating the presence of illuvial silt and clay in the profile (fig. A34). Differentiation of the B subhorizons is slightly more progressed in the Killey-age profile than in the Skilak-age profile, and they are slightly thicker (fig. 13). Comparison of the Bs horizons in both soils demonstrates that the hue in the Killey-age profile (10YR) is slightly more reddish than in the Skilak-age profile (2.5Y) (tables A4 and A5). Profile S1 has a markedly higher clay content and has the highest content of visible volcanic ash of the three sections studied.

The oldest Naptowne-age profile (S2) was documented at 91 m elevation on the flat crest of the type Moosehorn moraine (sheet 2, loc. KEN-80). The test pit was dug about 5 m from the pit in which section 32 (fig. A35) was measured. The loess cover is 13 cm thinner in the soil test pit. Silty pebble coatings are present throughout the section (fig. A36). There is incipient ped development in horizon Bs, which definitely has a more reddish hue (5YR) than the Bs horizon in the Killey-age profile (10YR) (tables A3 and A4). However, the bottoms of the B horizons are at about the same depth in both soils.

These three profiles are located in equable conditions of loess rain, materials (same till source), climate, vegetation, and there has been a history of fairly frequent wildfires. The main difference between the profiles should be the time of soil formation. However, we are not satisfied that our three Naptowne-age profiles constitute a reliable chronosequence. The Moosehorn-age profile (S2) appears to be very young for a soil that has been developing for about 18,000 <sup>14</sup>C yr (Reger and Pinney, 1996). We suspect that this profile has been truncated at some time in the past and is more representative of a profile that is intermediate in age between a Skilak profile and a Killey profile. This complex history may explain the inconsistent development of soil parameters among the three profiles (fig. 13). The magnitude and intensity of frost disturbance of the loess especially is an unevaluated condition that complicates profile development. The presence of at least one tephra layer in the Bw horizon of the Killey-age profile (table A3) and the likely presence of tephtras in loess in the other profiles also complicates profile interpretation. Clearly, more profiles need to be documented and evaluated before a reliable chronosequence can be developed.

### KACHEMAK BAY PROFILES

Profile S4 was documented in a test pit at 123 m elevation on the flat crest of the lobate moraine built by the Moosehorn advance of the Kachemak Bay lobe just south of Anchor River (Reger and Petrik, 1993) (sheet 3, loc. SEL-7). This pit was dug near section 72 (fig. A77) and exposed 62 cm of loess, tephtras, and redeposited tephtras over sandy drift (fig. A78). The E horizon is 2 to 10 cm thick, and the B horizon is strongly differentiated with Bw,

Bs, and Bhs subhorizons that range in moist colors from reddish brown to very dusky red (table A6). However, this color change is complicated by the presence of volcanic ash in subhorizon Bs. In fact, the entire profile, with its multiple soils and numerous tephtras, is complicated and difficult to interpret.

We measured profile S5 at 342 m elevation on the crest of the lateral moraine of the Moosehorn advance of the Kachemak Bay lobe (sheet 3, loc. SEL-13). The test pit was excavated close to the pit where we had earlier measured section 93 (fig. A79). The soil pit exposed 61 cm of loess and tephtras over sandy drift, but the profile, although complicated by the presence of a buried soil, is simpler than profile S4. The E horizon in profile S5 is discontinuous and up to 3 cm thick (fig. A80, table A7). Development of the B subhorizons is well advanced in both the surface and buried soils. In the buried soil, the Bhs subhorizon has a very dusky red moist color, and there is no recognized Bw subhorizon. In the surface soil, the Bhs subhorizon is also very dusky red, and the Bw subhorizon is dark reddish brown.

Comparison of the two soil profiles studied near Homer with soil development in the type area of the Naptowne glaciation is complicated by a higher rate of loess influx (including significant volcanic effluents), buried soils, different vegetation, and a much wetter climate with cloudier, slightly cooler summers in the Homer area. Wildfire frequency in the coastal rainforest, which is dominated by Sitka spruce, is undoubtedly much lower than in the mixed woodland of black and white spruce and hardwoods, which indicates a modified continental or continental climate in the Sterling area. The higher production of organic acids in the Homer area, due to greater rainfall and a more persistent, lush vegetation, is indicated by (a) the presence of Bh and Bhs subhorizons in the Moosehorn-age soils there and (b) the absence of these subhorizons in the Moosehorn profile (S2) in the Sterling area.

### TURNAGAIN ARM PROFILES

We recorded soil profile characteristics at two localities in the vicinity of Turnagain Arm. Soil profile S6 (fig. A83, table A8) was measured at an elevation of 25 m on the flat crest of the Elmendorf-age Bird Creek moraine, which is close to 14,000 <sup>14</sup>C yr old (Reger and others, 1995) (sheet 4, loc. SEW-2). In this profile, podzolization is slightly more advanced than in the slightly older Skilak-age profile (S3) in the Sterling area. In the Elmendorf-age soil, the Bs subhorizon is 5 cm thicker and slightly redder (table A8) than the Bs subhorizon in the Skilak-age soil (table A5)—yet the parent tills for both soils are derived from the same terrane and have an unweathered olive-

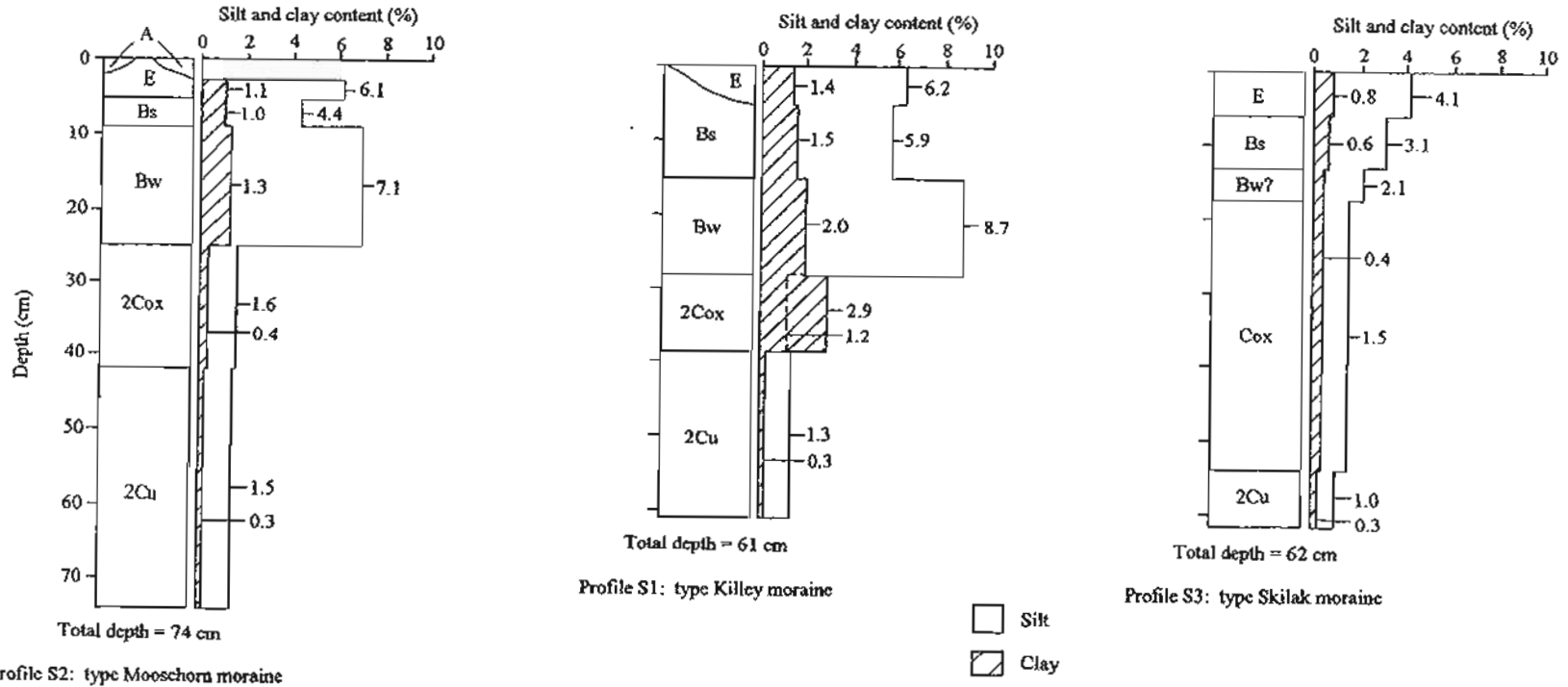


Figure 13. Comparison of soil profiles developed on type Moosehorn, Killey, and Skilak moraines in the type area of the Naptowne glaciation. Numbers for silt and clay content given to 0.1 percent to show values <1 percent. Soil horizon terminology slightly modified from system proposed by Birkeland and others (1991b).

gray color. The Bs subhorizon in profile S6 could be disturbed by frost action.

Soil profile S7 (fig. A84, table A9) was documented at an elevation of 297 m on the crest of a small 9,900-yr-old moraine of latest Elmendorf age in Turnagain Pass in the Kenai Mountains (sheet 4, loc. SEW-12). This is the youngest profile that we documented. Development of the spodic horizon is very advanced, as indicated by significant reddening and darkening of the B subhorizons compared to the olive gray of the parent till (table A9). The degree of change in hue in the Bhs and Bh subhorizons in profile S7 exceeds the greatest color change in the oldest Moosehorn-age soil in the Sterling area, and the B horizon is 18 cm thicker (table A3). Silt and clay caps are present in the Bhs, Bw, and Cox subhorizons. In the Bw subhorizon, the caps are a very bright dark-reddish brown and are moderately thick. Mottling of the Cox subhorizon could be due to frost action.

Soil horizons are strongly differentiated in profiles S6 and S7, which are younger than the profiles we measured on older moraines in Kenai Lowland. In our opinion, this strong horizon development reflects the very moist maritime climate of the Kenai Mountains. Burned spruce stumps at the site of profile S6 and small-diameter trees in the mixed conifer and hardwood woodland there are evidence of a fairly recent wildfire. Well-developed Bh and Bhs horizons demonstrate that humic-acid production has been intense beneath the subalpine vegetation at the site of profile S7, which is the younger of the two sites. Fire frequency at profile S7 was undoubtedly very low—if not zero—during the Holocene, so plant cover has probably remained generally undisturbed in Turnagain Pass. Precipitation increases dramatically with elevation in Alaska's coastal mountains, so there was almost certainly adequate moisture for producing considerable fulvic acid in Turnagain Pass.

## DISCUSSION

Comparison of hue and chroma values for horizons in profiles on the type Skilak, Killey, and Moosehorn moraines (tables A3-A5) clearly shows progressive reddening (changes of one to four hue units) and brightening (changes of one to six chroma units). As previously stated, interpretation of these values in two Moosehorn-age profiles in the Kachemak Bay area (tables A6 and A7) is difficult because of the complex stratigraphy and complicated histories of soil formation and loess deposition. However, differences of up to five hue units and five chroma units in horizons compared to the parent material indicate significant profile development. Two profiles of latest Wisconsin age in the vicinity of Turnagain Arm (tables A8 and A9) show remarkable reddening (changes of two to five hue units) and brightening (changes of one to five

chroma units) despite their youth relative to other Naptowne profiles. Clearly, rubification is locally progressive in older soil profiles of Naptowne age. However, we did not record dry soil color and could not calculate rubification indexes (Harden, 1982) for the seven profiles that we document. Complex local stratigraphy and the presence of numerous tephra in the profiles also frustrated our calculations of profile development indexes (Harden, 1982).

Our documentation of soil profiles in these three areas and casual observations of soils and vegetation elsewhere in the study region convince us that significant environmental gradients have existed in the past and still persist, even locally. These gradients affect rates of soil formation and seriously complicate the use of soils to date landforms. Because climate and vegetation are relatively continental in the area of the type Naptowne moraines and relatively maritime near the Cook Inlet coast and because annual precipitation increases with elevation (especially in the Kenai Mountains), rates of soil development are faster near the coast and at higher elevations than in low-level inland sites. Moraines that are known to be of the same age based on physiographic and stratigraphic relations bear very different soils in different areas.

## TILL-SOURCE STUDY

During the last major glaciation of Cook Inlet, ice entered the basin from centers of snow accumulation in the surrounding uplands, including the Kenai Mountains, the Chugach Mountains, the Talkeetna Mountains, and the Alaska-Aleutian Ranges (Schmoll and others, 1984, fig. 5). Sources of the resulting glacial deposits are obvious in the mouths of glaciated valleys or in moraines that are clearly related to nearby uplands. However, the dynamics of former glaciers were very complicated in parts of the upper Cook Inlet trough—for example, in the Swanson River-Moose River area—where ice could have come from several directions, depending on glaciological conditions in the uplands or conditions in the area of deposition. As a further complication in these areas, there likely was overriding and reworking of deposits from a given source by ice from other sources as conditions changed in ice-accumulation areas and in the basin of deposition.

Karlstrom (1964, plates 3 and 4) first plotted the distributions of moraines in the Cook Inlet trough and showed his interpretation of the extents of ice lobes from different sources by designating interlobate and other moraines. Our model of the Naptowne glaciation in this region evolved primarily from the study of landform distribution and interrelations and from stratigraphic evidence (Reger and Pinney, 1996). We commonly disagree with Karlstrom's (1964) interpretations of the ages and sources of various moraines, particularly in areas such as the northeastern Kenai Lowland, where landforms are

complex and till source is questionable. To test the validity of our model and develop a better understanding of the Naptowne glaciation, we collected 109 till samples and 92 collections of till pebbles to provide sedimentologic evidence that is independent of the evidence on which our model was developed. We reasoned that the compositions of the fine fractions and pebbles of the till samples reflect rock types in the source areas of the glaciers that deposited the tills.

## METHODOLOGY

During till sampling, great care was taken to collect only those samples that are not modified by running or standing water. Thus, we generally bagged basal tills and not ablation tills, and we tried to collect both matrix material and pebbles at each sample site, although this was possible at only 85 localities (table 1). Bag samples of till matrix were first sieved into six size fractions, and then, after weighing, we measured the total isotropic magnetic susceptibility of each size fraction. Work by Vonder Haar and Johnson (1973) and Gravenor and Stupavsky (1974) demonstrated that isotropic magnetic susceptibility, which is a function of the amount of ferromagnetic minerals (generally magnetite) in the sample, is useful for classifying and correlating tills. Chernicoff (1984) used isotropic magnetic susceptibility to establish the provenance of two tills in Minnesota. Our till-matrix experiment is based on the premise that isotropic magnetic susceptibility provides a reliable indirect measure of bedrock types in the source areas of the tills in the Cook Inlet trough.

Weights of magnetic-susceptibility samples were measured on a Mettler Electronic Scale, model PE-200, which has a capacity of 0.01 to 120 gm. Initially, three readings of the total magnetic susceptibility were made of each matrix sample by using a Bartington Instruments Magnetic Susceptibility Meter, model M.S. 2, and a Bartington Instruments Sensor, type M.S. 2B, which has a dual frequency. These readings were taken on the low-frequency setting, which provides readings in CGS units and has a scale factor of 0.1. Next, the means of the three initial readings were calculated. Because values measured by the instrument vary with the volume of the sample (which controls the number of ferromagnetic mineral grains present) and not all samples had the same volumes, we standardized mean magnetic-susceptibility readings to absolute units per gram of sample (table 15).

Pebble collections were initially washed and then each pebble was broken to expose a fresh surface. The lithology of each pebble was assigned to one of four general categories (table 16). We propose that the lithology of till pebbles provides a second reliable indicator of bedrock types in till-source areas.

On the basis of its location, each sample was initially

assigned by the proposed model to a particular source area. Most samples from the Talkeetna Mountains, Matanuska Valley, Chugach Mountains, Turnagain Arm, and Kenai Mountains were considered to be unambiguous because they were collected from moraines clearly related to these areas. However, only 23 of 48 till-matrix samples (48 percent) and 18 of 45 pebbles collections (40 percent) were clearly derived from the west side of Cook Inlet. For simplicity, in the glaciation model to be tested the majority of samples that were collected in Kenai Lowland outside of moraines obviously related to the west side of Cook Inlet and to the Turnagain Arm and Skilak Lake lobes (sheet 2 and table 1) were arbitrarily and questionably assigned to the west side of Cook Inlet. Samples of uncertain affinity were also collected from the "interlobate area" of the Matanuska-Knik lobe (Reger and Updike, 1983a), and other ambiguous samples were questionably assigned to Turnagain Arm and Kenai Mountains.

## INITIAL RESULTS AND ANALYSIS

Our analysis began with a calculation of mean values and standard deviations for the collections of samples from each source area (tables 17 and 18). Next, simple plots were made to relate the magnetic susceptibilities of till-matrix collections representing the six unambiguous source areas. Among these collections, mean magnetic susceptibilities clearly differentiate three groups of sources: (a) west side of Cook Inlet, (b) Talkeetna Mountains-Matanuska Valley, and (c) Chugach Mountains-Turnagain Arm-Kenai Mountains (fig. 14). Mean magnetic susceptibilities are relatively high in tills that are clearly derived from the west side of Cook Inlet, which is underlain by late Mesozoic and Cenozoic plutonic and associated volcanic, metasedimentary, and sedimentary rocks, including coal-bearing rocks of the Cook Inlet trough (Barnes, 1966; Magoon and others, 1976; Reed and others, 1983). Intermediate mean magnetic susceptibilities characterize till collections from the Talkeetna Mountains and Matanuska Valley. These terranes are dominated by Mesozoic and Cenozoic plutonic and metamorphic rocks of the Talkeetna batholith and associated sedimentary and volcanic rocks of Cenozoic age, including coal-bearing rocks of the Wishbone Hill coal district, as well as rocks from the slightly metamorphosed Mesozoic melange and flysch terranes of the northern Chugach Mountains (Ray, 1954; Barnes and Payne, 1956; Barnes, 1962; Magoon and others, 1976; Winkler, 1992). Mean magnetic susceptibilities are relatively low in tills that are clearly derived from Mesozoic terranes dominated by slightly metamorphosed melange and flysch sequences in the Chugach Mountains, Turnagain Arm, and Kenai Mountains (Martin and others, 1915; Barnes and Cobb, 1959; Clark, 1973; Magoon and others, 1976; Winkler, 1992). On the basis of (*Text cont'd. p. 63*)

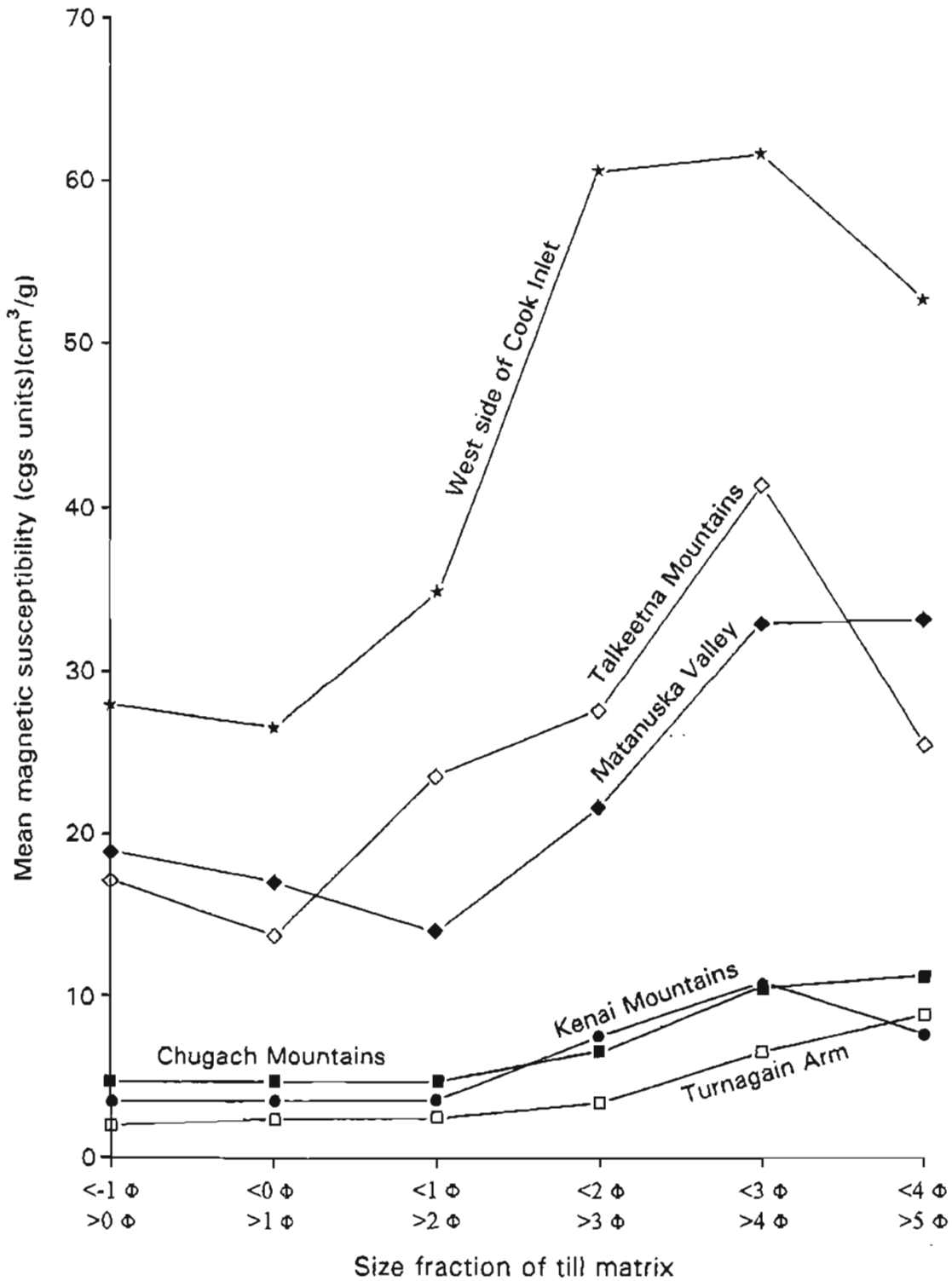


Figure 14. Mean magnetic susceptibility of six size fractions in 68 till samples from six known source areas in the Cook Inlet region.

**Table 15. Standardized mean magnetic susceptibility of six size fractions in 109 till samples collected in the Cook Inlet region. See table 1 and sheets 1–5 for sample locations**

Sample	Size fraction					
	<-1 $\Phi$ $\geq 0 \Phi$	<0 $\Phi$ $\geq 1 \Phi$	<1 $\Phi$ $\geq 2 \Phi$	<2 $\Phi$ $\geq 3 \Phi$	<3 $\Phi$ $\geq 4 \Phi$	<4 $\Phi$ $\geq 5 \Phi$
M1	1.3	1.3	1.2	1.7	3.1	2.9
M2	1.2	1.0	1.4	3.6	5.0	3.5
M3	0.9	1.2	1.4	1.8	2.3	2.3
M5	1.0	1.2	1.1	1.1	1.7	1.7
M6	0.8	0.8	1.0	2.8	4.0	2.0
M7	1.2	1.4	1.4	3.9	7.4	5.6
M8	0.8	0.8	0.7	0.7	1.1	1.0
M9	1.0	1.0	1.3	6.8	13.2	8.9
M10	1.7	2.6	1.7	3.4	5.6	7.0
M11	0.9	1.0	1.1	1.2	1.7	1.5
M12	0.9	0.8	0.9	2.1	4.4	3.8
M13	1.2	1.5	1.5	3.1	3.6	3.1
M14	0.9	1.0	1.0	1.5	2.0	2.0
M15	1.8	2.8	2.8	4.8	2.8	2.4
M16	1.1	1.1	1.1	1.6	2.3	2.4
M17	1.5	1.4	1.5	2.0	3.5	4.4
M18	1.5	1.6	1.8	4.7	7.5	4.9
M18	1.2	1.3	1.2	1.6	2.2	2.1
M19	2.5	2.3	2.4	3.6	5.5	5.3
M20	2.3	2.0	2.3	4.4	7.8	8.8
M21	2.3	2.4	2.6	8.9	13.8	8.4
M22	1.4	1.9	2.1	3.2	5.8	5.0
M23	1.7	1.8	1.8	5.5	34.9	12.8
M24	3.6	4.2	4.7	26.0	41.3	16.4
M25	1.6	2.0	3.4	6.1	11.5	7.3
M26	6.0	6.7	5.2	8.4	27.0	28.9
M27	6.4	6.6	5.6	10.1	21.6	17.6
M28	2.8	3.0	3.2	7.2	13.2	8.2
M29	1.2	1.7	1.8	2.8	3.2	2.5
M30	1.1	1.3	1.5	3.5	4.4	3.9
M31	1.6	1.2	1.9	3.0	4.5	3.3
M32	2.0	2.6	3.2	3.3	3.3	2.8
M33	6.6	6.6	6.5	10.7	19.9	15.1
M34	4.1	4.7	5.6	16.3	48.3	18.3
M35	8.0	7.9	6.4	11.9	25.3	17.2
M36	1.7	1.7	2.4	5.6	12.1	8.9
M37	8.6	8.9	6.8	12.7	40.3	21.9
M38	4.6	5.4	5.6	17.1	38.8	25.0
M39	3.4	4.1	4.1	7.5	8.5	8.4
M40	10.5	4.0	4.8	11.3	34.5	20.1
M41	26.7	23.6	20.2	27.0	42.5	14.5
M42	3.3	4.5	4.8	11.1	26.5	34.4
M43	14.6	14.3	12.7	24.6	37.2	33.7
M44	2.8	3.5	4.5	11.5	26.8	15.3
M45	4.9	4.6	8.3	44.0	5.6	23.2
M46	16.6	20.3	22.1	55.5	17.9	46.6
M47	21.9	21.7	22.1	33.6	53.8	46.7
M48	17.7	21.0	21.0	44.9	11.5	49.7
M49	15.9	1.2	8.5	14.4	26.9	29.0
M50	7.2	6.3	5.3	10.9	16.4	17.5
M51	10.1	7.2	7.6	19.4	52.1	23.7
M52	8.1	5.8	10.0	20.1	37.7	36.2
M53	12.7	8.8	11.3	46.9	46.5	28.6

Table 15. (continued)

Sample	Size fraction					
	<-1 $\Phi$ $\geq 0 \Phi$	<0 $\Phi$ $\geq 1 \Phi$	<1 $\Phi$ $\geq 2 \Phi$	<2 $\Phi$ $\geq 3 \Phi$	<3 $\Phi$ $\geq 4 \Phi$	<4 $\Phi$ $\geq 5 \Phi$
M54	18.5	16.2	42.3	5.9	31.2	7.2
M55	20.0	16.0	16.9	29.2	46.6	40.0
M56	21.2	15.8	12.1	34.2	59.8	49.3
M57	17.2	15.1	13.2	17.6	24.6	24.8
M58	15.3	15.0	12.5	14.6	21.9	26.1
M59	22.2	22.1	17.7	19.9	25.1	31.9
M60	15.9	13.5	13.3	22.1	29.7	23.3
M61	14.3	14.7	12.2	15.1	24.9	34.4
M62	13.0	9.8	9.9	13.9	26.7	21.3
M63	15.0	13.9	12.9	14.7	23.2	33.1
M64	0.7	6.8	9.0	10.6	18.2	20.5
M65	5.3	5.7	6.1	8.1	13.1	16.9
M66	2.0	2.2	2.4	3.1	4.1	4.1
M67	3.6	4.4	4.7	8.0	13.7	10.1
M68	6.8	5.9	5.8	8.0	11.1	14.6
M69	8.8	7.6	6.4	8.1	14.5	13.9
M70	2.1	2.3	2.5	2.7	5.6	6.5
M71	1.0	1.2	1.5	2.3	4.6	6.6
M72	2.9	3.3	3.5	4.3	8.4	11.0
M73	5.4	3.7	3.7	9.3	14.5	14.2
M74	3.9	3.6	3.6	6.5	12.5	13.3
M75	9.1	18.3	68.1	20.6	10.7	11.0
M76	5.1	4.6	4.9	7.9	12.3	12.9
M77	7.1	7.0	7.1	8.5	11.4	10.2
M78	6.9	4.5	7.6	16.1	17.2	10.9
M79	7.6	7.8	7.1	11.4	11.9	11.0
M80	6.4	8.3	7.6	11.7	12.4	12.4
M81	5.2	5.1	4.8	7.0	8.4	7.5
M82	7.3	6.9	6.4	10.9	12.5	11.4
M83	5.8	6.8	6.7	9.2	10.9	10.6
M84	6.5	5.6	4.9	9.7	20.0	13.3
M85	7.8	6.6	5.2	9.5	18.3	19.6
M86	8.3	6.8	6.1	13.1	14.7	13.6
M87	11.9	10.9	9.6	15.2	16.7	14.5
M88	11.5	6.6	7.4	13.4	17.2	17.3
M89	7.2	7.1	7.4	11.0	13.3	9.6
M90	13.5	12.6	12.4	19.9	22.4	9.7
M91	13.5	11.4	11.3	18.8	22.7	17.2
M92	9.2	10.1	10.6	22.1	24.7	22.0
M93	2.5	4.9	4.1	5.7	6.0	5.3
M94	7.9	7.0	7.4	14.9	21.9	29.5
M95	64.8	12.2	11.7	15.1	17.6	14.8
M96	13.2	15.7	15.6	20.2	25.5	24.3
M97	39.3	37.6	41.2	89.6	85.8	49.7
M98	18.0	18.6	18.6	21.7	25.1	25.7
M99	20.6	21.0	22.3	26.8	26.5	22.3
M100	6.8	5.8	5.9	7.1	8.3	6.6
M101	72.6	75.7	75.6	140.2	135.2	91.8
M102	52.5	53.2	100.2	141.4	108.2	85.3
M103	52.6	45.4	58.8	101.4	87.2	63.4
M104	30.1	27.5	90.8	180.2	228.8	169.2
M105	19.4	22.6	25.1	44.6	26.4	69.5
M106	53.9	43.0	39.0	62.1	59.6	38.4
M107	37.5	39.4	34.5	40.8	45.8	32.8
M108	44.3	43.0	42.5	48.9	48.8	42.6
M109	24.6	23.6	46.9	117.0	106.2	65.2

**Table 16.** *Composition of pebbles collected from tills at 92 sites in the Cook Inlet region. Number of pebbles per collection = n. See table 1 and sheets 1-5 for sample locations*

Pebble collection	n	Rock or mineral component (%)				Total
		Volcanic	Quartz	Plutonic	Metasedimentary <sup>a</sup>	
P1	135	0.7	1.5	0.7	97	99.9
P2	143	0.7	0	0	99.3	100
P3	119	0	0	0	100	100
P4	127	0	3.1	0	96.9	100
P5	270	1.1	0	2.2	96.7	100
P6	148	1.4	0	1.4	97.3	100.1
P7	144	0.7	0	0.7	98.6	100
P8	175	2.3	0	0	97.7	100
P9	196	0	0.5	2.6	96.9	100
P10	205	2.9	0	3.9	93.2	100
P11	70	1.4	2.9	4.3	91.4	100
P12	201	4	1	14.9	80.1	100
P13	60	11.7	1.7	25	61.7	100.1
P14	191	2.1	1	2.6	94.2	99.9
P15	176	4	1.1	8	86.9	100
P16	129	0	0	0.8	99.2	100
P17	226	0.4	0.9	2.2	96.5	100
P18	207	0.5	1	0.5	98.1	100.1
P19	165	0.6	0	0	99.4	100
P20	150	2	0	0.7	97.3	100
P21	256	2	0.4	3.1	94.5	100
P22	151	2.6	0.7	14.6	82.1	100
P23	187	0	1.1	4.3	94.7	100.1
P24	186	16.1	3.8	14.5	65.6	100
P25	246	2	1.2	2	94.7	99.9
P26	163	22.7	1.2	37.4	38.7	100
P27	188	1.6	0.5	4.3	93.6	100
P28	110	24.5	1.8	14.5	59.1	99.9
P29	280	6.8	1.8	10.4	81.1	100.1
P30	212	14.2	4.2	29.2	52.4	100
P31	164	19.5	3.7	31.7	45.1	100
P32	218	7.3	2.3	18.8	71.6	100
P33	298	5.4	6	15.8	72.8	100
P34	148	0.7	1.4	82.4	15.5	100
P35	176	0	3.4	59.1	37.5	100
P36	163	8	0	48.5	43.6	100.1
P37	247	6.5	0.8	39.7	53	100
P38	200	7	3.5	21	68.5	100
P39	227	8.4	3.1	38.8	49.8	100.1
P40	217	10.1	0.9	33.6	55.3	99.9
P41	158	4.4	1.9	31.6	62	99.9
P42	262	5.7	1.9	23.7	68.7	100
P43	130	11.5	0.8	23.1	64.6	100
P44	143	2.8	1.4	27.3	68.5	100
P45	236	7.6	1.7	21.6	69.1	100
P46	206	1.9	1	5.3	91.7	99.9
P47	163	0.6	0.6	6.1	92.6	99.9
P48	254	2	0	2.4	95.7	100.1
P49	306	2.3	0.3	3.9	93.5	100
P50	212	2.4	1.4	2.8	93.4	100
P51	171	4.1	0.6	5.3	90.1	100.1
P52	139	0.7	0	0	99.3	100
P53	191	0	0	0	100	100
P54	162	2.5	1.2	5.6	90.7	100

Table 16. (continued)

Pebble collection	n	Rock or mineral component (%)				Total
		Volcanic	Quartz	Plutonic	Metasedimentary <sup>a</sup>	
P55	299	0.7	1.3	21.1	76.9	100
P56	124	2.4	0.8	6.5	90.3	100
P57	90	3.3	1.1	14.4	81.1	99.9
P58	126	11.9	1.6	5.6	81	100.1
P59	42	2.4	0	11.9	85.7	100
P60	130	31.5	1.5	9.2	57.7	99.9
P61	107	37.4	0.9	10.3	51.4	100
P62	94	5.3	2.1	9.6	83	100
P63	52	21.2	0	19.2	59.6	100
P64	101	7.9	3	11.9	77.2	100
P65	88	9.1	4.5	8	78.4	100
P66	95	4.2	2.1	4.2	89.5	100
P67	93	8.6	1.1	9.7	80.6	100
P68	96	9.4	5.2	11.5	74	100.1
P69	85	7.1	7.1	11.8	74.1	100.1
P70	87	17.2	0	16.1	66.7	100
P71	100	2	0	3	95	100
P72	93	48.4	3.2	15.1	33.3	100
P73	78	19.2	2.6	19.2	59	100
P74	114	8.8	3.5	5.3	82.5	100.1
P75	73	6.8	0	8.2	84.9	99.9
P76	95	5.3	3.2	7.4	84.2	100.1
P77	88	9.1	4.5	2.3	84.1	100
P78	118	8.5	2.5	23.7	65.3	100
P79	163	40.5	1.2	52.1	6.1	99.9
P80	112	17.9	5.4	55.4	21.4	100.1
P81	112	16.1	0.9	55.4	27.7	100
P83	73	9.6	2.7	13.7	74	100
P84	171	87.7	1.8	7	3.5	100
P85	99	7.1	0	92.9	0	100
P86	63	15.9	0	84.1	0	100
P87	172	0.6	0	99.4	0	100
P88	137	48.2	0	27.7	24.1	100
P89	96	59.4	1	27.1	12.5	100
P90	65	63.1	1.5	15.4	20	100
P91	113	19.5	0	52.2	28.3	100
P92	151	41.1	0	45.7	13.2	100
P93	389	0.3	2.1	0.3	97.4	100.1

<sup>a</sup>Includes sedimentary and altered sedimentary lithologies.

standard deviations of mean magnetic susceptibility, the collection of samples from the west side of Cook Inlet is clearly more variable than the other collections, but collections from Talkeetna Mountains, Kenai Mountains, and Matanuska Valley have intermediate standard deviations in the finer size fractions (fig. 15).

These preliminary results persuaded us that our experiment could produce useful information on till sources. We reasoned that multivariate analysis, which can incorporate both magnetic-susceptibility and pebble-lithology values, could provide statistically significant results.

## RESULTS OF MULTIVARIATE ANALYSIS

The goal of the multivariate analysis was to develop an appropriate numerical scheme to accurately predict sources of tills in the eastern and northern Cook Inlet region. Our data set consists of 10 independent variables (magnetic-susceptibility readings of six size fractions of till matrix plus four compositional classes of till pebbles) and six dependent variables (the source areas identified in the model). Three multivariate programs were used in this evaluation: (a) CHAID, which detects data interactions by the use of decision trees; (b) multiple discriminant

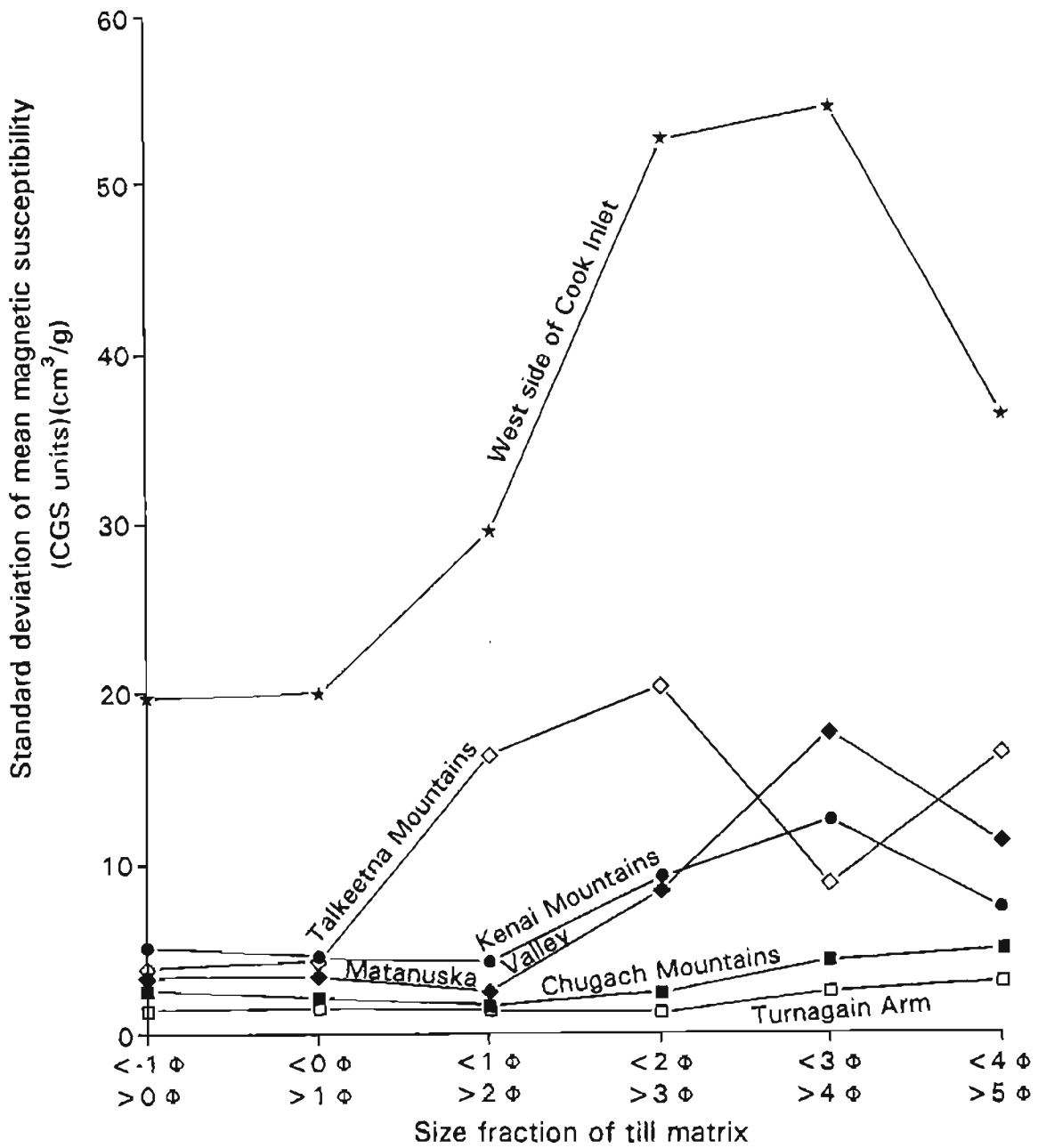


Figure 15. Standard deviation of mean magnetic susceptibility of six size fractions in 68 till samples from six known source areas in the Cook Inlet region.

Table 17a. Mean magnetic susceptibility of six size fractions in groups of Naptowne-age till samples derived from six known sources and from four areas where till source is uncertain in the Cook Inlet region

Source	n	Size fraction					
		<-1 $\phi$ >0 $\phi$	<0 $\phi$ >1 $\phi$	<1 $\phi$ >2 $\phi$	<2 $\phi$ >3 $\phi$	<3 $\phi$ >4 $\phi$	<4 $\phi$ >5 $\phi$
Talkeetna Mountains	3	17.1	13.7	23.5	27.3	41.4	25.3
Matanuska Valley	4	19.0	17.0	13.9	21.6	32.9	33.0
Chugach Mountains	6	4.8	4.7	4.7	6.3	10.4	11.0
Turnagain Arm	2	2.0	2.3	2.5	3.3	6.5	8.8
Kenai Mountains	35	3.5	3.5	3.5	7.5	10.7	7.6
West side of Cook Inlet	18	27.9	26.5	34.8	60.7	61.6	52.6
Matanuska-Knik "medial"	7	15.2	14.6	15.5	26.6	35.2	31.2
Turnagain Arm?	2	8.7	6.8	6.5	15.2	34.3	20.6
Kenai Mountains?	3	2.5	2.7	2.9	12.0	28.0	12.7
West side?	27	9.3	7.4	9.1	11.8	15.8	14.4

N = 107

Table 17b. Mean standard deviations of magnetic susceptibility in six size fractions in groups of Naptowne-age till samples derived from six known sources and from four areas where till source is uncertain in the Cook Inlet region

Source	n	Size fraction					
		<-1 $\phi$ >0 $\phi$	<0 $\phi$ >1 $\phi$	<1 $\phi$ >2 $\phi$	<2 $\phi$ >3 $\phi$	<3 $\phi$ >4 $\phi$	<4 $\phi$ >5 $\phi$
Talkeetna Mountains	3	3.9	4.2	16.5	20.6	8.9	16.7
Matanuska Valley	4	3.3	3.4	2.6	8.7	18.0	11.3
Chugach Mountains	6	2.7	2.1	1.8	2.7	4.4	5.0
Turnagain Arm	2	1.3	1.5	1.4	1.4	2.7	3.1
Kenai Mountains	35	5.2	4.7	4.2	9.3	12.8	7.7
West side of Cook Inlet	18	19.9	20.1	29.6	52.6	54.5	36.4
Matanuska-Knik "medial"	7	11.9	10.7	11.5	28.1	23.1	10.5
Turnagain Arm?	2	2.1	0.6	1.6	6.0	25.2	4.4
Kenai Mountains?	3	1.0	1.3	1.6	12.2	17.8	3.8
West side?	27	11.5	3.7	12.1	4.7	5.4	6.1

N = 107

analysis (MDA); and (c) AIM (abductive inference mechanism). Details of these analyses are provided in appendix B.

Predictions of till sources by the proposed model were significantly matched by CHAID predictions at both the 99- and 95-percent levels, which provides important confirmation of the proposed glaciation model (figs. 16 and 17). However, the location and nature of CHAID mismatches also provide important insights about the Naptowne glaciation in the Cook Inlet trough. A small number of samples collected in the eastcentral and southeastern Cook Inlet trough from moraines clearly related to ice from the Kenai Mountains was erroneously assigned (primarily at the 95-percent confidence level) to Turnagain Arm, which served as a major conduit for ice from virtually identical bedrock terranes in the northern Kenai Mountains and southern Chugach Mountains. At both

confidence levels, almost all mismatches occurred at sample sites where there is least confidence in the proposed glaciation model, namely in northern Kenai Lowland and in the interlobate belt associated with the Matanuska-Knik lobe north of Anchorage. In northern Kenai Lowland, samples assigned by the model to west side sources were assigned by CHAID to the Chugach Mountains, Kenai Mountains, or Matanuska Valley. Disparities among "interlobate" samples were assigned by CHAID to the Kenai Mountains, which is clearly not possible.

CHAID was also used to analyze the relative significance of the four lithologies in the pebble classification. Metasediment content was judged the only significant indicator among the four lithologic classes. However, limiting CHAID only to pebble lithology greatly blunted the sensitivity of the technique. CHAID chose magnetic susceptibility of the 1- $\phi$  (coarse-sand) fraction

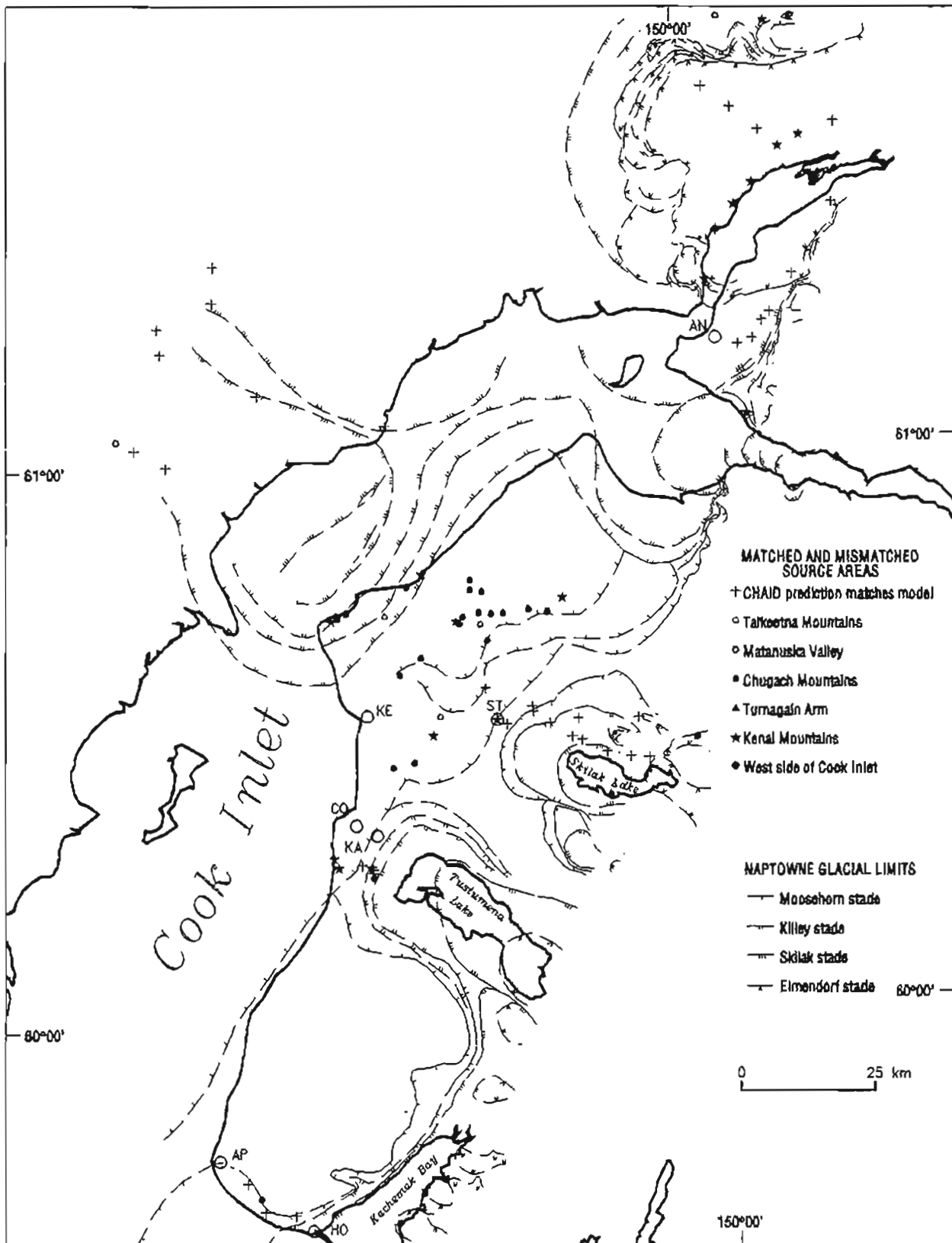


Figure 16. Comparison of CHAID predictions at the 99-percent confidence level and till sources predicted by the proposed glaciation model in the Cook Inlet region. Geographic localities: AN = Anchorage; AP = Anchor Point; CO = Cohoe; HO = Homer; KA = Kasilof; KE = Kenai; ST = Sterling.

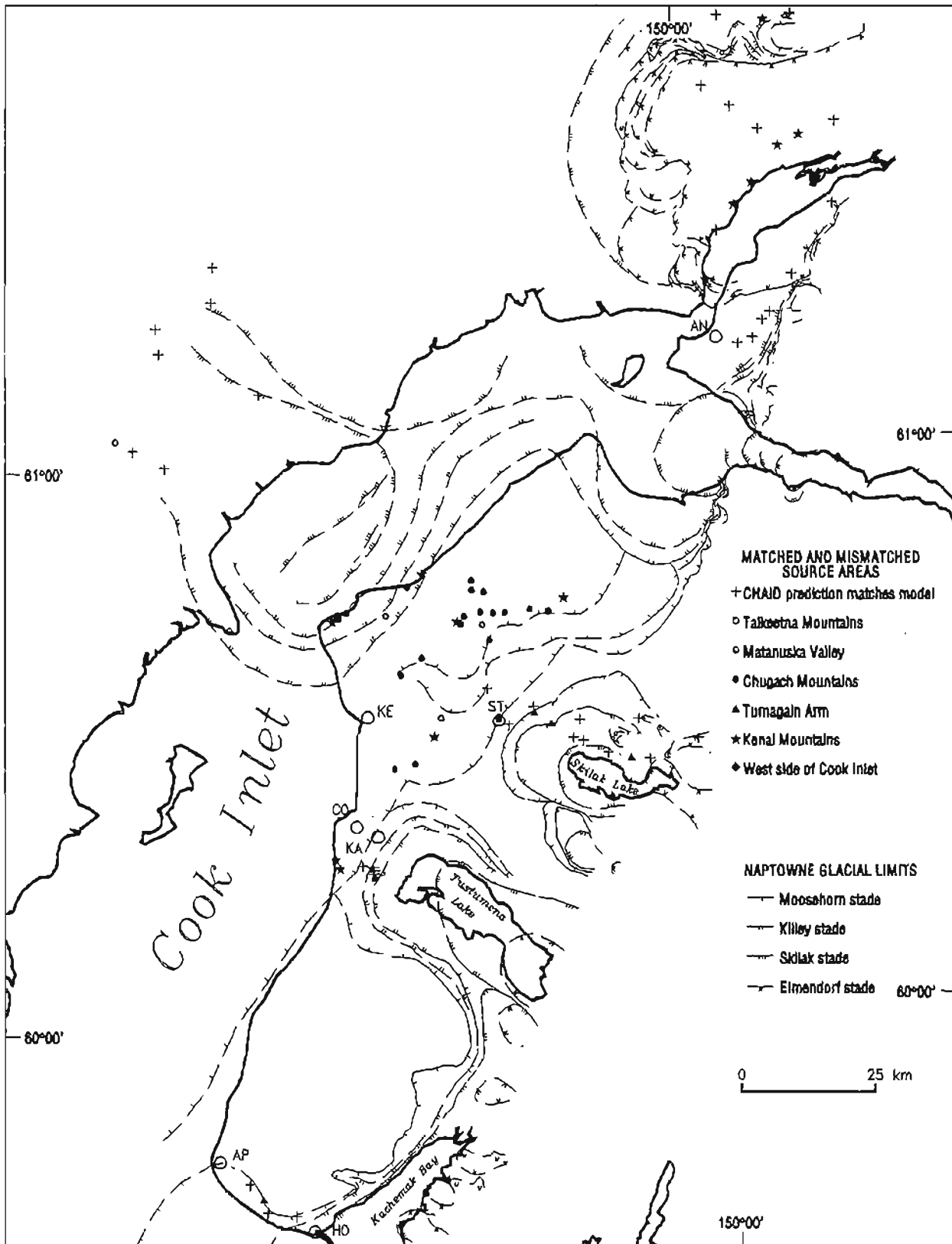


Figure 17. Comparison of CHAID predictions at the 95-percent confidence level and till sources predicted by the proposed glaciation model in the Cook Inlet region. Geographic localities: AN = Anchorage; AP = Anchor Point; CO = Cohoe; HO = Homer; KA = Kasilof; KE = Kenai; ST = Sterling.

**Table 18a.** Mean pebble compositions in groups of Naptowne-age tills derived from six known sources and from three areas where till source is uncertain in the Cook Inlet region

Source	n	Rock or mineral component (%)			
		Volcanic	Quartz	Plutonic	Metasedimentary
Talkeetna Mountains	3	2.9	1.6	63.3	32.2
Matanuska Valley	4	8.0	2.1	33.3	56.7
Chugach Mountains	6	2.2	0.7	4.3	92.8
Turnagain Arm	2	0.4	0.0	0.0	99.7
Kenai Mountains	19	1.1	0.6	1.5	96.7
West side of Cook Inlet	23	26.4	1.7	36.2	35.6
Matanuska-Knik "medial"	7	6.6	2.3	23.8	67.3
Kenai Mountains?	3	0.5	1.1	2.6	95.8
West side?	25	9.4	2.0	10.4	78.3
N = 92					

**Table 18b.** Mean standard deviations of pebble compositions in groups of Naptowne-age tills derived from six known sources and from three areas where till source is uncertain in the Cook Inlet region

Source	n	Rock or mineral component (%)			
		Volcanic	Quartz	Plutonic	Metasedimentary
Talkeetna Mountains	3	4.4	1.7	17.3	14.8
Matanuska Valley	4	1.6	1.4	8.6	8.2
Chugach Mountains	6	1.1	0.5	1.5	1.9
Turnagain Arm	2	0.5	0.0	0.0	0.5
Kenai Mountains	19	0.9	0.9	1.5	2.0
West side of Cook Inlet	23	22.3	1.5	26.9	27.7
Matanuska-Knik "medial"	7	2.9	1.7	4.9	3.6
Kenai Mountains?	3	0.8	1.6	1.8	4.0
West side?	25	9.0	1.8	5.6	11.0
N = 92					

and 4- $\phi$  (very fine sand) fraction of the till matrix and contents of metasediment and plutonic pebbles as significant predictors of till source in this study.

Although the basic requirements of MDA were not satisfied by our data set because of its limited size, MDA clearly indicates that percentages of metasediment and plutonic lithologies in till pebble collections are significant indicators of till sources in the eastern and northern Cook Inlet trough. Many model predictions were confirmed by MDA, which produced only a few more mismatches (fig. 18) than did CHAID. Mismatches in Skilak Lake, Tustumena Lake, and Kachemak Bay samples result from MDA assignments (in decreasing order) to Turnagain Arm, Chugach Mountains, and Matanuska Valley. Mismatches of granitic-rich and locally derived till samples from the west side of Cook Inlet resulted from MDA assignments to the Talkeetna Mountains, which are cored by the extensive Talkeetna batholith. As with CHAID, most MDA mismatches are concentrated in northern Kenai Lowland, where model predictions are shakiest. There, tills attributed

to the west side of Cook Inlet by the glacial model were assigned about equally by MDA to Matanuska Valley and Chugach Mountains.

AIM could not successfully partition our data set. However, it determined (although not conclusively) that three factors are significant for differentiating till sources in the eastern and northern Cook Inlet trough: (a) magnetic susceptibility of the 4- $\phi$  (very fine sand) fraction, (b) percentage of metasediment pebbles, and (c) percentage of plutonic pebbles.

## IMPLICATIONS

Multivariate analysis successfully partitioned our data set to identify the six till sources predicted by the glaciation model. However, the data set probably provides indicative and not conclusive results because it is too small to comprehensively represent the complex glacial deposits in the Cook Inlet trough. Nonetheless, the three approaches tested produce mutually supportive results. Disparities

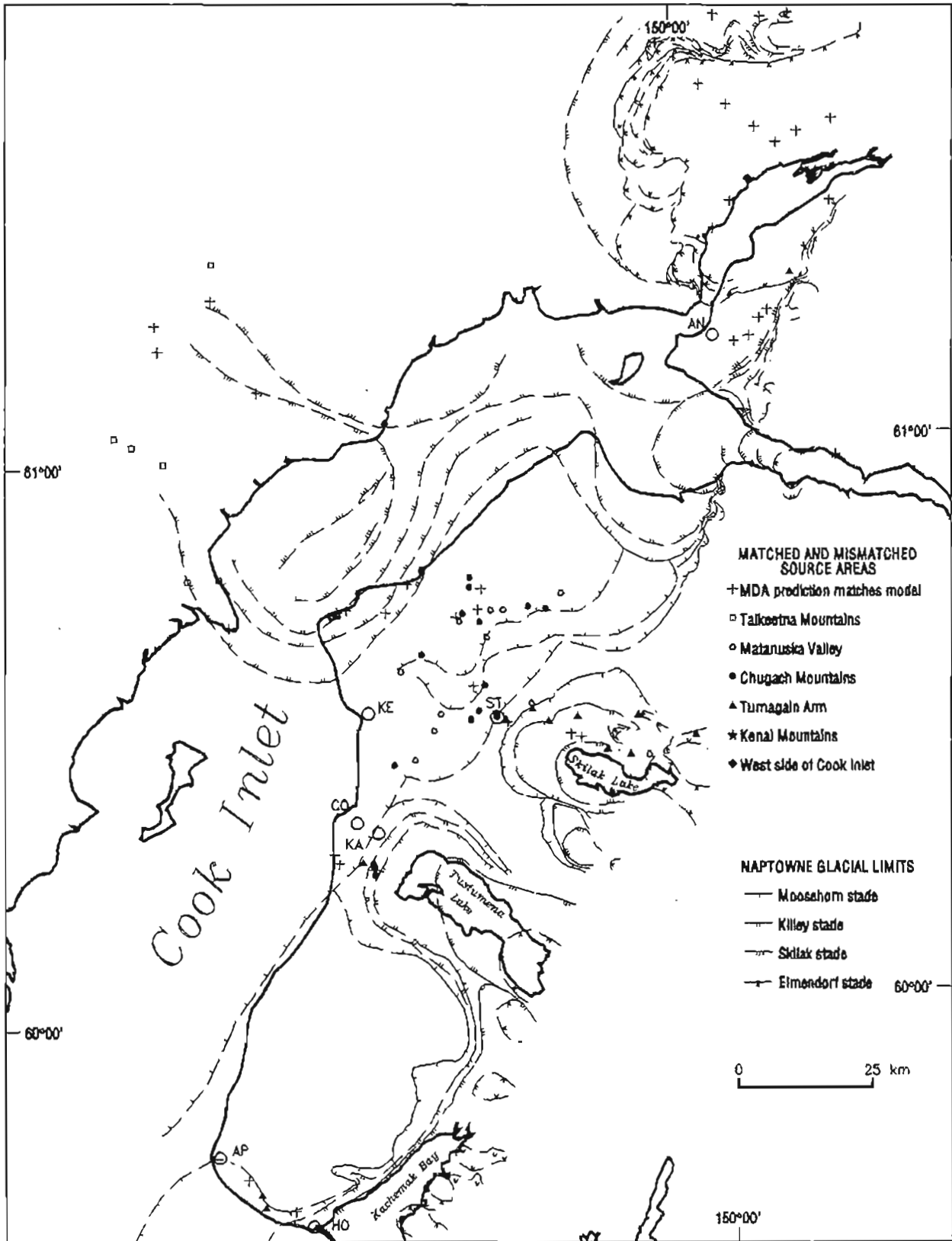


Figure 18. Comparison of till sources predicted by multiple discriminant analysis and sources predicted by the proposed glaciation model in the Cook Inlet region. Geographic localities: AN = Anchorage; AP = Anchor Point; CO = Cohoe; HO = Homer; KA = Kasilof; KE = Kenai; ST = Sterling.

between model predictions and predictions by CHAID and MDA are generally related to lack of confidence in model assignments.

Differences in the proposed glaciation model and statistical predictions in "known" moraines are probably due to the inability of CHAID and MDA to distinguish between subtle differences of bedrock in different source areas based on this data set. Concentrations of mismatches probably indicate that ice of Naptowne age entered northern Kenai Lowland not just from the northwest but also from the north and northeast (fig. 19), similar to the glacioestuarine model proposed by Schmoll and others (1984, fig. 7). However, based on near-surface stratigraphy and landform interrelations in Kenai Lowland, we have a different interpretation than them for the nature, extent, and age of former waterbodies in the Cook Inlet trough (Reger and Pinney, 1996). Complications for an interpretation of statistical mismatches in northern Kenai Lowland include (a) scouring and incorporation of weakly cemented Tertiary bedrock (particularly on the west side of Cook Inlet) and (b) probable reworking during the Naptowne advance of older Pleistocene deposits, perhaps from more than one source.

On the basis of our pilot study, we suggest that a final resolution of a model of Naptowne glaciation in the Cook Inlet trough should include a consideration of the results of multivariate analysis of a data set produced by an expanded and more intensive till sampling program. Initial results indicate that this program can be limited to measuring the isotropic magnetic susceptibility of the coarse-sand and very fine sand fractions of the till matrix and to determining the percentages of metasediment and plutonic till pebbles. Results of this statistical approach should be compatible with landform interrelations and stratigraphy.

## CONCLUSIONS

The most widespread and chronologically most important tephra we document in Kenai Lowland is the Lethe tephra, which is the key to correlating morainal sequences from Kachemak Bay to Turnagain Arm (Reger and Pinney, 1996). This dacitic airfall tephra strongly correlates with complex pyroclastics in the the Windy Creek area near Mt. Katmai, based on ferromagnesian mineral content, distinctive shard morphology, and very consistent shard geochemistry. Stratigraphic and physiographic evidence in Kenai Lowland indicates that the Lethe tephra was deposited after 16,000 <sup>14</sup>C yr B.P. late in the Killey stade of the Naptowne glaciation.

We recognize nine Holocene tephtras and tentatively recognize four tephtras in Kenai Lowland. On the basis of shard geochemistry, we tentatively suggest that several of these tephtras could have been erupted from Mt. Augustine, Mt. Redoubt, and Hayes volcano on the west side of Cook Inlet.

However, the Crooked Creek and Funny River tephtras, which are best represented among the Holocene tephtras in our sampling program, have no known correlatives.

Our investigations of the regionally important section at Goose Bay on the west side of Knik Arm indicate that the Goose Bay peat, its enclosed tephtras, and the underlying type till of the Knik glaciation are middle Pleistocene in age. In several attempts to date the Goose Bay tephtra, which is the thickest volcanic ash in the section, we conclude that the best result is a three-sample (composite) isochron <sup>40</sup>Ar/<sup>39</sup>Ar age of 378 ± 0.67 ka, obtained by the laser method. We also confirm the presence of the Stampede tephtra, previously identified by Begét and Keskinen (1991), at the base of the Goose Bay peat.

Evidence in the bluff at Kenai demonstrates that a tide-water glacier floated there late in the Killey stade shortly after 16,480 ± 170 <sup>14</sup>C yr B.P. and that a marine connection existed between middle Cook Inlet and the North Pacific Ocean. Stratigraphic and paleontologic evidence in the Kasilof-Kalifornsky area indicates that inlet waters were very cold with variable turbidity and salinity about 16,000 <sup>14</sup>C yr B.P. and that debris-laden icebergs were present.

Macrofossil collections from the Bootlegger Cove Formation in upper Cook Inlet are dominated by pelecypods with minor gastropod and barnacle components. These assemblages are rich in species compared to the modern *Macoma balthica* fauna. Between 14,900 ± 400 and 13,470 ± 120 <sup>14</sup>C yr B.P., BCF faunas probably lived in conditions that were very similar to some modern fjords along the southcentral and southeastern coast of Alaska, except there was strong tidal action.

Our pedologic observations raise serious questions about past practices of correlating moraines by similar soil development. We conclude that significant environmental gradients in the Cook Inlet region probably affected rates of soil formation and seriously complicate the use of soils to date landforms.

Multivariate analysis of six size fractions of till matrix and four compositional classes of till pebbles was successfully used to test a model of Naptowne glaciation in the eastern and northern Cook Inlet region. Concentrations of discrepancies between model and statistical predictions probably indicate that Naptowne ice entered the northern Kenai Lowland from the northwest, north, and northeast.

## ACKNOWLEDGMENTS

We gratefully acknowledge the critical contributions made by many of our colleagues during field and laboratory phases of this investigation. Able assistance was provided in the field by Rod Combellick, Cheri Daniels, Jeff Kline, Sven Lagerberg, Bill Petrik, Doug Reger, and Fred Sturmman. On numerous occasions, we depended on

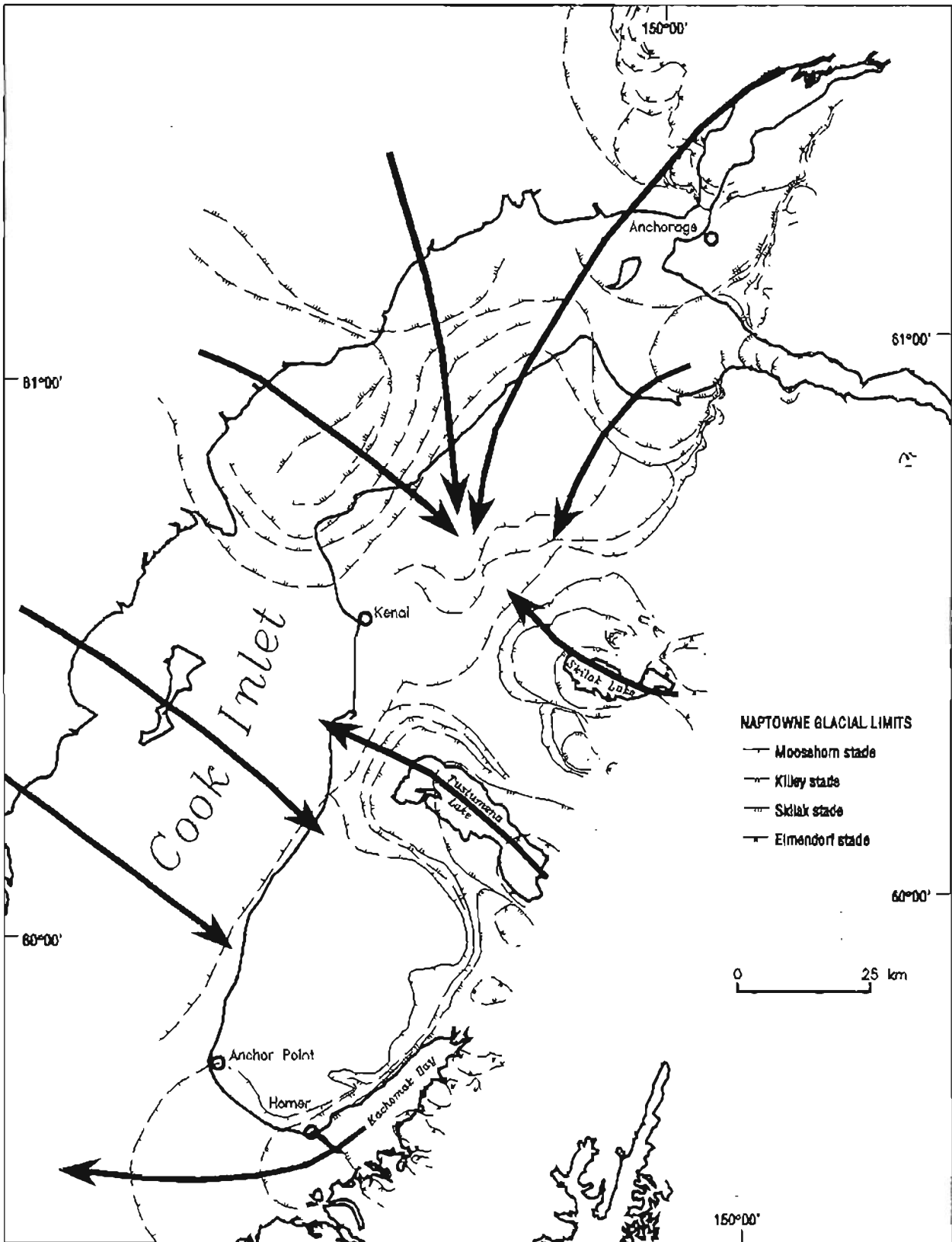


Figure 19. Revised model of Naptowne glaciation in the Cook Inlet region, showing major ice-flow directions (arrows) inferred from multivariate analysis of magnetic-susceptibility and pebble compositions of till samples.

the expert advice and outstanding cartographic products provided by Sturmman. We appreciate permission to map and sample the Kenai National Moose Range by Dan Doshier, U.S. Fish and Wildlife Service.

Several folks helped analyze the many samples we collected during the past 19 years. We are particularly appreciative of the friendly hospitality and technical support provided by Scott Cornelius and Diane Johnson, who expertly program and maintain the electron microprobe in the Washington State University Geochronology Laboratory. Preliminary correlations of Holocene tephra in the Cook Inlet region were facilitated by our access to unpublished geochemical data that were kindly provided to Pinney by Jim Begét, Kathy Campbell, Tom Dilley, Sam Swanson, and Victoria Avery. Dr. Paul Layer, University of Alaska (Fairbanks) Geochronology Laboratory, kindly analyzed tephra samples that ultimately provided the important  $^{40}\text{Ar}/^{39}\text{Ar}$  date of the Goose Bay tephra. Dr. Bob Zimmerman, U.S. Geological Survey, searched thousands of apatite grains in the Goose Bay tephra for fission tracks and ultimately provided a mean fission-track age for that tephra. Our radiocarbon samples were analyzed by the University of Arizona (AA); Beta Analytic, Inc. (Beta); Teledyne Isotopes (I); Geochron Laboratories (GX), Washington State University Radiocarbon Dating Laboratory (WSU), and University of Washington Quaternary Isotope Laboratory (QL). John Roe measured the paleomagnetism of our Goose Bay samples with the permission of Dr. David Stone, University of Alaska (Fairbanks) Geophysical Institute. Nora Foster, University of Alaska (Fairbanks) Museum, efficiently identified the constituents of our macrofossil collections from the Bootlegger Cove Formation. Our collections of microfossils from the Bootlegger Cove Formation were inventoried by Micropaleo Consultants, Inc. We are grateful to Al Kimker, Alaska Department of Fish and Game, for discussions on the distributions and habitat requirements of modern pelecypods in Cook Inlet.

We thank Dr. Tom Ager, U.S. Geological Survey, for letting us use the unpublished radiocarbon date from the bottom of his Circle Lake core.

A special tip of our hats goes to Dr. Dan Hawkins, geostatistician extraordinaire now enjoying a busy retirement from the University of Alaska (Fairbanks). Dan became intrigued by the the potential of using a combination of magnetic susceptibility and pebble contents in till samples to identify till sources. He efficiently ran our data through their statistical paces and, in the process, segregated key parameters for six source areas. In addition to his obvious technical expertise and review of appendix B, we are grateful for Dan's enthusiastic support and patience in answering many questions asked by these statistical neophytes.

We are thankful for technical reviews of this report

by Dr. Troy Péwé, Department of Geology, Arizona State University; Kristine Crossen, Department of Geology, University of Alaska (Anchorage); and Karen Clautice, DGGs. We especially hope that Kris will pursue similar studies in the Cook Inlet region in the future. And last, but not least by any measure, we give well-earned credit to Fran Tannian, who patiently and efficiently answered our many editorial questions, and to Frank Larson, whose editing skills and attention to detail helped us find elusive typos, clarify awkward sentences, and apply the final polish to this report.

## REFERENCES CITED

- Ager, T.A., and Shaw, E.G., 1986, Postglacial pollen record from Circle Lake, Kachemak Bay, south-central Alaska [abs.]: American Association of Stratigraphic Palynologists Program and Abstracts, 19th Annual Meeting, v. 19, p. 1.
- Barnes, F.F., 1962, Geologic map of lower Matanuska Valley, Alaska: U.S. Geological Survey Miscellaneous Geologic Investigations Map I-359, 1 sheet, scale 1:63,360.
- \_\_\_\_\_, 1966, Geology and coal resources of the Beluga-Yentna region, Alaska: U.S. Geological Survey Bulletin 1202-C, 54 p.
- Barnes, F.F., and Cobb, E.H., 1959, Geology and coal resources of the Homer district, Kenai coal field, Alaska: U.S. Geological Survey Bulletin 1058-F, p. 217-260, 12 sheets, various scales.
- Barnes, F.F., and Payne, T.G., 1956, The Wishbone Hill district, Matanuska coal field, Alaska: U.S. Geological Survey Bulletin 1016, 88 p., 20 sheets, various scales.
- Bartsch-Winkler, Susan, Ovenshine, A.T., and Kachadoorian, Reuben, 1983, Holocene history of the estuarine area surrounding Portage, Alaska, as recorded in a 93 m core: Canadian Journal of Earth Sciences, v. 20, no. 5, p. 802-820.
- Bartsch-Winkler, Susan, and Schmoll, H.R., 1984, Guide to late Pleistocene and Holocene deposits of Turnagain Arm: Anchorage, Alaska Geological Society guidebook, 70 p.
- \_\_\_\_\_, 1992, Utility of radiocarbon-dated stratigraphy in determining late Holocene earthquake recurrence intervals, upper Cook Inlet region, Alaska: Geological Society of America Bulletin, v. 104, no. 6, p. 684-694.
- Baxter, Rae, 1983, Mollusks of Alaska: Homer, China Poot Bay Society report, 86 p.
- Begét, James, Edwards, Mary, Hopkins, David, Keskinen, Mary, and Kukla, George, 1991, Old Crow tephra found at the Palisades of the Yukon: Quaternary Research, v. 35, no. 2, p. 291-297.
- Begét, J.E., and Keskinen, Mary, 1991, The Stampede tephra: A middle Pleistocene marker bed in glacial and

- olian deposits of central Alaska: *Canadian Journal of Earth Sciences*, v. 28, no. 7, p. 991-1002.
- Begét, J.E., and Kienle, Juergen, 1992, Cyclic formation of debris avalanches at Mount St Augustine volcano: *Nature*, v. 356, no. 6371, p. 701-704.
- Begét, J.E., and Nye, C.J., 1994, Postglacial eruption history of Redoubt Volcano, Alaska: *Journal of Volcanology and Geothermal Research*, v. 62, nos. 1-4, p. 31-54.
- Begét, J.E., Reger, R.D., Pinney, DeAnne, Gillispie, Tom, and Campbell, Kathy, 1991, Correlation of the Holocene Jarvis Creek, Tangle Lakes, Cantwell, and Hayes tephra in south-central and central Alaska: *Quaternary Research*, v. 35, no. 2, p. 174-189.
- Begét, J.E., Stihler, S.D., and Stone, D.B., 1994, A 500-year-long record of tephra falls from Redoubt Volcano and other volcanoes in upper Cook Inlet, Alaska: *Journal of Volcanology and Geothermal Research*, v. 62, nos. 1-4, p. 55-67.
- Berry, M.E., 1994, Soil-geomorphic analysis of late-Pleistocene glacial sequences in the McGee, Pine, and Bishop Creek drainages, east-central Sierra Nevada, California: *Quaternary Research*, v. 41, no. 2, p. 160-175.
- Biggs, David, de Ville, Barry, and Suen, Edward, 1991, A method of choosing multiway partitions for classification and decision trees: *Journal of Applied Statistics*, v. 18, no. 1, p. 49-62.
- Birkeland, P.W., 1984, *Soils and geomorphology*: New York, Oxford University Press, 372 p.
- Birkeland, P.W., Berry, M.E., and Swanson, D.K., 1991a, Use of soil catena field data for estimating relative ages of moraines: *Geology*, v. 19, no. 3, p. 281-283.
- Birkeland, P.W., Machette, M.N., and Haller, K.M., 1991b, Soils as a tool for applied Quaternary geology: *Utah Geological and Mineralogical Survey Miscellaneous Publication 91-3*, 63 p.
- Borchardt, G.A., Aruscavage, P.J., and Millard, H.T., Jr., 1972, Correlation of the Bishop Ash, a Pleistocene marker bed, using instrumental neutron activation analysis: *Journal of Sedimentary Petrology*, v. 42, no. 2, p. 301-306.
- Broecker, W.S., Kulp, J.L., and Tucek, C.S., 1956, Lamont natural radiocarbon measurements III: *Science*, v. 124, no. 3213, p. 154-165.
- Cameron, C.C., Malterer, T.J., Rawlinson, S.E., and Hardy, S.B., 1981, Surficial geology and peat resources of the Rogers Creek area, Susitna Valley, Alaska: U.S. Geological Survey Open-File Report 81-1302, 3 sheets, scale 1:15,840.
- Clark, S.H.B., 1973, The McHugh Complex of south-central Alaska: U.S. Geological Survey Bulletin 1372-D, p. D1-D11.
- Chernicoff, S.E., 1984, Using isotropic magnetic susceptibility to delineate glacial tills: *Journal of Geology*, v. 92, no. 1, p. 113-118.
- Combellick, R.A., 1990, Evidence for episodic late-Holocene subsidence in estuarine deposits near Anchorage, Alaska: Basis for determining recurrence intervals of major earthquakes: Alaska Division of Geological & Geophysical Surveys Public-Data File 90-29, 67 p.
- \_\_\_\_\_, 1991, Paleoseismicity of the Cook Inlet region, Alaska: Evidence from peat stratigraphy in Turnagain and Knik Arms: Alaska Division of Geological & Geophysical Surveys Professional Report 112, 52 p.
- Combellick, R.A., and Pinney, D.S., 1995, Radiocarbon age of probable Hayes tephra, Kenai Peninsula, Alaska, in Combellick, R.A., and Tannian, Fran, eds., *Short Notes on Alaska Geology 1995*: Alaska Division of Geological & Geophysical Surveys Professional Report 117, p. 1-9.
- Combellick, R.A., and Reger, R.D., 1988, Engineering-geologic assessment of the proposed Hatcher Pass ski resort at Government Peak, southcentral Alaska: Alaska Division of Geological & Geophysical Surveys Public-Data File 88-39, 24 p.
- \_\_\_\_\_, 1994, Sedimentological and radiocarbon-age data for tidal marshes along eastern and upper Cook Inlet, Alaska: Alaska Division of Geological & Geophysical Surveys Report of Investigations 94-6, 60 p.
- Daniels, C.L., 1981a, Geologic and materials maps of the Anchorage C-7 SE Quadrangle, Alaska: Alaska Division of Geological & Geophysical Surveys Geologic Report 67, 2 sheets, scale 1:25,000.
- \_\_\_\_\_, 1981b, Geologic and materials maps of the Anchorage C-7 SW Quadrangle, Alaska: Alaska Division of Geological & Geophysical Surveys Geologic Report 71, 2 sheets, scale 1:25,000.
- Dilley, T.E., 1988, Holocene tephra stratigraphy and pedogenesis in the middle Susitna River valley, Alaska: Fairbanks, University of Alaska MS thesis, 98 p.
- Foster, N.R., 1991, Intertidal bivalves: Fairbanks, University of Alaska Press, 152 p.
- Gravenor, C.P., and Stupavsky, M., 1974, Magnetic susceptibility of the surface tills of southern Ontario: *Canadian Journal of Earth Sciences*, v. 11, no. 5, p. 658-663.
- Hair, J.F., Jr., Anderson, R.E., Tatham, R.L., and Black, W.C., 1995, *Multivariate data analysis with readings*: Englewood Cliffs, Prentice Hall, 745 p.
- Harden, J.W., 1982, A quantitative index of soil development from field descriptions—examples from a chronosequence in central California: *Geoderma*, v. 28, no. 1, p. 1-28.
- Karlstrom, T.N.V., 1957, Tentative correlation of Alaskan glacial sequences, 1956: *Science*, v. 125, no. 3237, p. 73-74.
- \_\_\_\_\_, 1964, Quaternary geology of the Kenai Lowland and glacial history of the Cook Inlet region, Alaska:

- U.S. Geological Survey Professional Paper 443, 69 p., 7 sheets, various scales.
- Kienle, Jürgen, and Nye, C.J., 1990, Volcanoes of Alaska, in Wood, C.A., and Kienle, Jürgen, eds., Volcanoes of North America: Cambridge, Cambridge University Press, p. 17-109.
- Kulp, J.L., Feely, H.W., and Tryon, L.E., 1951, Lamont natural radiocarbon measurements I: Science, v. 114, no. 2970, p. 565-568.
- Kulp, J.L., Tryon, L.E., Eckelman, W.R., and Snell, W.A., 1952, Lamont natural radiocarbon measurements II: Science, v. 116, no. 3016, p. 409-414.
- Lewinson, Lisa, 1993, Data mining: Intelligent technology gets down to business: PC AI, v. 7, no. 6, p. 16-23.
- Magoon, L.B., Adkison, W.L., and Egbert, R.M., 1976, Map showing geology, wildcat wells, Tertiary plant fossil localities, K-Ar dates, and petroleum operations, Cook Inlet area, Alaska: U.S. Geological Survey Miscellaneous Investigations Map I-1019, 3 sheets, scale 1:250,000.
- Marsters, Beverly, Spiker, Elliott, and Rubin, Meyer, 1969, U.S. Geological Survey radiocarbon dates X: Radiocarbon, v. 11, no. 1, p. 210-227.
- Martin, G.C., Johnson, B.L., and Grant, U.S., 1915, Geology and mineral resources of Kenai Peninsula, Alaska: U.S. Geological Survey Bulletin 587, 243 p., 3 sheets, various scales.
- Miller, R.D., and Dobrovolny, Ernest, 1959, Surficial geology of Anchorage and vicinity, Alaska: U.S. Geological Survey Bulletin 1093, 128 p., 1 sheet, scale 1:63,360.
- Olson, E.A., and Broecker, W.S., 1959, Lamont natural radiocarbon measurements V: American Journal of Science, v. 257, no. 1, p. 1-28.
- Pinney, D.S., 1991, Laboratory procedures for processing tephra samples: Alaska Division of Geological & Geophysical Surveys Public-Data File 91-30, 30 p.
- \_\_\_\_\_, 1993, Late Quaternary glacial and volcanic stratigraphy near Windy Creek, Katmai National Park, Alaska: Fairbanks, University of Alaska MS thesis, 185 p.
- Pinney, D.S., and Begét, J.E., 1991a, Deglaciation and latest Pleistocene and early Holocene glacier readvances on the Alaska Peninsula: Records of rapid climate change due to transient changes in solar intensity and atmospheric CO<sub>2</sub> content?, in Weller, Gunter, Wilson, C.L. and Severin, B.A.B., eds., Proceedings of the International Conference on the Role of the Polar Regions in Global Change: Fairbanks, University of Alaska Geophysical Institute and Center for Global Change and Arctic System Research, v. 2, p. 634-640.
- \_\_\_\_\_, 1991b, Late Pleistocene volcanic deposits near the Valley of Ten Thousand Smokes, Katmai National Park, Alaska, in Reger, R.D., ed., Short Notes on Alaska Geology 1991: Alaska Division of Geological & Geophysical Surveys Professional Report 111, p. 45-53.
- Plafker, George, 1956, Occurrence of diatomaceous earth near Kenai, Alaska: U.S. Geological Survey Bulletin 1039B, p. 25-31, 1 sheet, scale 1:3,000.
- Rawlinson, S.E., 1986, Peat-resource and surficial-geologic map of the southern Kenai area, Kenai Peninsula, Alaska: Alaska Division of Geological & Geophysical Surveys Report of Investigations 86-15, 1 sheet, scale 1:31,680.
- Ray, R.G., 1954, Geology and ore deposits of the Willow Creek mining district, Alaska, U.S. Geological Survey Bulletin 1004, 86 p., 9 sheets, various scales.
- Reed, B.L., Miesch, A.T., and Lanphere, M.A., 1983, Plutonic rocks of Jurassic age in the Alaska-Aleutian Range batholith: Chemical variations and polarity: Geological Society of America Bulletin, v. 94, no. 10, p. 1232-1240.
- Reger, R.D., 1977, Photointerpretive map of the surficial geology of the southern Kenai lowlands, Alaska: Alaska Division of Geological & Geophysical Surveys Open-File Report 111A, 1 sheet, scale 1:63,360.
- \_\_\_\_\_, 1978a, Reconnaissance geology of the Talkeetna-Kashwitna area, Susitna River basin, Alaska: Alaska Division of Geological & Geophysical Surveys Open-File Report 107A, 1 sheet, scale 1:63,360.
- \_\_\_\_\_, 1978b, Reconnaissance geology of the new capital site and vicinity, Anchorage Quadrangle, Alaska: Alaska Division of Geological & Geophysical Surveys Open-File Report 113A, 1 sheet, scale 1:63,360.
- \_\_\_\_\_, 1981a, Geology and geologic materials maps of the Anchorage C-8 SE Quadrangle, Alaska: Alaska Division of Geological & Geophysical Surveys Geologic Report 65, 2 sheets, scale 1:25,000.
- \_\_\_\_\_, 1981b, Geology and geologic materials maps of the Anchorage C-8 SW Quadrangle, Alaska: Alaska Division of Geological & Geophysical Surveys Geologic Report 68, 2 sheets, scale 1:25,000.
- \_\_\_\_\_, 1981c, Geology and geologic materials maps of the Anchorage B-8 NE Quadrangle, Alaska: Alaska Division of Geological & Geophysical Surveys Geologic Report 69, 2 sheets, scale 1:25,000.
- \_\_\_\_\_, 1981d, Geology and geologic materials maps of the Anchorage B-8 NW Quadrangle, Alaska: Alaska Division of Geological & Geophysical Surveys Geologic Report 70, 2 sheets, scale 1:25,000.
- \_\_\_\_\_, 1985, Brief overview of the surficial geology and glacial history of the Kenai Lowland, in Sisson, Alexander, ed., Guide to the geology of the Kenai Peninsula, Alaska: Anchorage, Alaska Geological Society guidebook, p. 20-23.
- Reger, R.D., and Carver, C.L., 1977, Photointerpretive map

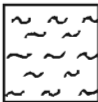
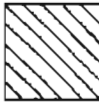
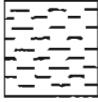
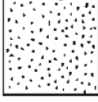
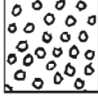
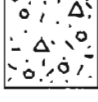
- of geologic materials of the southern Kenai lowlands, Alaska: Alaska Division of Geological & Geophysical Surveys Open-File Report 111B, 1 sheet, scale 1:63,360.
- \_\_\_\_\_. 1978a, Reconnaissance map of geologic materials, Talkeetna-Kashwitna area, Susitna River basin, Alaska: Alaska Division of Geological & Geophysical Surveys Open-File Report 107B, 1 sheet, scale 1:63,360.
- \_\_\_\_\_. 1978b, Reconnaissance geologic materials map of the new capital site and vicinity, Anchorage Quadrangle, Alaska: Alaska Division of Geological & Geophysical Surveys Open-File Report 113B, 1 sheet, scale 1:63,360.
- Reger, R.D., Combellick, R.A., and Brigham-Grette, Julie, 1995, Update of latest Wisconsin events in the upper Cook Inlet region, southcentral Alaska, in Combellick, R.A., and Tannian, Fran, eds., Short Notes on Alaska Geology 1995: Alaska Division of Geological & Geophysical Surveys Professional Report 117, p. 33-45.
- Reger, R.D., Combellick, R.A., and Pinney, D.S., 1994a, Geologic and derivative materials maps of the Anchorage C-7 NE Quadrangle, Alaska: Alaska Division of Geological & Geophysical Surveys Report of Investigations 94-24, 2 sheets, scale 1:25,000.
- \_\_\_\_\_. 1994b, Geologic and derivative materials maps of the Anchorage C-7 NW Quadrangle, Alaska: Alaska Division of Geological & Geophysical Surveys Report of Investigations 94-25, 2 sheets, scale 1:25,000.
- \_\_\_\_\_. 1994c, Geologic and derivative materials maps of the Anchorage C-8 NE Quadrangle, Alaska: Alaska Division of Geological & Geophysical Surveys Report of Investigations 94-26, 2 sheets, scale 1:25,000.
- \_\_\_\_\_. 1994d, Geologic and derivative materials maps of the Anchorage C-8 NW Quadrangle, Alaska: Alaska Division of Geological & Geophysical Surveys Report of Investigations 94-27, 2 sheets, scale 1:25,000.
- Reger, R.D., and Petrik, W.A., 1993, Surficial geology and late Pleistocene history of the Anchor Point area, Alaska: Alaska Division of Geological & Geophysical Surveys Public-Data File 93-50b, 8 p., 1 sheet, scale 1:25,000.
- Reger, R.D., and Pinney, D.S., 1996, Late Wisconsin glaciation of the Cook Inlet region with emphasis on Kenai Lowland and implications for early peopling, in Davis, N.Y., and Davis, W.E., eds., Adventures through time: Readings in the anthropology of Cook Inlet, Alaska: Anchorage, Cook Inlet Historical Society, p. 15-35.
- Reger, R.D., and Updike, R.G., 1983a, Upper Cook Inlet region and the Matanuska Valley, in Péwé, T.L., and Reger, R.D., eds., Guidebook to permafrost and Quaternary geology along the Richardson and Glenn Highways between Fairbanks and Anchorage, Alaska: Alaska Division of Geological & Geophysical Surveys Guidebook 1, p. 185-263, 1 sheet, scale 1:250,000.
- \_\_\_\_\_. 1983b, A working model for late Pleistocene glaciation of the Anchorage lowland, upper Cook Inlet, Alaska, in Thorson, R.M., and Hamilton, T.D., eds., Glaciation in Alaska: Extended abstracts from a workshop: University of Alaska Museum Occasional Paper 2, p. 71-74.
- Rieger, Samuel, 1983, The genesis and classification of cold soils: New York City, Academic Press, 230 p.
- Riehle, J.R., 1983, Preliminary Holocene tephrochronology of the upper Cook Inlet region of Alaska [abs.]: Geological Society of American Abstracts with Programs, v. 15, no. 5, p. 331-332.
- \_\_\_\_\_. 1985, A reconnaissance of the major tephra deposits in the upper Cook Inlet region, Alaska: Journal of Volcanology and Geothermal Research, v. 26, no. 1/2, p. 37-74.
- \_\_\_\_\_. 1994, Heterogeneity, correlatives, and proposed stratigraphic nomenclature of Hayes tephra set H, Alaska: Quaternary Research, v. 41, no. 3, p. 285-288.
- Riehle, J.R., Bowers, P.M., and Ager, T.A., 1990, The Hayes tephra deposits, an upper Holocene marker horizon in south-central Alaska: Quaternary Research, v. 33, no. 3, p. 276-290.
- Riehle, J.R., Kienle, Juergen, and Emmel, K.S., 1981, Lahars in Crescent River valley, lower Cook Inlet, Alaska: Alaska Division of Geological & Geophysical Surveys Geologic Report 53, 10 p.
- Riehle, J.R., Meyer, C.E., Ager, T.A., Kaufman, D.S., and Ackerman, R.E., 1987, The Aniakchak tephra deposit, a late Holocene marker horizon in western Alaska, in Hamilton, T.D., and Galloway, J.P., eds., Geologic studies in Alaska by the U.S. Geological Survey during 1986: U.S. Geological Survey Circular 998, p. 19-22.
- Rubin, Meyer, and Alexander, Corrine, 1958, U.S. Geological Survey radiocarbon dates IV: Science, v. 127, no. 3313, p. 1476-1487.
- \_\_\_\_\_. 1960, U.S. Geological Survey radiocarbon dates V: American Journal of Science Radiocarbon Supplement, v. 2, p. 129-185.
- Rubin, Meyer, and Suess, H.E., 1956, U.S. Geological Survey radiocarbon dates III: Science, v. 123, no. 3194, p. 442-448.
- Rymer, M.J., and Sims, J.D., 1982, Lake-sediment evidence for the date of deglaciation of the Hidden Lake area, Kenai Peninsula, Alaska: Geology, v. 10, no. 6, p. 314-316.
- Schmidt, R.A.M., 1963, Pleistocene marine microfauna in the Bootlegger Cove Clay, Anchorage, Alaska: Science, v. 141, no. 3578, p. 350-351.
- Schmoll, H.R., Dobrovolny, Ernest, and Gardner, C.A., 1981, Preliminary geologic map of Fire Island, Municipality of Anchorage, Alaska: U.S. Geological Survey Open-File Report 81-552, 4 p., 1 sheet, scale 1:25,000.
- Schmoll, H.R., Szabo, B.J., Rubin, Meyer, and Dobrovolny,

- Ernest, 1972, Radiometric dating of marine shells from the Bootlegger Cove Clay, Anchorage area, Alaska: Geological Society of America Bulletin, v. 83, no. 4, p. 1107-1114.
- Schmoll, H.R., and Yehle, L.A., 1983, Glaciation in the upper Cook Inlet basin: A preliminary re-examination based on geologic mapping in progress, in Thorson, R.M., and Hamilton, T.D., eds., Glaciation in Alaska: Extended abstracts from a workshop: University of Alaska Museum Occasional Paper 2, p. 75-100.
- \_\_\_\_\_, 1986, Pleistocene glaciation of the upper Cook Inlet basin, in Hamilton, T.D., Reed, K.M., and Thorson, R.M., eds., Glaciation in Alaska—the geologic record: Anchorage, Alaska Geological Society, p. 193-218.
- Schmoll, H.R., Yehle, L.A., Gardner, C.A., and Odum, J.K., 1984, Guide to surficial geology and glacial stratigraphy in the upper Cook Inlet basin: Anchorage, Alaska Geological Society guidebook, 89 p.
- Science Applications, Inc., 1977, Environmental assessment of the Alaskan continental shelf: Interim lower Cook Inlet synthesis report: Washington, D.C., National Oceanic and Space Administration report, 136 p.
- Spiker, Elliott, Kelley, Lea, Oman, Charles, and Rubin, Meyer, 1977, U.S. Geological Survey radiocarbon dates XII: Radiocarbon, v. 19, no. 2, p. 332-353.
- Stihler, S.D., 1991, Paleomagnetic investigation of seismic and volcanic activity recorded in the sediments of Skilak Lake: Fairbanks, University of Alaska MS thesis, 197 p.
- Suess, H.E., 1954, U.S. Geological Survey radiocarbon dates I: Science, v. 120, no. 3117, p. 467-473.
- Sullivan, B.M., Spiker, Elliott, and Rubin, Meyer, 1970, U.S. Geological Survey radiocarbon dates XI: Radiocarbon, v. 12, no. 1, p. 319-334.
- Soil Survey Staff, 1975, Soil taxonomy, a basic system of soil classification for making and interpreting soil surveys: Washington, D.C., U.S. Department of Agriculture Soil Conservation Service Agriculture Handbook 436, 754 p.
- Thorson, R.M., 1986, Late Cenozoic glaciation of the northern Nenana River valley, in Hamilton, T.D., Reed, K.M., and Thorson, R.M., eds., Glaciation in Alaska, the glacial record: Anchorage, Alaska Geological Society, p. 99-121.
- Urdike, R.G., and Ulery, C.A., 1983a, Preliminary geologic map of the Anchorage B-6 NW (Eklutna Lake) Quadrangle: Alaska Division of Geological & Geophysical Surveys Report of Investigations 83-3, 2 sheets, scale 1:10,000.
- \_\_\_\_\_, 1983b, Subsurface structure of the cohesive facies of the Bootlegger Cove Formation, southwest Anchorage: Alaska Division of Geological & Geophysical Surveys Professional Report 84, 5 p., 3 sheets, scale 1:15,840.
- \_\_\_\_\_, 1986, Engineering-geology map of southwest Anchorage: Alaska Division of Geological & Geophysical Surveys Professional Report 89, 1 sheet, scale 1:15,840.
- Vonder Haar, S.P., and Johnson, W.H., 1973, Mean magnetic susceptibility: A useful parameter for stratigraphic studies of glacial till: Journal of Sedimentary Petrology, v. 43, no. 4, p. 1148-1151.
- Westgate, J.A., 1988, Isothermal plateau fission-track age of the Old Crow tephra: Geophysical Research Letters, v. 15, p. 376-379.
- Westgate, J.A., Hamilton, T.D., and Gorton, M.P., 1983, Old Crow tephra—a new late Pleistocene stratigraphic marker across northcentral Alaska and western Yukon Territory: Quaternary Research, v. 38, no. 1, p. 38-54.
- Westgate, J.A., Stemper, B.A., and Péwé, T.L., 1990, A 3 m.y. record of Pliocene-Pleistocene loess in interior Alaska: Geology, v. 18, no. 9, p. 858-861.
- Wilcox, R.E., 1959, Some effects of recent volcanic ash falls with especial reference to Alaska: U.S. Geological Survey Bulletin 1028-N, p. 409-476.
- Wiles, G.C., 1992, Holocene glacial fluctuations in the southern Kenai Mountains, Alaska: Buffalo, State University of New York, PhD dissertation, 333 p.
- Wiles, G.C., and Calkin, P.E., 1994, Late Holocene, high-resolution glacial chronologies and climate, Kenai Mountains, Alaska: Geological Society of America Bulletin, v. 106, no. 2, p. 281-303.
- Williams, J.R., 1986, New radiocarbon dates from the Matanuska Glacier bog section, in Bartsch-Winkler, Susan, and Reed, K.M., eds., Geologic studies in Alaska by the U.S. Geological Survey during 1985: U.S. Geological Survey Circular 978, p. 85-88.
- Winkler, G.R., 1992, Geologic map and summary geochronology of the Anchorage 1° x 3° quadrangle, southern Alaska: U.S. Geological Survey Miscellaneous Investigations Map I-2283, 1 sheet, scale 1:250,000.
- Yehle, L.A., and Schmoll, H.R., 1989, Surficial geologic map of the Anchorage B-7 SW Quadrangle, Alaska: U.S. Geological Survey Open-File Report 89-318, 33 p., 1 sheet, scale 1:25,000.
- Yehle, L.A., Schmoll, H.R., and Dobrovolsky, Ernest, 1990, Geologic map of the Anchorage B-8 SE and part of the Anchorage B-8 NE Quadrangles, Alaska: U.S. Geological Survey Open-File Report 90-238, 37 p., 1 sheet, scale 1:25,000.
- \_\_\_\_\_, 1991, Geologic map of the Anchorage B-8 SW Quadrangle, Alaska: U.S. Geological Survey Open-File Report 91-143, 30 p., 1 sheet, scale 1:25,000.

## **APPENDIX A**

Stratigraphic sections and soil profiles associated with middle to late Pleistocene deposits in the Cook Inlet region. Observation dates are shown at the top of the sections. Stratigraphic symbols and terminology are defined in table A.1. Soil-profile terminology is defined in table A.2. Geochemistry of glass shards in tephtras with asterisk (\*) numbers was analyzed by electron microprobe but is not reported because of great variation. Question mark after tephtra number indicates that tephtra designation is very tentative due to small number of shards segregated. Tephtras without numbers were not sampled.

Table 1A. Symbols and terminology used in stratigraphic sections

	Organic material or peat		Loess (eolian silt)
	Clay		Tephra
	Silt		Silt and clay rhythmite
	Sand		Sand and silt rhythmite
	Pebble gravel		Blocky rubble
	Diamicton, mixed coarse and fine material		Invertebrate fossil sample
	Wood		Microfossil sample
	Dropstone		Fission-track sample
	Radiocarbon sample		Sand wedge
	<sup>39</sup> Ar/ <sup>40</sup> Ar sample		

Estimated content of silt, sand, and gravel is based on field observations and general composition in summary descriptions of stratigraphic sections as indicated by nonquantitative terms:

Some = 12 to 30 percent

Trace = 4 to 12 percent

Not recorded <4 percent

Estimated content of cobbles and boulders is based on field observations and general composition in summary descriptions of stratigraphic sections as indicated by nonquantitative terms:

Numerous = two cobbles or boulders in 0.6 m section

Scattered = two cobbles or boulders in 3 to 4.5 m section

Rare = two cobbles or boulders in section >4.5 m

Table A2. Definitions of symbols in summary soil descriptions (Soil Survey Staff, 1975; modified by Harden, 1982; Birkeland, 1984; Birkeland and others, 1991b; and this study)

Characteristic	Symbol	Definition	Measure
Structure	l	Few present	Few/dm <sup>2</sup>
	m	Massive	No peds developed
	sg	Single grained	No particle bonding
	vl	Very weak	Very few, indistinct peds
	f	Fine or thin	Plates 1-2 mm, blocks 5-10 mm
	pl	Platy	Particles oriented in horizontal planes
	sbk	Subangular blocks	Peds faces round and planar
Consistence	lo	Loose (dry and moist)	Noncoherent
	so	Weakly coherent (dry)	Powders easily
	so	Nonsticky (wet)	No adherence
	ss	Slightly sticky (wet)	Slight adherence, stretches
	po	Nonplastic (wet)	No rod forms
	ps	Slightly plastic (wet)	Weak rod forms
Roots	v)	Very few present	Very few/dm <sup>2</sup>
	1	Few present	Few/dm <sup>2</sup>
	2	Commonly present	Common/dm <sup>2</sup>
	3	Many present	Many/dm <sup>2</sup>
	vf	Very fine	<1 mm dia
	f	Fine	1 to 2 mm dia
	m	Medium	2 to 5 mm dia
	co	Coarse	>5 mm dia
Pores	1	Few present	Few/dm <sup>3</sup>
	2	Commonly present	Common/dm <sup>3</sup>
	3	Many present	Many/dm <sup>3</sup>
	vf	Very fine	0.1 to 0.5 mm dia
	f	Fine	0.5 to 2 mm dia
	m	Medium	2 to 5 mm dia
	tub	Tubular shape	Cylindrical, elongate pores
	ves	Vesicular shape	Spherical or elliptical pores
	ir	Irregular shape	Walls of pores curves or angular
Lower boundary	a	Abrupt	Transition w/in 1 mm to 2.5 cm
	c	Clear	Transition w/in 2.5 to 6 cm
	g	Gradual	Transition w/in 6 to 12.5 cm
	d	Diffuse	Transition >12.5 cm
	i	Irregular	Undulates, pocket depths >widths
	s	Smooth	Parallel to ground surface
	w	Wavy	Undulates, pocket depths <widths
b	Broken	Parts of horizon laterally discontinuous	

\*Exact number varies with size of structure, root, or pore (Soil Survey Staff, 1975, p. 479-481).

**Table A3.** Summary field description of soil profile S1 measured 08-14-90 on flat crest of type Killey moraine (60°31'25"N, 150°37'42"W), Kenai C-2 SW Quadrangle (KEN-79, sheet 2). Elevation 101 m. Horizons according to Soils Survey Staff (1975), modified by Birkeland and others (1991b) and this study

Horizon	E	Bs	Bw <sup>a</sup>	2Cox	2Cu
Depth (cm)	0-5	5-15	15-28	28-39	39-61
Moist Munsell color	2.5Y5/2 (grayish brown)	10YR5/6 (yellowish brown)	70% 2.5Y5/6 (loess) (light olive brown) 30% 2.5Y5/2 (tephra) (grayish brown)	5Y5/3 (olive)	5Y4/3 (olive)
Texture (% gravel)	sand (- - -)	sand (trace)	sand (trace)	sand (50)	sand (50)
Structure	sg	sg	v1 fsbk to sg	sg	sg
Dry consistence	- - -	lo	so	- - -	- - -
Moist consistence	- - -	- - -	- - -	- - -	- - -
Wet consistence	so, ps	so, ps	ss, ps	ss, po	so, po
Roots	3f, 2m, 1co	3f, 2vf, 2m	2m, 1co, 1f	1f	v1f
Pores	- - -	- - -	3f ir	- - -	- - -
Lower boundary	c,s	c,w	c,w	c,s	- - -

<sup>a</sup>Complex mixture of loess and tephra.

Vegetation: Post-1947 open woodland of white spruce (*Picea glauca*), black spruce (*Picea mariana*), and quaking aspen (*Populus tremuloides*) with scattered highbush cranberry (*Viburnum edule*) shrubs, lupine (*Lupinus* spp.), and a discontinuous, thin ground cover of lingonberry (*Vaccinium vitis-idaea*), bearberry (*Arctostaphylos uva-ursi*), feathermosses, and foliose lichens.

**Table A4.** Summary field description of soil profile S2 measured 08-14-90 on flat crest of type Moosehorn moraine (60°31'23"N, 150°42'34"W), Kenai C-2 SW Quadrangle (KEN-80, sheet 2). Elevation 91 m. Horizons according to Soils Survey Staff (1975), modified by Birkeland and others (1991b) and this study

Horizon	A	E	Bs <sup>a</sup>	Bw	2Cox	2Cu
Depth (cm)	0-2	2-5	5-9	9-25	25-42	42-74
Moist Munsell color	10YR4/2 (dark grayish brown)	10YR6/1 (gray)	5YR5/8 (yellowish red)	10YR6/4 (light yellowish brown)	5Y5/3 (olive)	5Y4/2 (olive gray)
Texture (% gravel)	- - - (- - -)	sand (- - -)	sand (trace)	sand (trace)	sand (50)	sand (50)
Structure <sup>b</sup>	- - -	v lfsbk to m	v lfsbk to sg	v lfsbk to sg	sg	lfsbk to sg
Dry consistence	- - -	lo	lo	so	- - -	- - -
Moist consistence	- - -	- - -	- - -	- - -	- - -	- - -
Wet consistence	- - -	so, ps	so, ps	so, ps	so, po	so, po
Roots	2f, 1m	2f, 1m	2f, 1m	2f, 1m	vlf	- - -
Pores	- - -	- - -	- - -	3f ir	- - -	- - -
Lower boundary	c,b	c,w	c,w	c,w	c,s	- - -

<sup>a</sup>Hydrophobic because of organic matter.

<sup>b</sup>Mixture of silt and clay forms pebble caps throughout section.

Vegetation: Post-1947 open woodland of black spruce (*Picea mariana*), white spruce (*Picea glauca*), birch (*Betula papyrifera* ssp.), and quaking aspen (*Populus tremuloides*) with scattered highbush cranberry (*Viburnum edule*) shrubs, lupine (*Lupinus* spp.), and a discontinuous, thin ground cover of lingonberry (*Vaccinium vitis-idaea*), bearberry (*Arctostaphylos uva-ursi*), mosses, and foliose lichens.

**Table A.5.** Summary field description of soil profile S3 measured 08-14-90 on flat crest of type Skilak moraine (60°28'45"N, 150°27'24"W), Kenai B-2 NE Quadrangle (KEN-101, sheet 2). Elevation 89 m. Horizons according to Soils Survey Staff (1975), modified by Birkeland and others (1991b) and this study

Horizon	E	Bs	Bw? <sup>a</sup>	Cox	Cu
Depth (cm)	0-6	6-13	13-17	17-54	54-74
Moist Munsell color	5Y6/3 (pale olive)	2.5Y5/6 (light olive brown)	5Y6/4 (pale olive)	5Y5/2 (olive gray)	5Y4/2 (olive gray)
Texture (% gravel)	sand (trace)	sand (trace)	sand (trace)	sand (trace)	sand (50)
Structure <sup>b</sup>	m to sg	m to sg	m to sg	sg	sg
Dry consistence	---	---	---	---	---
Moist consistence	---	---	---	---	---
Wet consistence	so, po	so, po	so, po	so, po	so, po
Roots	1f, 1m	1f, 1m	3vf, 2f	1f	---
Pores	---	---	---	---	---
Lower boundary	c,w	c,d	c,w	c,s	---

<sup>a</sup>Bw is a weakly developed, borderline Cox.

<sup>b</sup>Mixture of silt and clay forms thin caps.

Vegetation: Post-1947 open woodland of white spruce (*Picea glauca*), black spruce (*Picea mariana*), and quaking aspen (*Populus tremuloides*) with a ground cover of narrow-leaf Labrador tea (*Ledum decumbens*) and foliose lichens.

**Table A6.** Summary field description of soil profile S4 measured 08-16-90 on flat crest of Moosehorn-age moraine of the Kachemak Bay lobe (59°43'33"N, 151°44'02"W), Seldovia C-5 NW Quadrangle (SEL -7, sheet 3). Elevation 123 m. Horizons according to Soils Survey Staff (1975), modified by Birkeland and others (1991b) and this study

Horizon	Ap <sup>a</sup>	A/E	Bhs	Bs (tephra)	Bw	2Ab <sup>b</sup>	2Bwb	2Coxb	3Coxb	3Cub
Depth (cm)	0-9	9-16	16-24	24-36	36-47	47-57	57-62	62-78	78-93	93-107
Moist Munsell color	---	5YR2/1 (A) (black) 10YR4/2 (E) (dark grayish brown)	10R2/2 (very dusky red)	5YR4/8 (reddish brown)	5YR3/3 (dark reddish brown)	5YR2/2 (dark reddish brown)	10YR4/4 (dark yellowish brown)	2.5Y5/4 (light olive brown)	2.5Y4/4 (olive brown)	10YR3/3 (dark brown)
Texture (% gravel)	---	sand (trace)	loamy sand (trace)	sand (trace)	sand (trace)	sand (trace)	sand (trace)	sand (trace)	sand (20)	sand (40-50)
Structure	---	m	m	m <sup>c</sup>	m to v lfsbk	m	lfsbk	m to sg	m	m to sg
Dry consistence	---	---	---	---	---	---	---	---	---	---
Moist consistence	---	---	---	---	---	---	---	---	---	---
Wet consistence	---	ss, ps	so, ps	so, ps	so, ps	ss, ps	ss, ps	ss, ps	so, ps	so, po
Roots	---	3co, 3m, 2f, 2vf	3f, 2co, 2m	lf, 1vf	2f, 2vf	2f, 2vf	2f, 2vf, 1m	1f, 1vf	v 1vf	---
Pores	---	3vf tub, 2f tub	1f tub	---	3vf tub	2f ir	3f tub, 1m tub	3vf tub, 1f tub	1f tub	---
Lower boundary	---	c,w	c,w	c,w	c,w	c,w	c,s	g,s	c,s	---

<sup>a</sup>Disturbed so not described.

<sup>b</sup>Lowest 1 cm is Eb, which is not described.

<sup>c</sup>Breaks where directed because of presence of tephra shards.

Vegetation: Open Sitka spruce (*Picea sitkensis*) woodland with understory dominated by ferns, tall fireweed (*Epilobium angustifolium*), and scattered grasses (*Calamagrostis* spp.) and a widespread 15-cm-thick ground cover of feathermosses and clubmoss (*Lycopodium annotinum*), which also covers downed trees.

**Table A7.** Summary field description of soil profile S5 measured 08-15-90 on flat crest of Moosehorn-age moraine of the Kachemak Bay lobe (59°39'49"N, 151°32'13"W), Seldovia C-5 NW Quadrangle (SEL-13, sheet 3). Elevation 342 m. Horizons according to Soils Survey Staff (1975), modified by Birkeland and others (1991b) and this study

Horizon	E	Bhs	Bw	2Bhsb <sup>a</sup>	2Cox1b	2Cox2b	3Cox3b	3Cub <sup>b</sup>
Depth (cm)	0-3	3-9	9-31	31-40	40-53	53-61	61-103	103-116
Moist Munsell color	10YR4/2 (dark grayish brown)	2.5YR2/2 (very dusky red)	5YR2/2 (dark reddish brown)	10R2/2 (very dusky red)	10YR3/3 (dark brown)	10YR4/4 (dark yellowish brown)	10YR3/4 (dark yellowish brown)	2.5Y5/4 (light olive brown)
Texture (% gravel)	sand (---)	sand (---)	sand (---)	sand (---)	sand (---)	sand (trace) <sup>c</sup>	sand (trace) <sup>c</sup>	sand (---)
Structure	---	m	m to v lfsbk	m	m to sg	m to sg	m to lfsbk	---
Dry consistence	---	---	---	---	---	---	---	---
Moist consistence	---	---	---	---	---	---	---	---
Wet consistence	so, ps	so, ps	ss, ps	ss, ps	ss, ps	ss, ps	ss, ps	---
Roots	---	3m, 3f, 1 co	3m, 2f, 2co	3m, 2f, 1co	1f, 1m	1f, 1m	1m, v1f	---
Pores	---	2vf ir	3vf ir, 1f tub	3f ir, 1f tub	3f ir	2f ir	3f ir	---
Lower boundary	a,w	c,w	c,i	c,i	c,w	c,w	---	---

<sup>a</sup>Some bioturbation.

<sup>b</sup>Sandy phase of Moosehorn drift.

<sup>c</sup>Frost-jacked stones.

Vegetation: Open Sitka spruce (*Picea sitkensis*) woodland with scattered Kenai birch (*Betula papyrifera* var. *kenaica*), an understory of ferns, highbush cranberry (*Viburnum edule*), twisted stalk (*Streptopus amplexifolius*), and a ground cover of feathermosses and grasses.

**Table A8.** Summary field description of soil profile S6 measured 08-13-90 on flat crest of Elmendorf-age Bird Creek moraine (60°58'07"N, 149°26'39"W), Turnagain Arm, Seward D-7 NW Quadrangle (SEW-2, sheet 4). Elevation 25 m. Horizons according to Soils Survey Staff (1975), modified by Birkeland and others (1991b) and this study

Horizon	A	E	Bs	Bw <sup>a</sup>	Cox1	Cox2	Cu
Depth (cm)	0-2	2-10	10-22	22-28	28-46	46-52	52-94
Moist Munsell color	10YR5/1 (gray)	10YR7/1 (light gray)	10YR5/7 (yellowish brown)	10YR6/4 (light yellowish brown)	5Y5/3 (olive)	5Y5/2+ (olive gray)	5Y5/2 (olive gray)
Texture (% gravel)	---	sand (---)	sand (---)	sand (---)	sand (---)	sand (---)	sand (---)
Structure	---	sg	sg	m to sg	sg	sg to v1fpl	sg to 1fpl
Dry consistence	---	lo	lo	lo	lo	lo	lo
Moist consistence	---	lo	lo	lo	lo	lo	lo
Wet consistence	---	ss, ps	ss, ps	ss, ps	so, ps	so, ps	so, ps
Roots	---	3m, 3f, 3vf, 1 co	3f, 2m, 2vf	3f, 2m, 1co	2f, 1vf, 1m	1f, 1m	1f, 1m
Pores	---	---	3f ves, 1f tub	3vf ves, 1f tub	2f ves, 1f tub	—	1m tub, 1f ves
Lower boundary	c,b	c,i	c,w	c,w	c,s	c,s	—

<sup>a</sup>Appears to be mixed Bs and Cox1, perhaps as a transition or by seasonal-frost stirring.

Vegetation: A 30- to 40-yr-old birch (*Betula papyrifera* spp.) woodland with scattered alder (*Alnus* sp.) shrubs, an understory of red-berried elder (*Sambucus racemosa*), highbush cranberry (*Viburnum edule*), dwarf dogwood (*Cornus canadensis*), scattered tall fireweed (*Epilobium angustifolium*), and grasses (*Calamagrostis* spp.), and a thin ground cover of foliose lichens and mosses. Numerous burned spruce (*Picea* sp.) stumps.

**Table A9.** Summary field description of soil profile S7 measured 08-13-90 on crest of 9,900-yr-old latest-Naptowne moraine in Turnagain Pass (60°47'39"N, 149°13'12"W), southwestern quarter of Seward D-6 Quadrangle (SEW-12, sheet 4). Elevation 297 m. Horizons according to Soils Survey (1975), modified by Birkeland and others (1991b) and this study

Horizon	A <sup>a</sup>	Bhs <sup>b</sup>	Bw <sup>b</sup>	Cox <sup>b</sup>	Cu	A (east wall)	E (east wall)	Bh (east wall)
Depth (cm)	0-9	9-24	24-43	43-72	72-79	0-3	3-7	7-11
Moist Munsell color	2.5YR2/4 (dark reddish brown)	2.5YR2/2 (very dusky red)	5YR3/2 <sup>c</sup> (dark reddish brown)	60% 5Y5/2 (olive gray) <sup>d</sup> 40% 5Y4/3	5Y4/2 (olive gray)	2.5YR2/4 (dark reddish brown)	5YR3/2 (dark reddish brown)	2.5YR2/4 (dark reddish brown)
Texture (% gravel)	sand (- - -)	sand (10)	sand (60)	sand (60)	sand (60)	- - - (- - -)	sand (- - -)	sand (10)
Structure	m to sg	m to sg	sg	sg	sg	m to sg	m to sg	m to sg
Dry consistence	- - -	- - -	- - -	- - -	- - -	- - -	- - -	- - -
Moist consistence	- - -	- - -	- - -	- - -	- - -	- - -	- - -	- - -
Wet consistence	so, ps	ss, ps	ss, ps	so, po	ss, ps	so, ps	so, ps	so, ps
Roots	2f	1f, 2vf	1f	v1f	- - -	2f	2f	2f
Pores	- - -	3f ir	- - -	- - -	- - -	- - -	- - -	- - -
Lower boundary	d,s	c,w	c,s	c,s	- - -	d,s	d,s	d,s

<sup>a</sup>Cumulic?

<sup>b</sup>Mixture of silt and clay form caps on pebbles. Coatings are moderately thick in Bw.

<sup>c</sup>Very bright (5YR3/4 (dark reddish brown)) stone coatings.

<sup>d</sup>Slightly mottled.

Vegetation: Alpine meadow of crowberry (*Empetrum nigrum*) mat with scattered cloudberry (*Rubus chamaemorus*), grasses (*Calamagrostis* sp.), spirea (*Spirea Beauverdiana*) shrubs, lingonberry (*Vaccinium vitis-idaea*), and tall fireweed (*Epilobium angustifolium*).

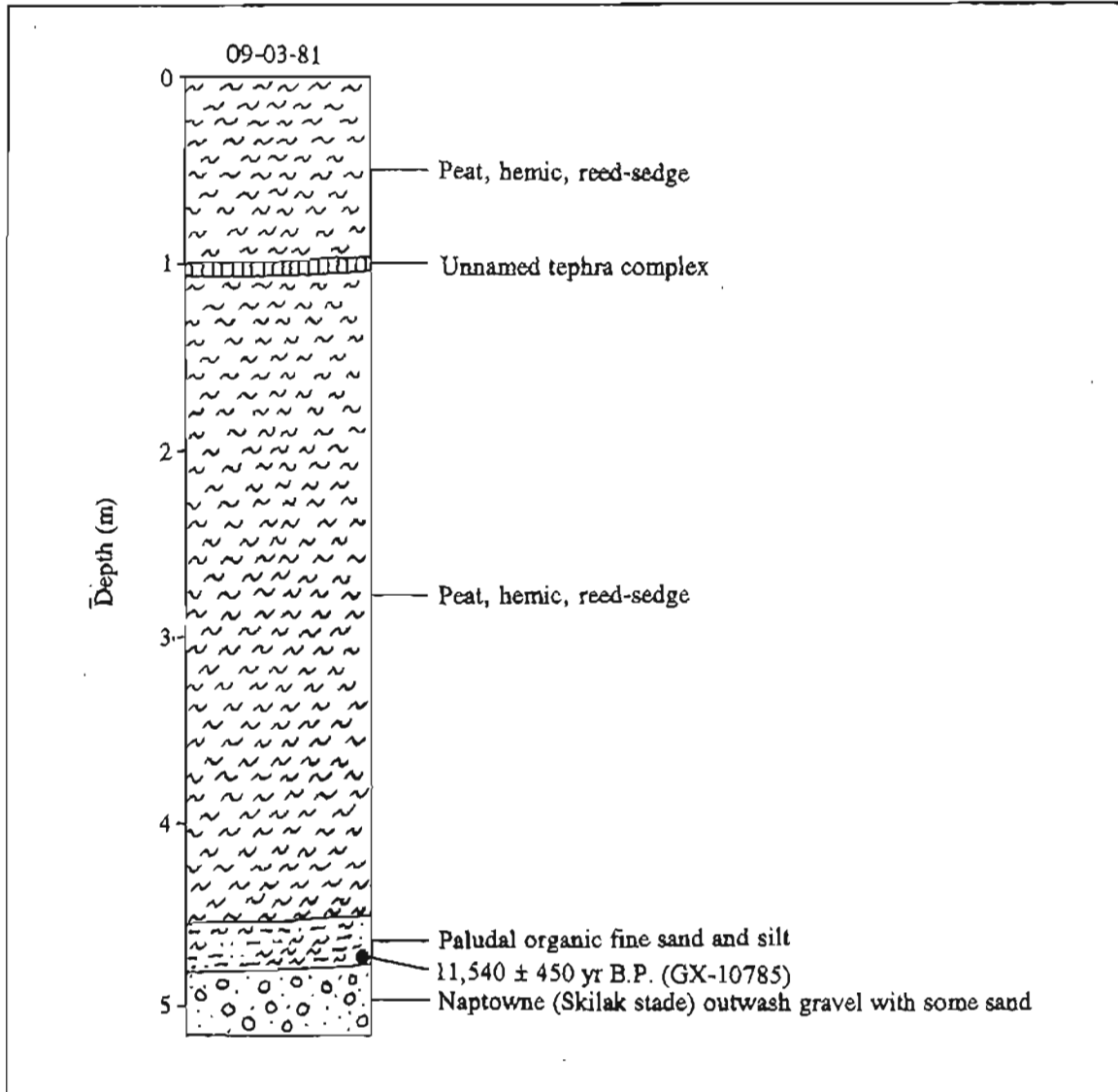


Figure A1. Stratigraphy exposed in section 1 (61°50'05"N, 149°58'39"W), Anchorage D-8 SW Quadrangle (ANC-1, sheet 1). Chronologic significance of radiocarbon date given in table 2.

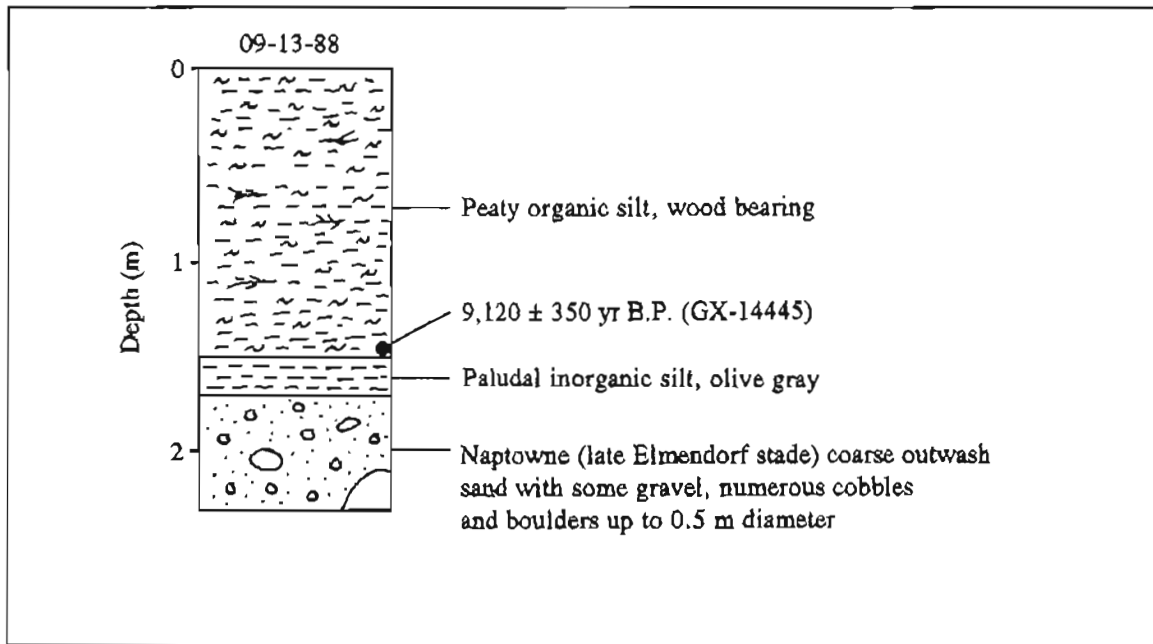


Figure A2. Stratigraphy exposed in section 2 (61°41'44"N, 149°15'05"W), Anchorage C-7 NE Quadrangle (ANC-9, sheet 1). Chronologic significance of radiocarbon date given in table 2.

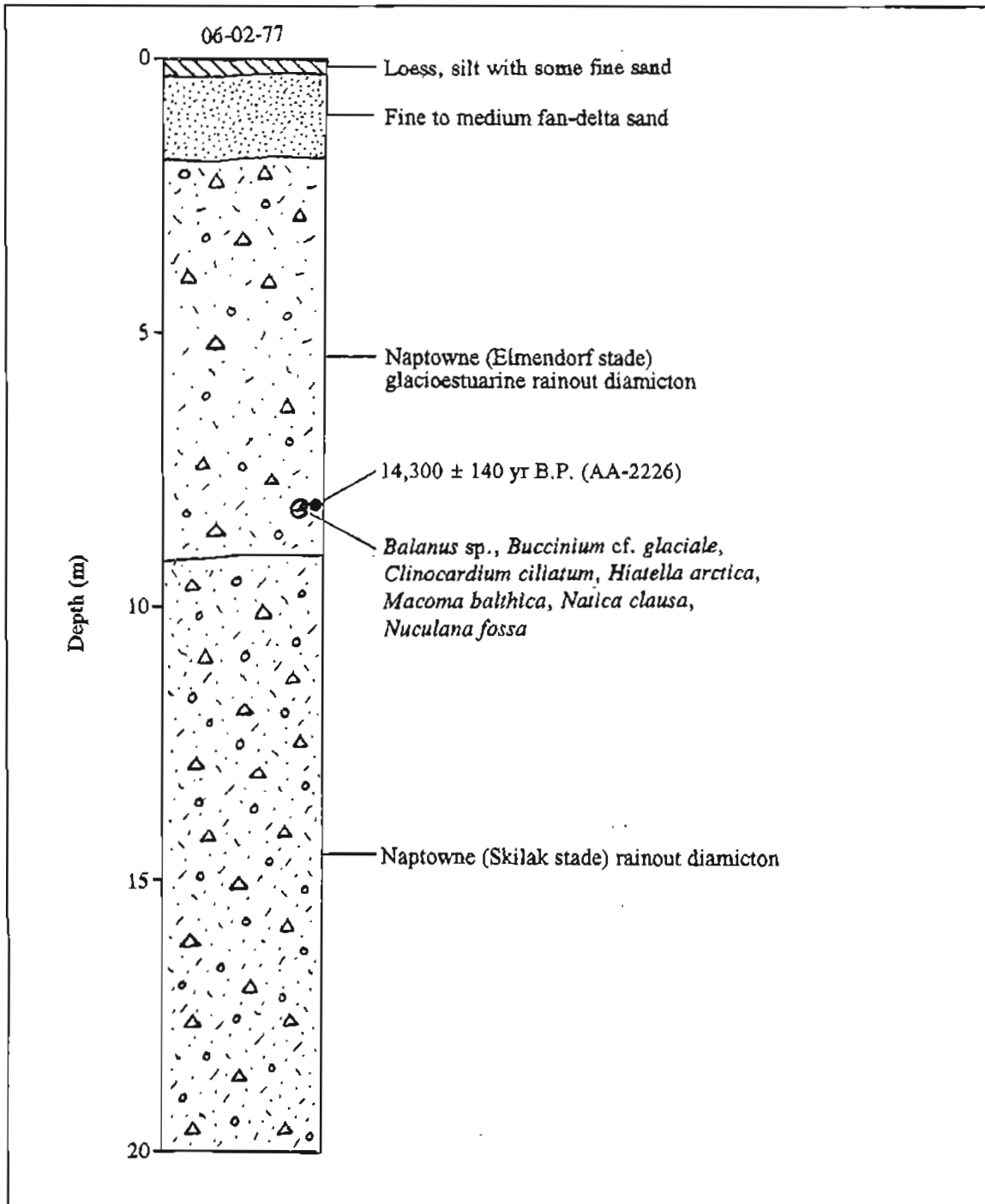


Figure A4. Stratigraphy exposed in section 4 (61°15'34"N, 149°55'57"W), Anchorage B-8 SW Quadrangle (ANC-36, sheet 1). Chronologic significance of radiocarbon date given in table 2.

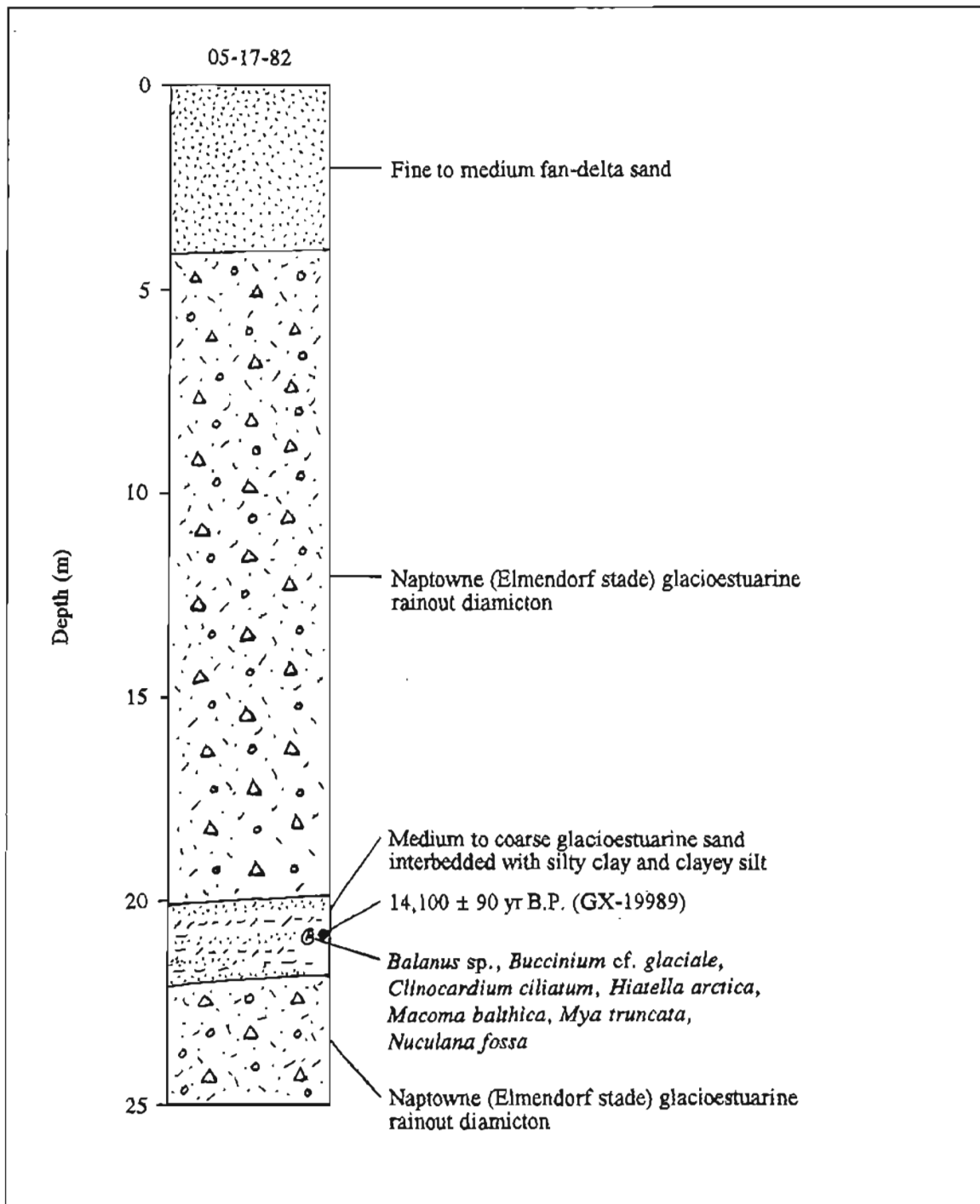


Figure A5. Stratigraphy exposed in section S (61°14'17"N, 149°58'57"W), Anchorage A-8 NW Quadrangle (ANC-39, sheet 1). Chronologic significance of radiocarbon date given in table 2.

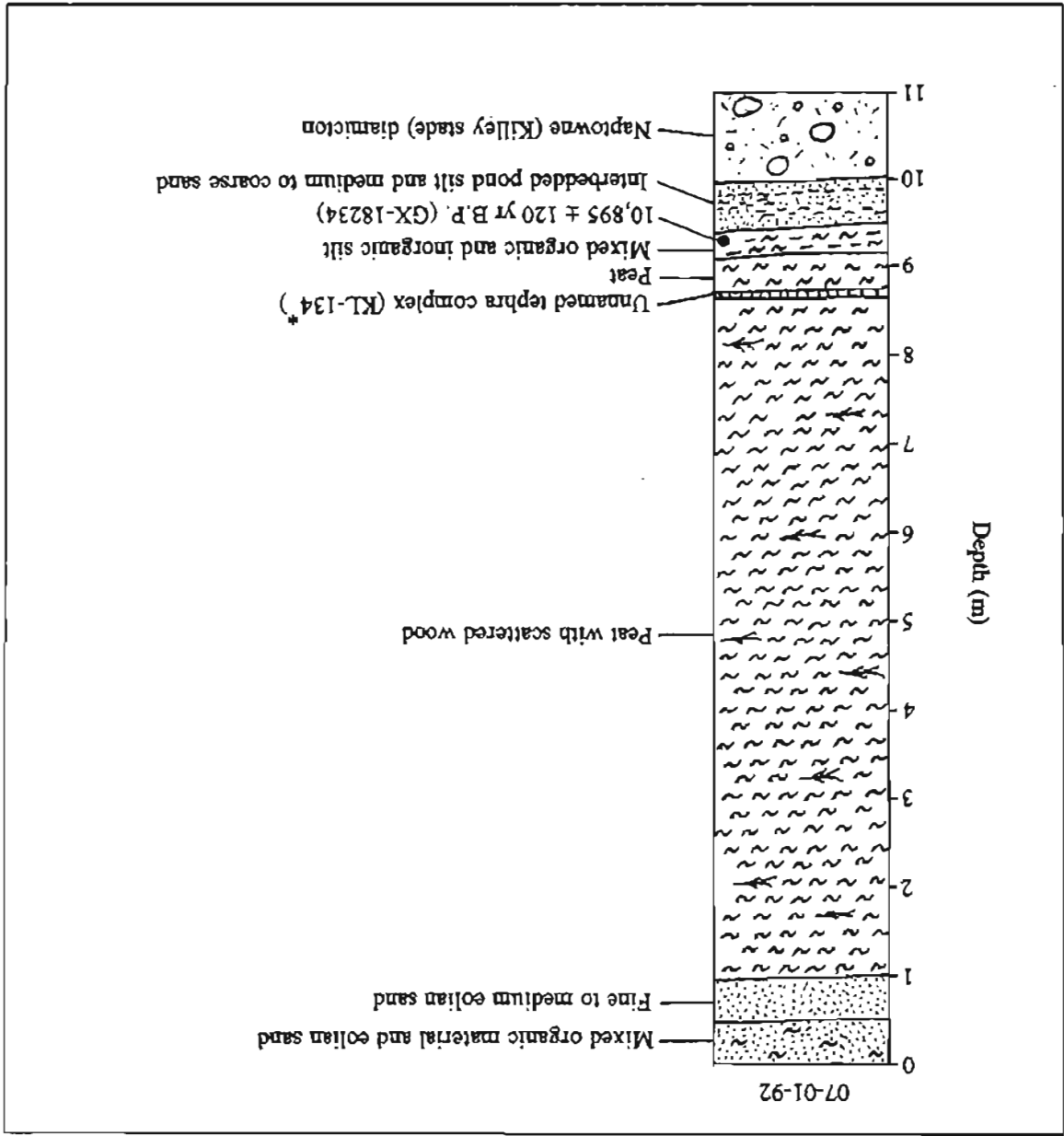


Figure A6. Stratigraphy exposed in section 6 (60°58'48"N, 150°18'11"W), Kenai D-1 NW Quadrangle (KEN-1, sheet 2). Chronologic significance of radiocarbon date given in table 2.

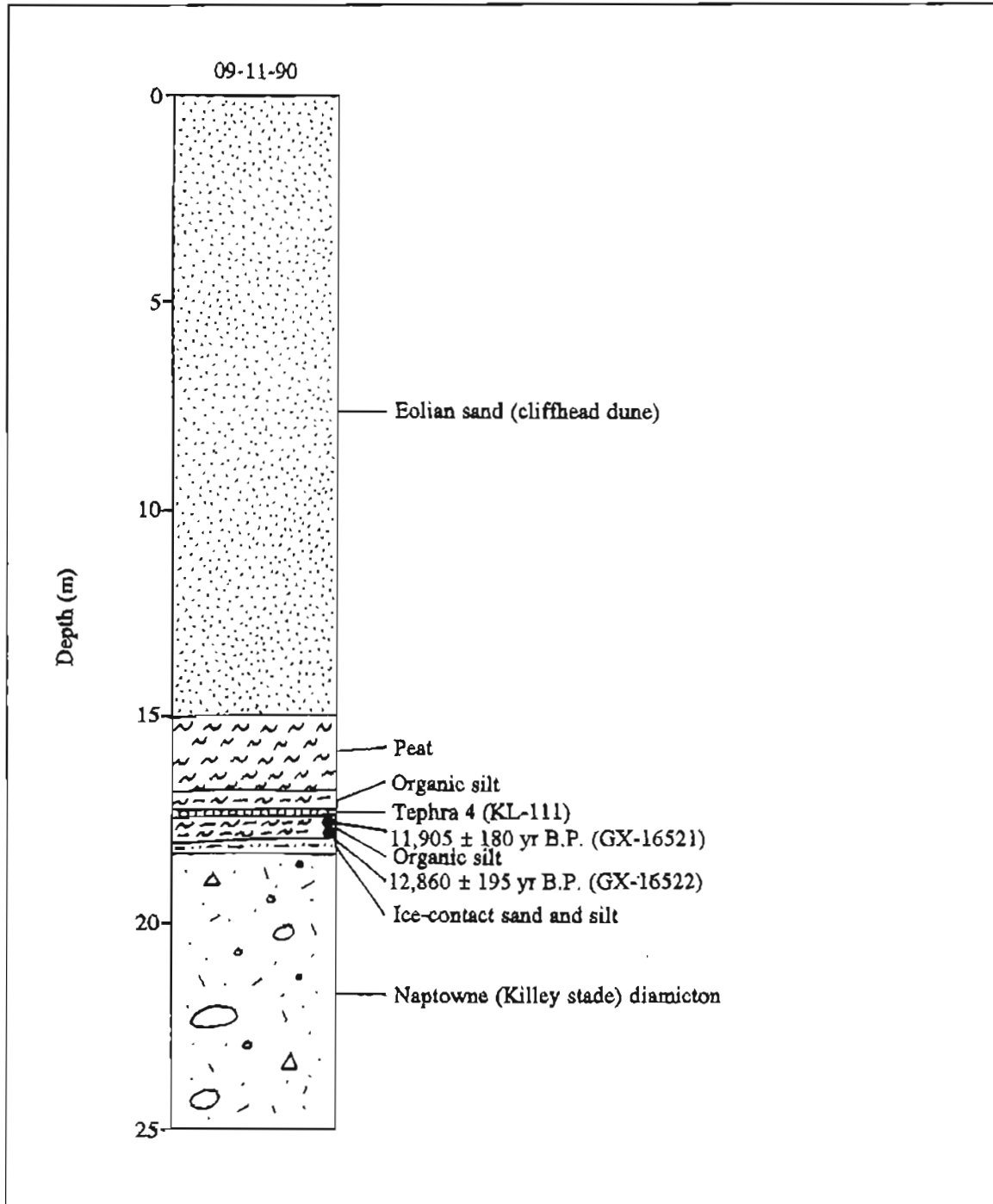


Figure A7. Stratigraphy exposed in section 7 (60°58'02"N, 150°17'20"W), Kenai D-1 NW Quadrangle (KEN-2, sheet 2). Chronologic significance of radiocarbon dates given in table 2. Tephra geochemistry given in table 3.

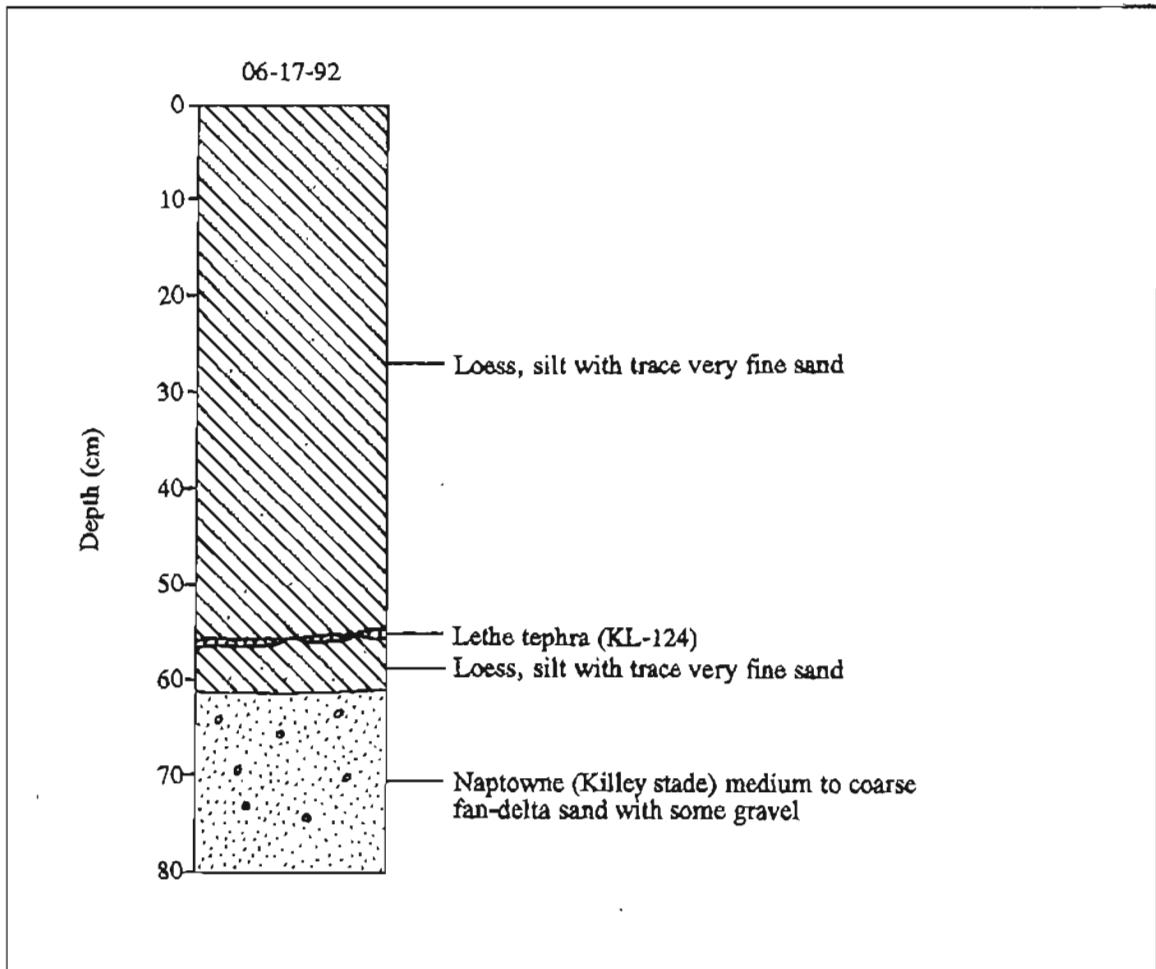


Figure A17. Stratigraphy exposed in section 17 (60°37'25"N, 151°07'54"W), Kenai C-4 SE Quadrangle (KEN-44, sheet 2). Tephra geochemistry given in table 3. Section indicates Killey age for fan delta near Kenai.

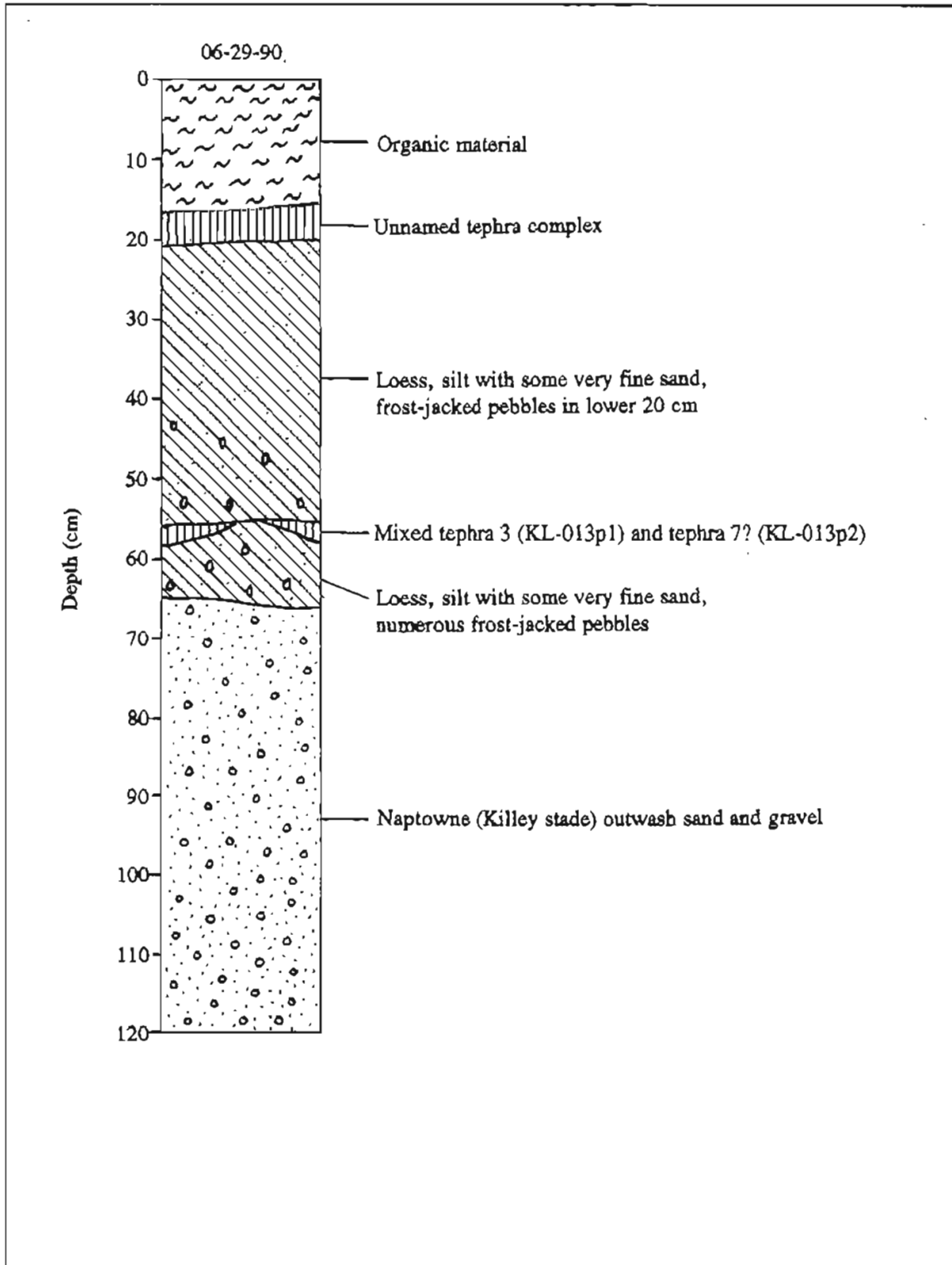


Figure A16. Stratigraphy exposed in section 16 (60°38'05"N, 151°20'02"W), Kenai C-4 NW Quadrangle (KEN-41, sheet 2). Tephra geochemistry given in table 3, except for unnamed tephra complex.

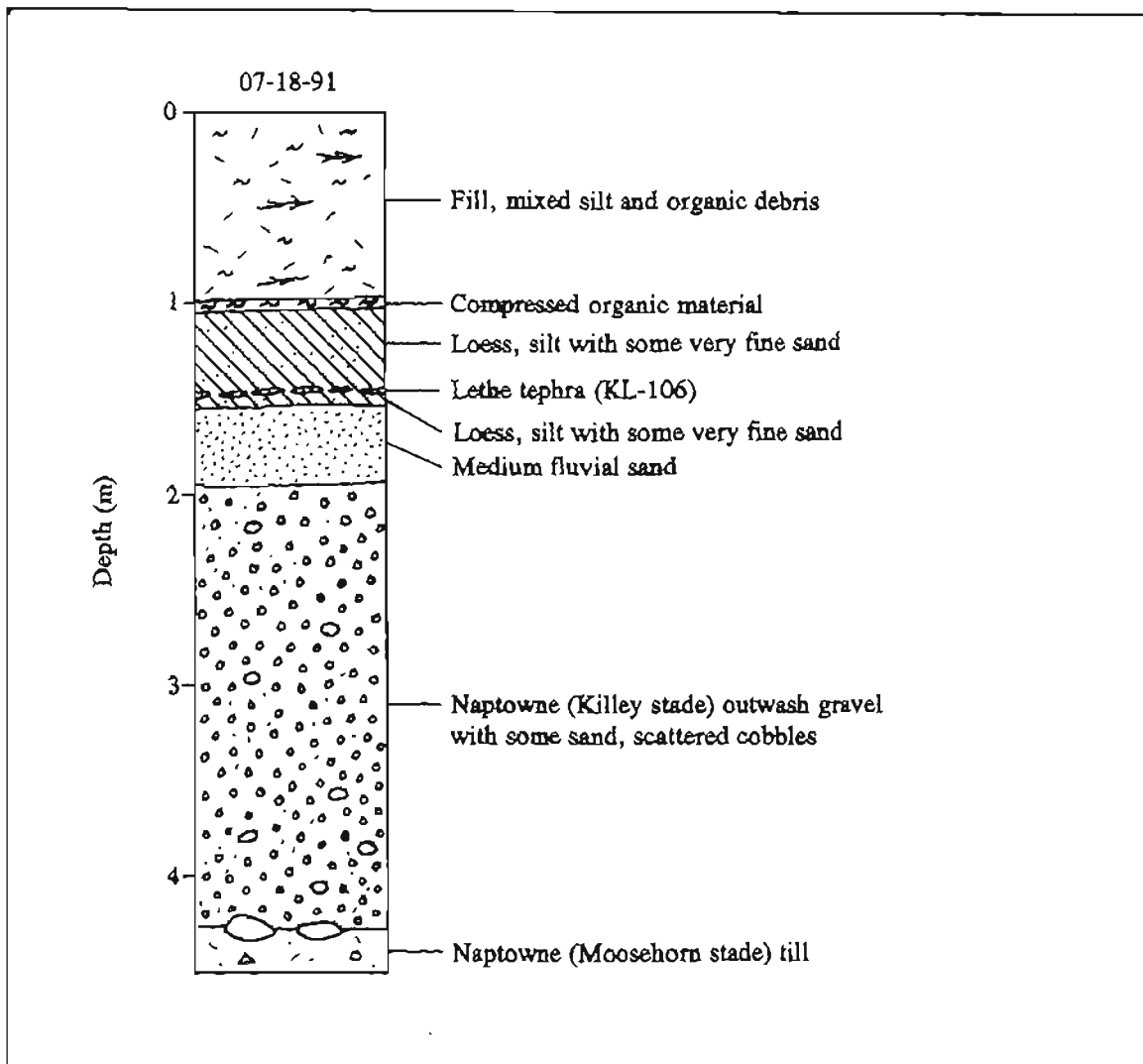


Figure A15. Stratigraphy exposed in section 15 ( $60^{\circ}38'17''N$ ,  $151^{\circ}04'22''W$ ), Kenai C-3 NW Quadrangle (KEN-40, sheet 2). Tephra geochemistry given in table 3. Section indicates Killey age for upper terrace on east side of Beaver Creek and associated paleodrainage system down Swanson River from terminal moraines of Turnagain Arm lobe.

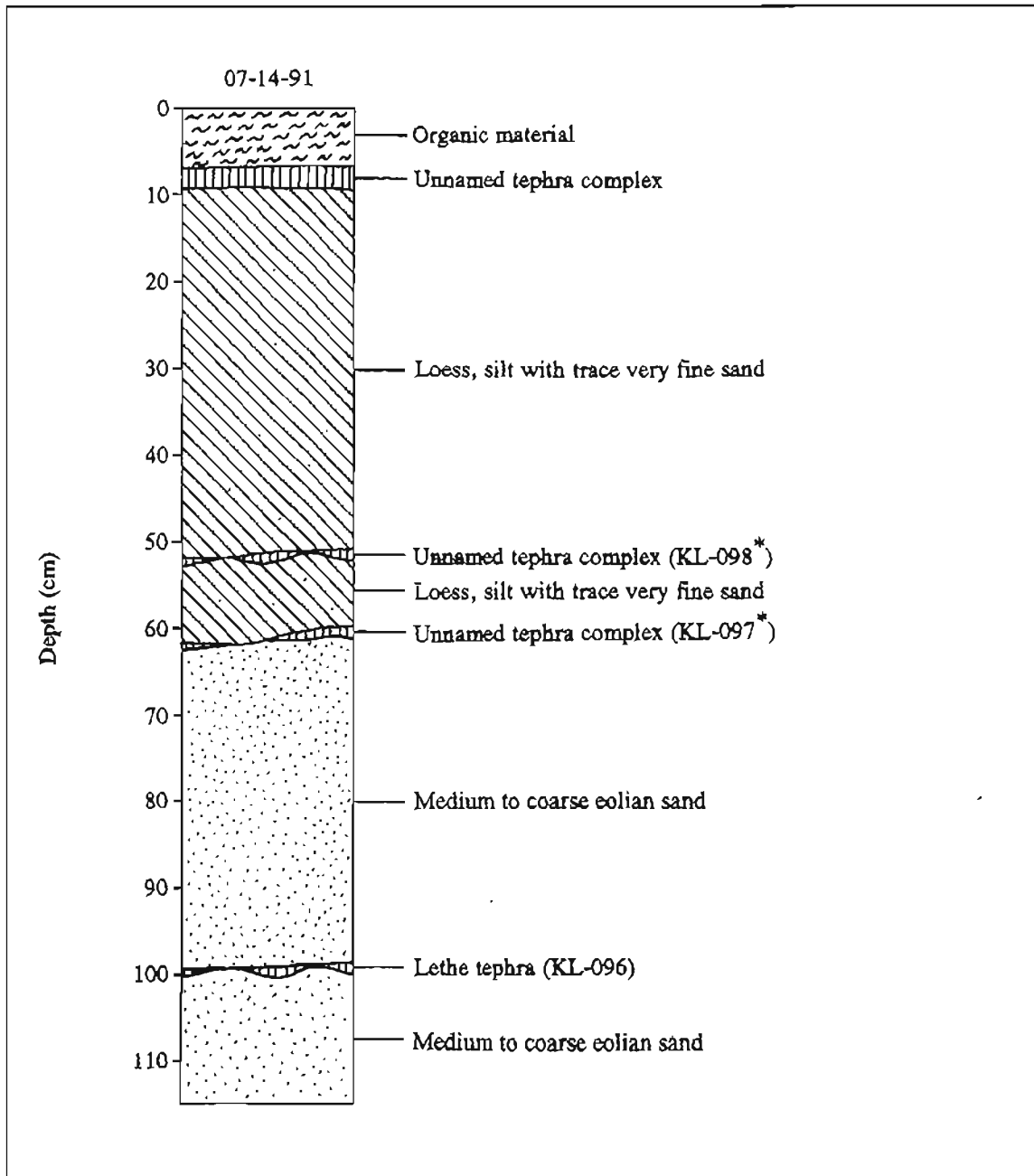


Figure A14. Stratigraphy exposed in section 14 (60°38'58"N, 150°49'21"W), Kenai C-3 NE Quadrangle (KEN-38, sheet 2). Tephra geochemistry given in table 3. Section demonstrates late Killey age for eolian sand in meltwater channels through Moosehorn moraine in finger Lakes area.

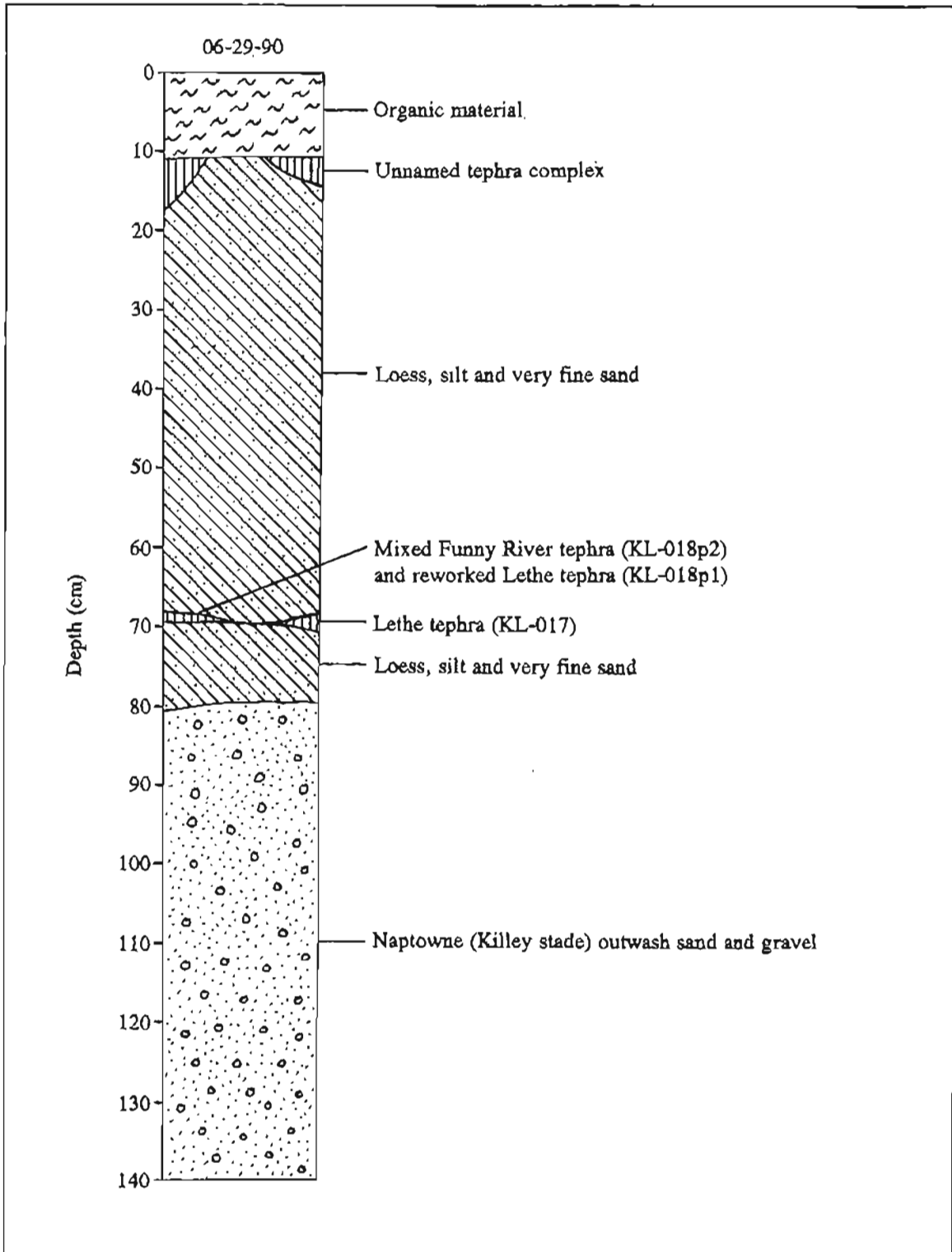


Figure A13. Stratigraphy exposed in section 13 (60°39'38"N, 151°18'55"W), Kenai C-4 NW Quadrangle (KEN-36, sheet 2). Tephra geochemistry given in table 3, except for unnamed tephra complex. Section indicates Killey age for outwash in Salamatof area.

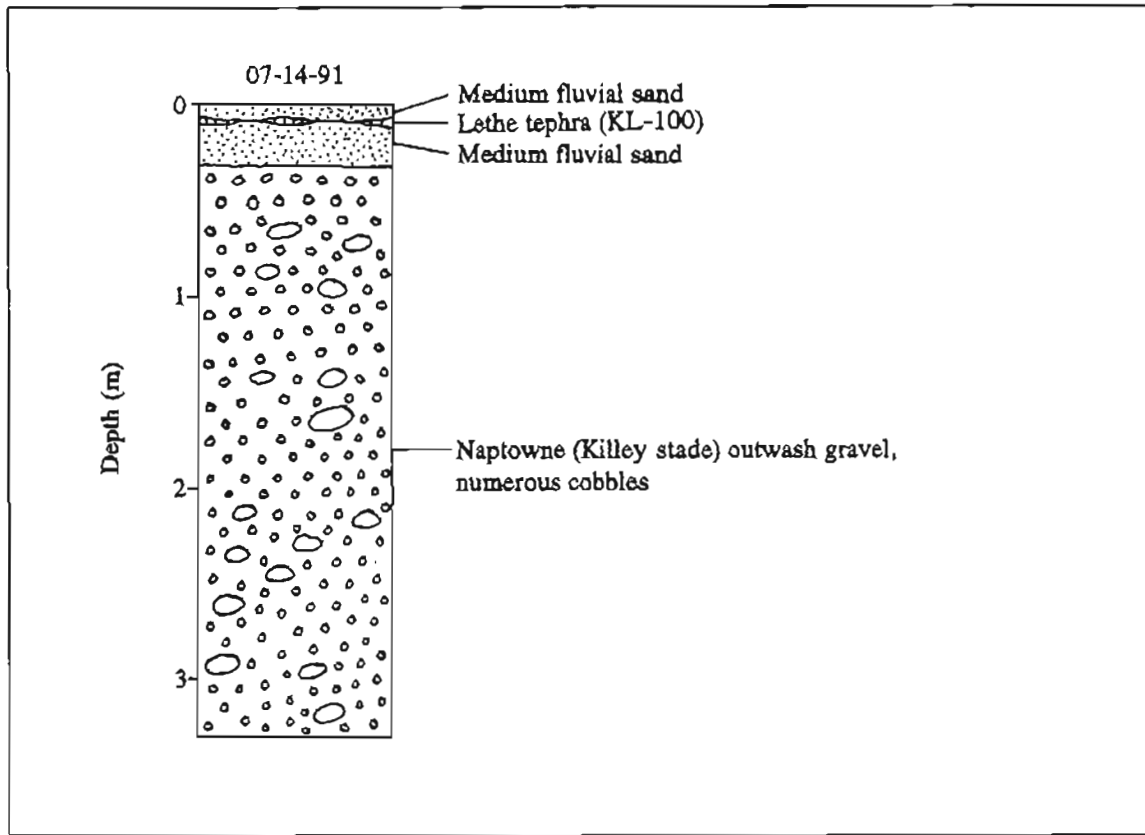


Figure A12. Stratigraphy exposed in section 12 ( $60^{\circ}43'25''N$ ,  $151^{\circ}54'15''W$ ), Kenai C-3 NE Quadrangle (KEN-27, sheet 2). Tephra geochemistry given in table 3. Section indicates Killey age for Swanson River paleodrainage system from moraines of Turnagain Arm lobe to 25-m marine terrace at Kenai.

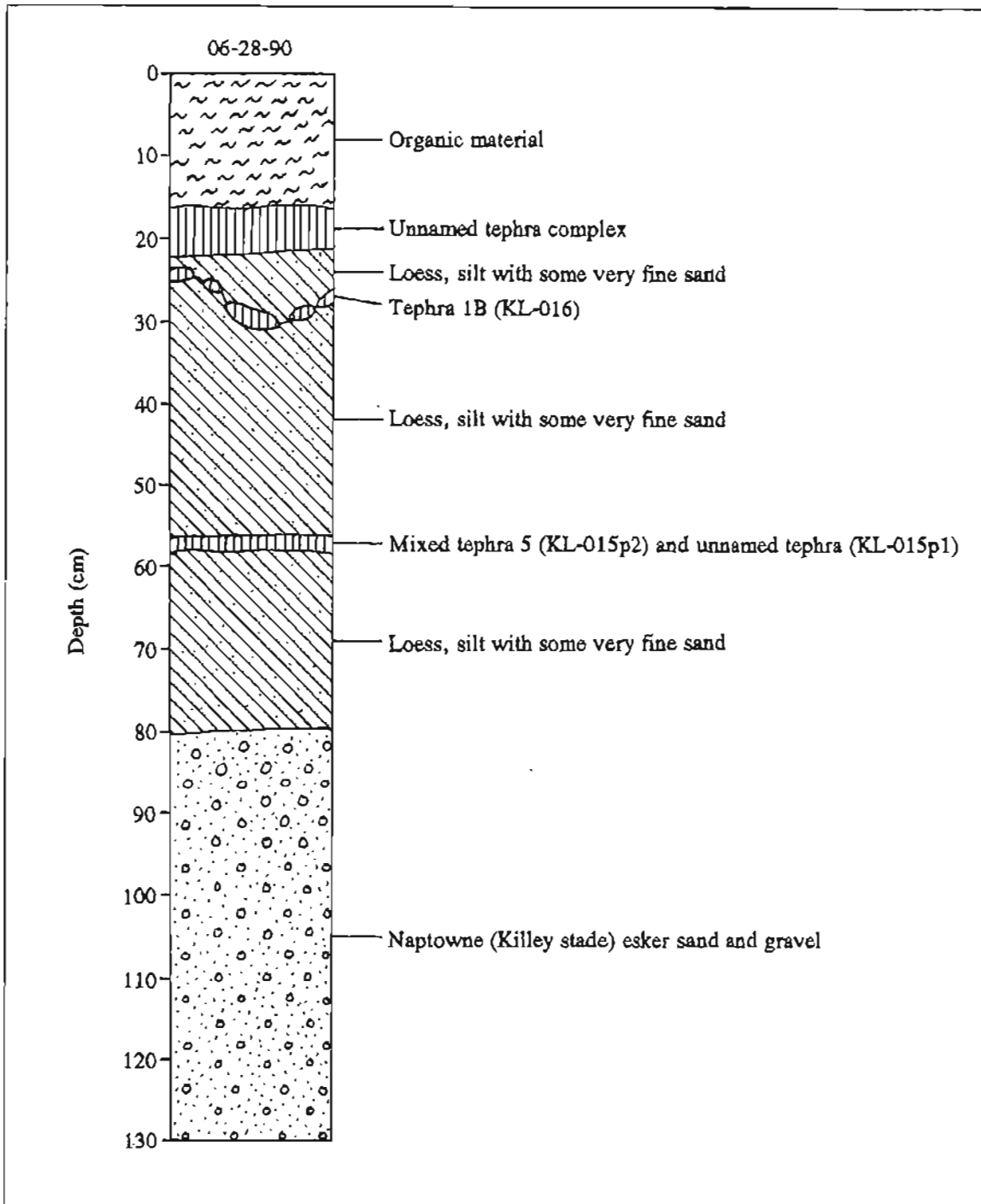


Figure A11. Stratigraphy exposed in section 11 (60°43'59"N, 151°09'37"W), Kenai C-4 NE Quadrangle (KEN-18, sheet 2). Tephra geochemistry given in table 3, except for unnamed tephra complex.

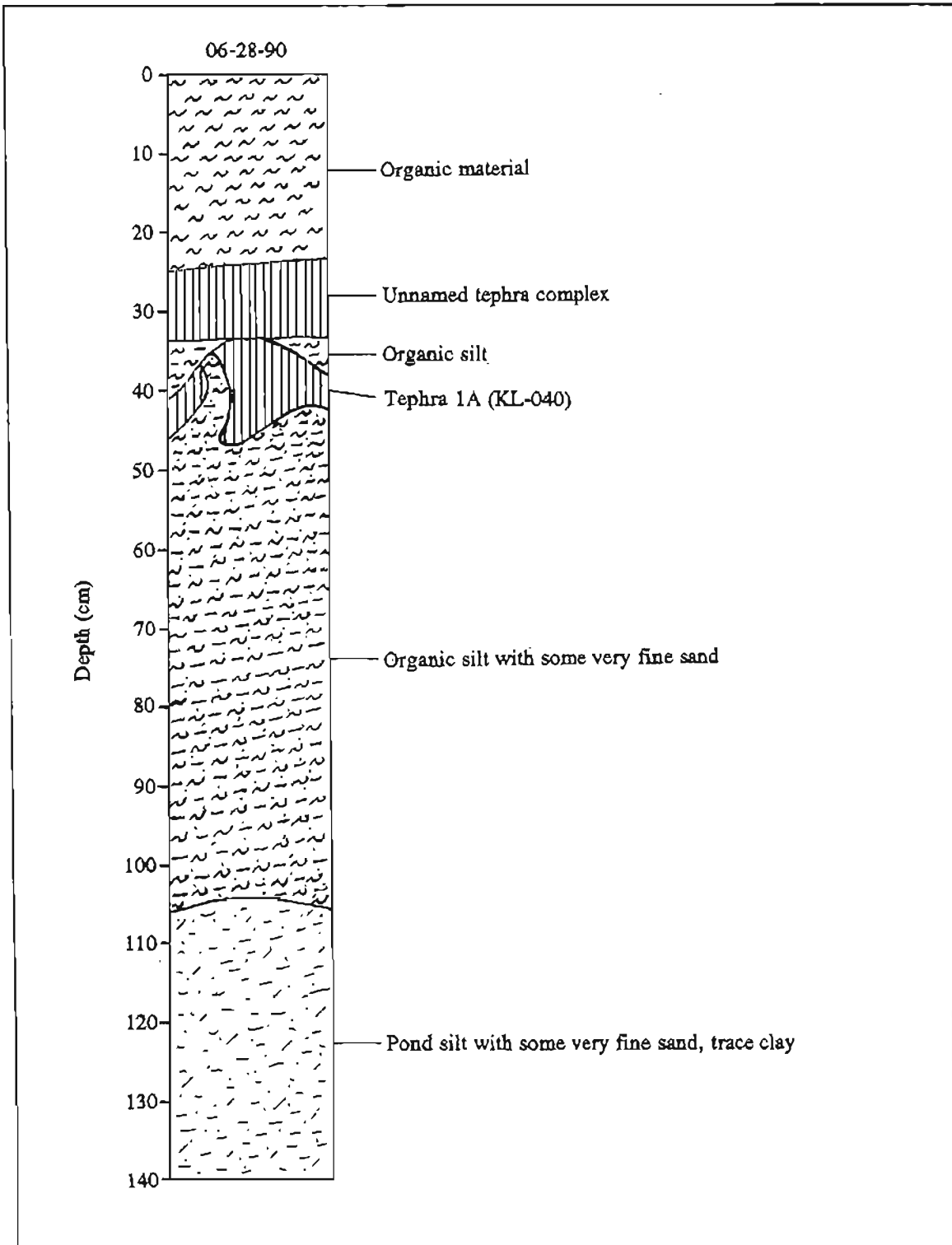


Figure A10. Stratigraphy exposed in section 10 (60°44'27"N, 151°18'07"W), Kenai C-4 NE Quadrangle (KEN-15, sheet 2). Tephra geochemistry given in table 3, except for unnamed tephra complex.

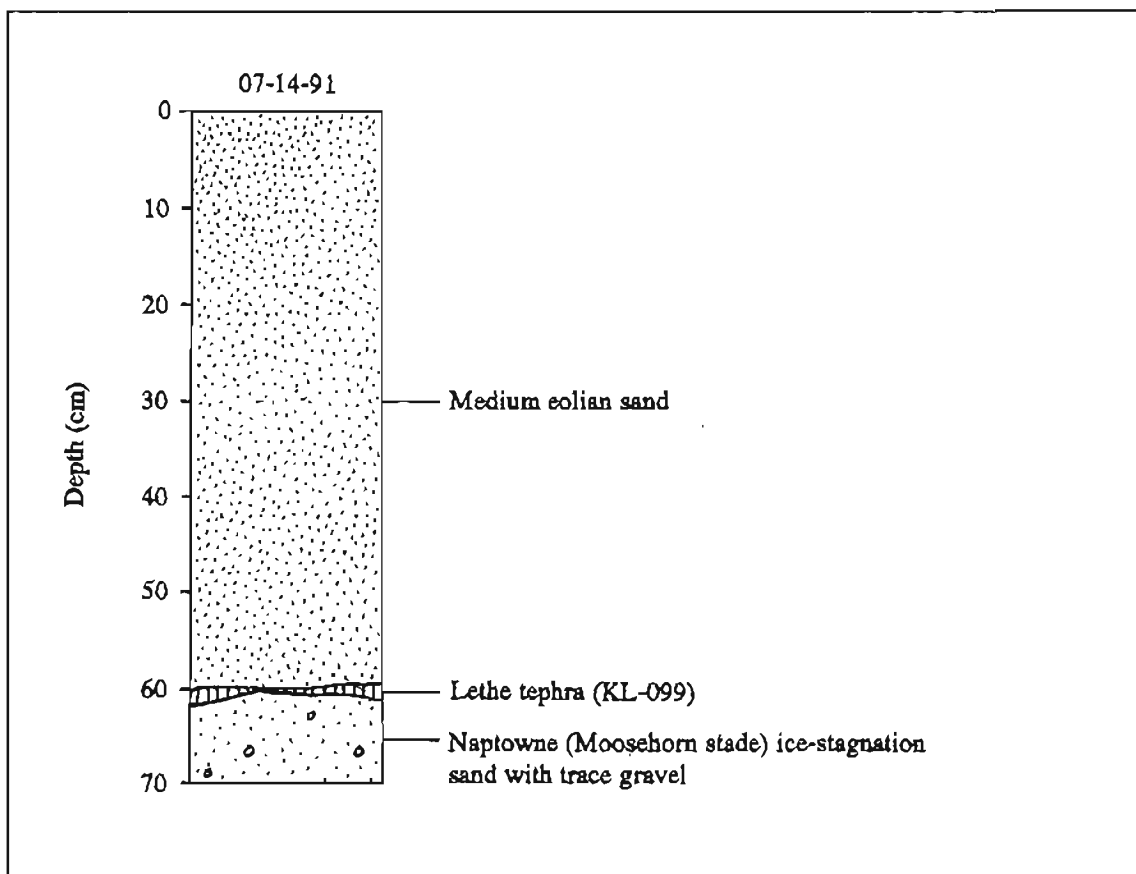


Figure A9. Stratigraphy exposed in section 9 (60°44'58"N, 150°51'27"W), Kenai D-3 SE Quadrangle (KEN-14, sheet 2). Tephra geochemistry given in table 3.

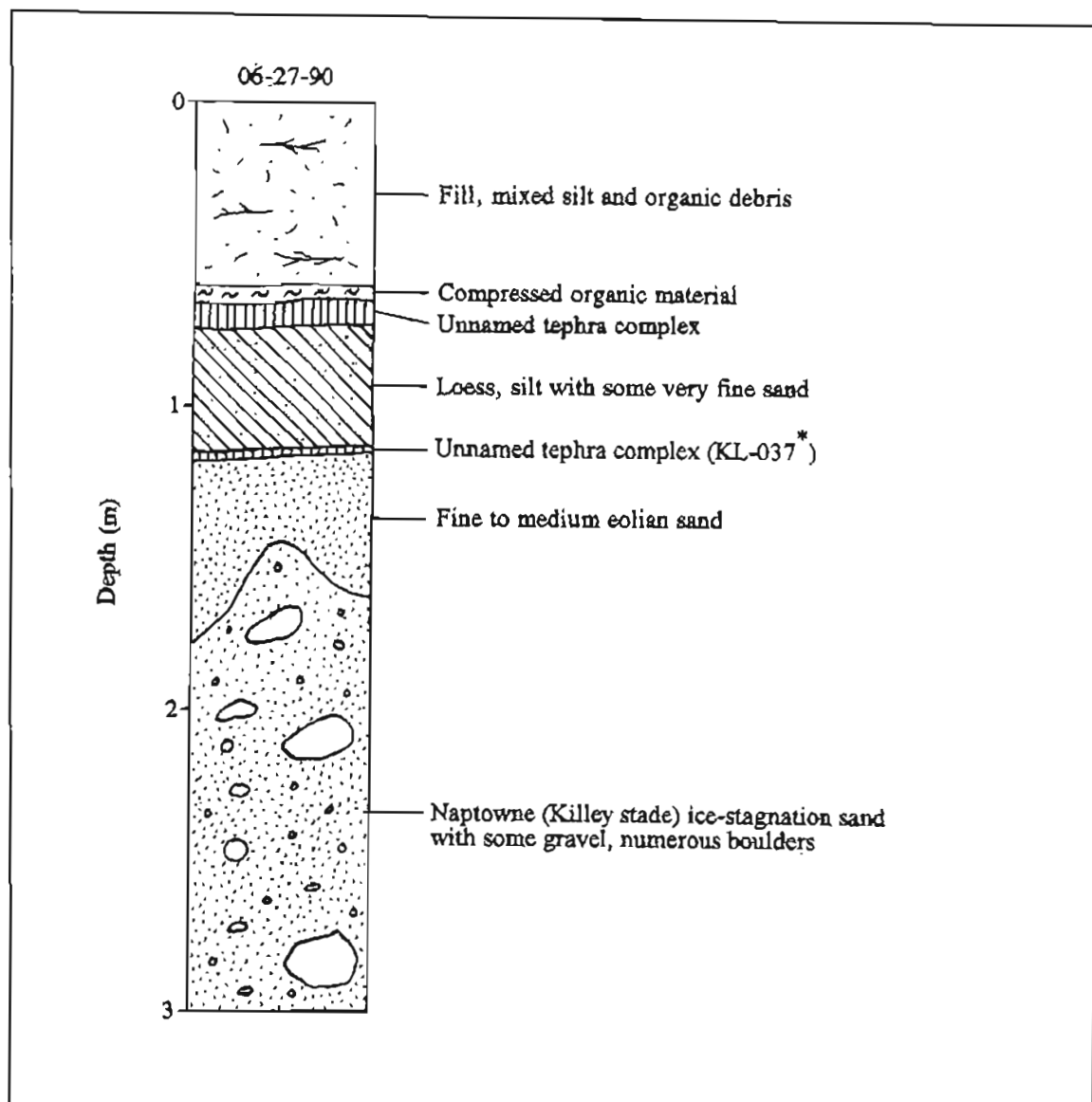


Figure A8. Stratigraphy exposed in section 8 (60°47'59"N, 151°00'56"W), Kenai D-3 SW Quadrangle (KEN-6, sheet 2).

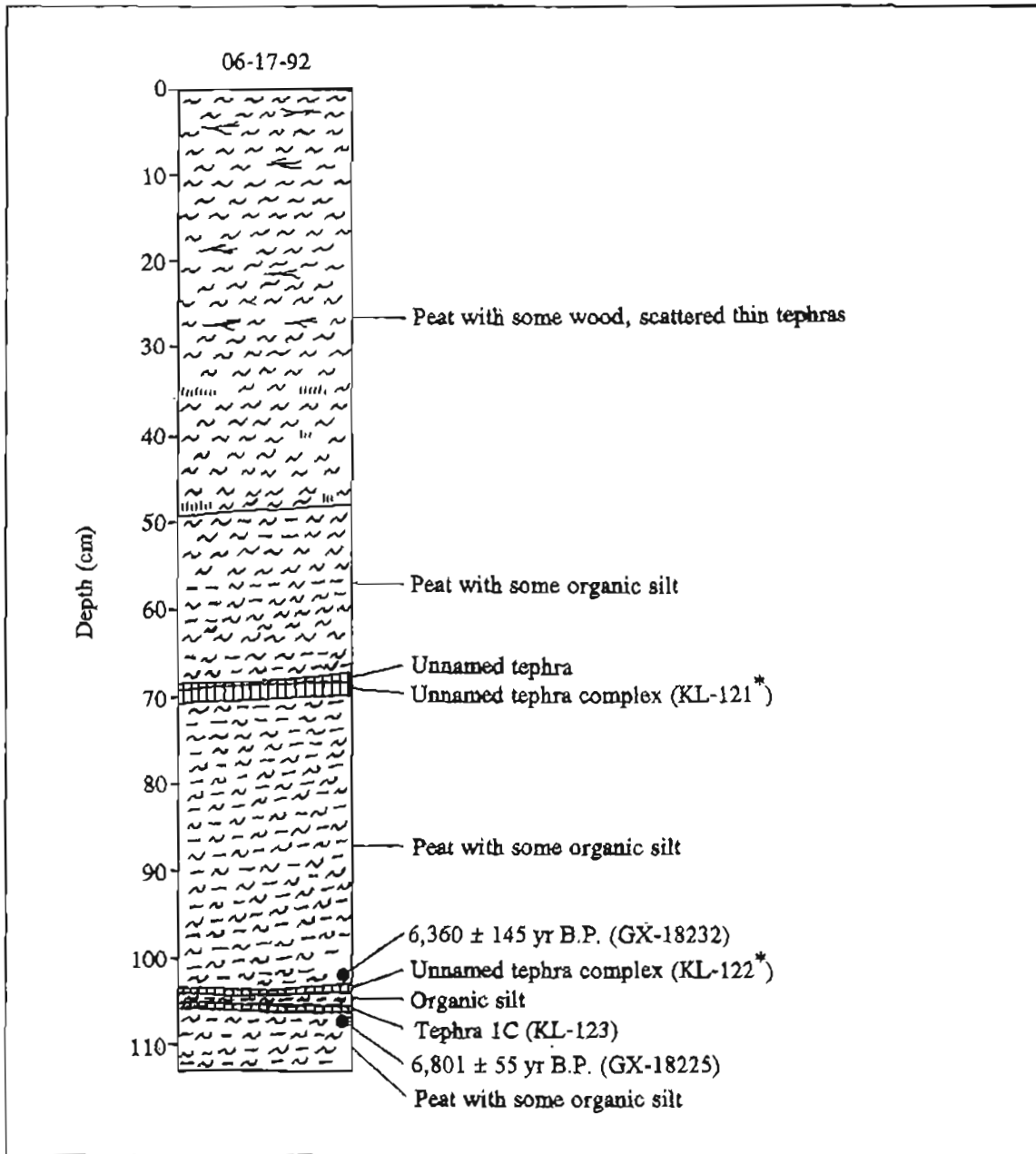


Figure A18. Stratigraphy exposed in section 18 (60°35'47"N, 151°12'49"W), Kenai C-4 SE Quadrangle (KEN-46, sheet 2). Chronologic significance of radiocarbon dates given in table 2. Tephra geochemistry given in table 3, except for unnamed tephra complexes.

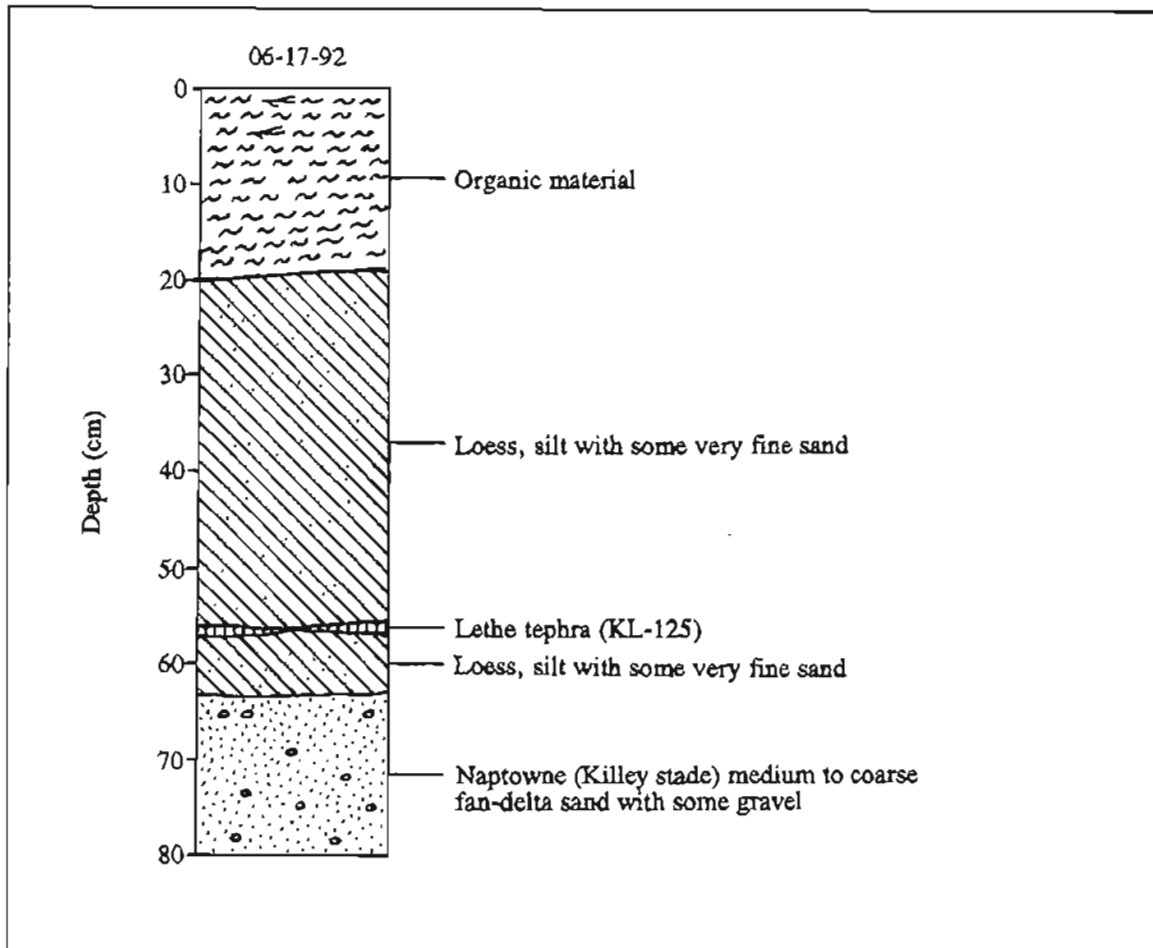


Figure A19. Stratigraphy exposed in section 19 (60°34'24"N, 151°13'46"W), Kenai C-4 SE Quadrangle (KEN-50, sheet 2). Tephra geochemistry given in table 3. Section indicates Killey age for fan delta at Kenai.

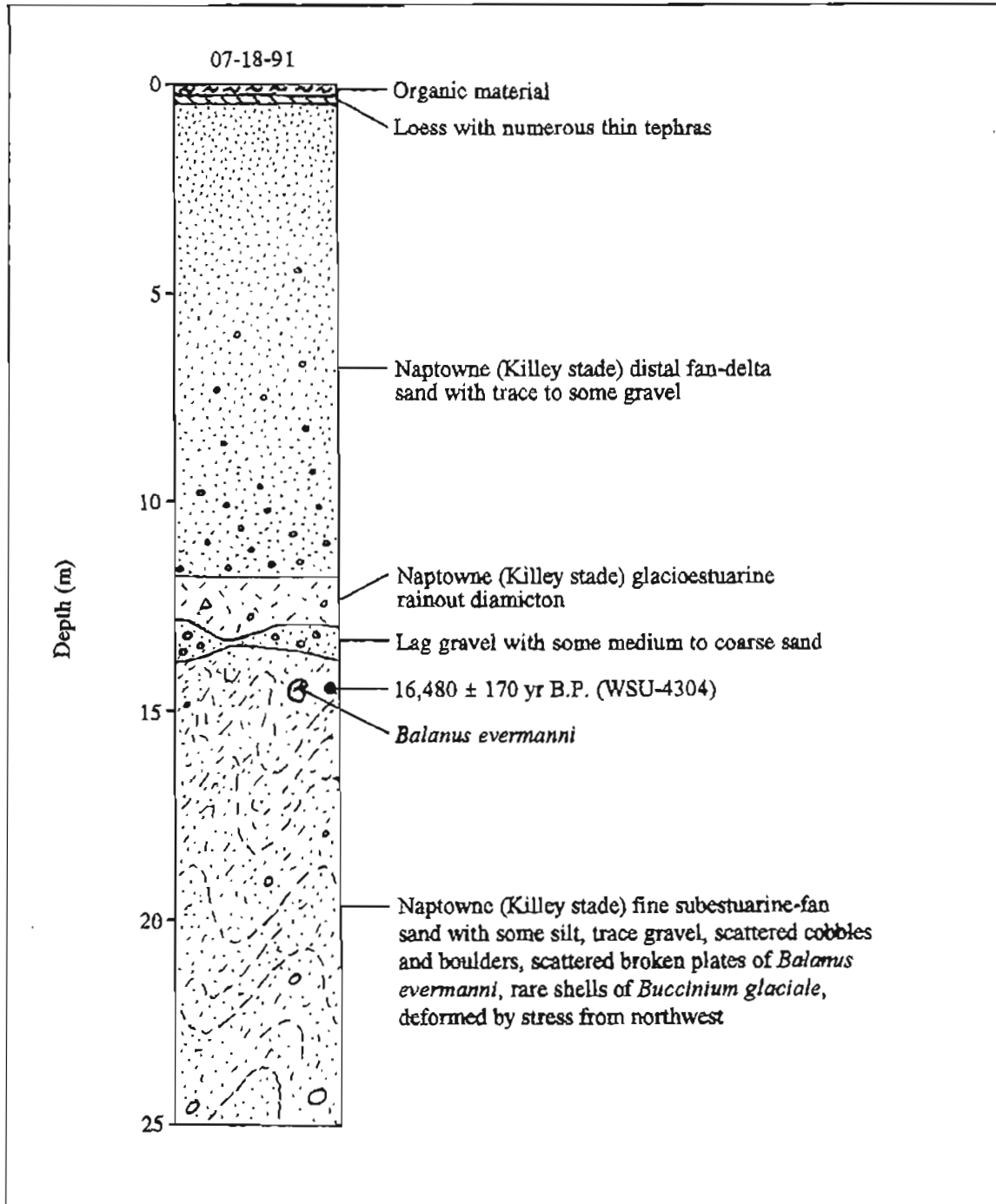


Figure A20. Stratigraphy exposed in section 20 (60°33'07"N, 151°14'17"W), Kenai C-4 SE Quadrangle (KEN-53, sheet 2). Chronologic significance of radiocarbon date given in table 2.

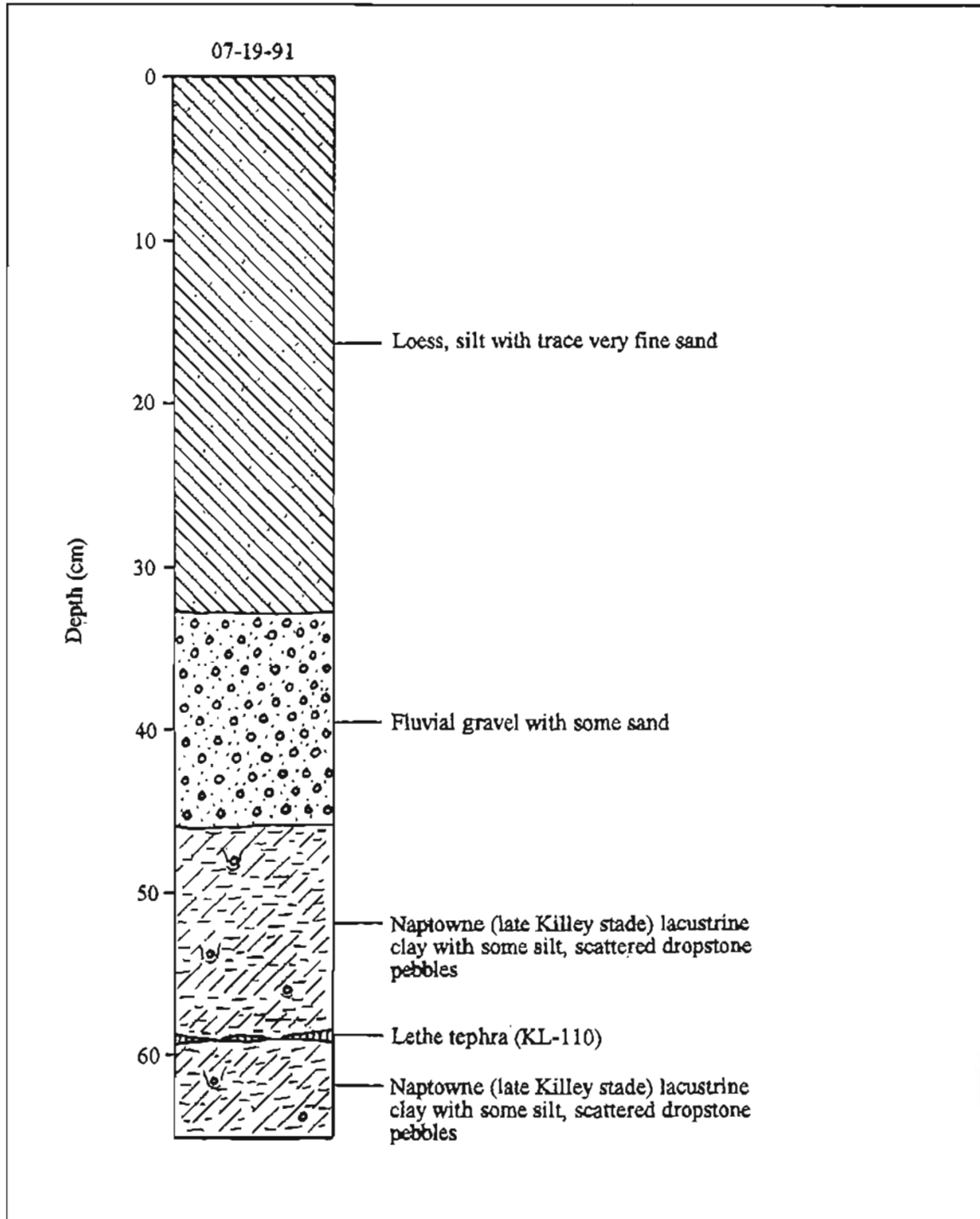


Figure A21. Stratigraphy exposed in section 21 (60°32'58"N, 150°59'25"W), Kenai C-3 SW Quadrangle (KEN-56, sheet 2). Tephra geochemistry given in table 3. Section establishes late Killey age for upper local lake deposits on drift of Moosehorn age northeast of Soldotna.

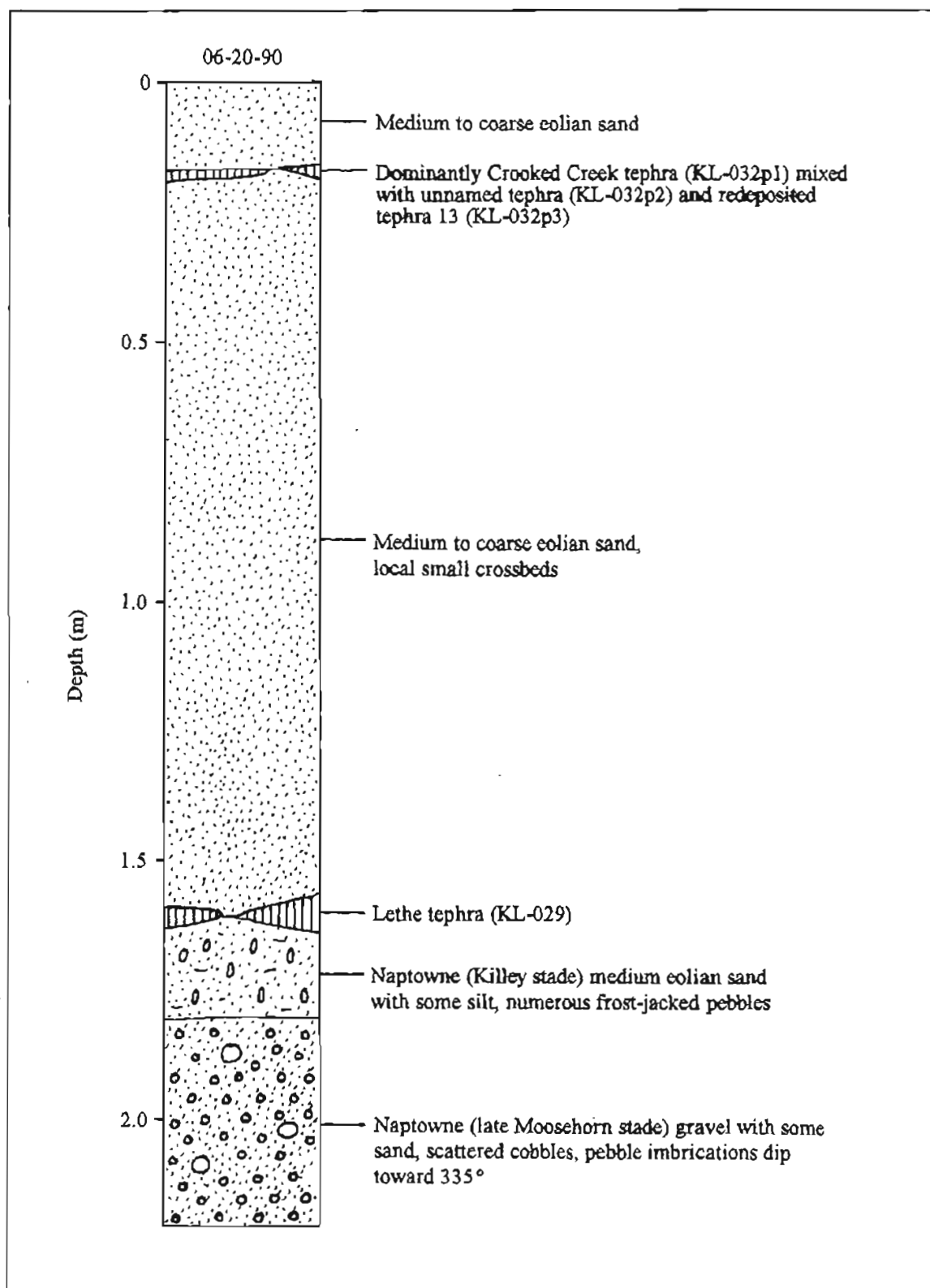


Figure A22. Stratigraphy exposed in section 22 (60°32'50"N, 150°48'17"W), Kenai C-3 SE Quadrangle (KEN-58, sheet 2). Tephra geochemistry given in table 3. Section establishes late Killey age for eolian sand overlying alluvium of late Moosehorn age in meltwater channels west of Moose River.

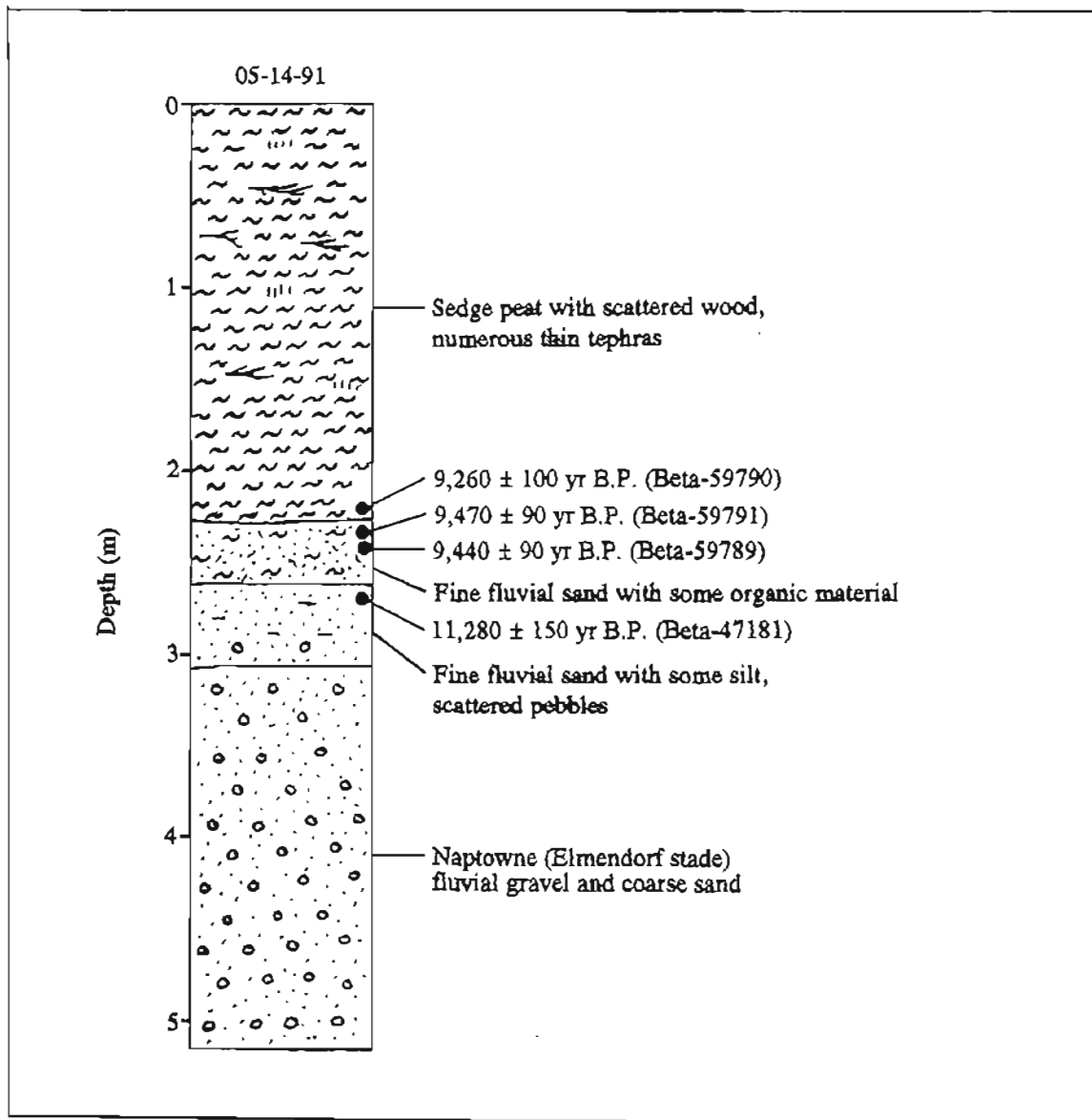


Figure A23. Stratigraphy exposed in section 23 (60°32'28"N, 151°10'42"W), Kenai C-4 SE Quadrangle (KEN-60, sheet 2). Chronologic significance of radiocarbon dates given in table 2.

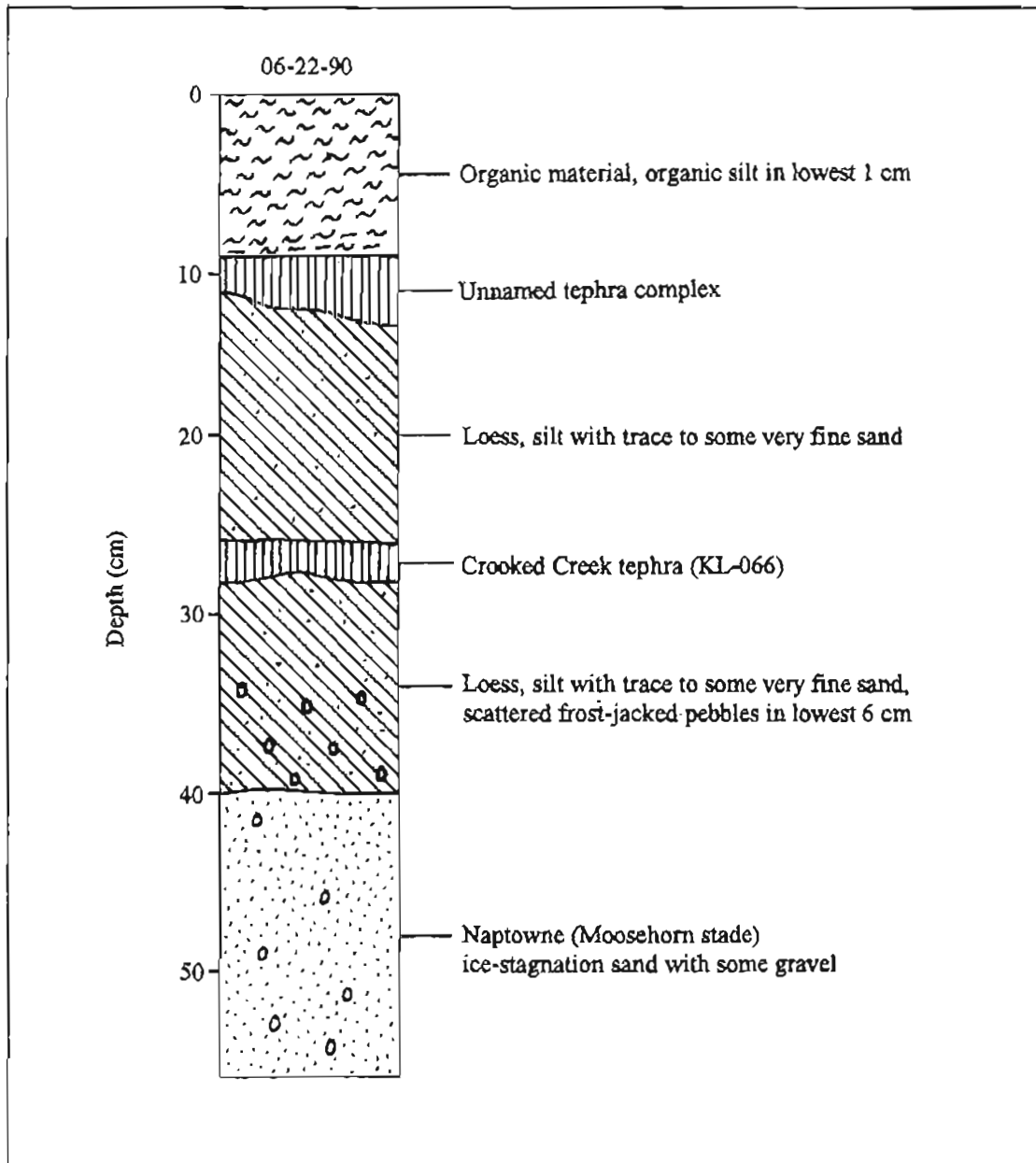


Figure A24. Stratigraphy exposed in section 24 (60°32'21"N, 150°49'46"W), Kenai C-3 SE Quadrangle (KEN-62, sheet 2). Tephra geochemistry given in table 3, except for unnamed tephra complex.

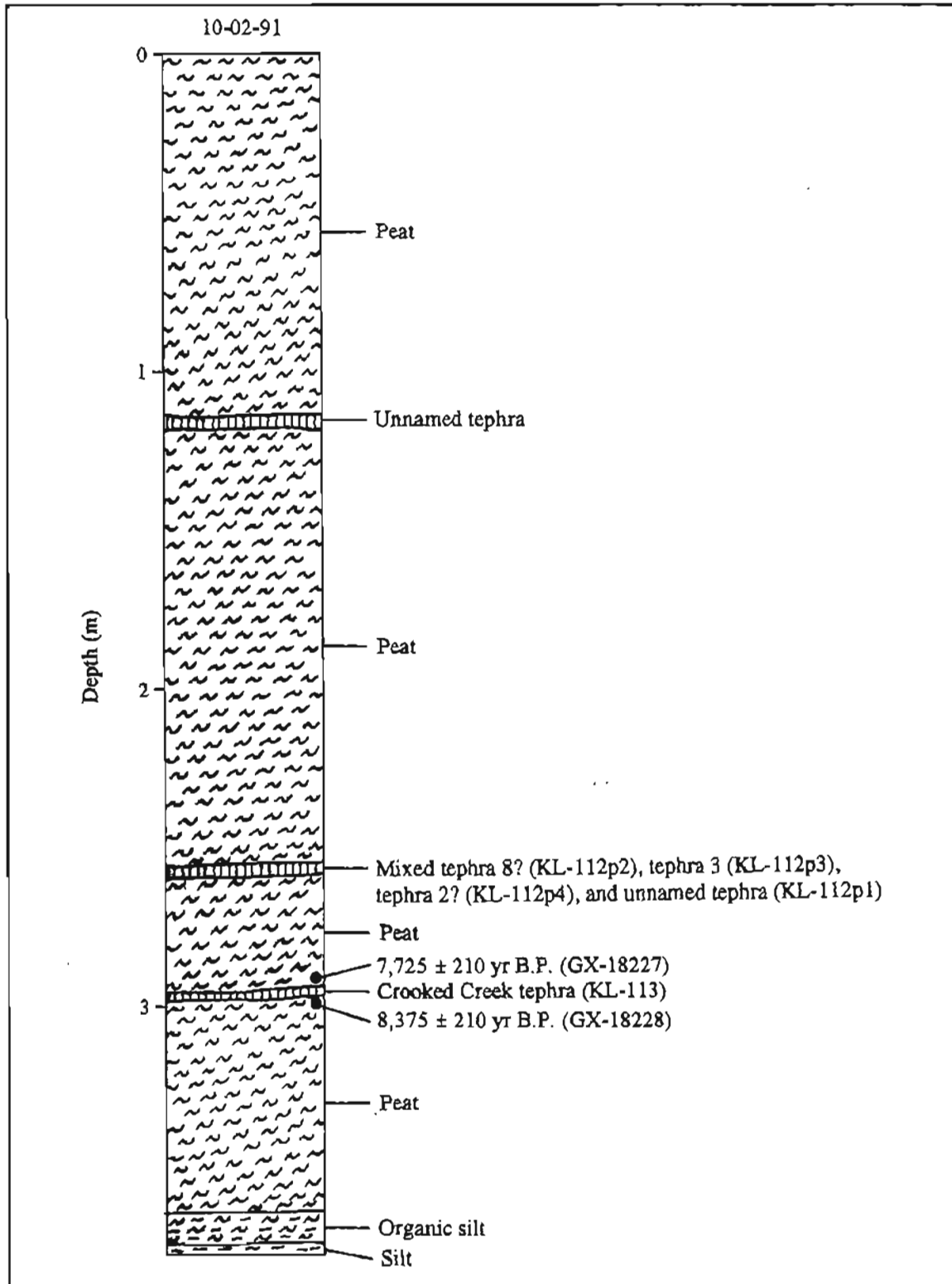


Figure A25. Stratigraphy exposed in section 25 (60°32'13"N, 150°46'15"W), Kenai C-3 SE Quadrangle (KEN-64, sheet 2). Chronologic significance of radiocarbon dates given in table 2. Tephra geochemistry given in table 3, except for unnamed tephra complex.

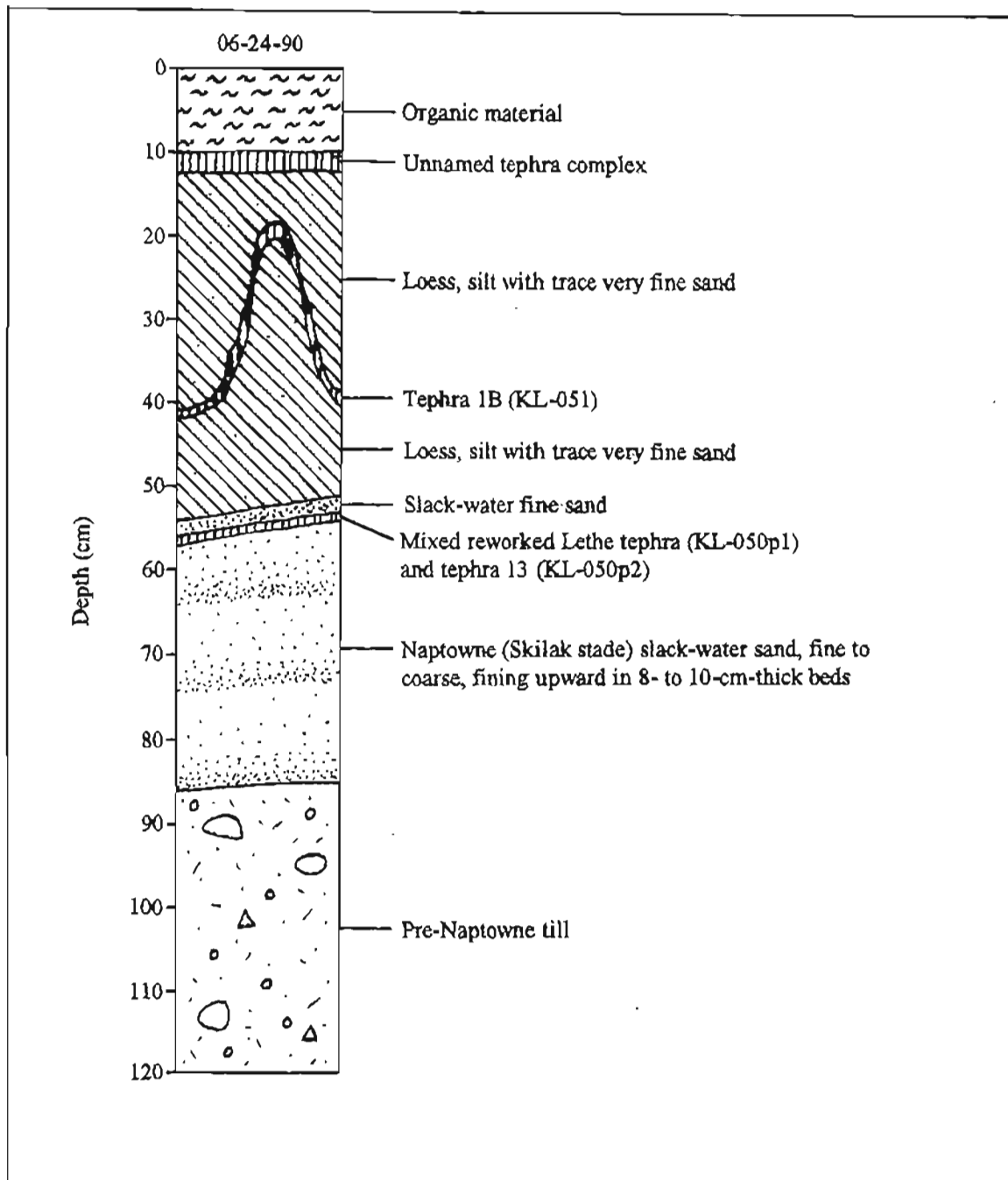


Figure A26. Stratigraphy exposed in section 26 ( $60^{\circ}32'05''N$ ,  $150^{\circ}44'54''W$ ), Kenai C-2 SW Quadrangle (KEN-65, sheet 2). Tephra geochemistry given in table 3, except for unnamed tephra complex. Section indicates Skilak age for slack-water sands on second-highest terrace of Kenai River in Sterling area.

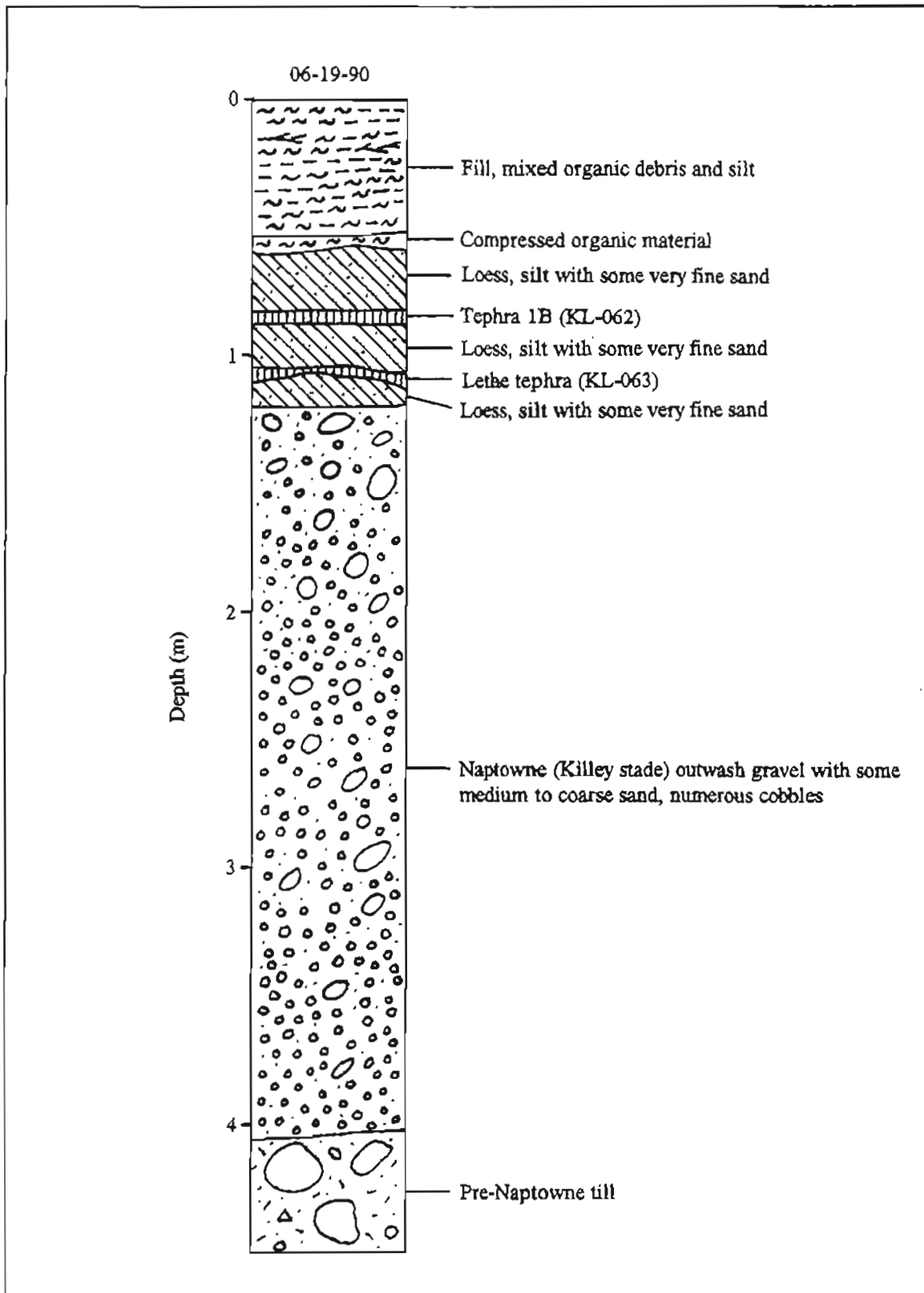


Figure A27. Stratigraphy exposed in section 27 (60°32'04"N, 150°43'53"W), Kenai C-2 SW Quadrangle (KEN-66, sheet 2). Tephra geochemistry given in table 3. Section demonstrates deposition of Lethe tephra after gravel outwash from nearby type Killey moraine.

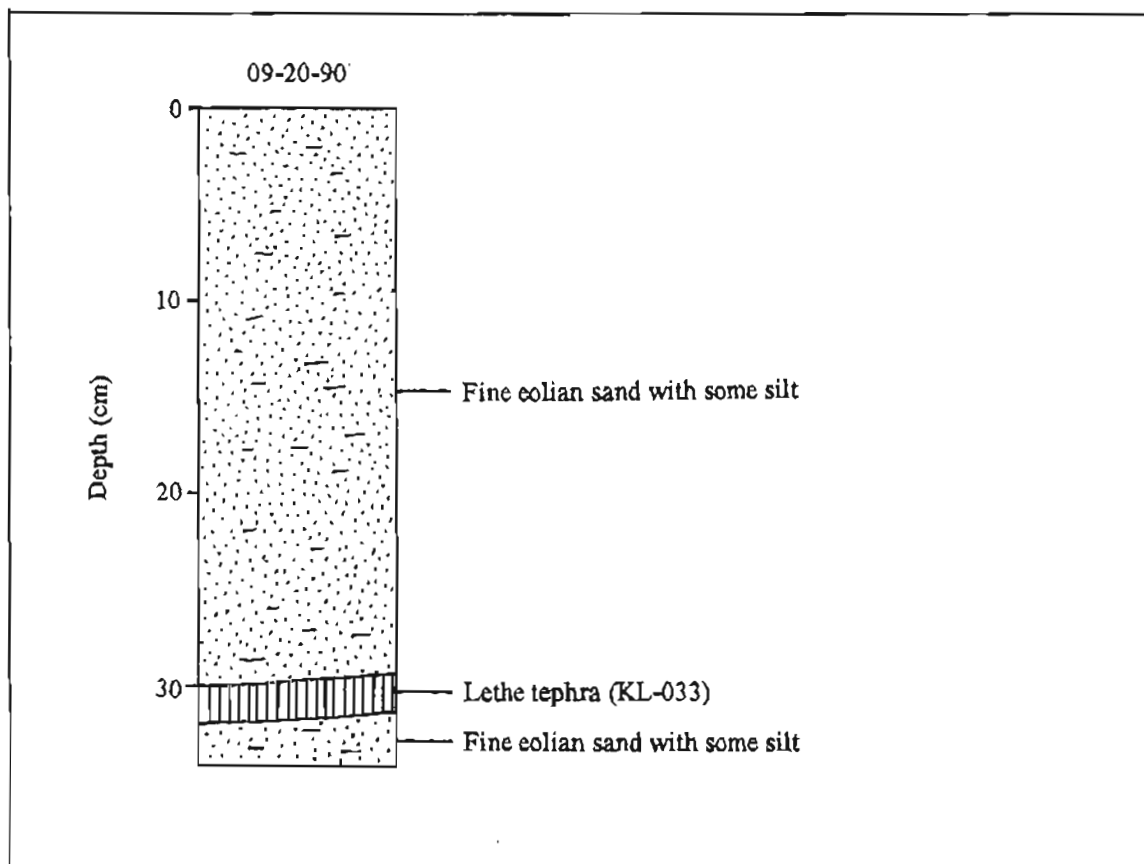


Figure A28. Stratigraphy exposed in section 28 (60°31'57"N, 150°55'10"W), Kenai C-3 SE Quadrangle (KEN-68, sheet 2). Tephra geochemistry given in table 3, except for unnamed tephra complex. Section establishes late Killey age for dune sand north of Whisper Lake.

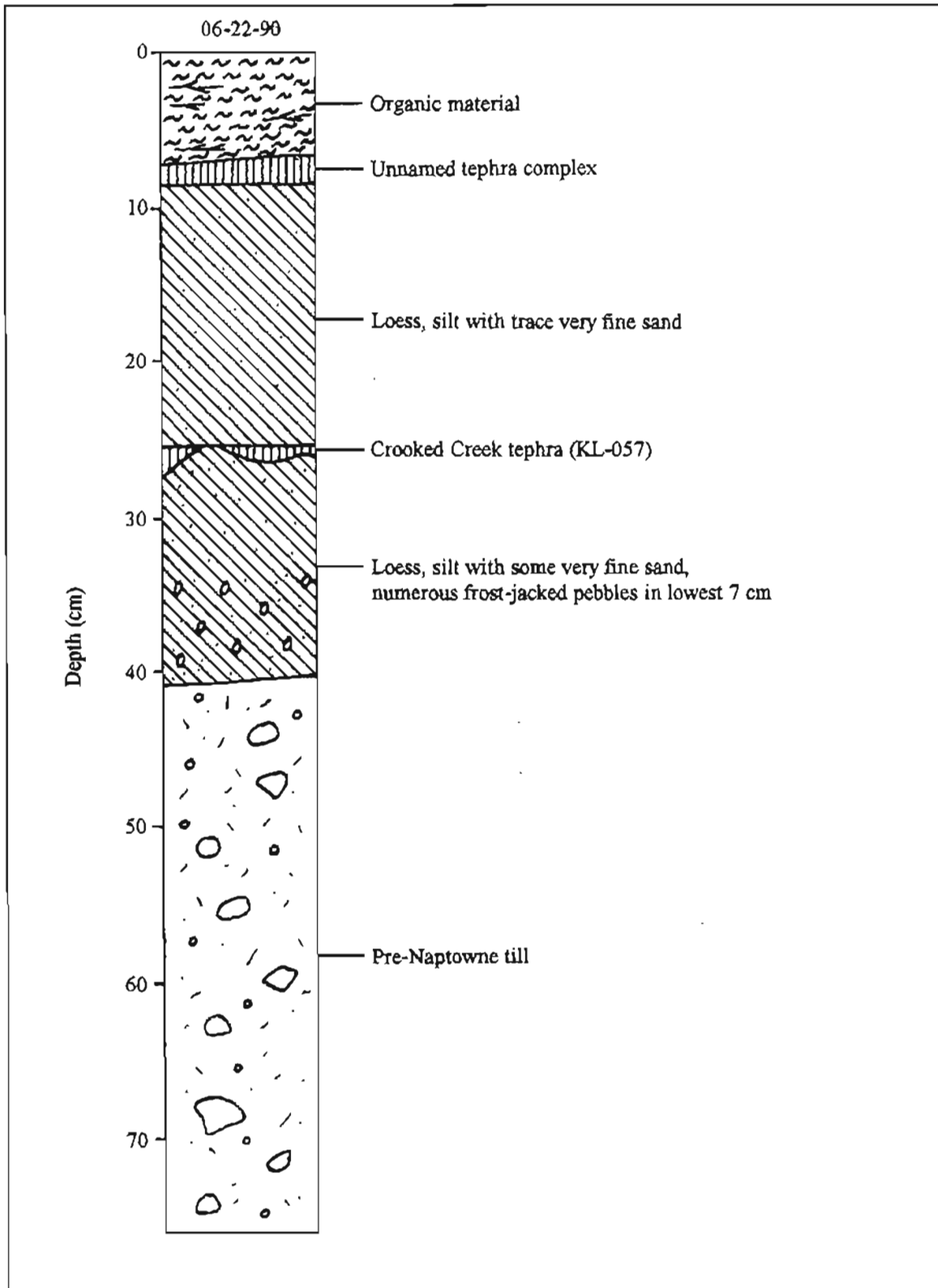


Figure A29. Stratigraphy exposed in section 29 (60°31'49"N, 150°44'01"W), Kenai C-2 SW Quadrangle (KEN-71, sheet 2). Tephra geochemistry given in table 3, except for unnamed tephra complex.

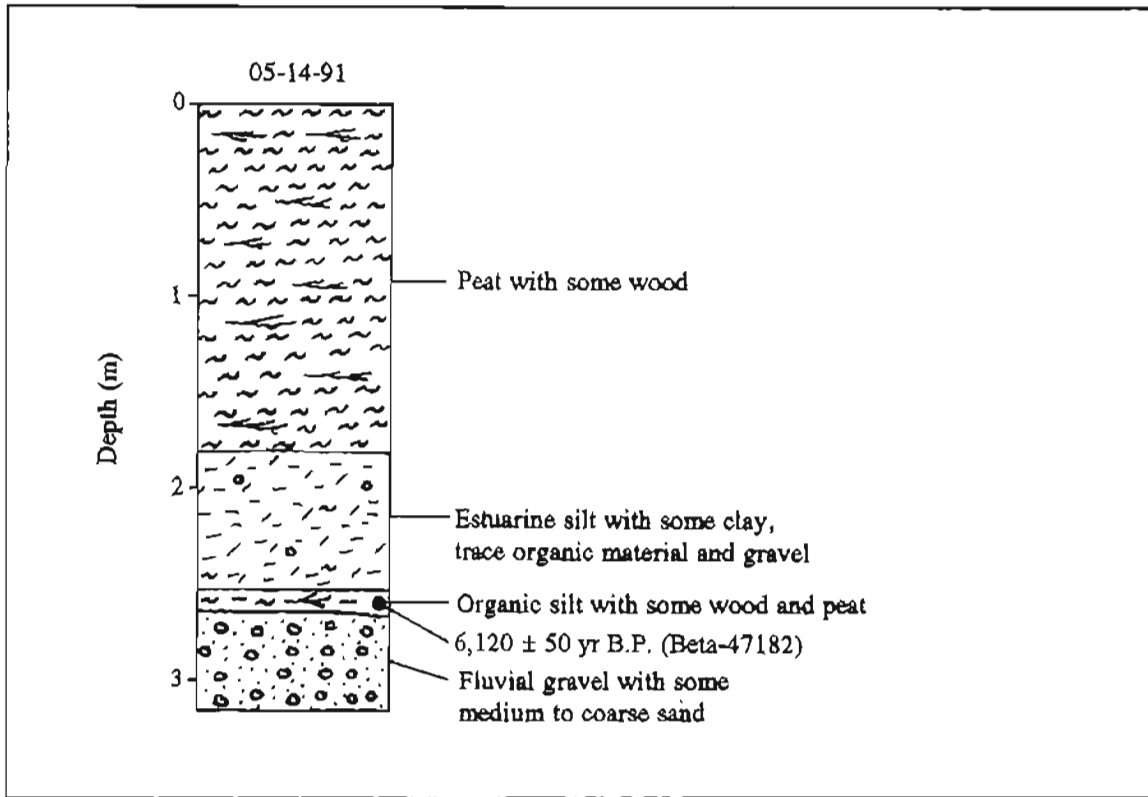


Figure A30. Stratigraphy exposed in section 30A (60°31'30"N, 151°12'31"W), Kenai C-4 SE Quadrangle (KEN-78, sheet 2). Chronologic significance of radiocarbon date given in table 2.

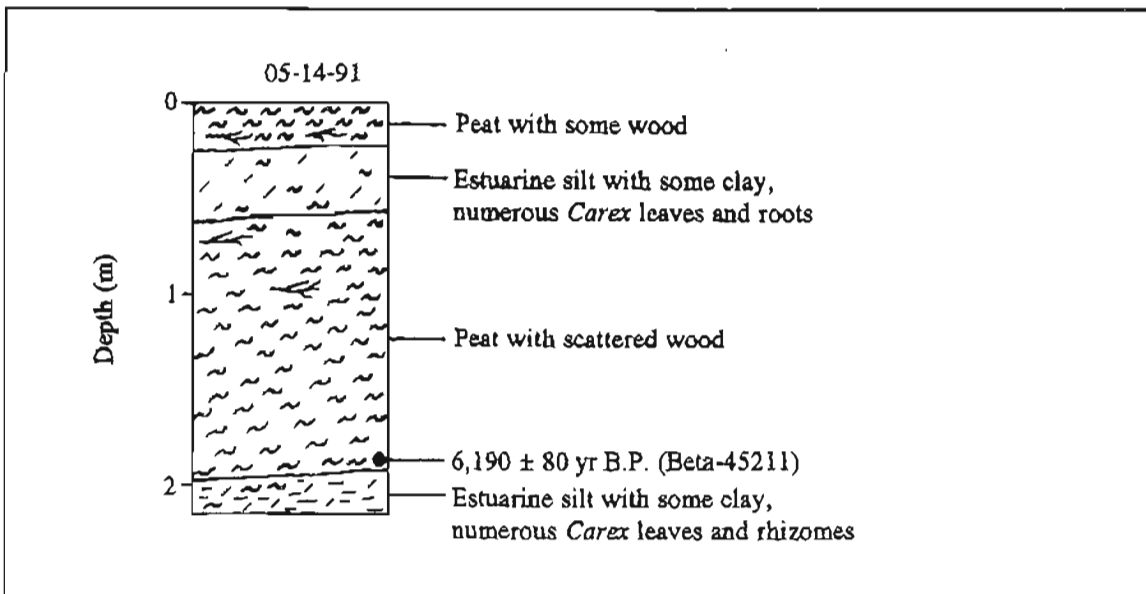


Figure A31. Stratigraphy exposed in section 30B (60°31'30"N, 151°12'31"W), Kenai C-4 SE Quadrangle (KEN-78, sheet 2). Chronologic significance of radiocarbon date given in table 2.

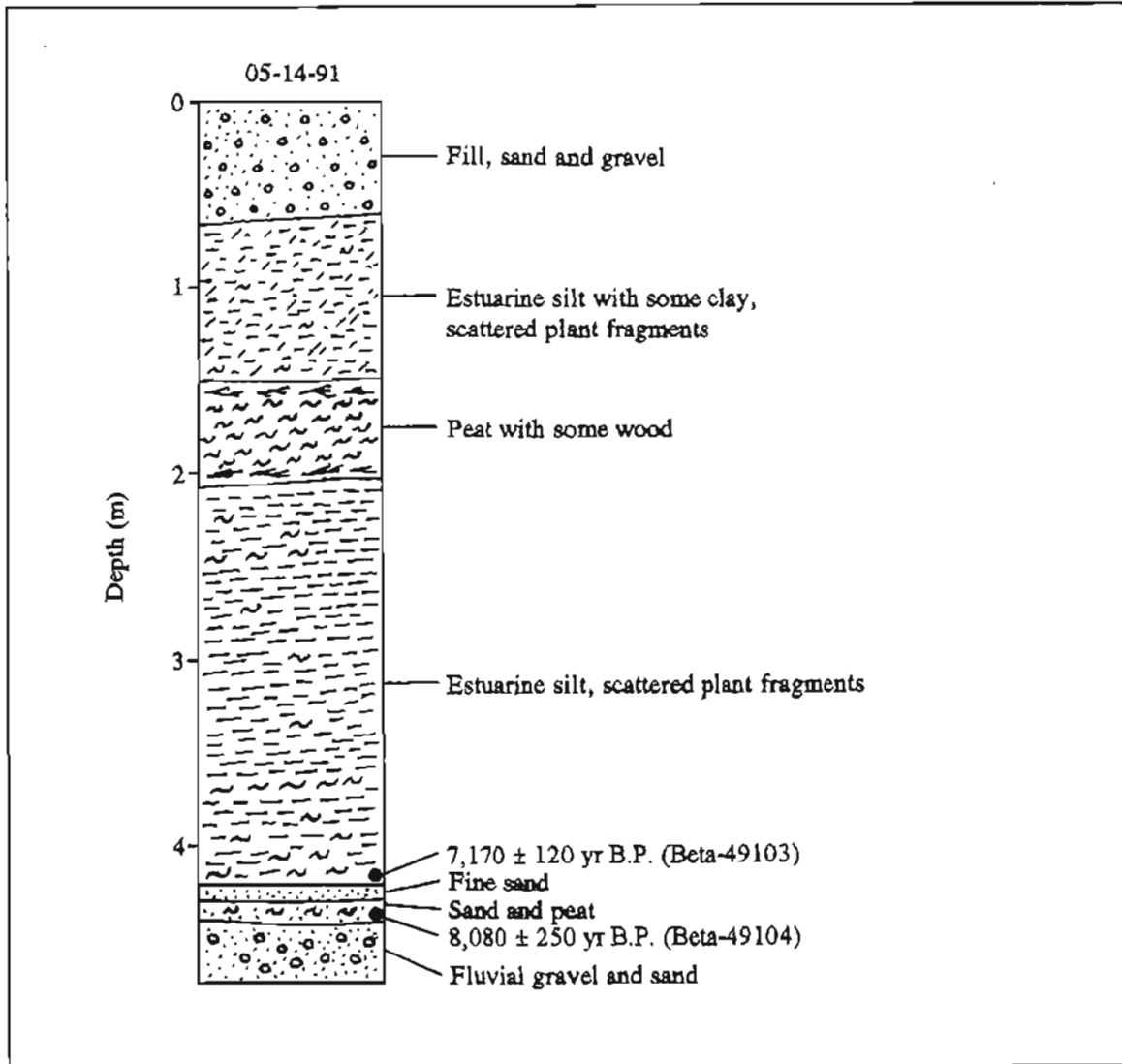


Figure A32. Stratigraphy exposed in section 30C (60°31'30"N, 151°12'31"W), Kenai C-4 SE Quadrangle (KEN-78, sheet 2). Chronologic significance of radiocarbon dates given in table 2.

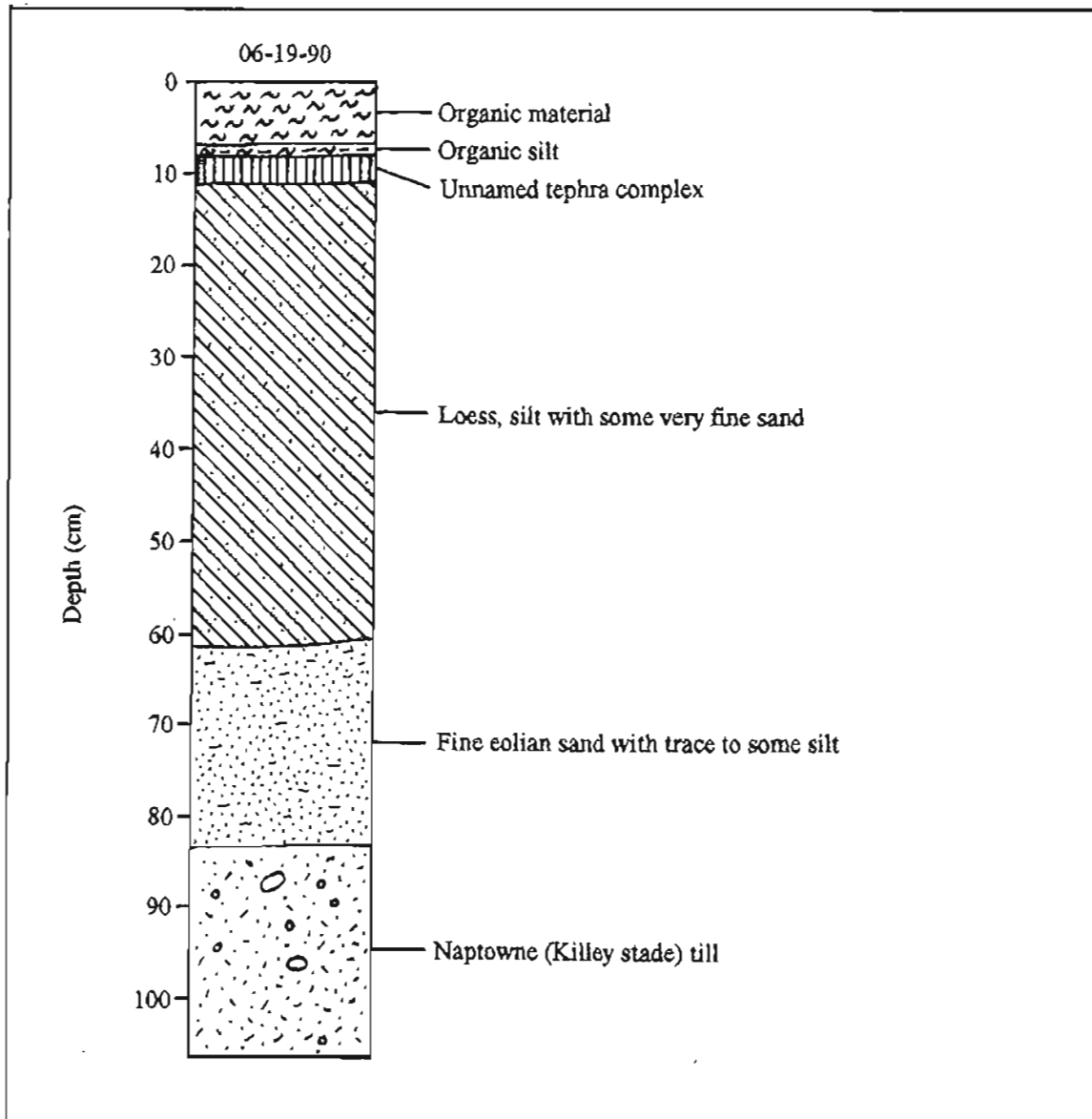


Figure A33. Stratigraphy exposed in section 31 ( $60^{\circ}31'25''N$ ,  $150^{\circ}37'42''W$ ) on type Killey moraine, Kenai C-2 SW Quadrangle (KEN-79, sheet 2).

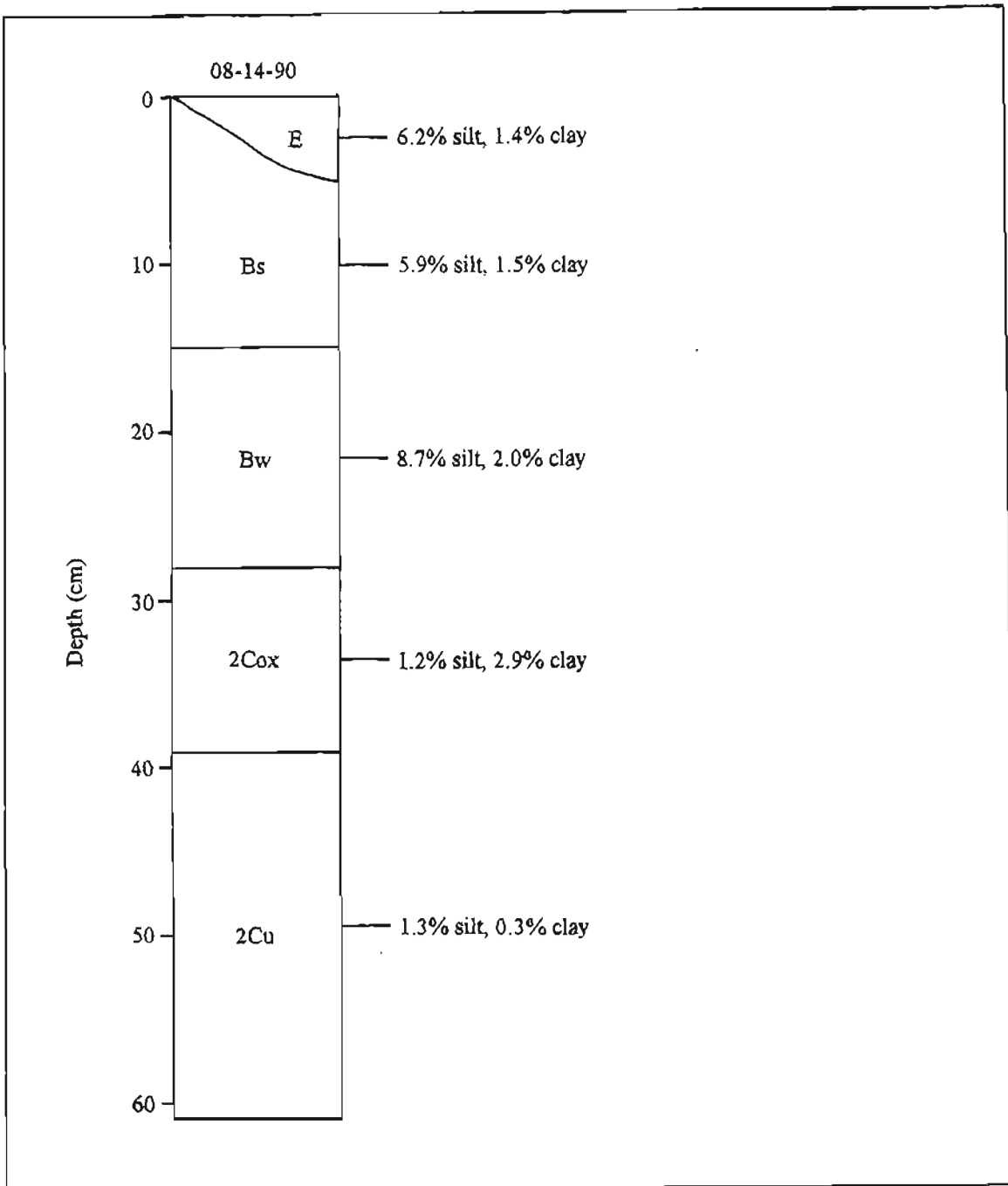


Figure A34. Distribution of silt and clay (calculated as percent of <2-mm fraction) with depth in soil profile S1 on flat crest of type Killey moraine (60°31'25"N, 150°37'42"W), Kenai C-2 SW Quadrangle (KEN-79, sheet 2). Elevation 101 m. Horizons according to Soil Survey Staff (1975), modified by Birkeland and others (1991b) and this study. Horizons O and A not shown above horizon E. Detailed profile description summarized in table A3.

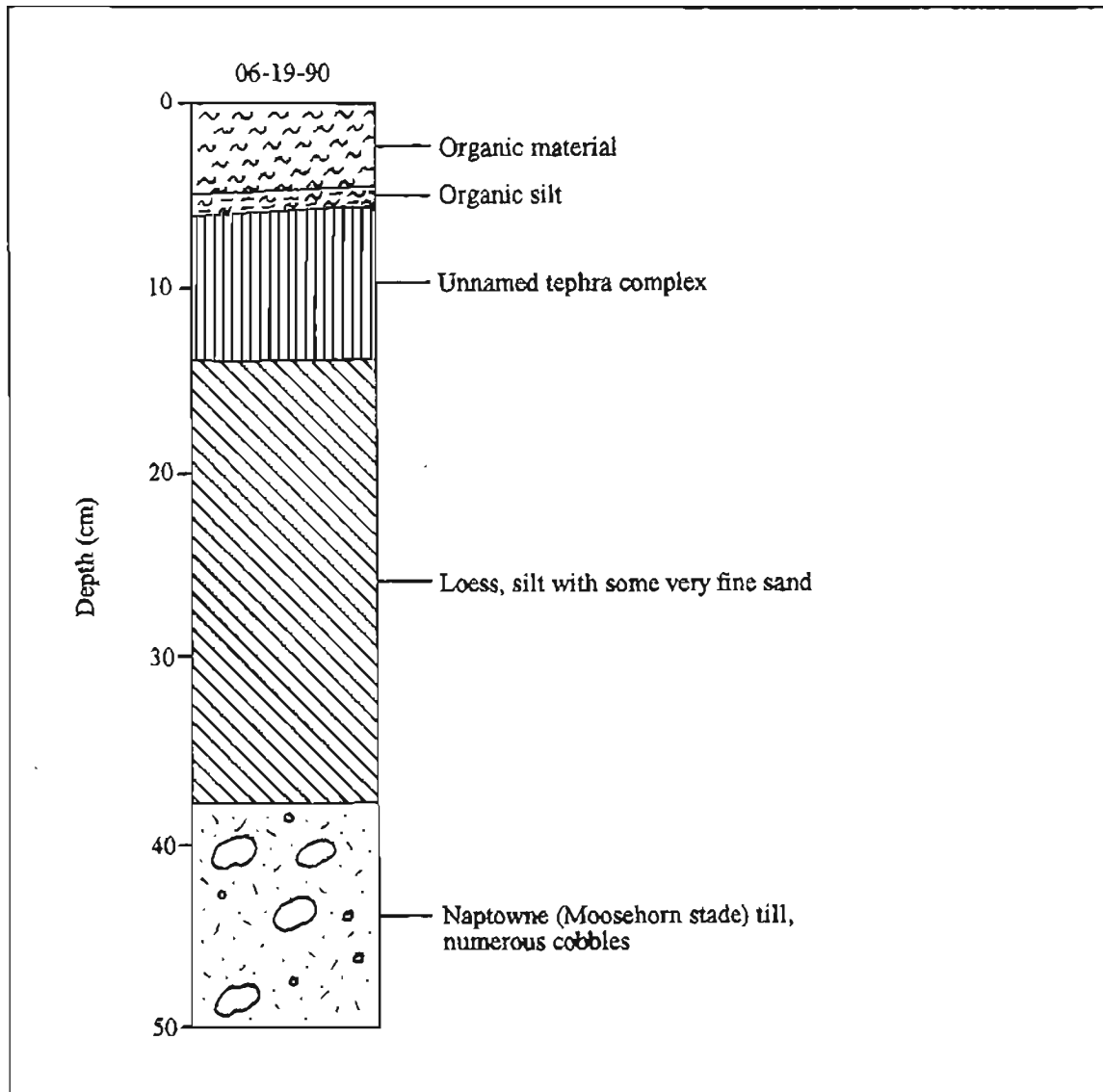


Figure A35. Stratigraphy exposed in section 32 ( $60^{\circ}31'23''N$ ,  $150^{\circ}42'34''W$ ) on type Moosehorn moraine, Kenai C-2 SW Quadrangle (KEN-80, sheet 2).

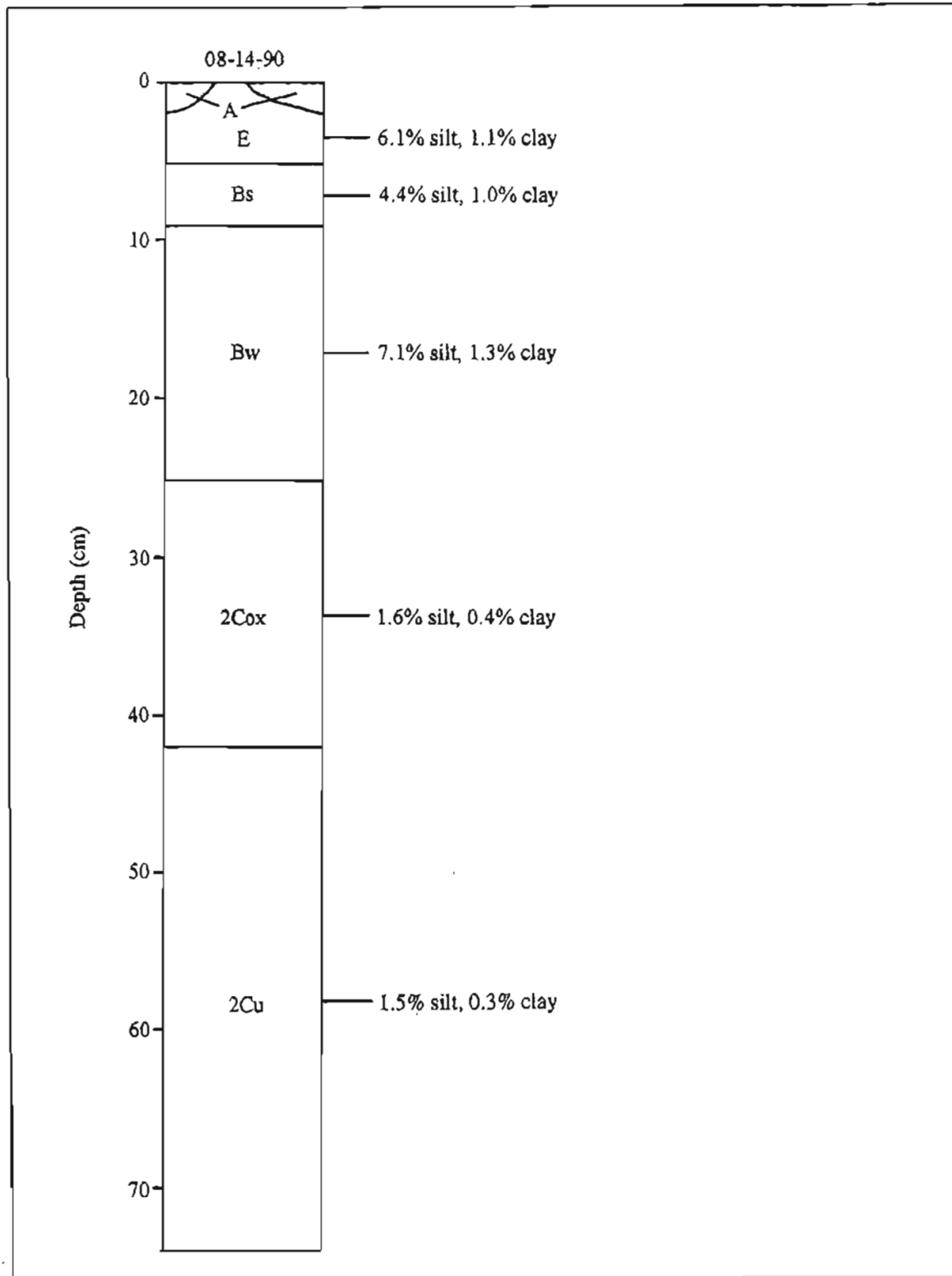


Figure A36. Distribution of silt and clay (calculated as percent of <2-mm fraction) with depth in soil profile S2 on flat crest of type Moosehorn moraine (60°31'23"N, 150°42'34"W), Kenai C-2 SW Quadrangle (KEN-80, sheet 2). Elevation 91 m. Horizons according to Soil Survey Staff (1975), modified by Birkeland and others (1991b) and this study. Horizon O not shown above horizon A. Detailed profile description summarized in table A4.

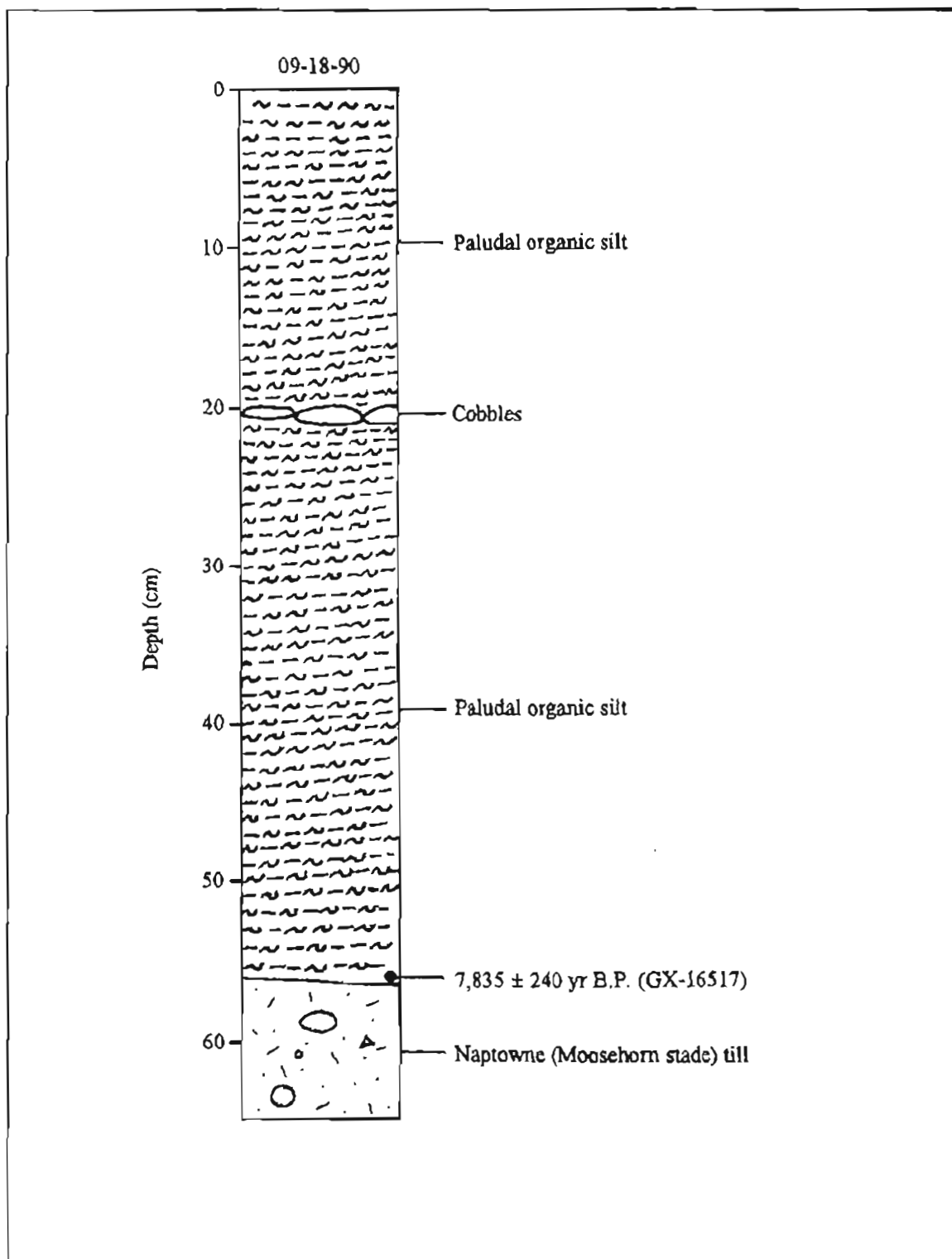


Figure A37. Stratigraphy exposed in section 33 (60°31'23"N, 150°40'38"W), Kenai C-2 SW Quadrangle (KEN-81, sheet 2). Chronologic significance of radiocarbon date given in table 2.

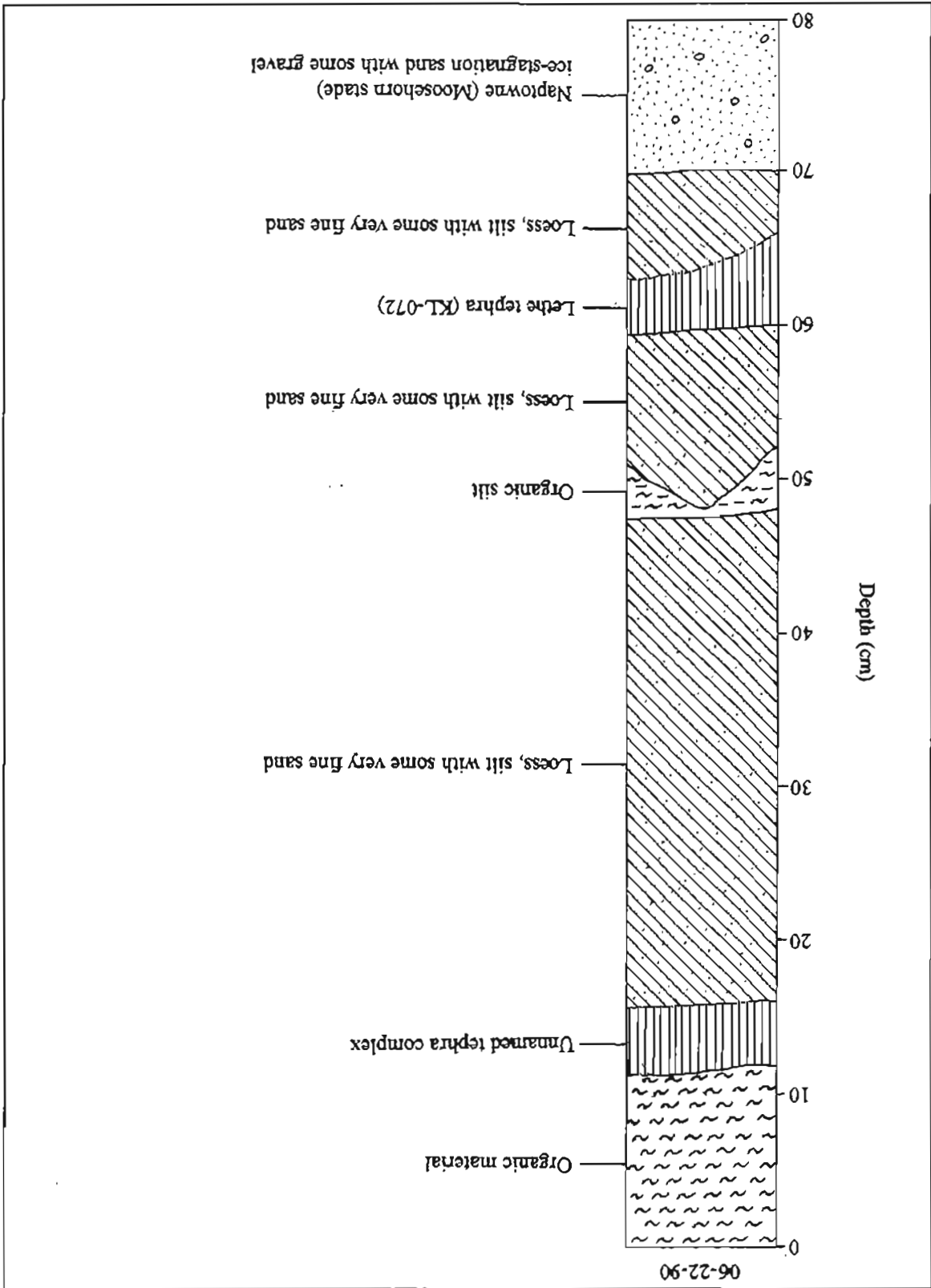


Figure A38. Stratigraphy exposed in section 34 (60°31'13"N, 150°53'13"W), Kenai C-3 SE Quadrangle (KEN-82, sheet 2). Tephra geochemistry given in table 3, except for unnamed tephra complex. Section establishes late Killey age for loess overlying ice-stagnation deposits of Moosehorn age near Whisper Lake.

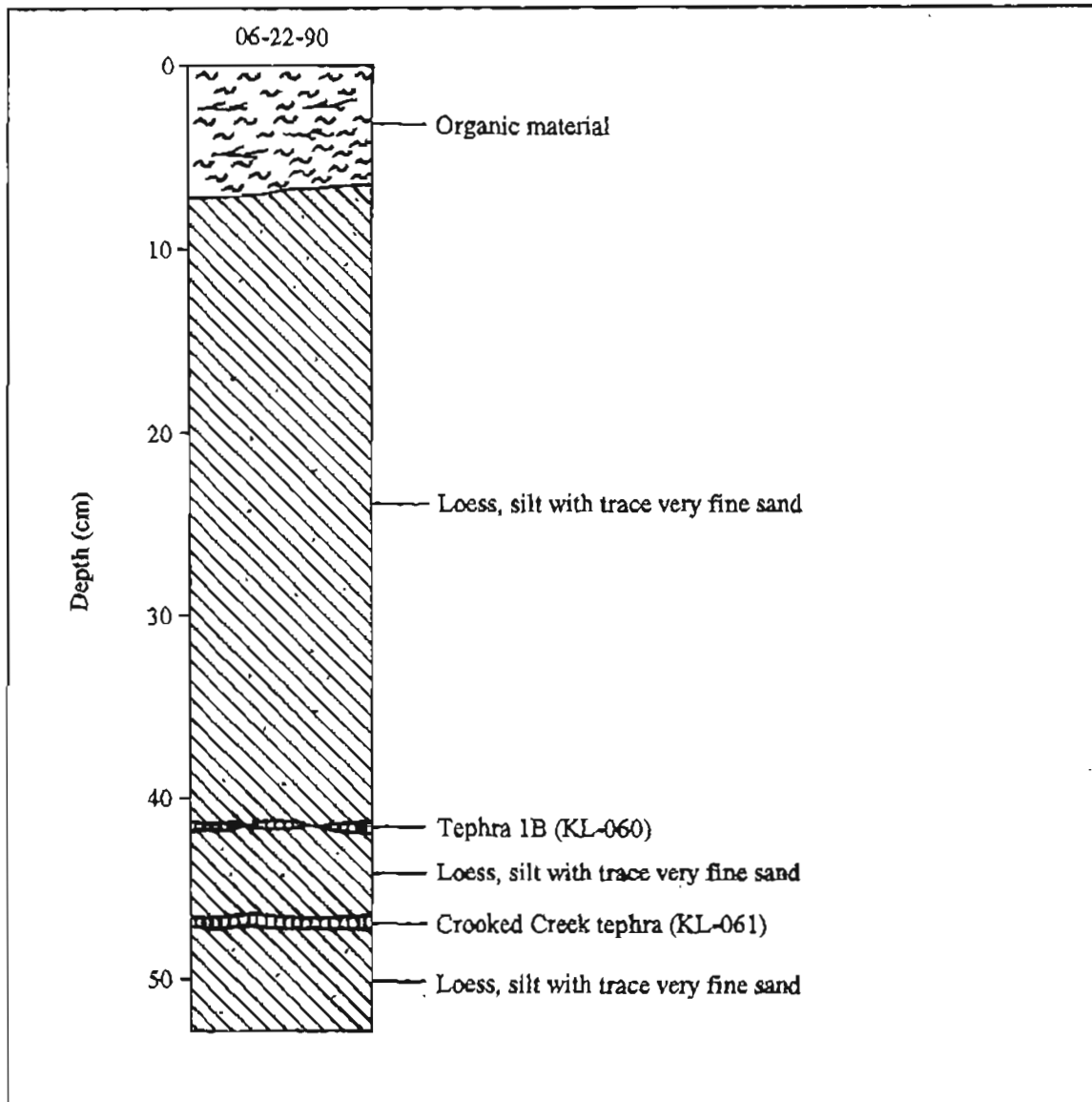


Figure A39. Stratigraphy exposed in section 35 (60°31'06"N, 150°47'45"W), Kenai C-3 SE Quadrangle (KEN-83, sheet 2). Tephra geochemistry given in table 3.

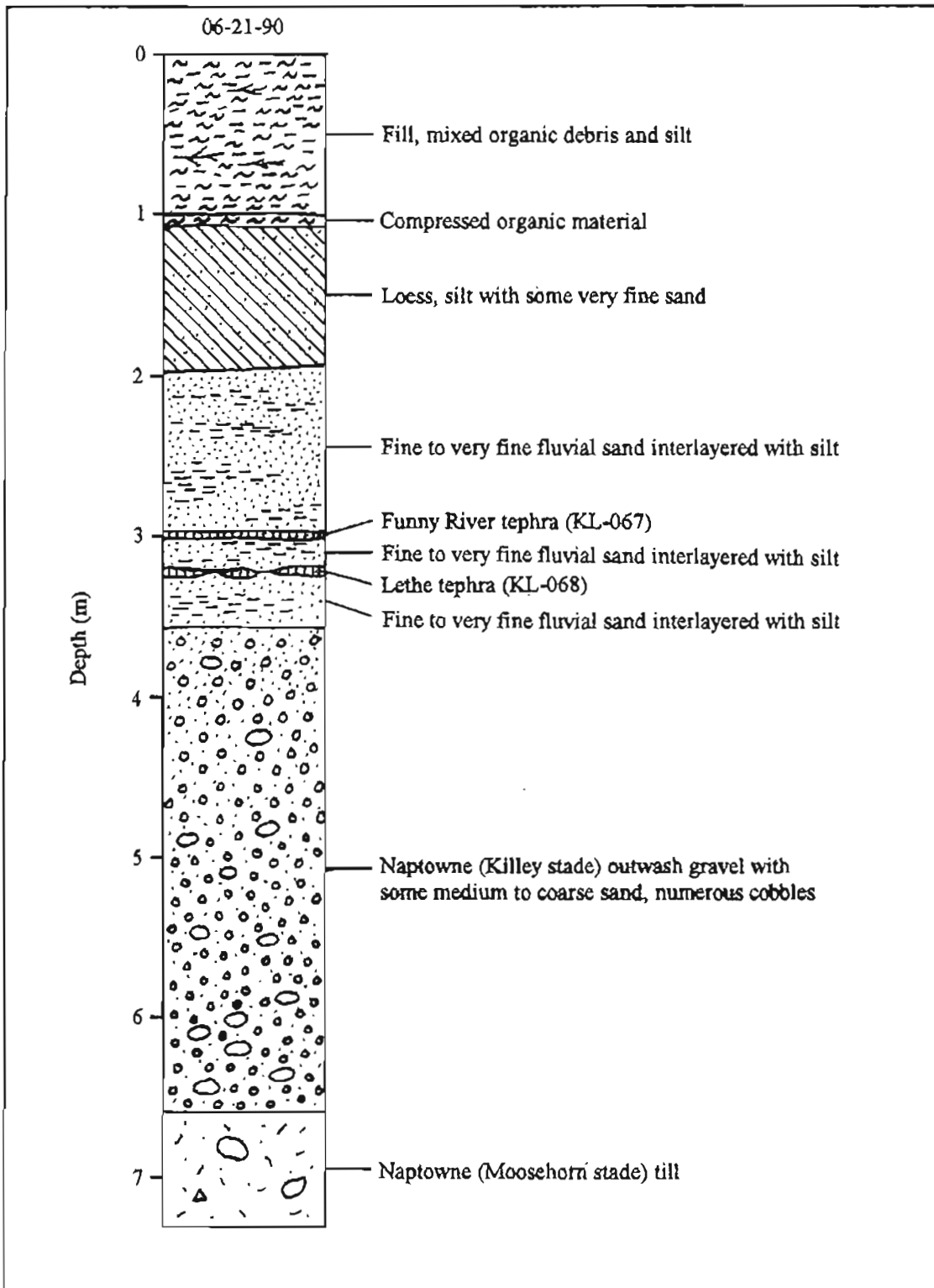


Figure A40. Stratigraphy exposed in section 36 (60°30'58"N, 150°45'30"W), Kenai C-3 SE Quadrangle (KEN-85, sheet 2). Tephra geochemistry given in table 3. Section demonstrates deposition of Lethe tephra after gravel outwash from nearby type Killey moraine.

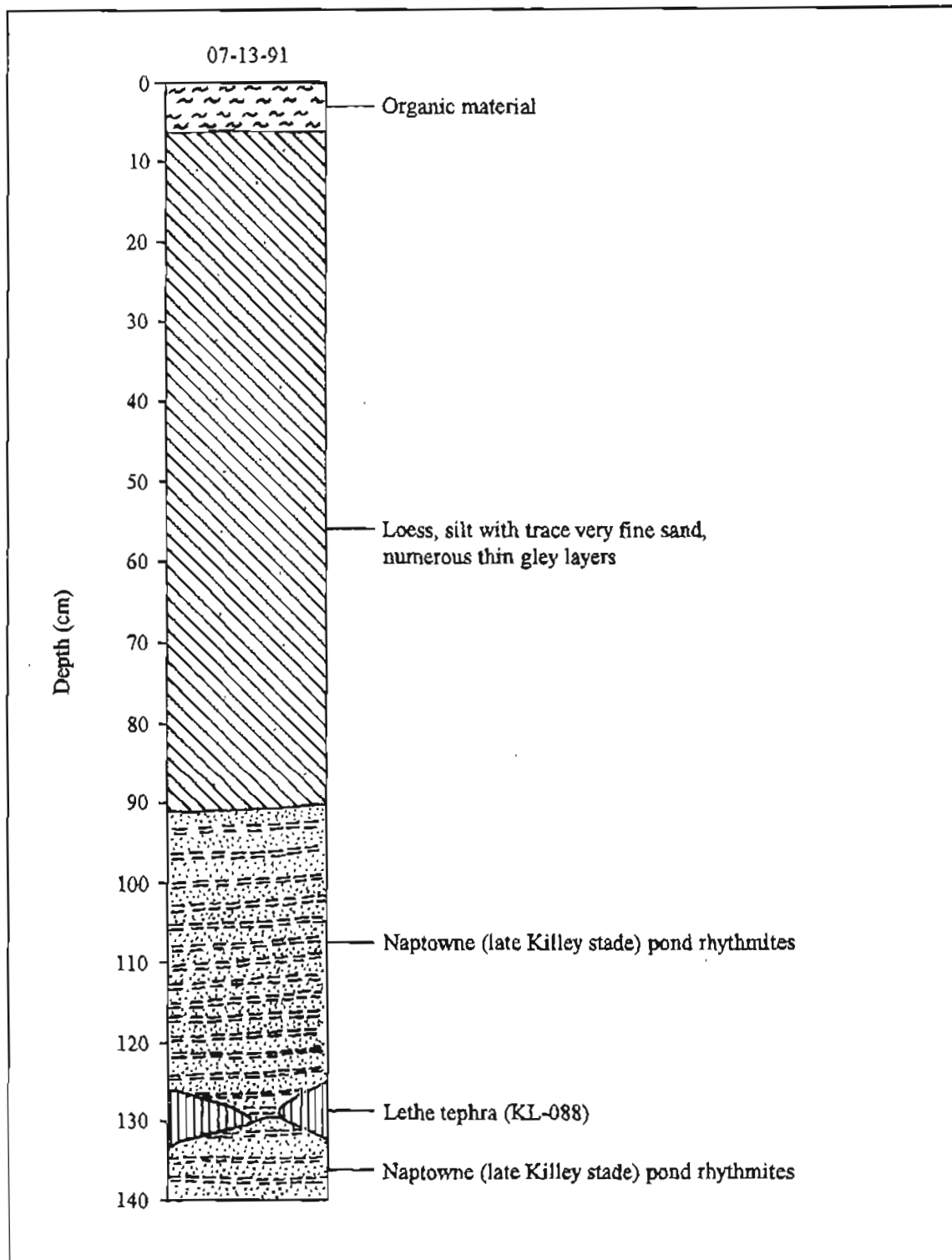


Figure A41. *Stratigraphy exposed in section 37 (60°30'57"N, 150°38'48"W), Kenai C-2 SW Quadrangle (KEN-86, sheet 2). Tephra geochemistry given in table 3. Section establishes late Killey age for pond sediments on type Killey moraine.*

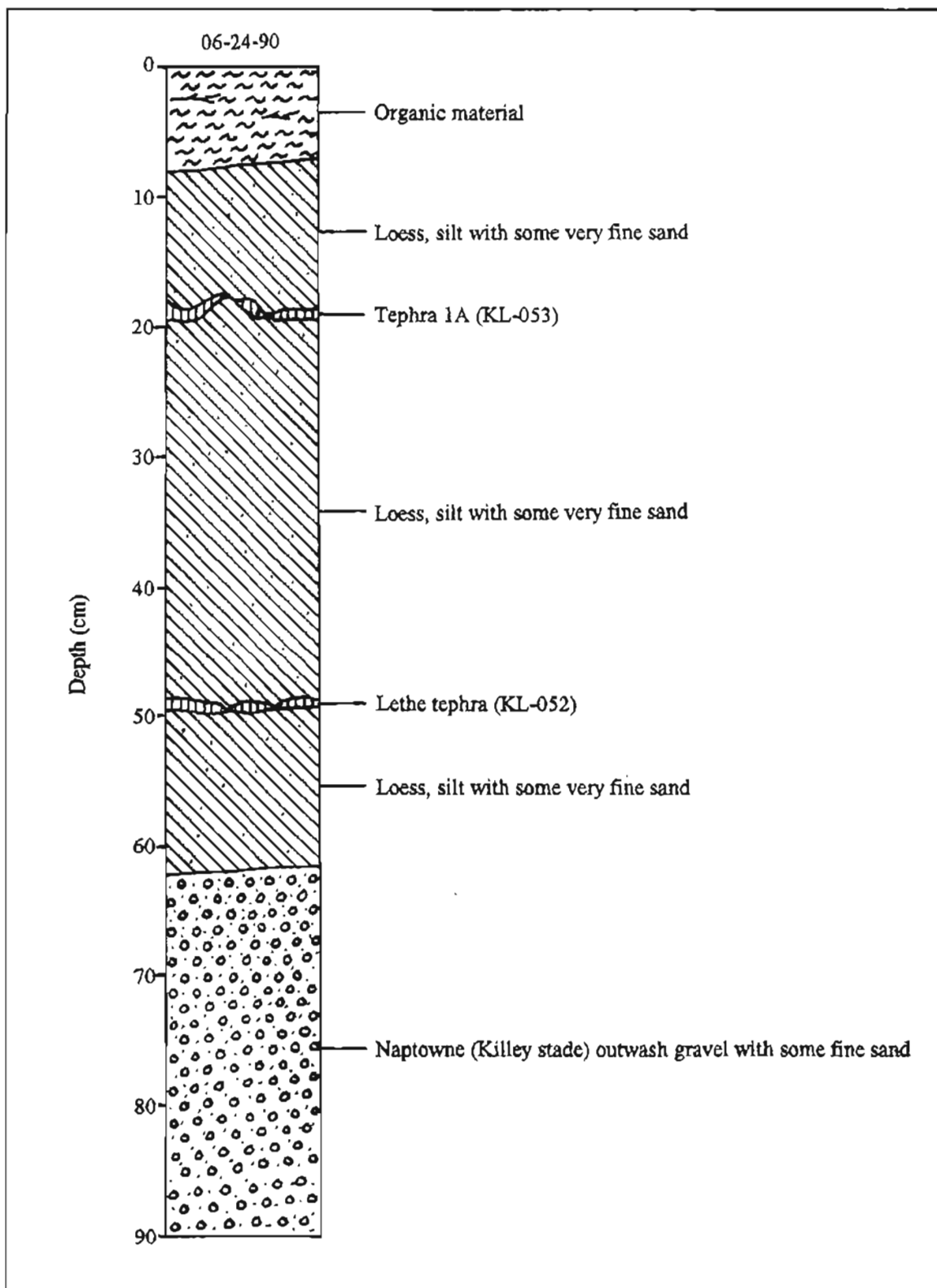


Figure A42. Stratigraphy exposed in section 38 ( $60^{\circ}30'55''N$ ,  $150^{\circ}40'51''W$ ), Kenai C-2 SW Quadrangle (KEN-87, sheet 2). Tephra geochemistry given in table 3. Section demonstrates deposition of Lethe tephra after gravel outwash from the type Killey moraine.

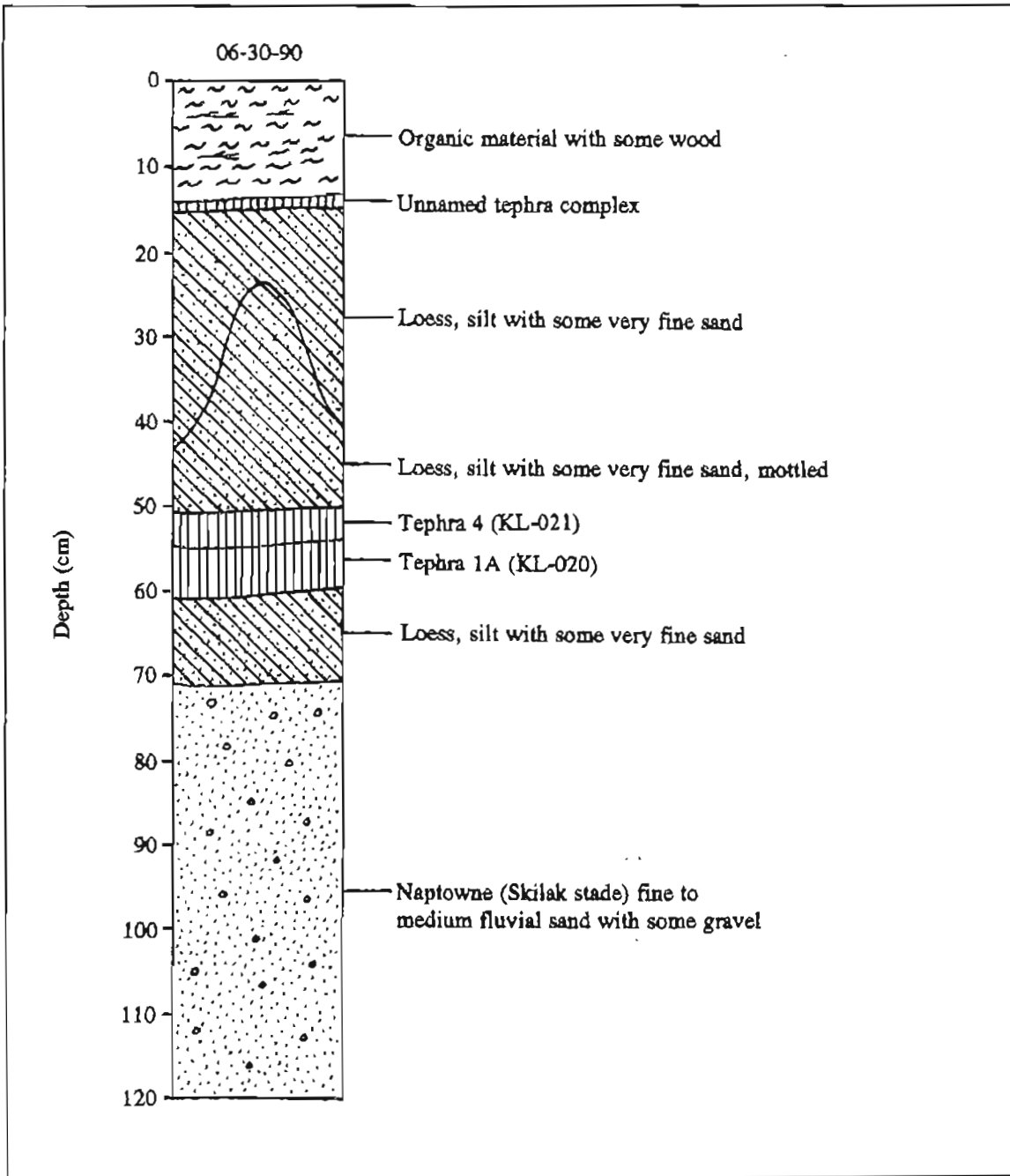


Figure A43. Stratigraphy exposed in section 39 (60°30'41"N, 151°16'18"W), Kenai C-4 SE Quadrangle (KEN-88, sheet 2). Tephra geochemistry given in table 3, except for unnamed tephra complex.

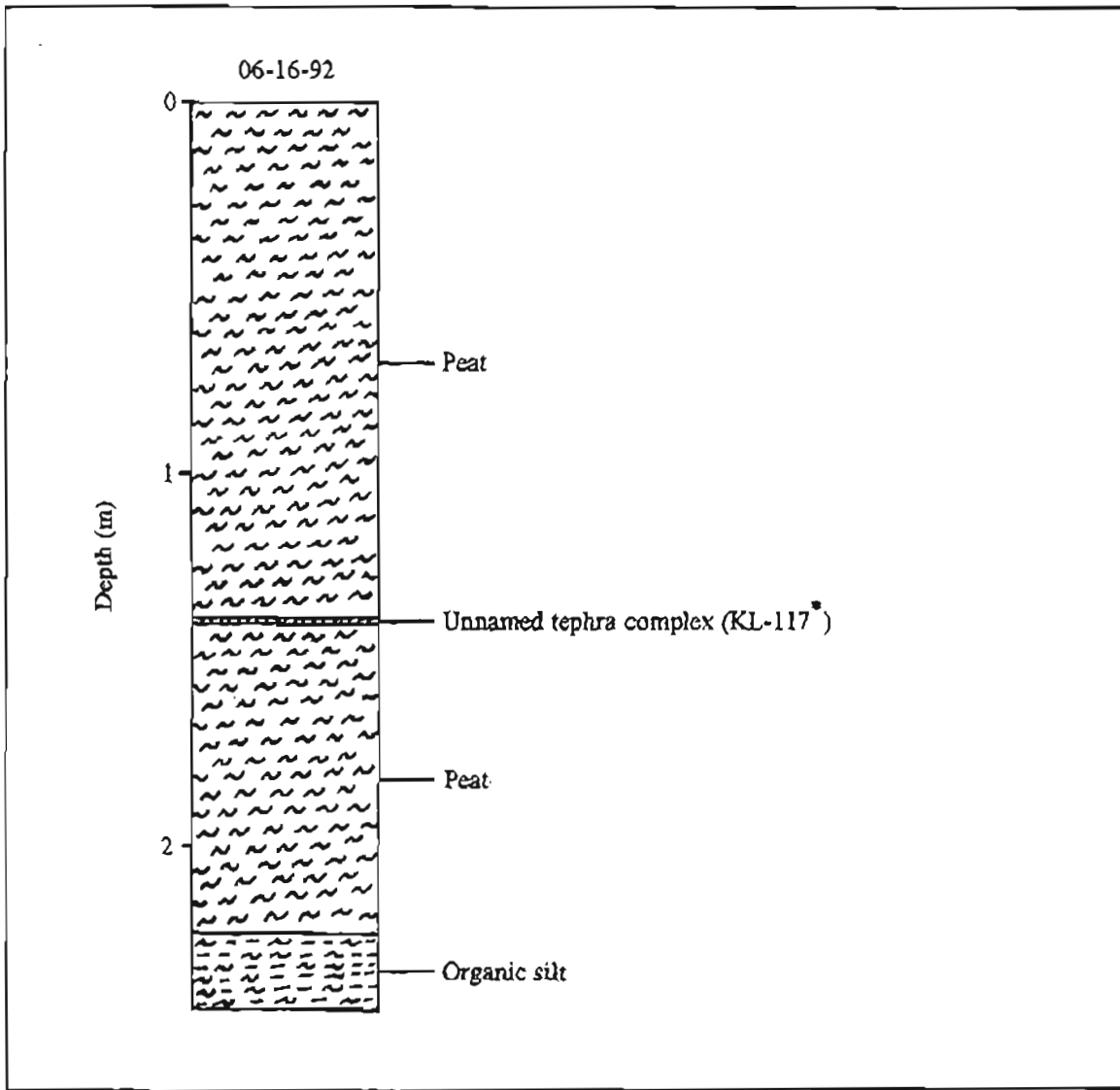


Figure A44. Stratigraphy exposed in section 40 (60°30'11"N, 150°36'42"W), Kenai C-2 SW Quadrangle (KEN-90, sheet 2).

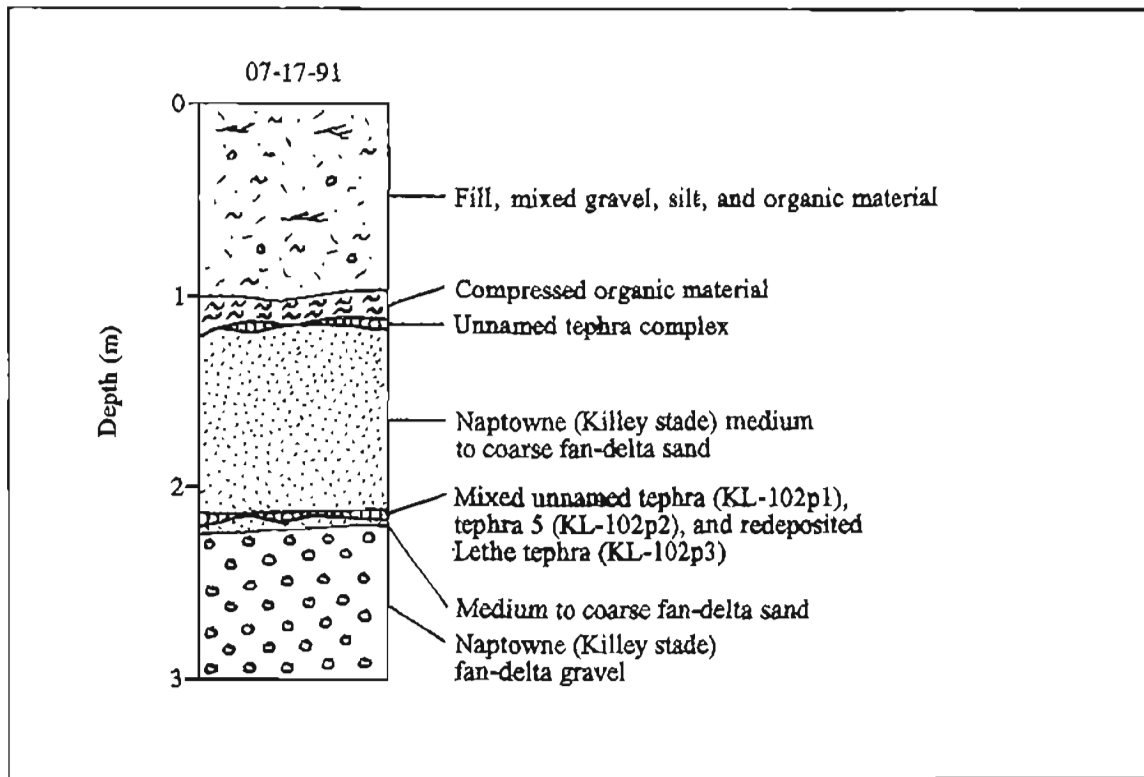


Figure A45. Stratigraphy exposed in section 41 (60°29'20"N, 151°11'59"W), Kenai B-4 NE Quadrangle (KEN-96, sheet 2). Tephra geochemistry given in table 3, except for unnamed tephra complex. Section indicates Killey age for fan delta related to upper terrace of lower Kenai River.

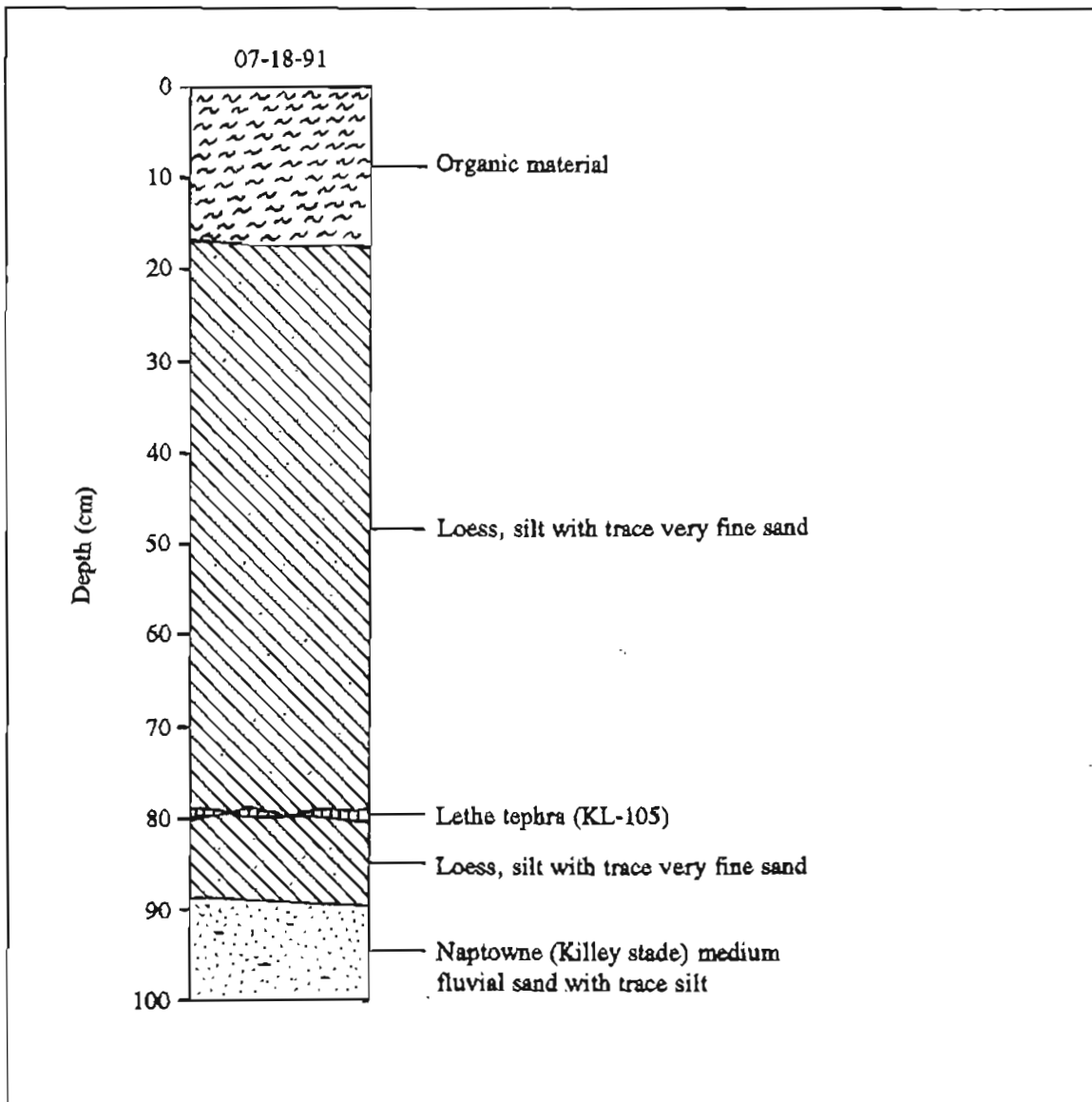


Figure A46. Stratigraphy exposed in section 42 (60°29'17"N, 151°03'07"W), Kenai B-3 NW Quadrangle (KEN-97, sheet 2). Tephra geochemistry given in table 3. Section indicates Killey age for upper terrace of Kenai River at Soldoma.

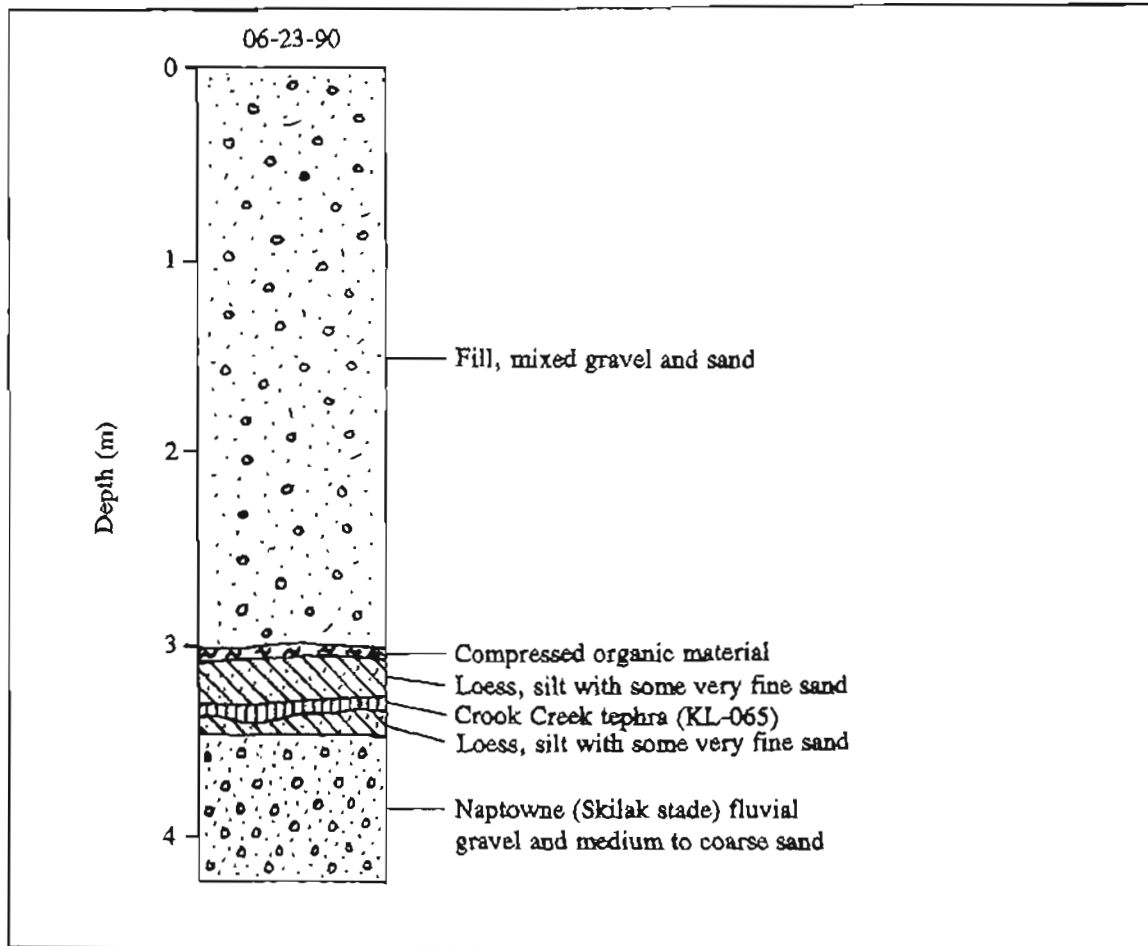


Figure A47. Stratigraphy exposed in section 43 (60°28'47"N, 151°03'22"W), Kenai B-3 NW Quadrangle (KEN-100, sheet 2). Tephra geochemistry given in table 3.

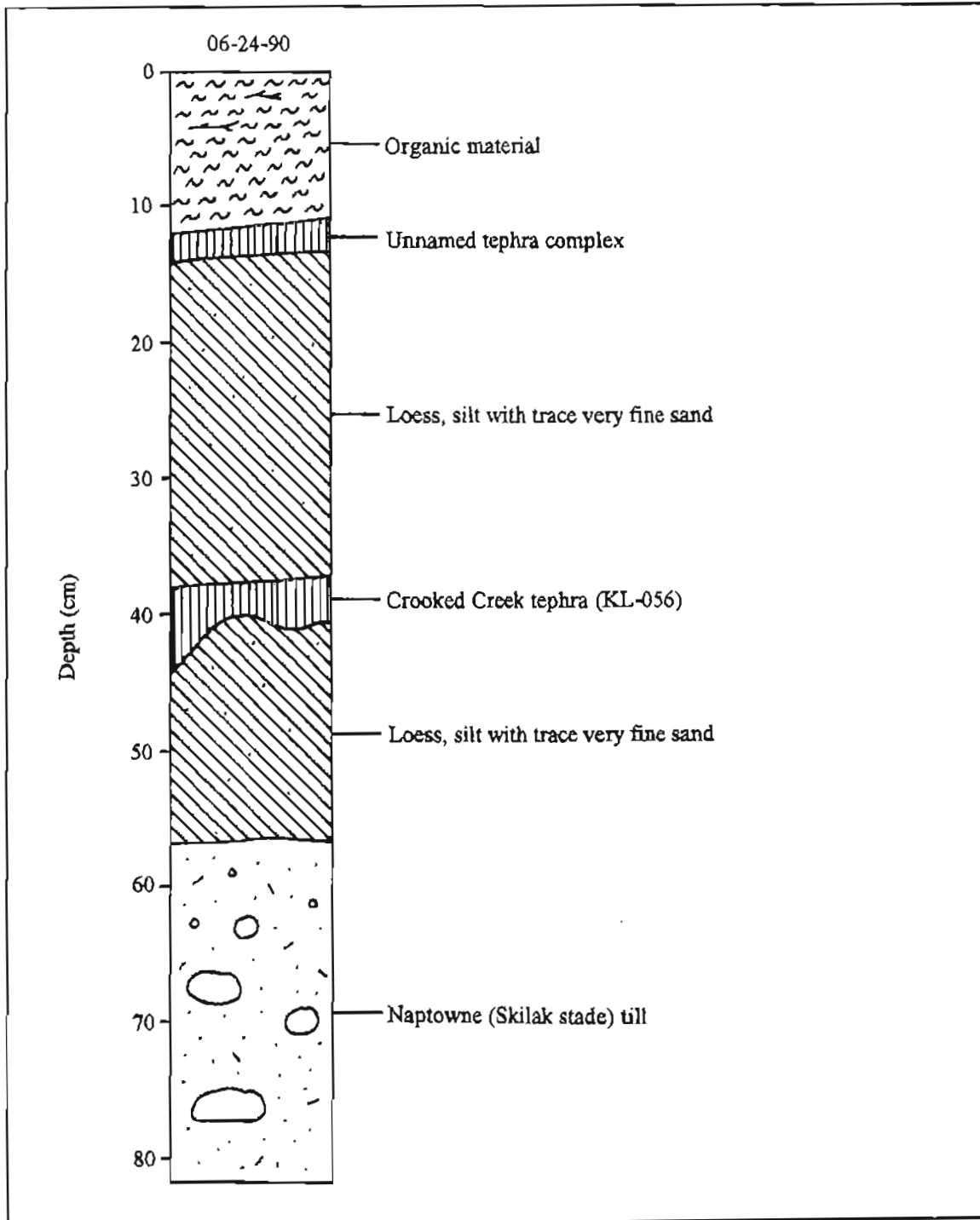


Figure A48. Stratigraphy exposed in section 44 ( $60^{\circ}28'45''N$ ,  $150^{\circ}27'24''W$ ) on type Skilak moraine, Kenai B-2 NE Quadrangle (KEN-101, sheet 2). Tephra geochemistry given in table 3, except for unnamed tephra complex.

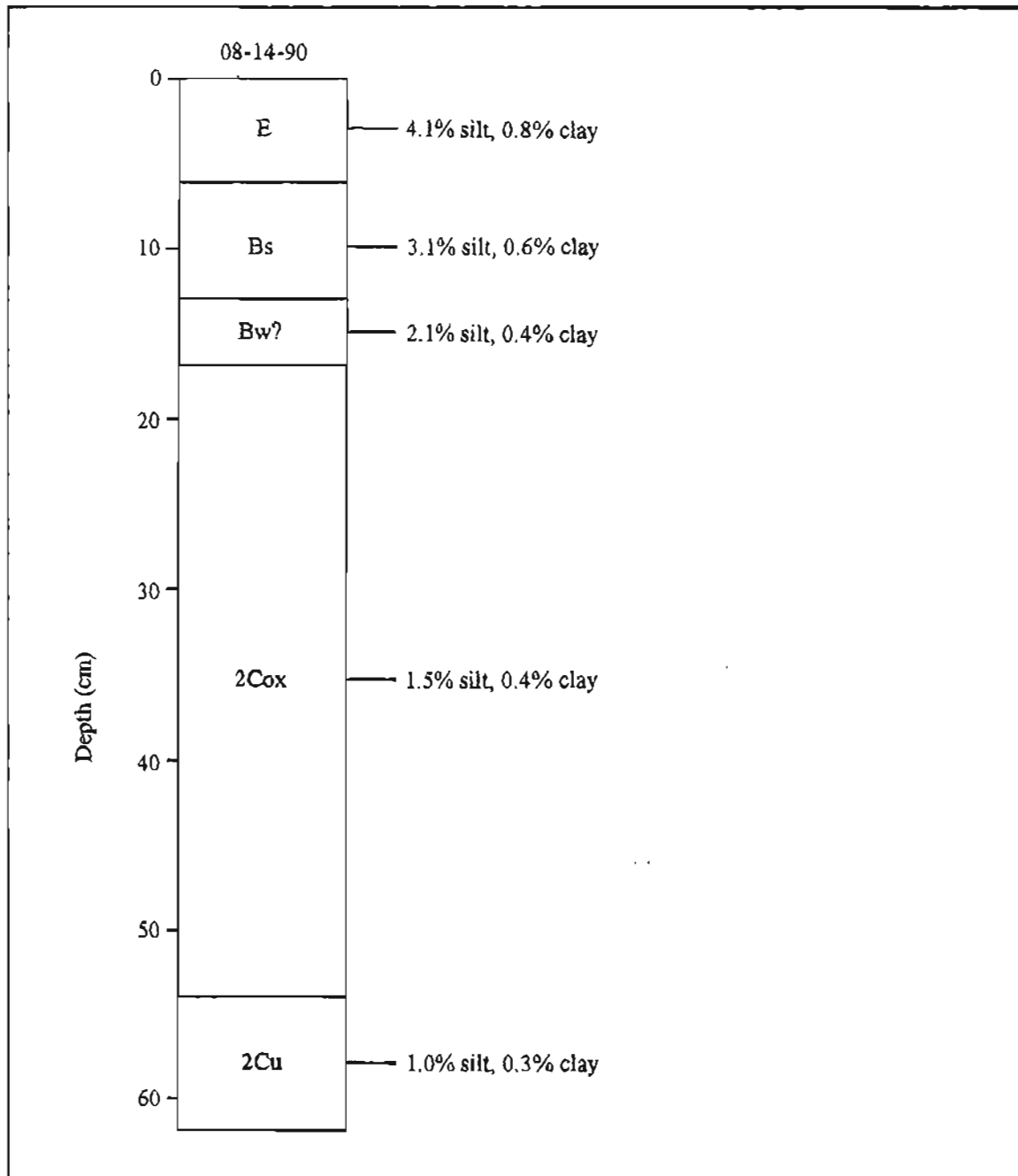


Figure A49. Distribution of silt and clay (calculated as percent of <2-mm fraction) with depth in soil profile S3 on flat crest of type Skilak moraine (60°28'45"N, 150°27'24"W), Kenai B-2 NE Quadrangle (KEN-101, sheet 2). Elevation 89 m. Horizons according to Soil Survey Staff (1975), modified by Birkeland and others (1991b) and this study. Horizons O and A not shown above horizon E. Detailed profile description summarized in table A5.

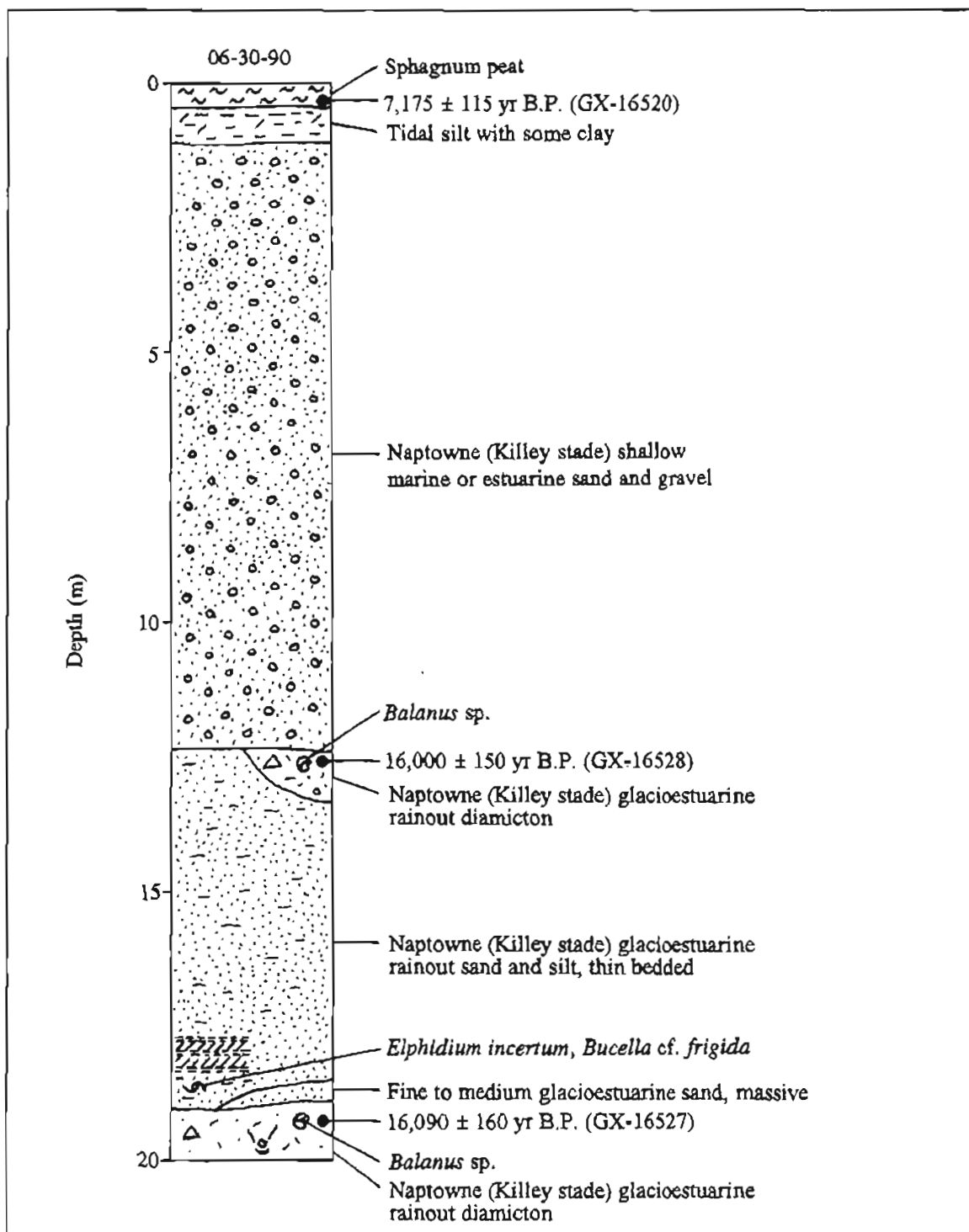


Figure A50. Stratigraphy exposed in section 45 (60°28'29"N, 151°16'38"W), Kenai B-4 NE Quadrangle (KEN-103, sheet 2). Chronologic significance of radiocarbon dates given in table 2.

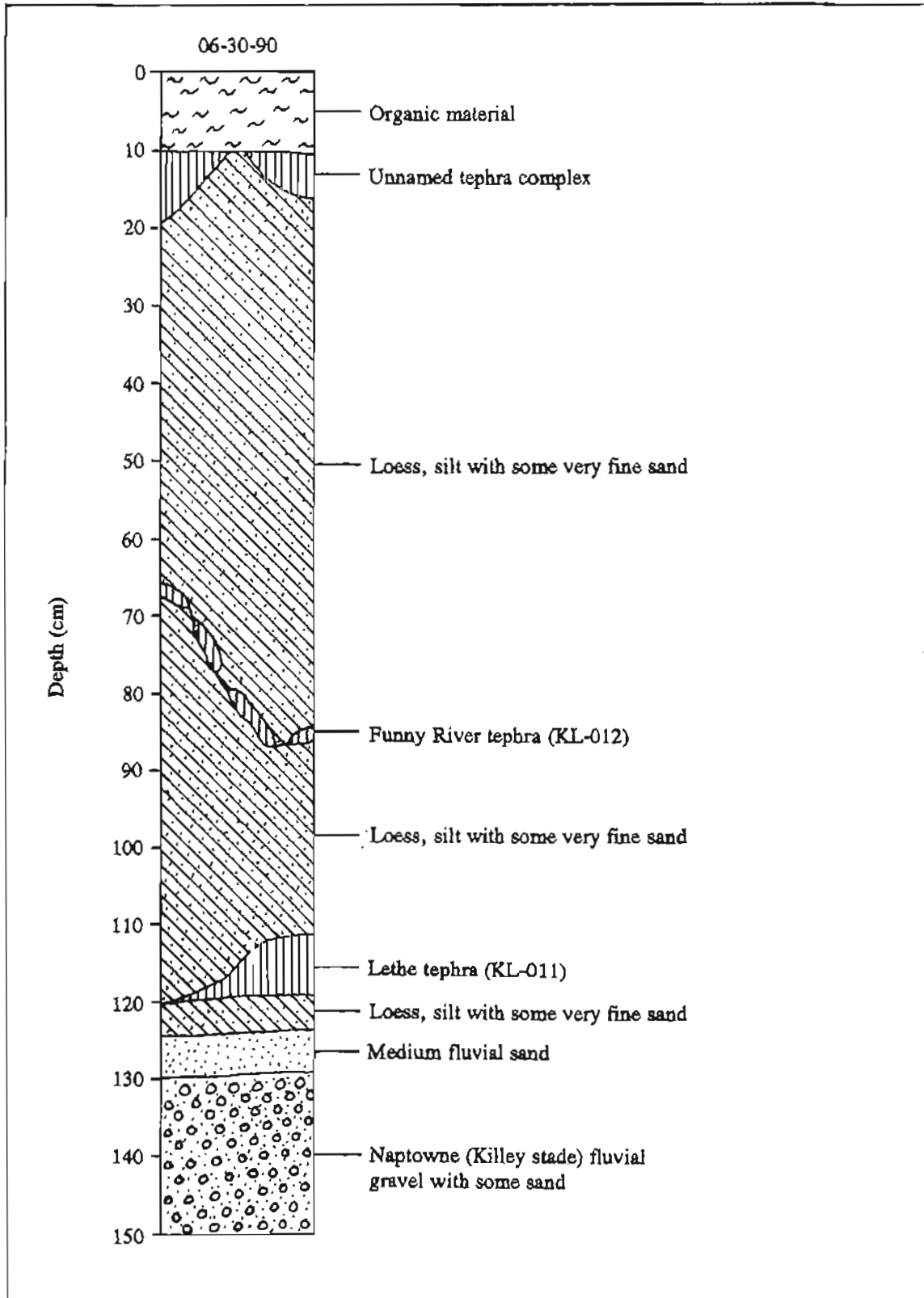


Figure A51. Stratigraphy exposed in section 46 (60°28'17"N, 151°07'10"W), Kenai B-3 NW Quadrangle (KEN-105, sheet 2). Tephra geochemistry given in table 3, except for unnamed tephra complex. Section indicates Killey age for upper terrace of Kenai River at Soldoma and associated fan of lower Slikok Creek.

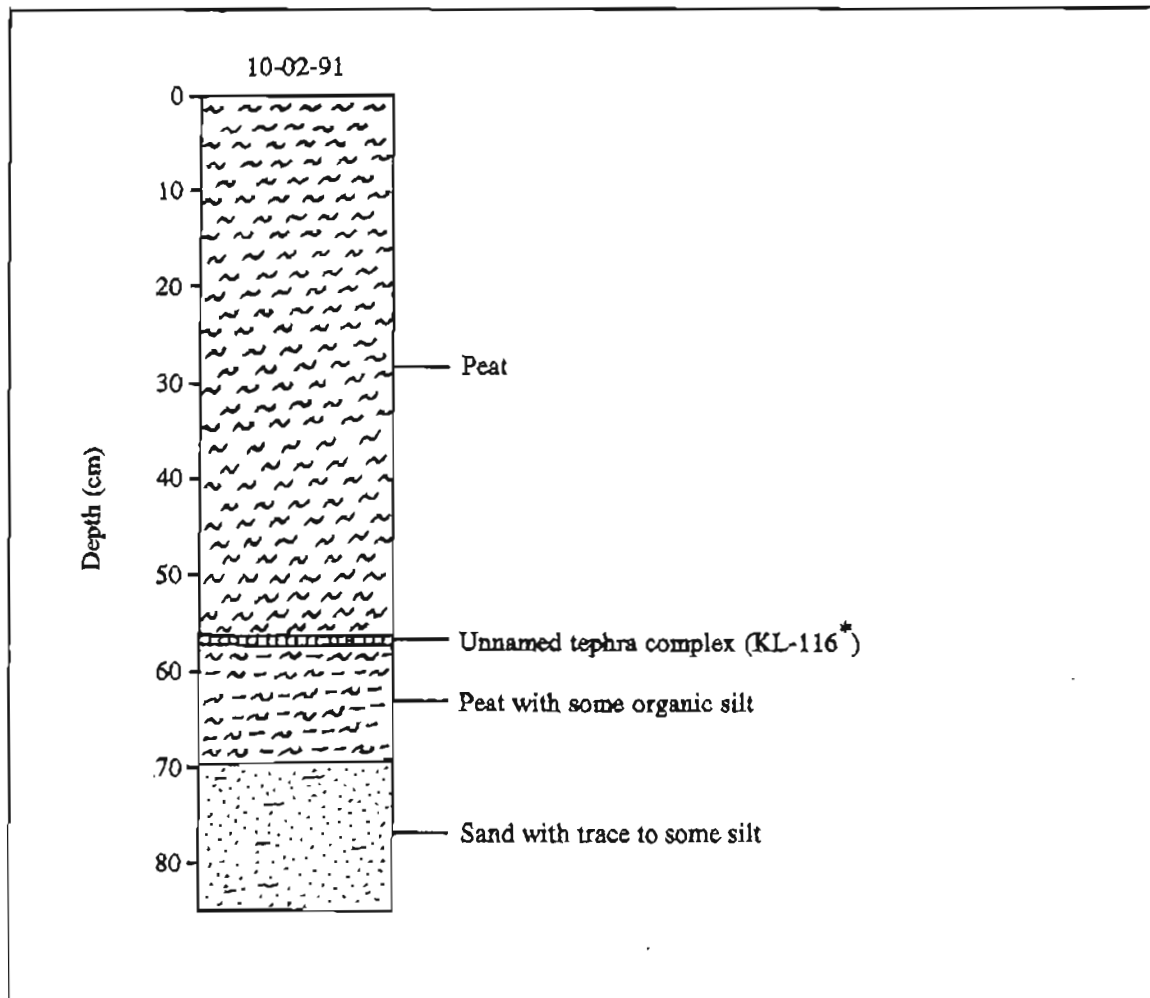


Figure A52. Stratigraphy exposed in section 47 (60°28'05"N, 151°04'51"W), Kenai B-3 NW Quadrangle (KEN-107, sheet 2).

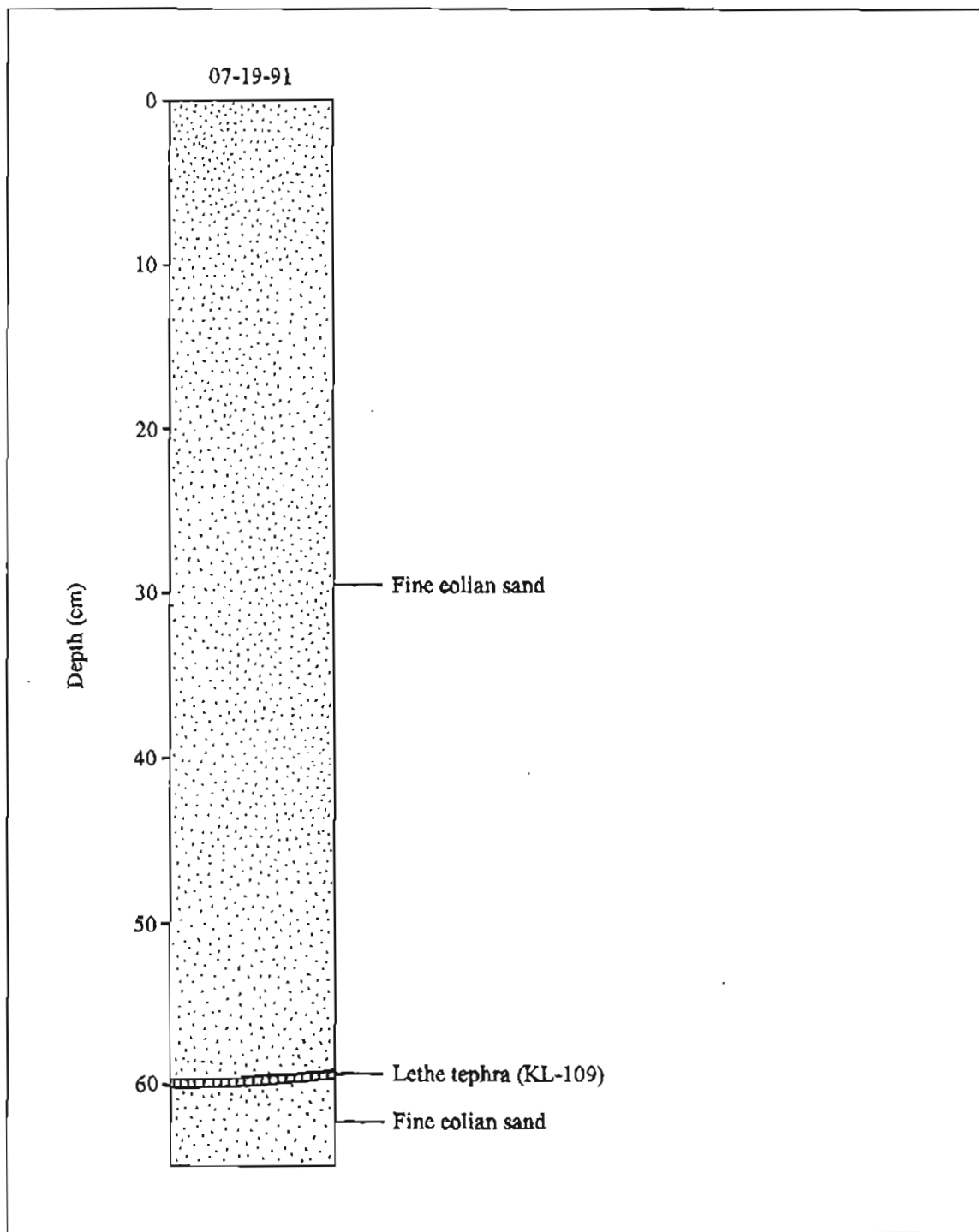


Figure A53. Stratigraphy exposed in section 48 ( $60^{\circ}27'37''N$ ,  $151^{\circ}57'48''W$ ), Kenai B-3 NW Quadrangle (KEN-110, sheet 2). Tephra geochemistry given in table 3. Section establishes late Killey age for eolian sand on drift of Moosehorn age on southern wall of Kenai River valley south of Soldotna.

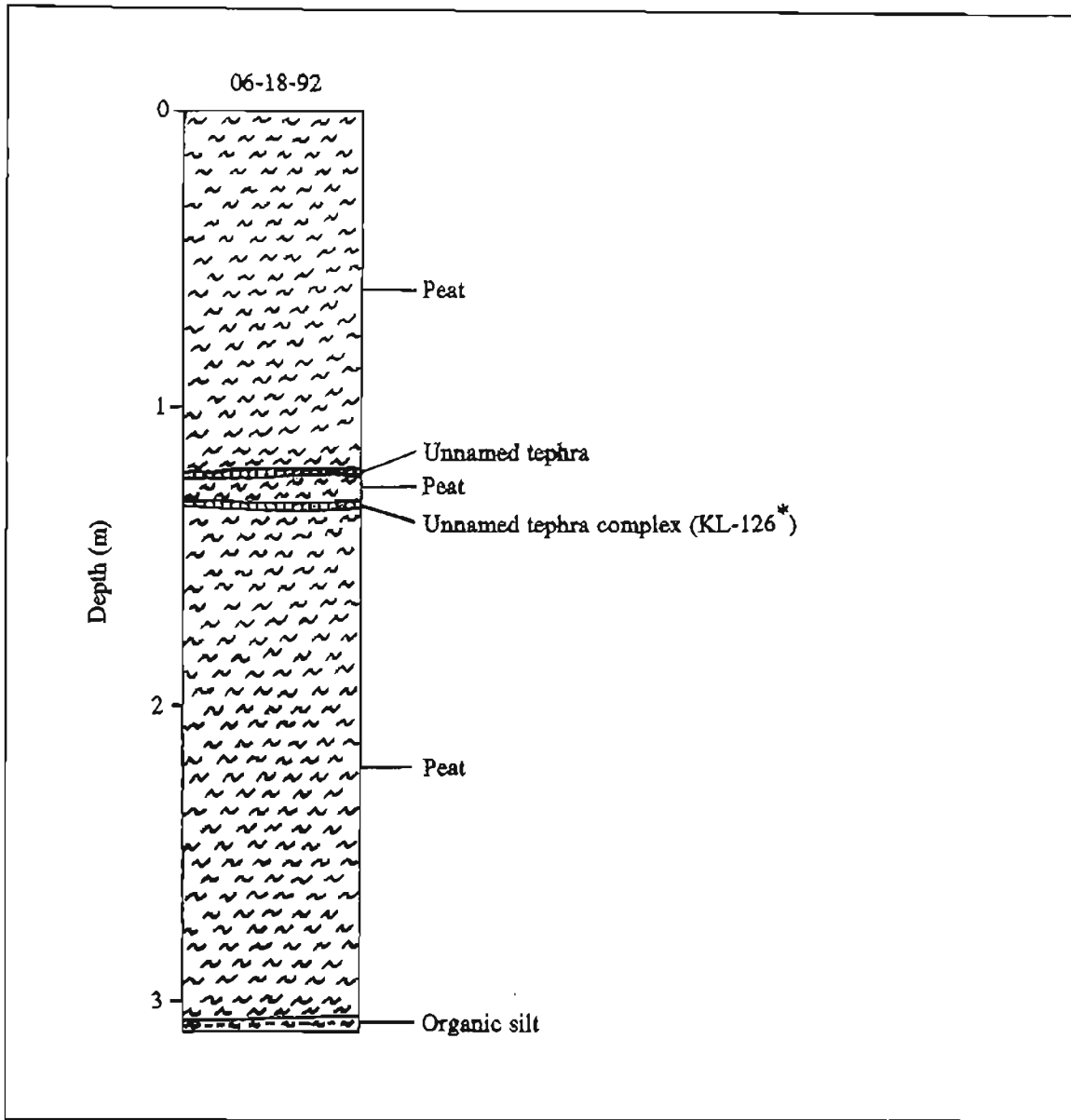


Figure A54. Stratigraphy exposed in section 49 (60°27'00"N, 151°14'14"W), Kenai B-4 NE Quadrangle (KEN-113, sheet 2).

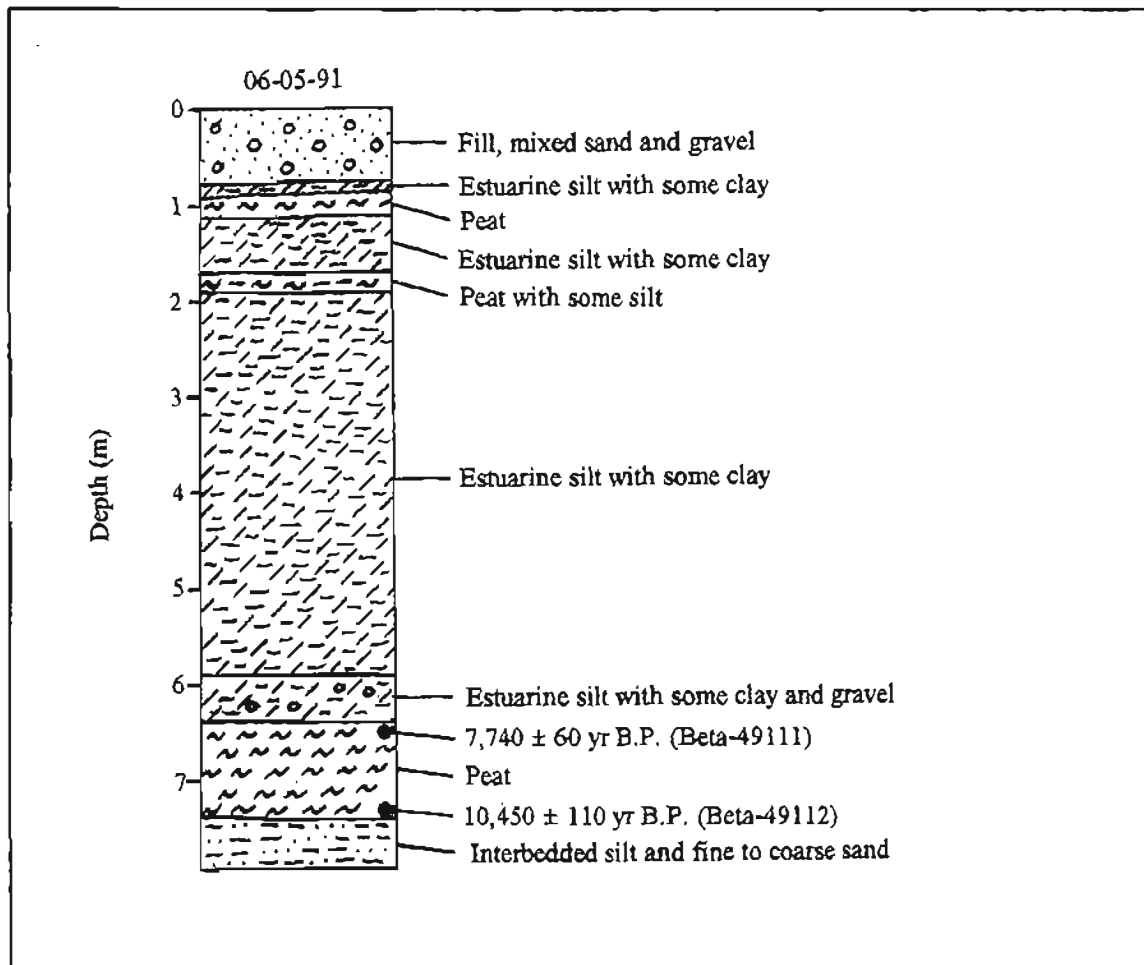


Figure A55. Stratigraphy exposed in section 50 (60°23'00"N, 151°16'54"W), Kenai B-4 NE Quadrangle (KEN-115, sheet 2). Chronologic significance of radiocarbon dates given in table 2.

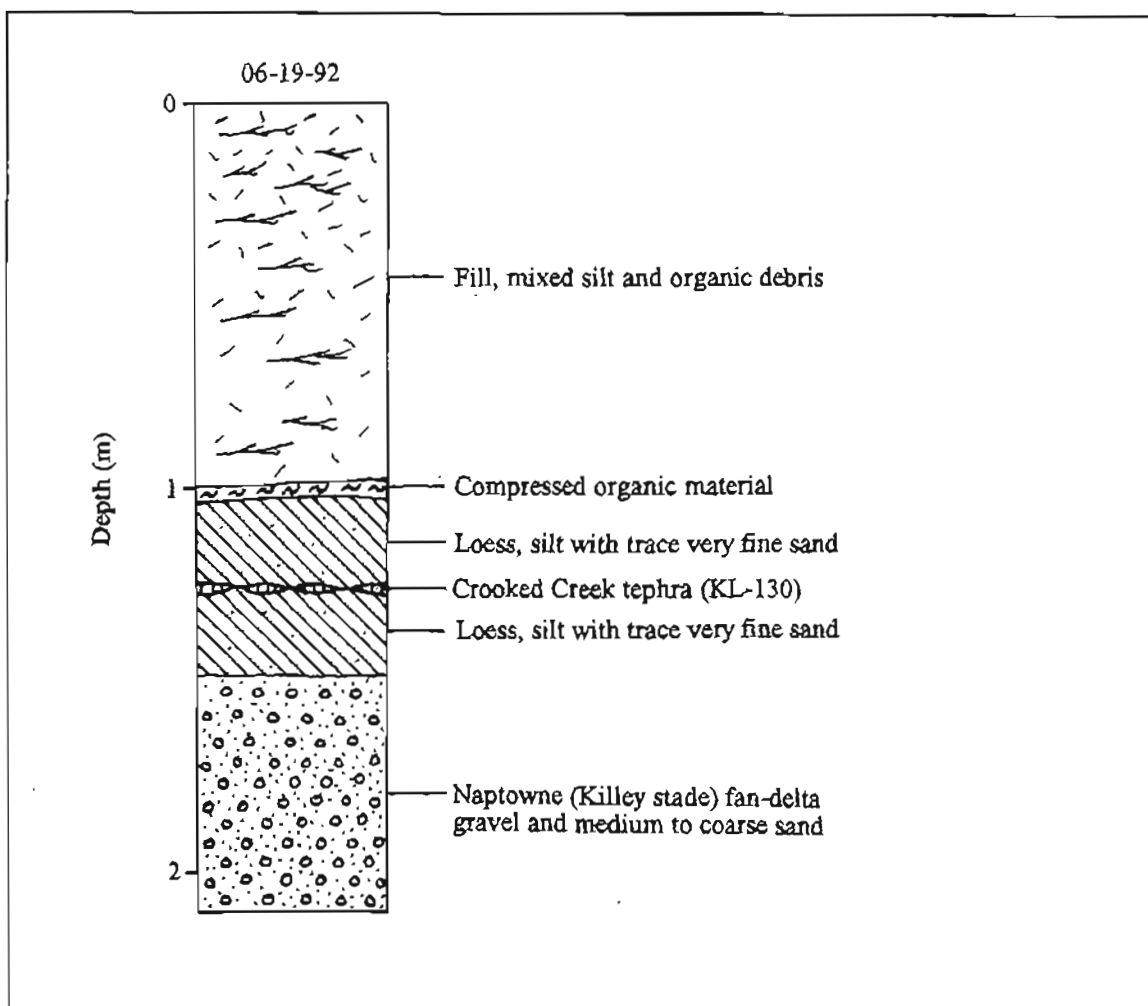


Figure A56. Stratigraphy exposed in section 51 (60°22'37"N, 151°18'57"W), Kenai B-4 NW Quadrangle (KEN-116, sheet 2). Tephra geochemistry given in table 3.

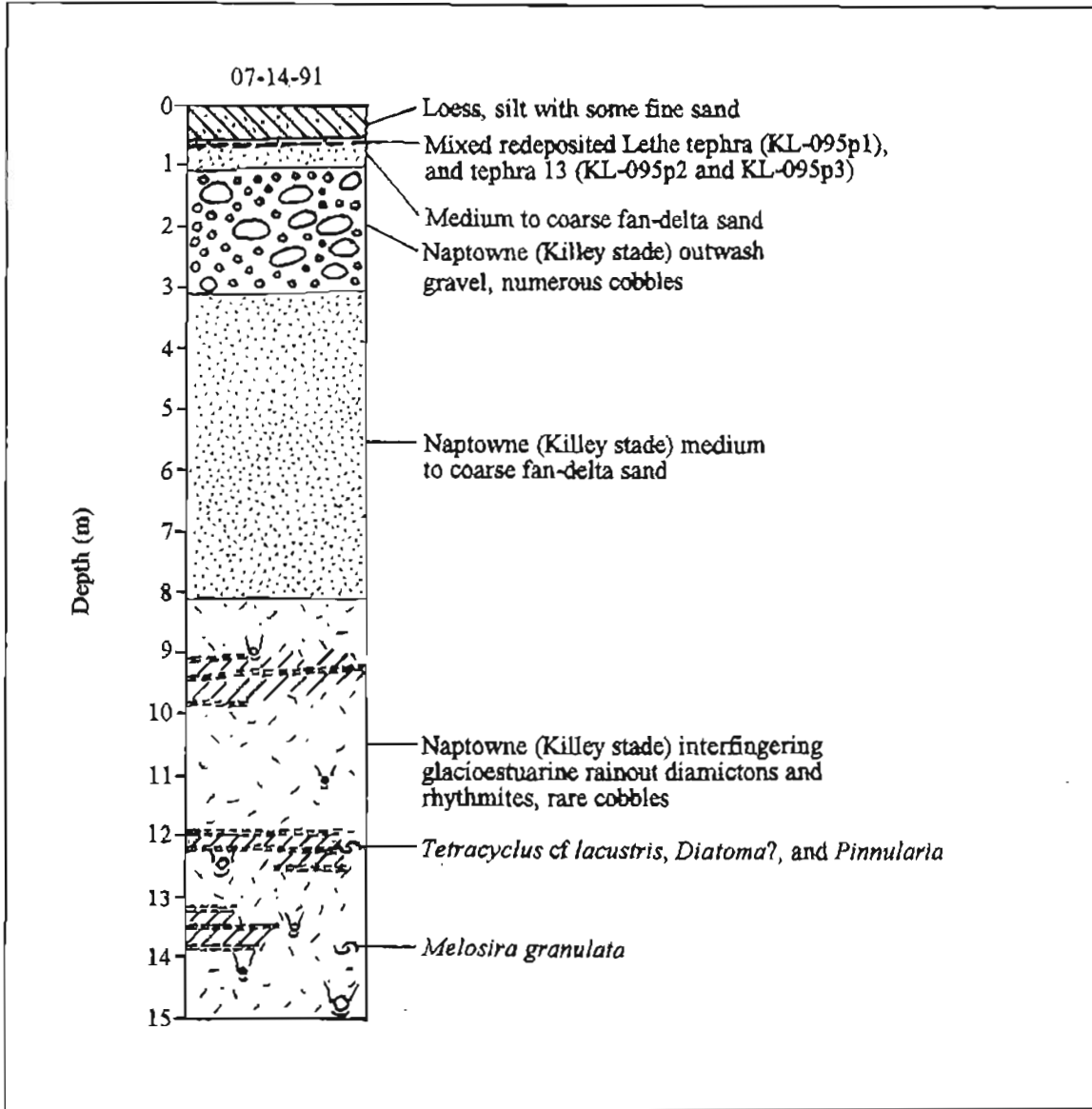


Figure A57. Stratigraphy exposed in section 52 (60°22'18"N, 151°17'59"W), Kenai B-4 SE Quadrangle (KEN-117, sheet 2). Tephra geochemistry given in table 3. Section indicates Killey age for fan-delta sediments and associated diamicton at mouth of Kasilof River.

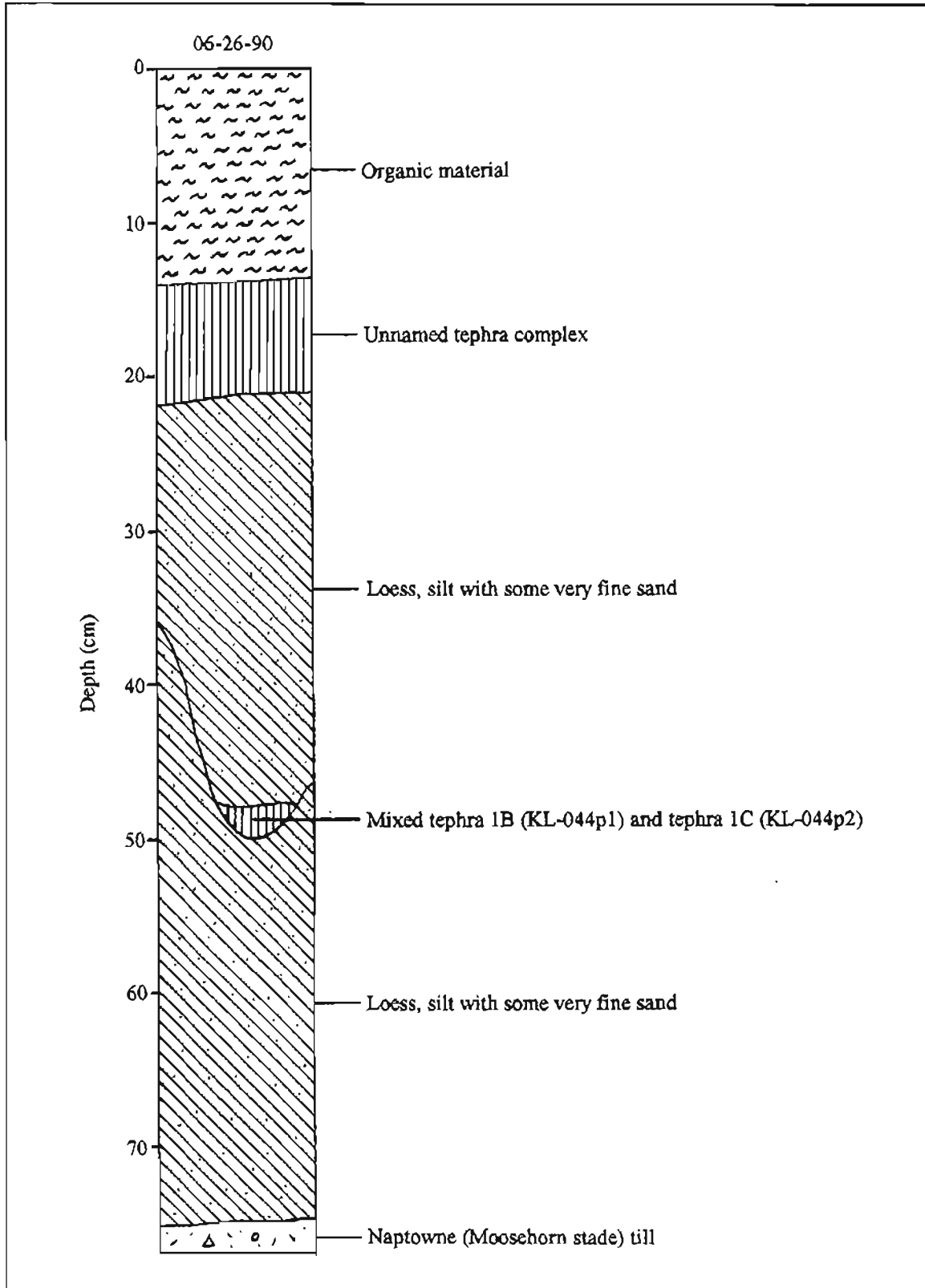


Figure A58. Stratigraphy exposed in section 53 (60°22'11"N, 151°11'40"W), Kenai B-4 SE Quadrangle (KEN-118, sheet 2). Tephra geochemistry given in table 3, except for unnamed tephra complex.

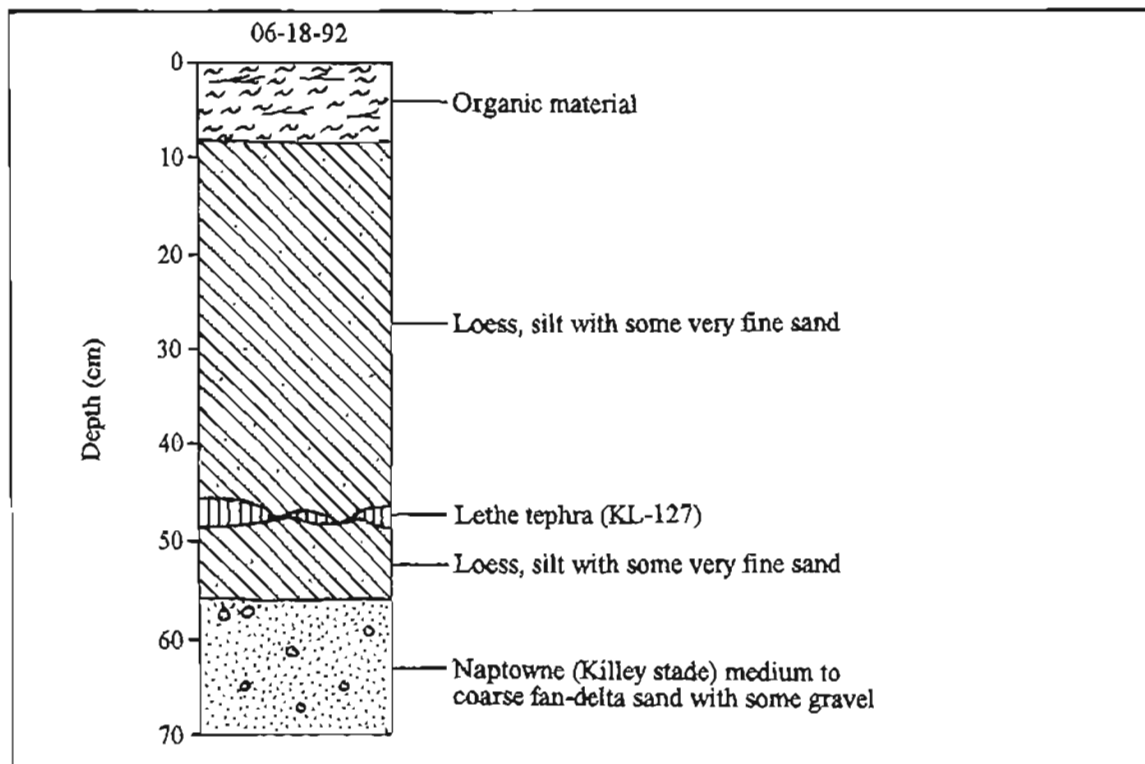


Figure A59. Stratigraphy exposed in section 54 (60°21'18"N, 151°15'58"W), Kenai B-4 SE Quadrangle (KEN-119, sheet 2). Tephra geochemistry given in table 3. Section indicates Killey age for fan delta at Kasilof and associated highest marine terrace between Kasilof and Kenai.

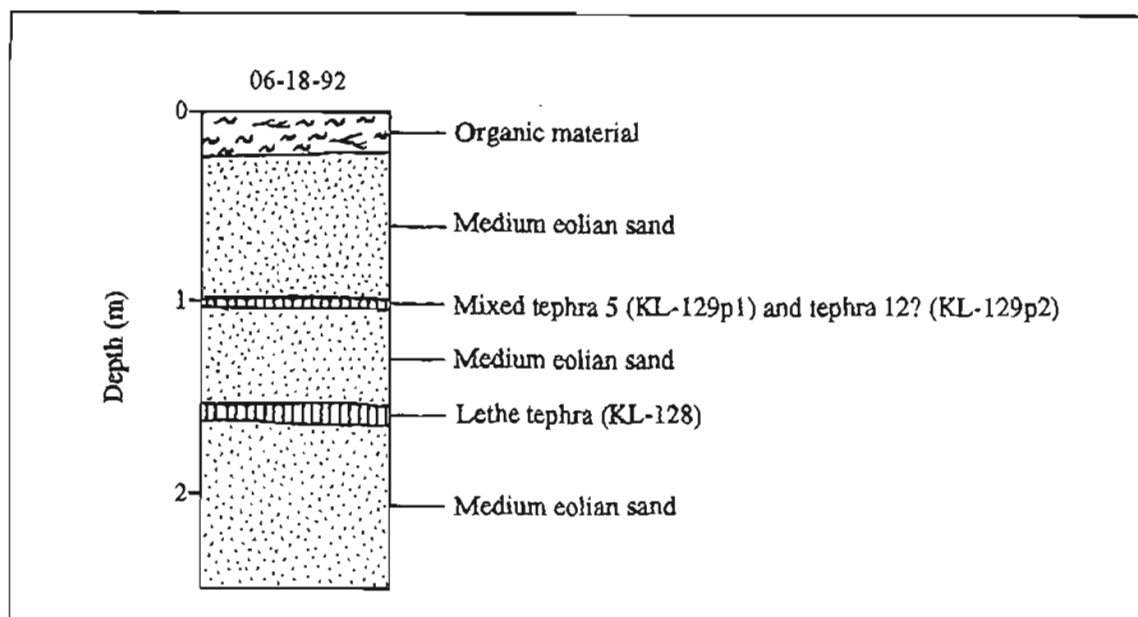


Figure A60. Stratigraphy exposed in section 55 (60°20'46"N, 151°13'07"W), Kenai B-4 SE Quadrangle (KEN-120, sheet 2). Tephra geochemistry given in table 3. Section demonstrates late Killey age for sand dunes along Sterling Highway at Coal Creek.

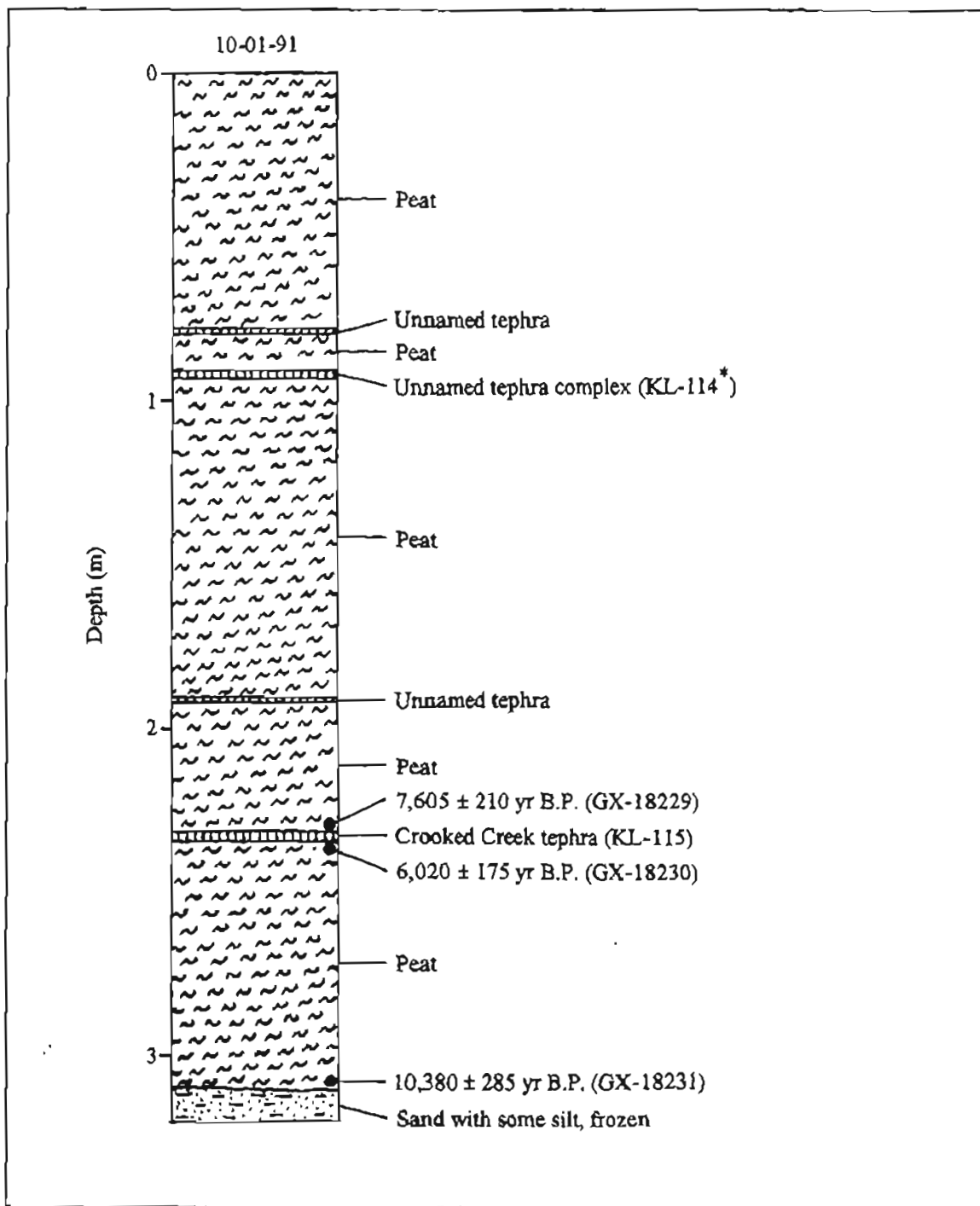


Figure A61. Stratigraphy exposed in section 56 (60°20'21"N, 151°13'39"W), Kenai B-4 SE Quadrangle (KEN-122, sheet 2). Chronologic significance of radiocarbon dates given in table 2. Tephra geochemistry given in table 3, except for unnamed tephtras.

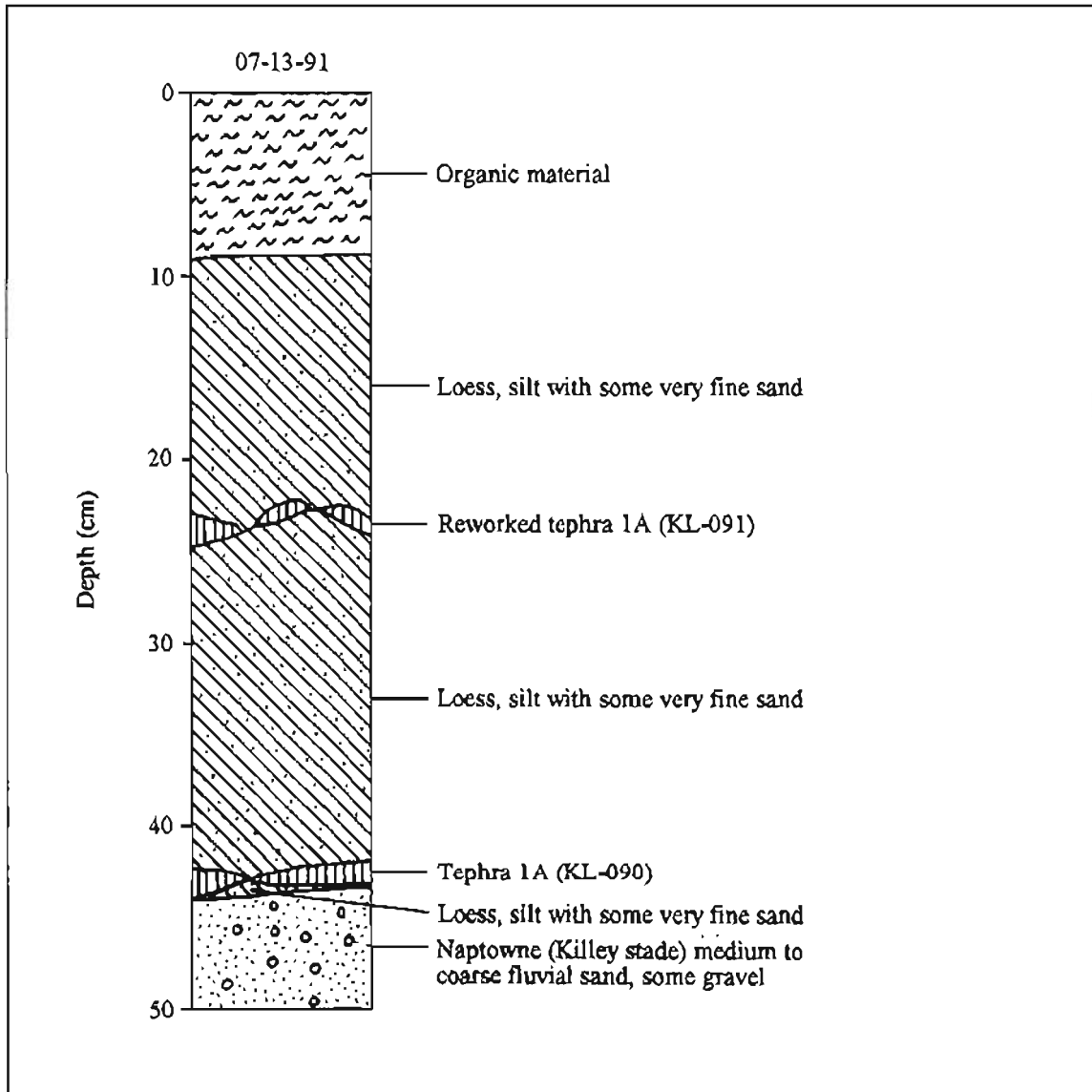


Figure A62. Stratigraphy exposed in section 57 (60°19'58"N, 151°16'02"W), Kenai B-4 SE Quadrangle (KEN-123, sheet 2). Tephra geochemistry given in table 3.

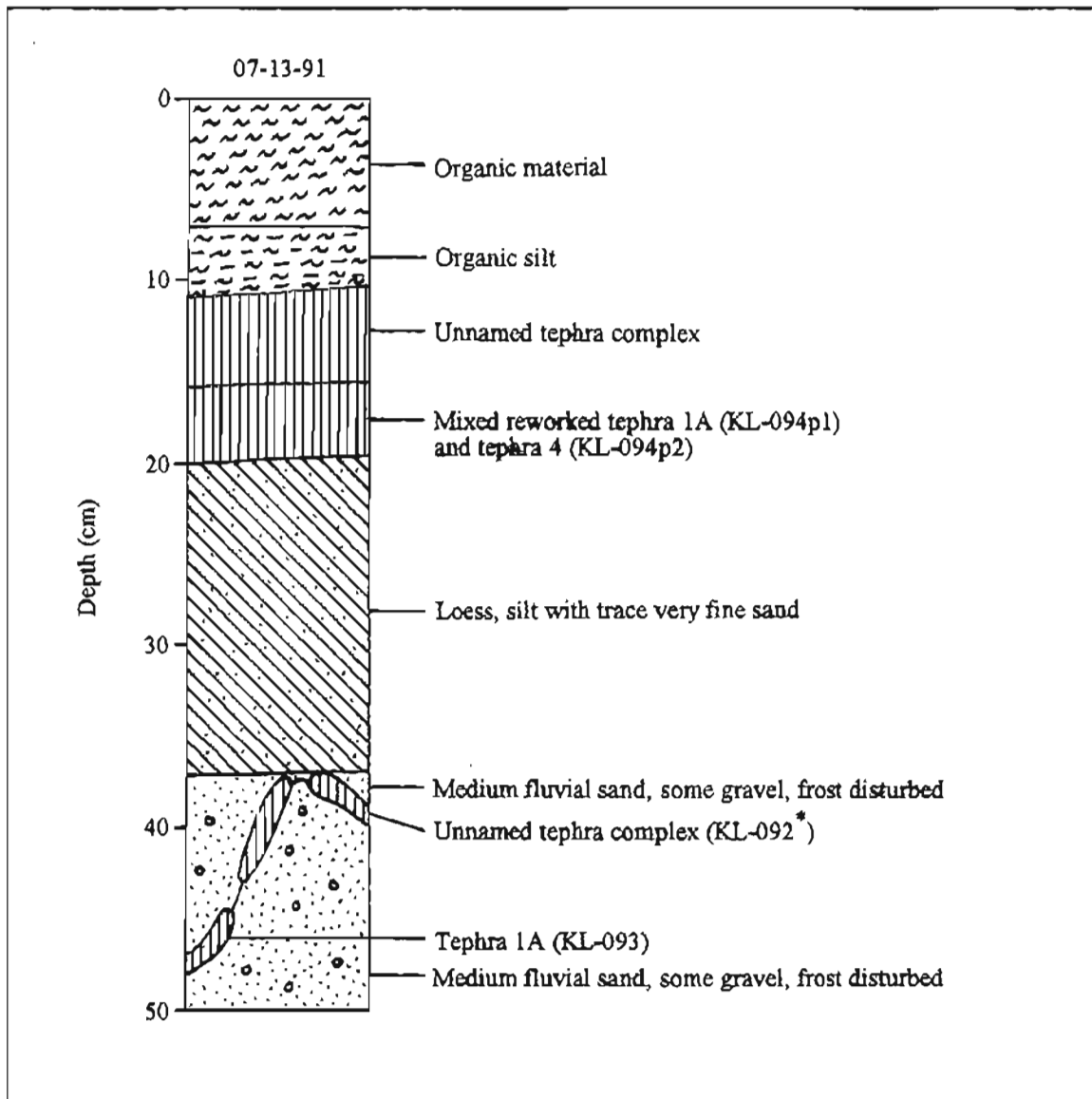


Figure A63. Stratigraphy exposed in section 58 (60°18'25"N, 151°15'33"W), Kenai B-4 SE Quadrangle (KEN-124, sheet 2). Tephra geochemistry given in table 3, except for unnamed tephra complex.

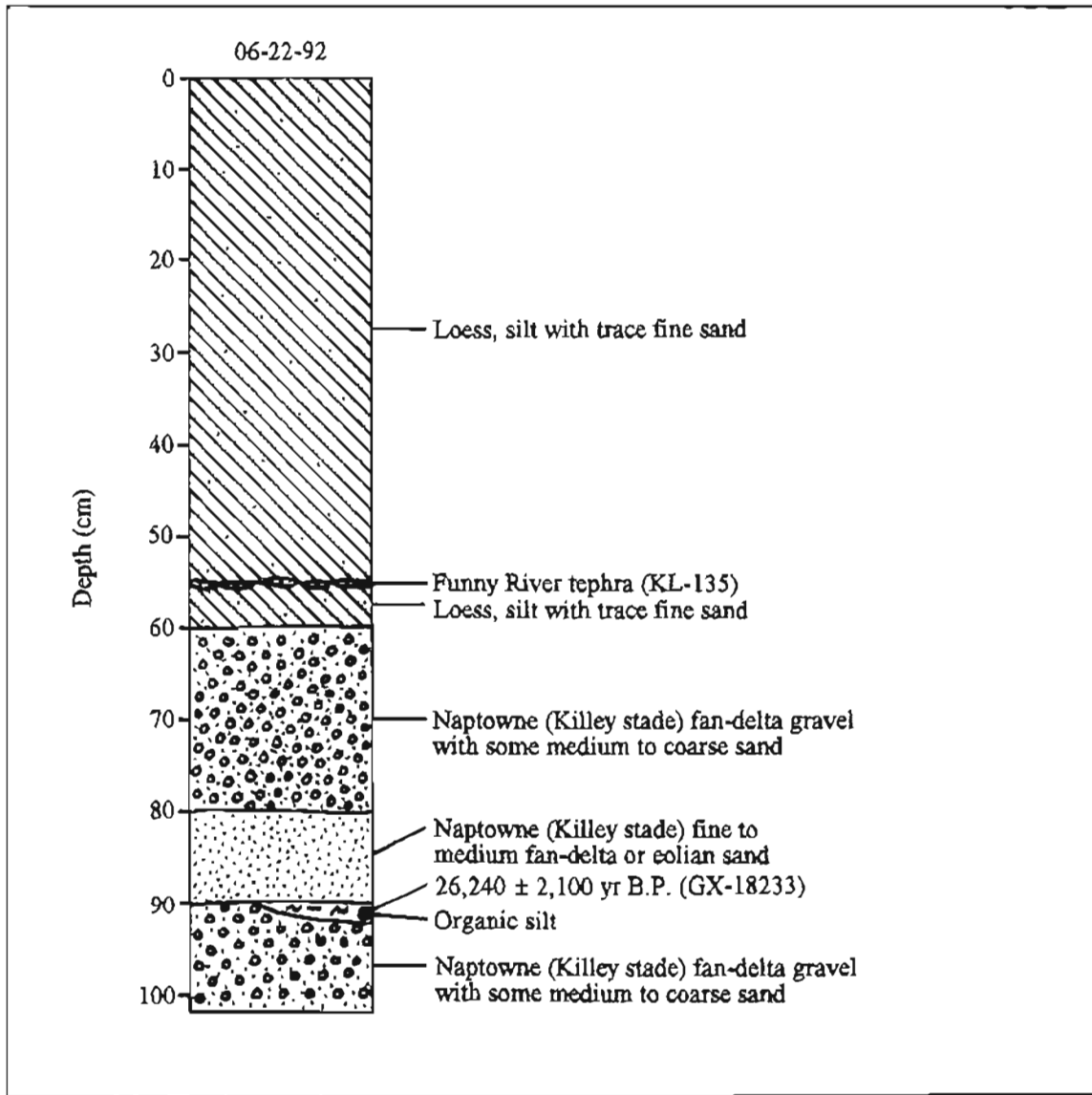


Figure A64. Stratigraphy exposed in section 59 (60°18'08"N, 151°15'37"W), Kenai B-4 SE Quadrangle (KEN-126, sheet 2). Chronologic significance of radiocarbon date given in table 2. Tephra geochemistry given in table 3.

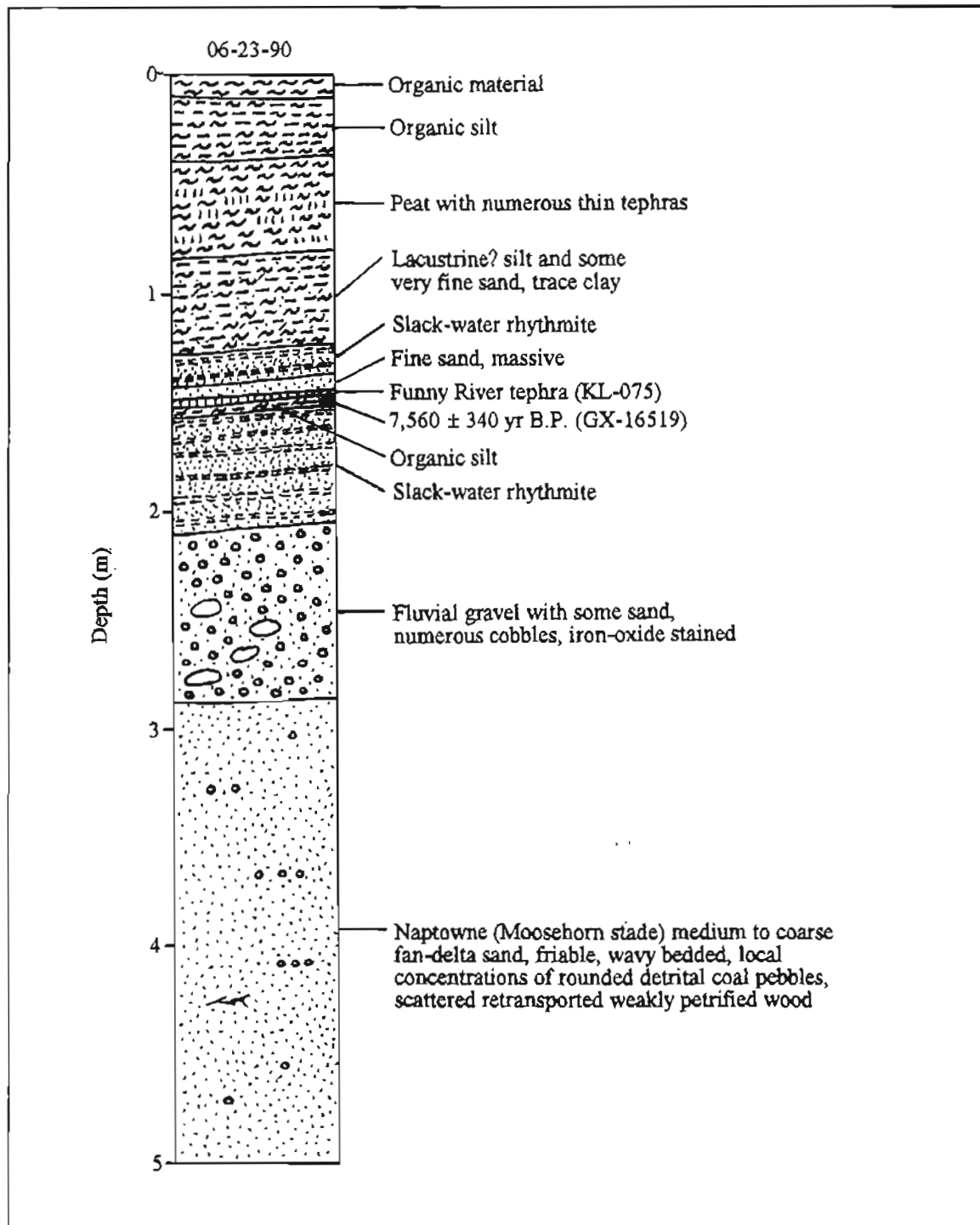


Figure A65. Stratigraphy exposed in section 60 (60°17'57"N, 151°22'21"W), Kenai B-4 SW Quadrangle (KEN-128, sheet 2). Chronologic significance of radiocarbon date given in table 2. Tephra geochemistry given in table 3.

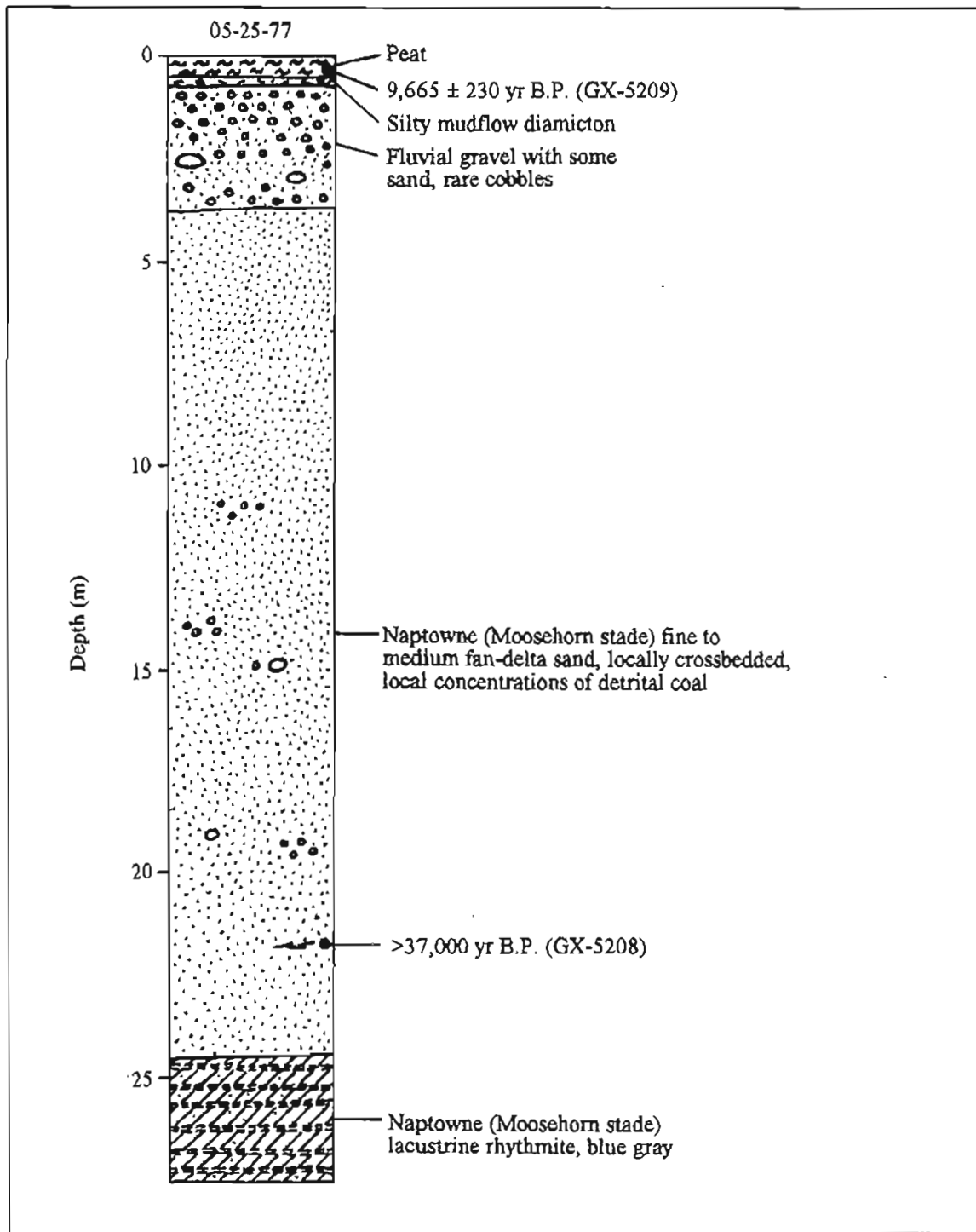


Figure A66. Stratigraphy exposed in section 61 (60°17'56"N, 151°22'53"W), Kenai B-4 SW Quadrangle (KEN-129, sheet 2). Chronologic significance of radiocarbon dates given in table 2.

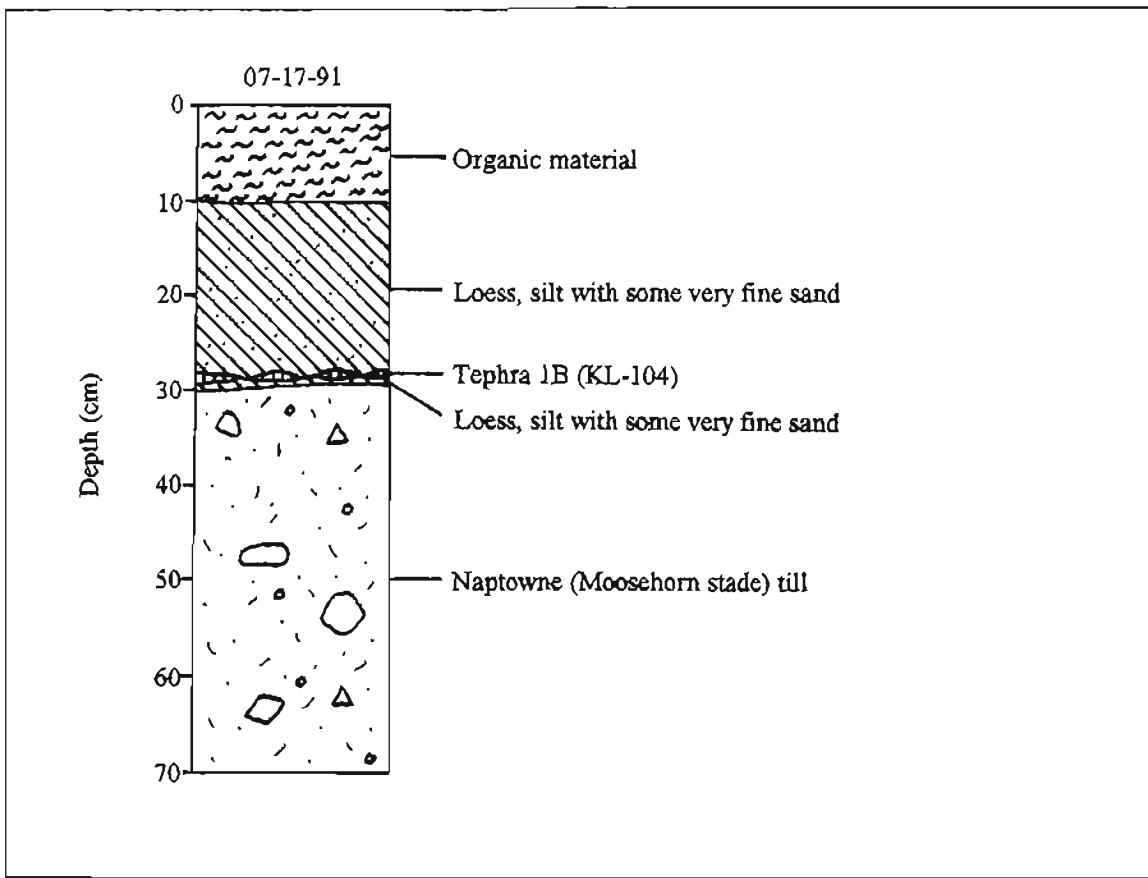


Figure A67. Stratigraphy exposed in section 62 (60°17'15"N, 151°16'45"W), Kenai B-4 SE Quadrangle (KEN-130, sheet 2). Tephra geochemistry given in table 3.

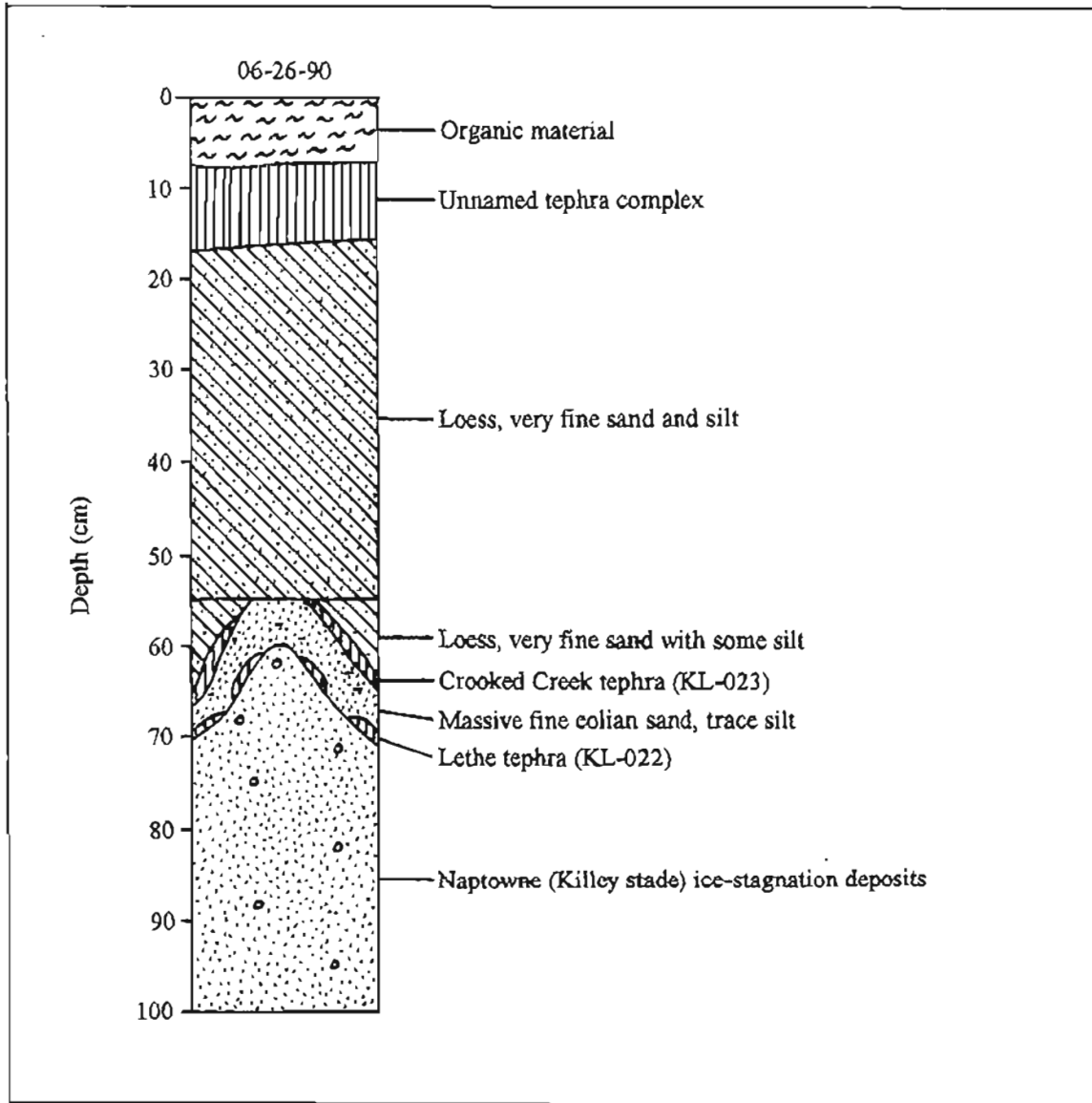


Figure A68. Stratigraphy exposed in section 63 ( $60^{\circ}17'02''N$ ,  $151^{\circ}14'33''W$ ), Kenai B-4 SE Quadrangle (KEN-132, sheet 2). Tephra geochemistry given in table 3, except for unnamed tephra complex. Section indicates Killey age for outer end moraine of Tiustumena Lake lobe along Kasilof River.

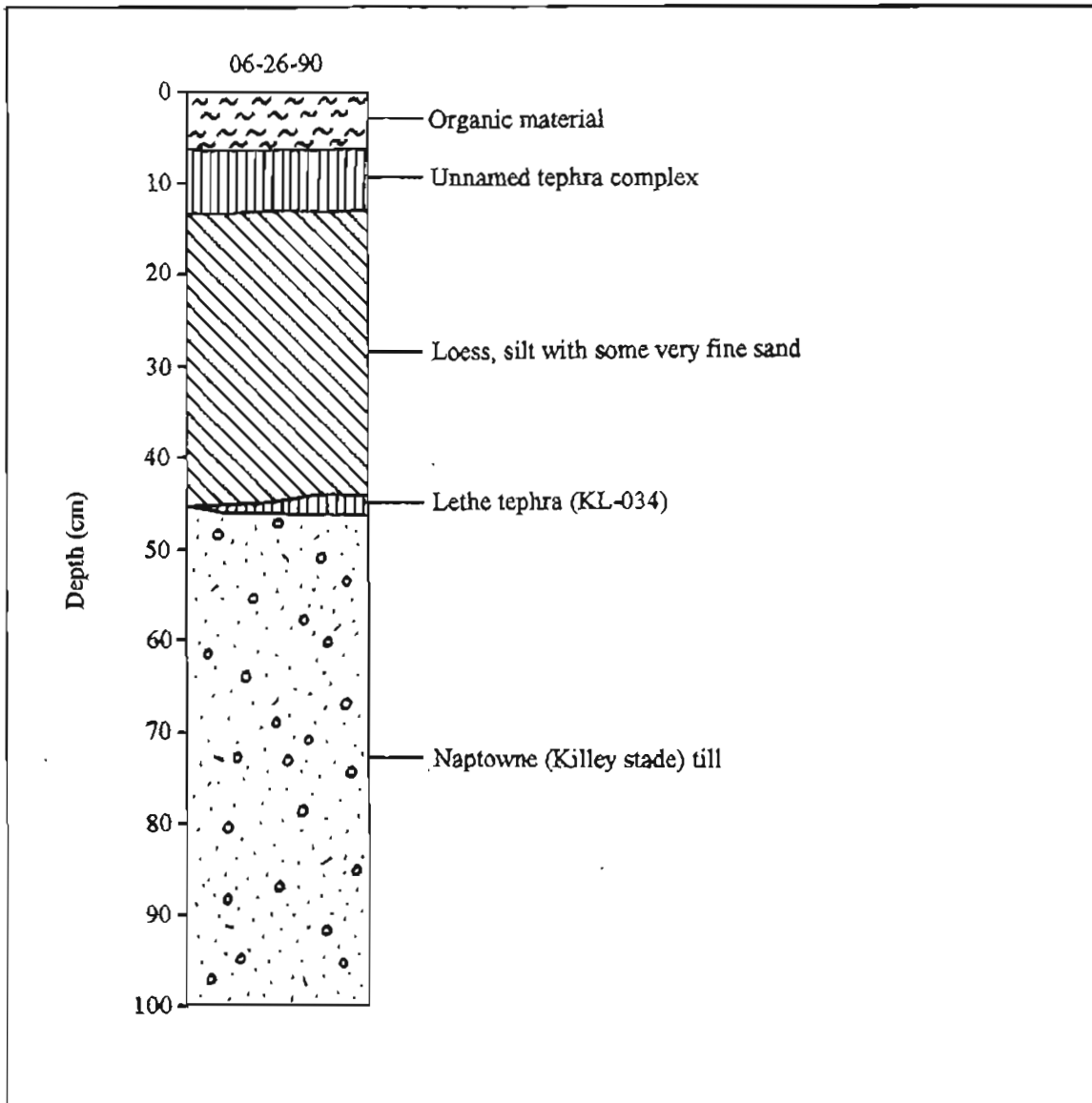


Figure A69. Stratigraphy exposed in section 64 (60°15'16"N, 151°13'06"W), Kenai B-4 SE Quadrangle (KEN-139, sheet 2). Tephra geochemistry given in table 3, except for unnamed tephra complex. Section indicates Killey age for second outer end moraine of Tustumena Lake lobe along Kaslof River.

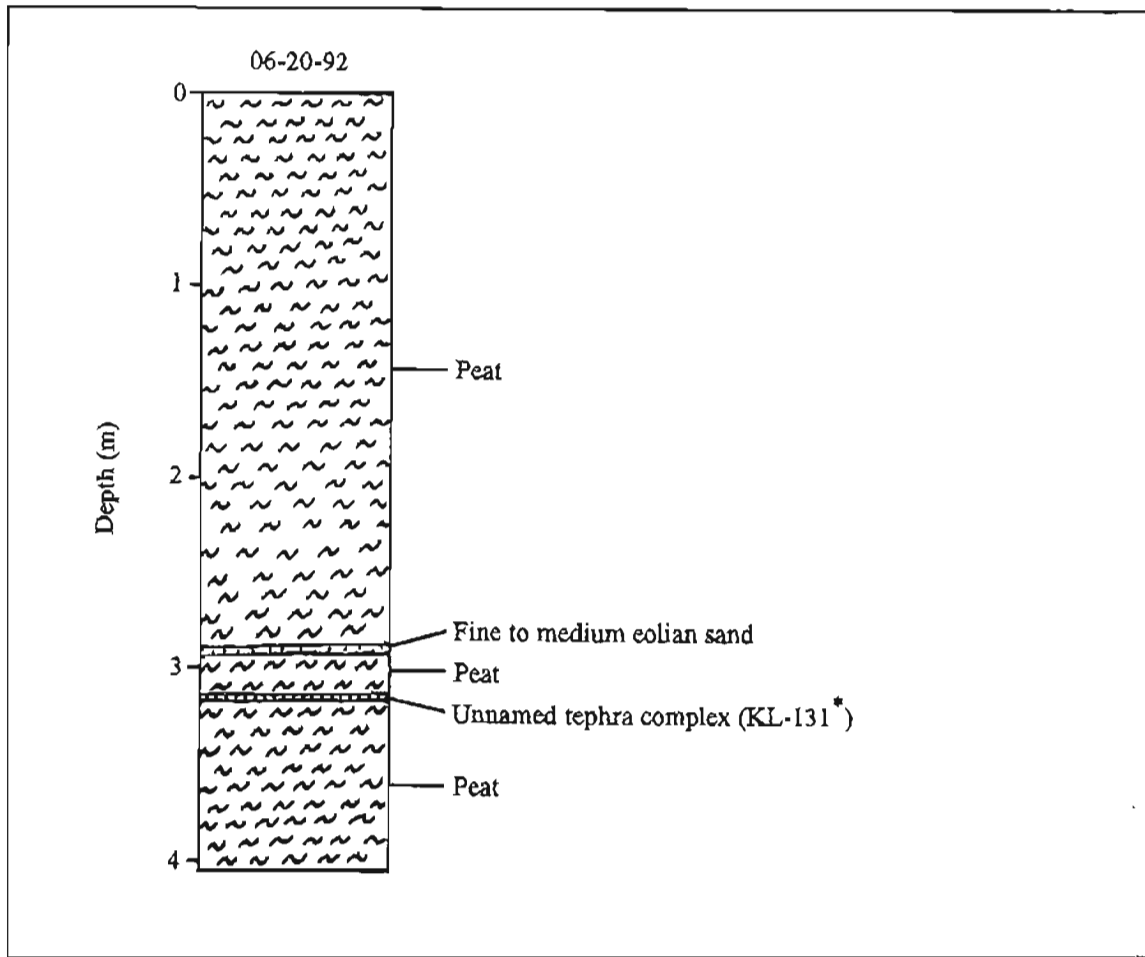


Figure A70. Stratigraphy exposed in section 65 (60°10'03"N, 151°26'46"W), Kenai A-4 NW Quadrangle (KEN-140, sheet 2).

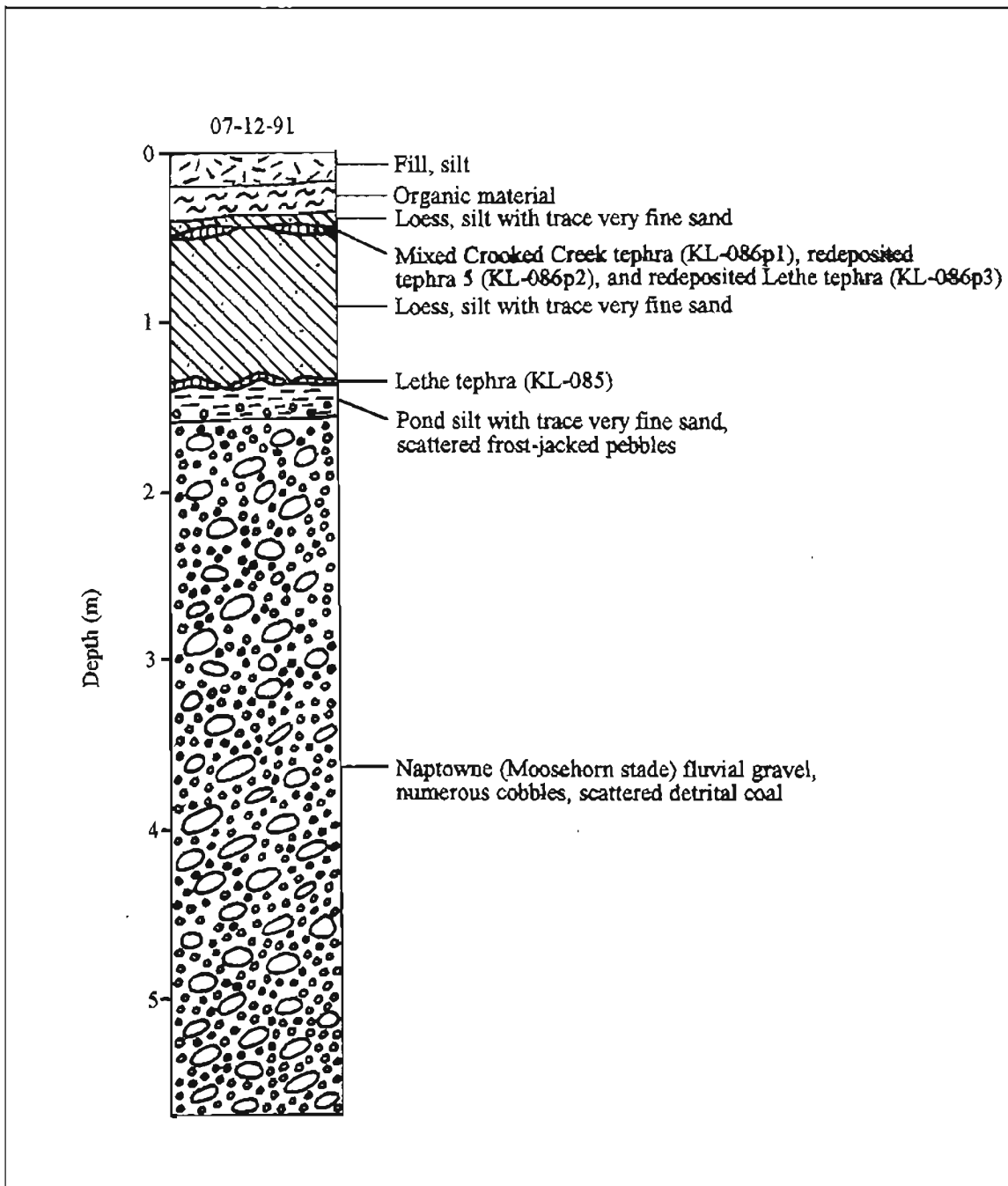


Figure A71. Stratigraphy exposed in section 66 (60°08'21"N, 151°31'18"W), Kenai A-5 SE Quadrangle (KEN-141, sheet 2). Tephra geochemistry given in table 3.

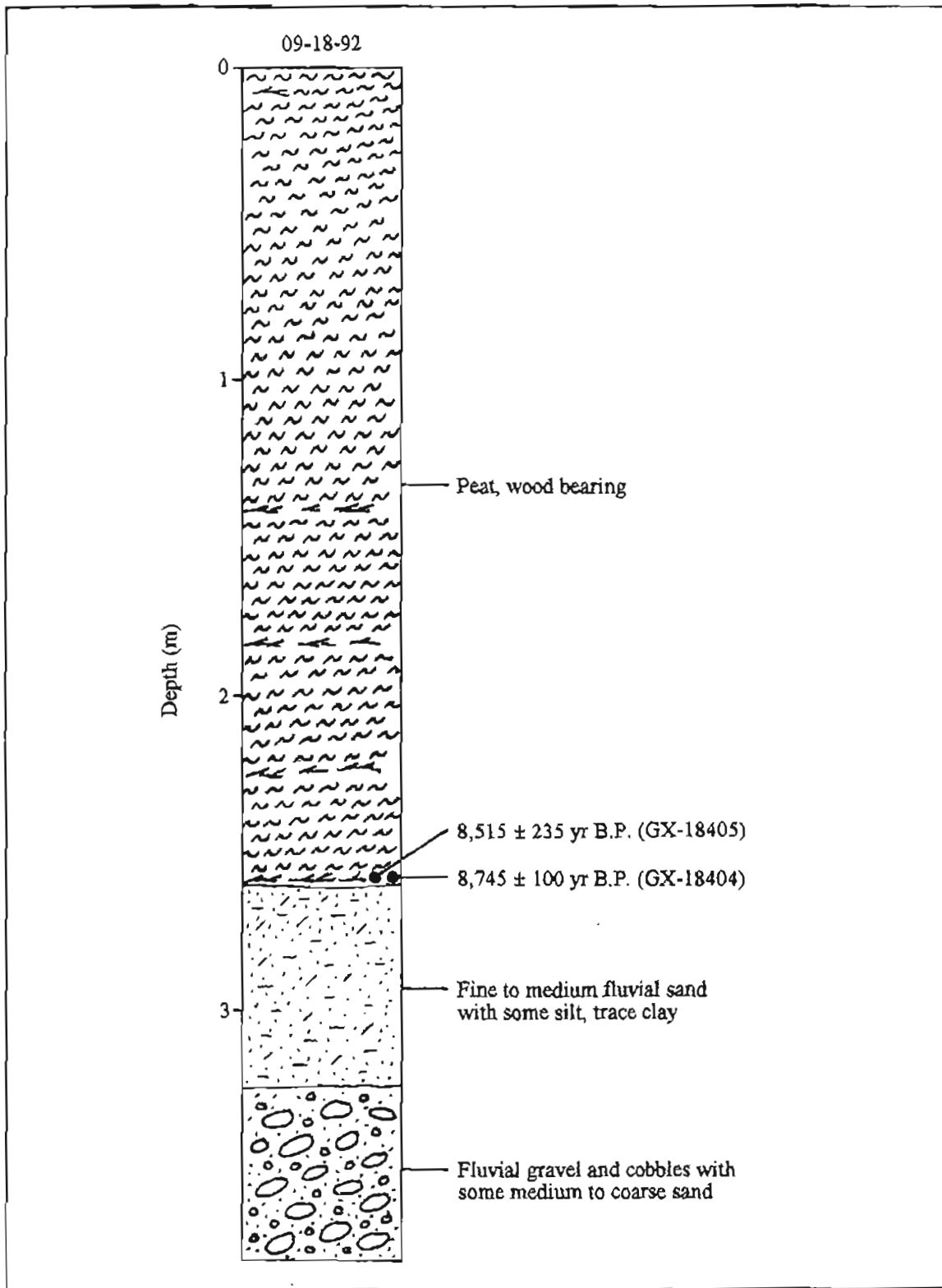


Figure A72. Stratigraphy exposed in section 67 (59°47'42"N, 151°47'31"N), Seldovia D-5 SW Quadrangle (SEL-2, sheet 3). Chronologic significance of radiocarbon dates given in table 2.

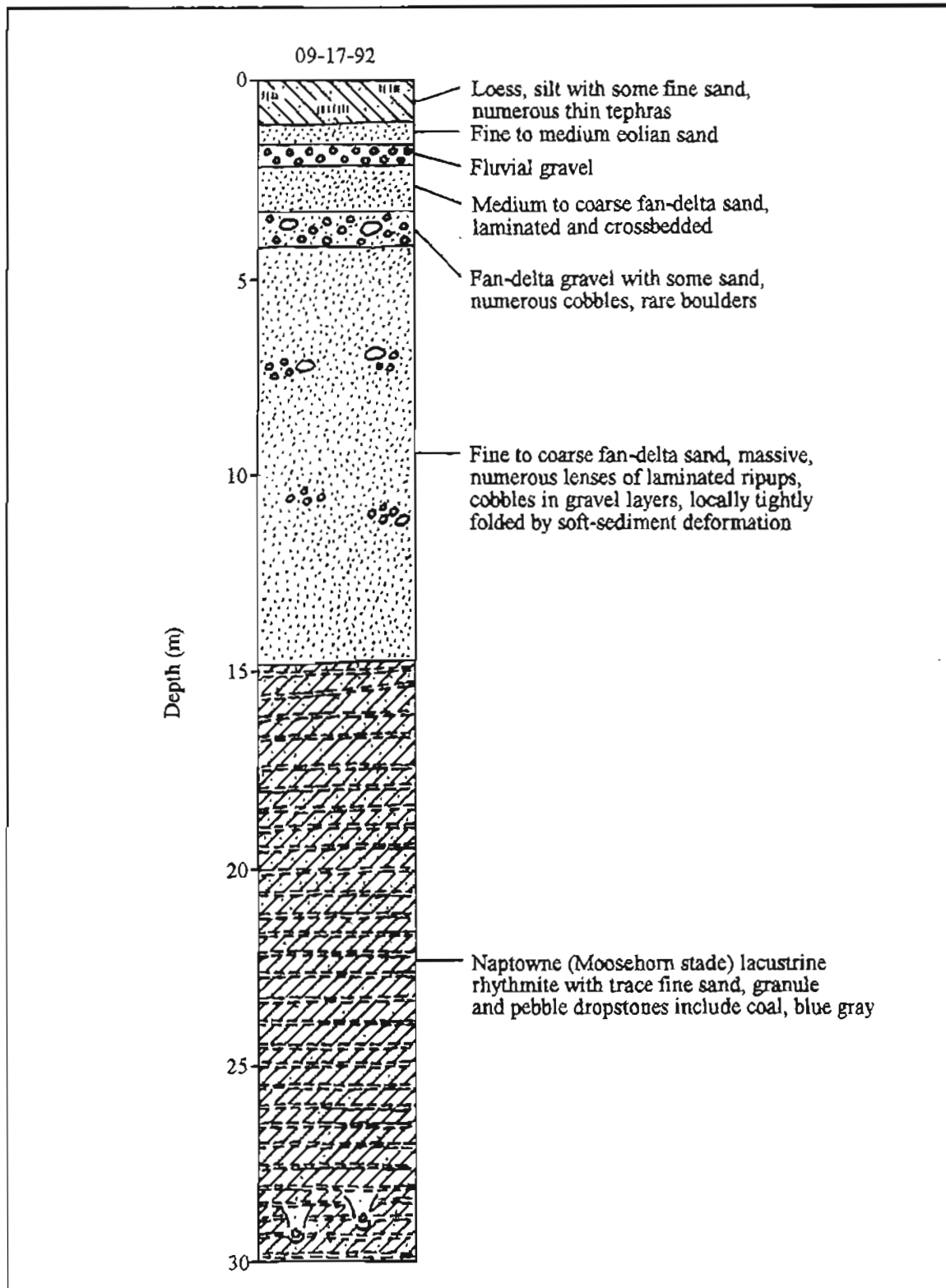


Figure A73. Stratigraphy exposed in section 68 (59°47'15"N, 151°51'20"W), Seldovia D-5 SW Quadrangle (SEL-3, sheet 3) (Reger and Petrik, 1993).

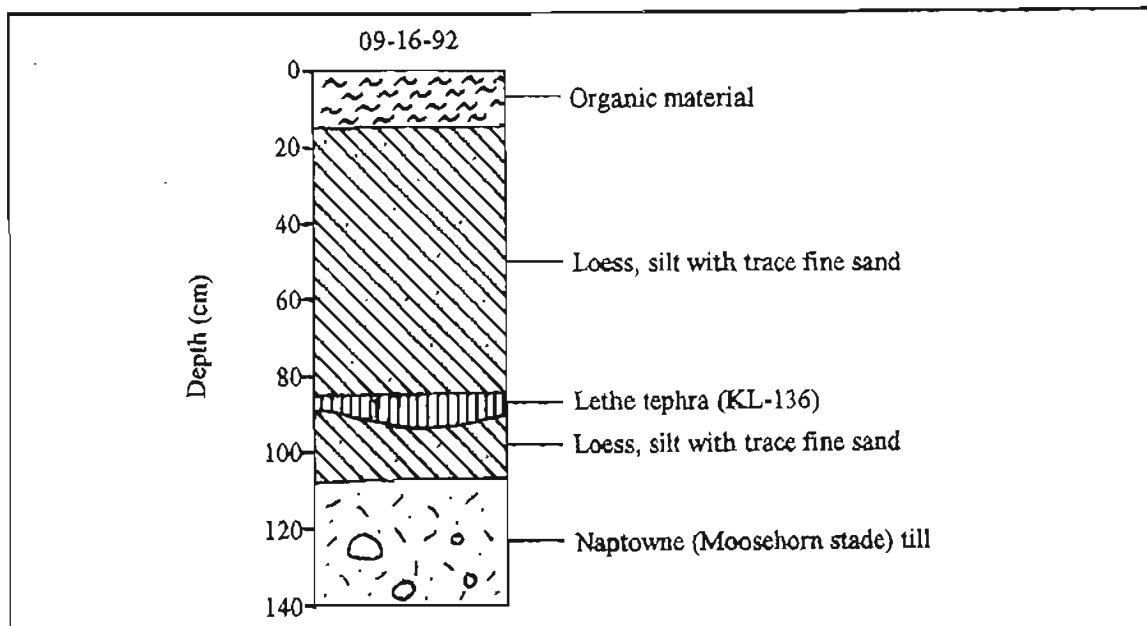


Figure A74. Stratigraphy exposed in section 69 (59°46'12"N, 151°51'22"W), Seldovia C-5 NW Quadrangle (SEL-4, sheet 3). Tephra geochemistry given in table 3.

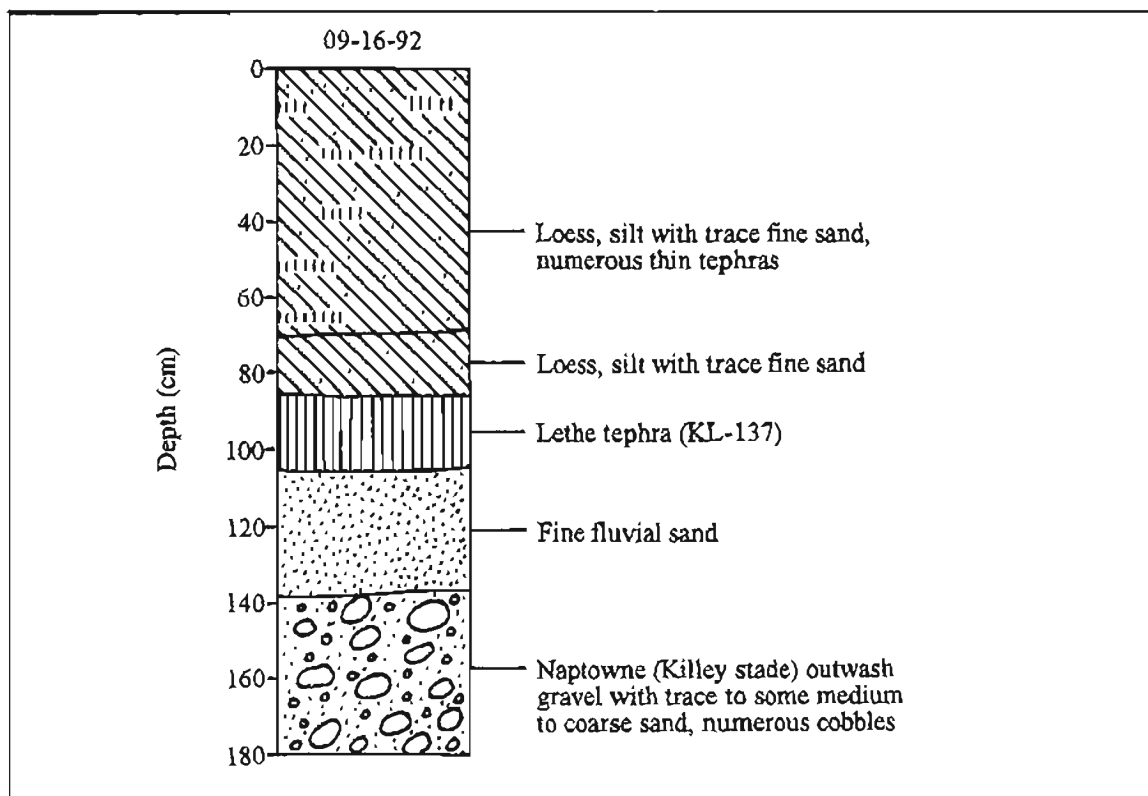


Figure A75. Stratigraphy exposed in section 70 (59°43'50"N, 151°50'05"W), Seldovia D-5 SW Quadrangle (SEL-5, sheet 3). Tephra geochemistry given in table 3, except for unnamed tephras. Section indicates deep lower valley of Anchor River incised before Killey stade.

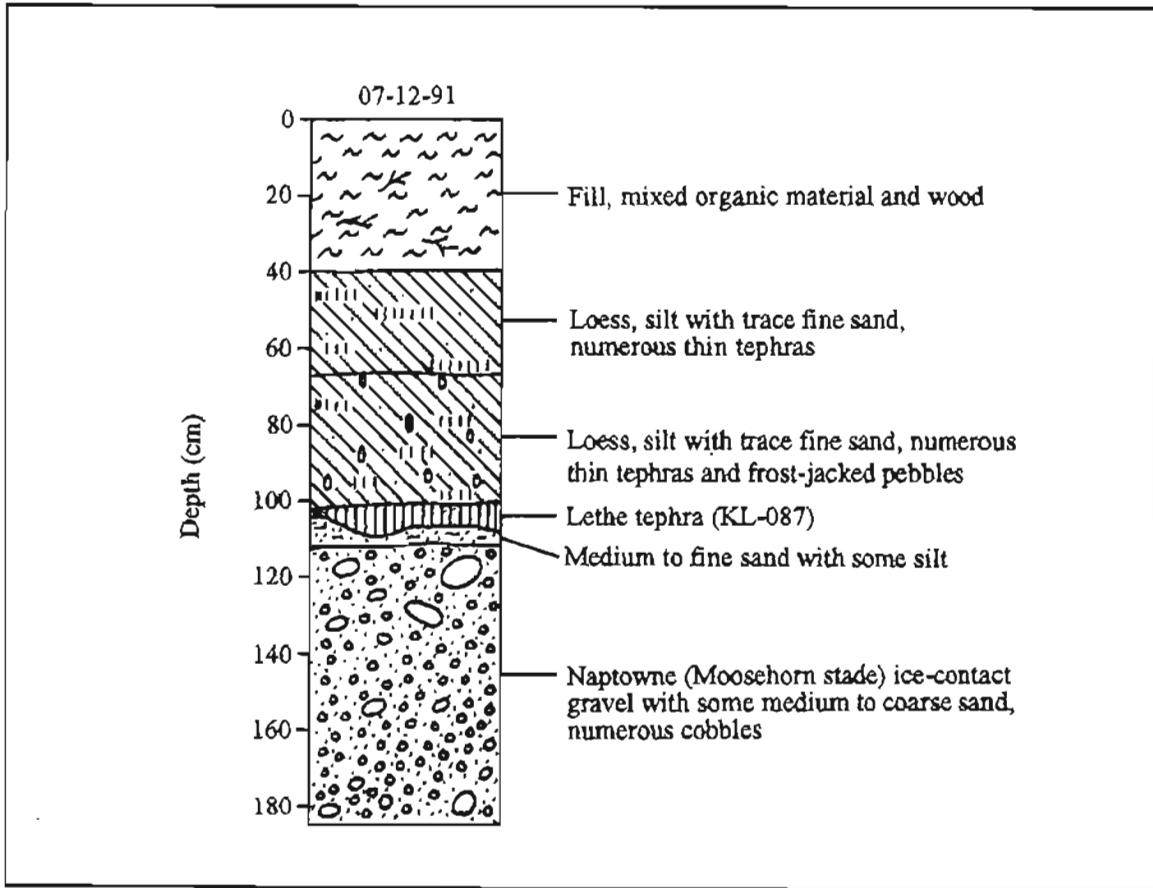


Figure A76. Stratigraphy exposed in section 71 (59°43'49"N, 151°46'06"W), Seldovia C-5 NW Quadrangle (SEL-6, sheet 3). Tephra geochemistry given in table 3, except for unnamed tephras.

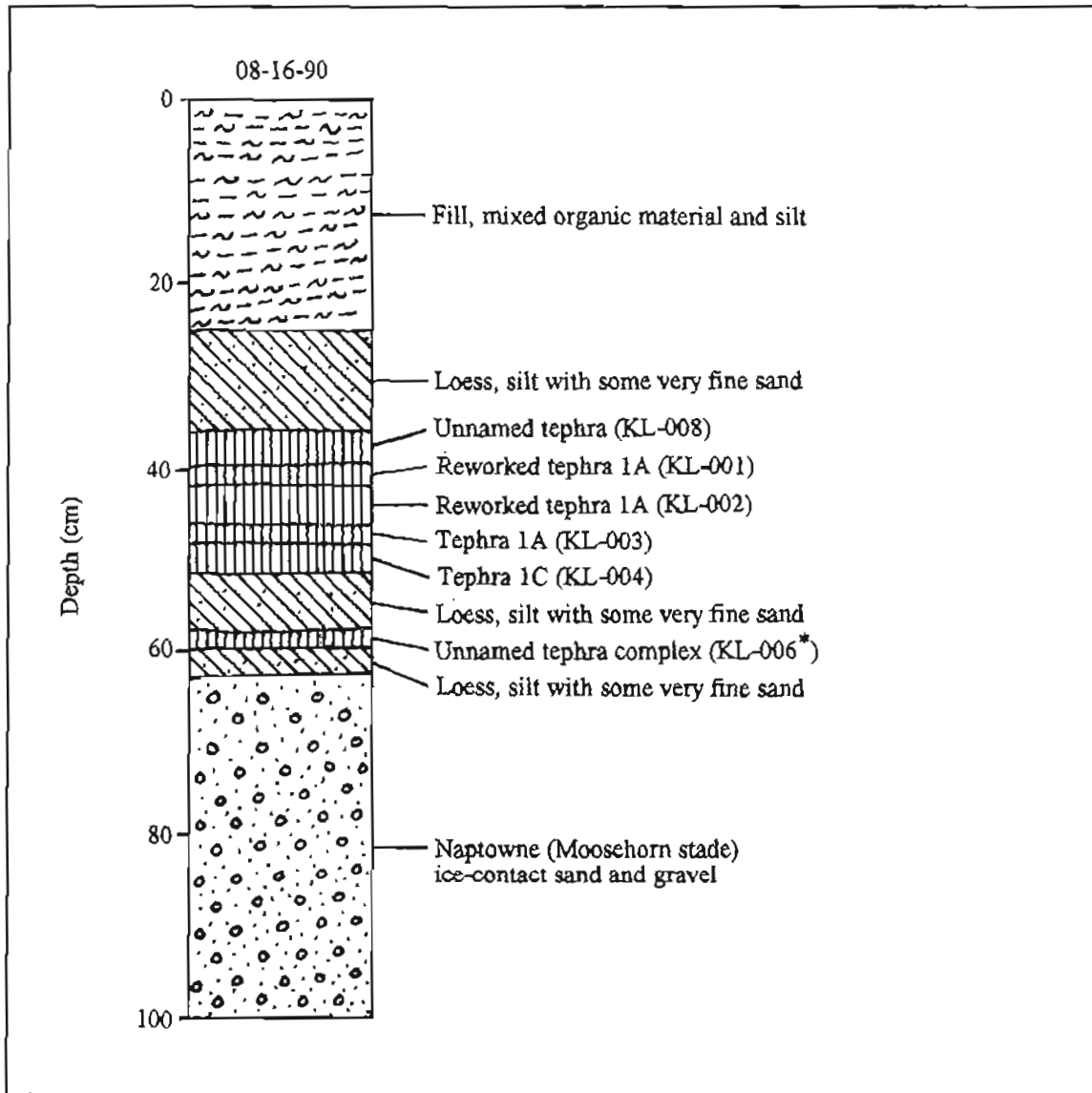


Figure A77. Stratigraphy exposed in section 72 ( $59^{\circ}43'33''N$ ,  $151^{\circ}44'02''W$ ), Seldovia C-5 NW Quadrangle (SEL-7, sheet 3). Tephra geochemistry given in table 3.

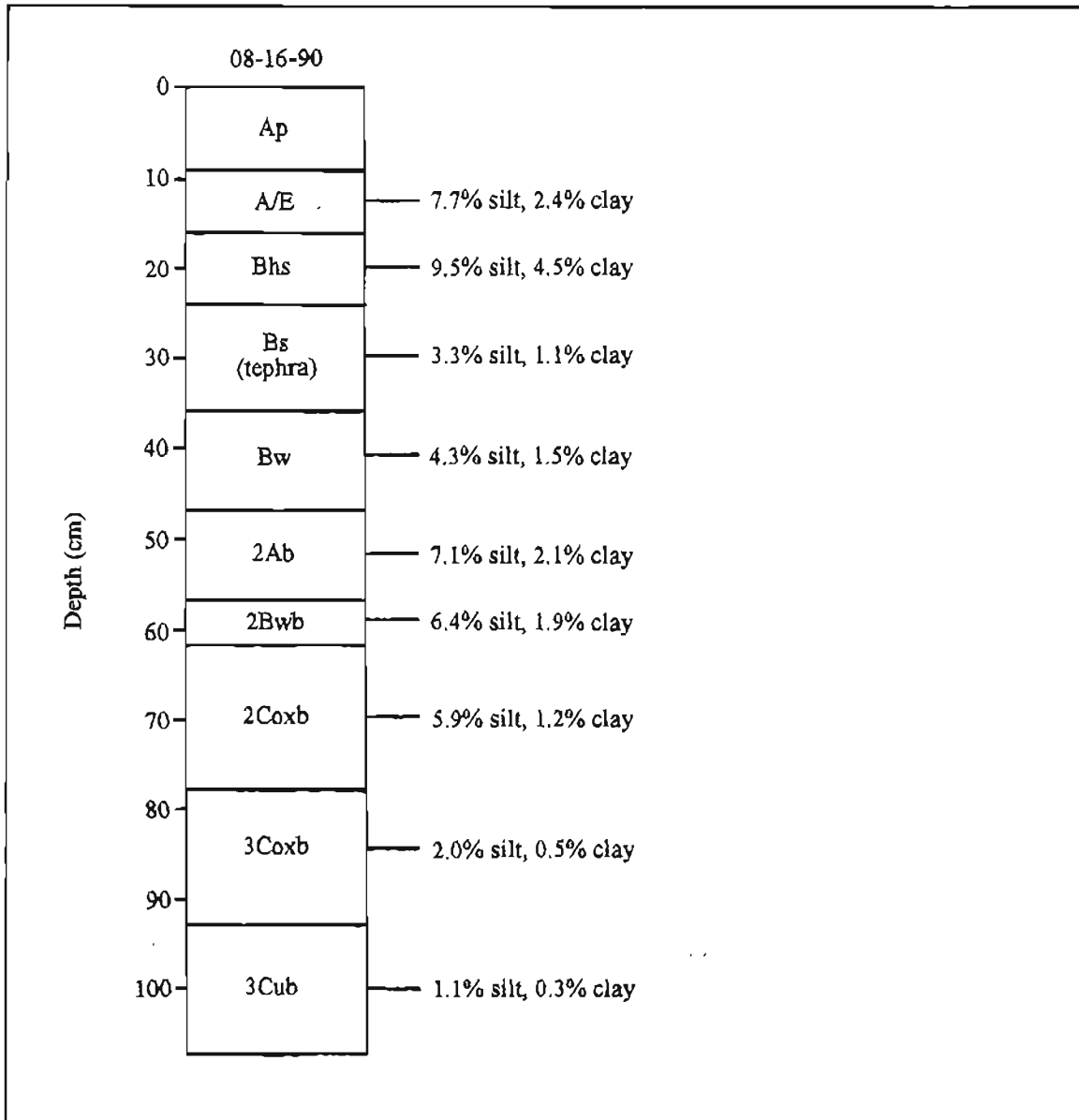


Figure A78. Distribution of silt and clay (calculated as percent of <2-mm fraction) with depth in soil profile S4 on flat crest of Moosehorn-age moraine of Kachemak Bay lobe (59°43'33"N, 151°44'02"W), Seldovia C-5 NW Quadrangle (SEL-7, sheet 3). Elevation 123 m. Horizons according to Soil Survey Staff (1975), modified by Birkeland and others (1991b) and this study. Horizon O not shown above horizon A. Detailed profile description summarized in table A6.

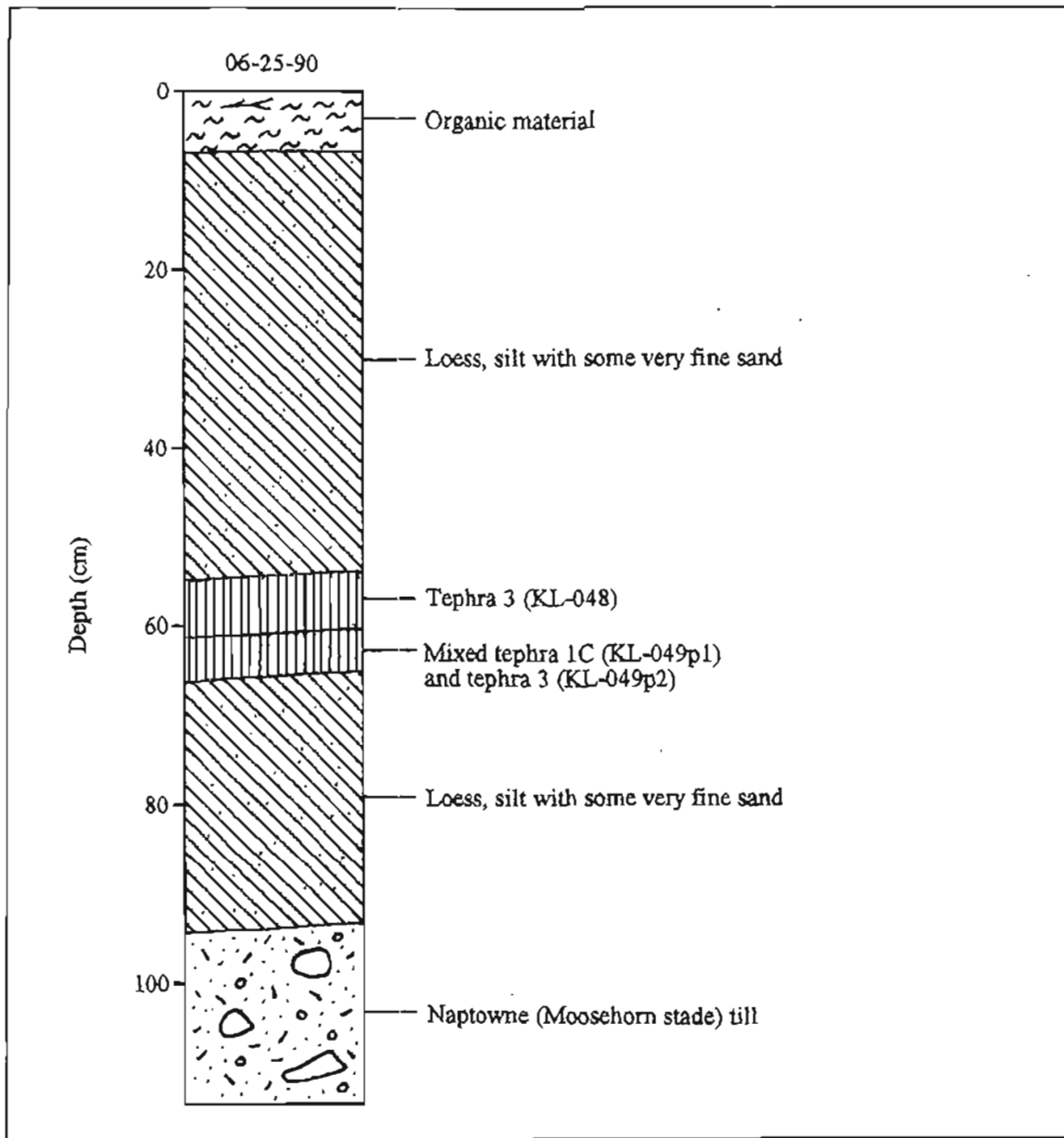


Figure A79. Stratigraphy exposed in section 73 (59°39'49"N, 151°32'13"W), Seldovia C-5 NE Quadrangle (SEL-13, sheet 3). Tephra geochemistry given in table 3.

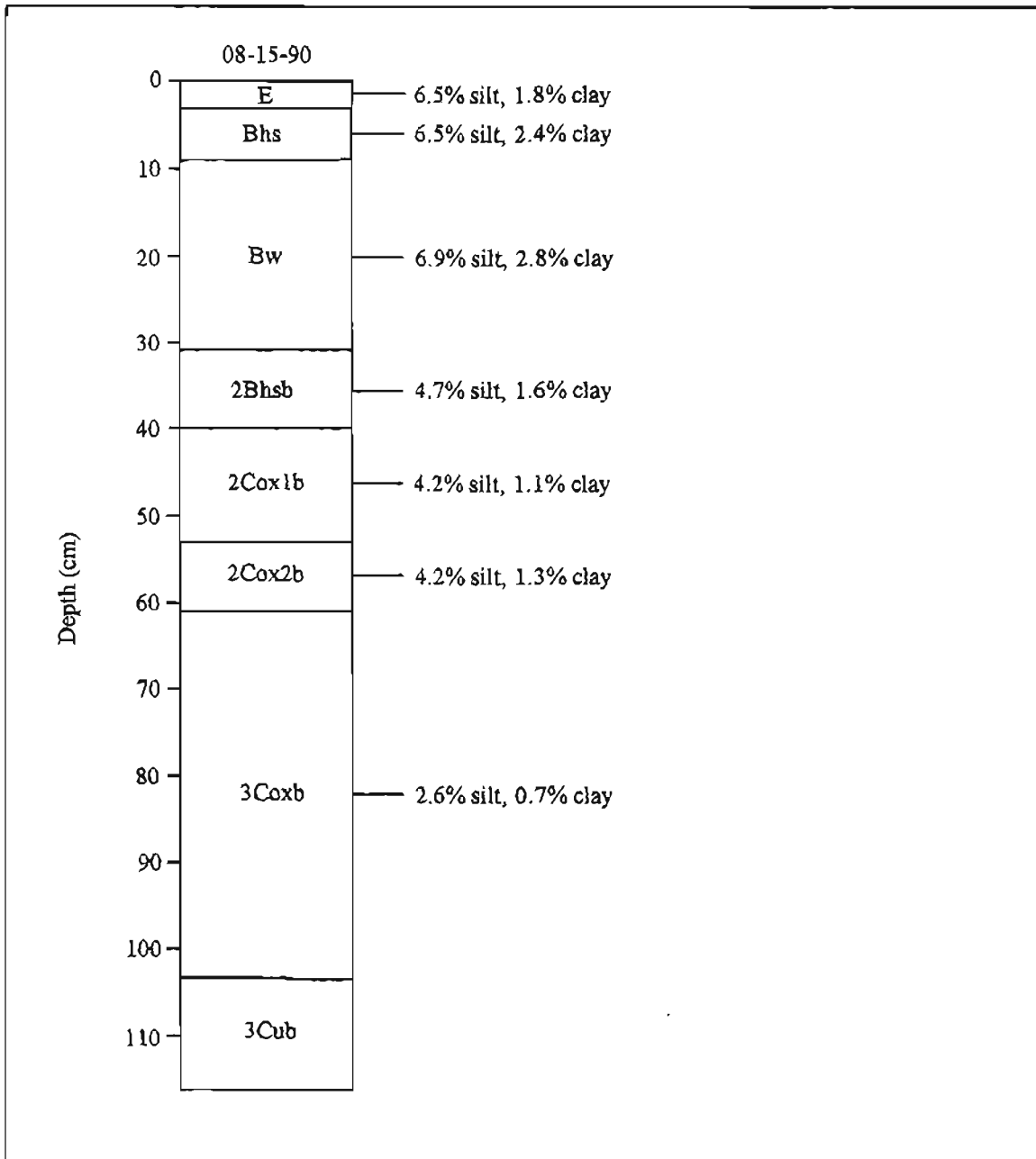


Figure A80. Distribution of silt and clay (calculated as percent of <2-mm fraction) with depth in soil profile S5 on flat crest of Moosehorn-age moraine of Kachemak Bay lobe (59°39'49"N, 151°32'13"W), Seldovia C-5 NE Quadrangle (SEL-13, sheet 3). Elevation 342 m. Horizons according to Soil Survey Staff (1975), modified by Birkeland and others (1991b) and this study. Horizons O and A not shown above horizon E. Detailed profile description summarized in table A7.

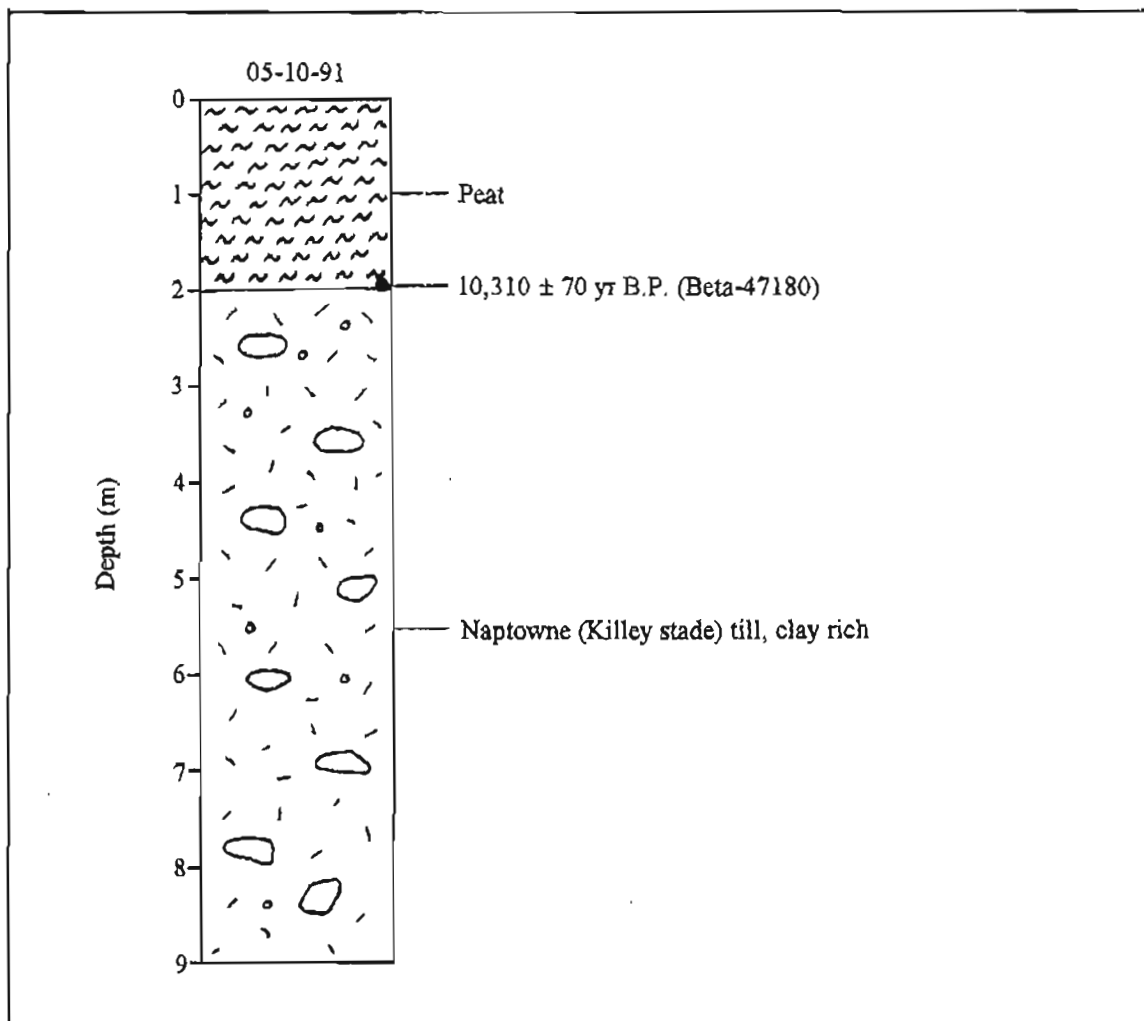


Figure A81. Stratigraphy exposed in section 74 (59°38'06"N, 151°30'41"W), Seldovia C-5 NE Quadrangle (SEL-14, sheet 3). Chronologic significance of radiocarbon date given in table 2.

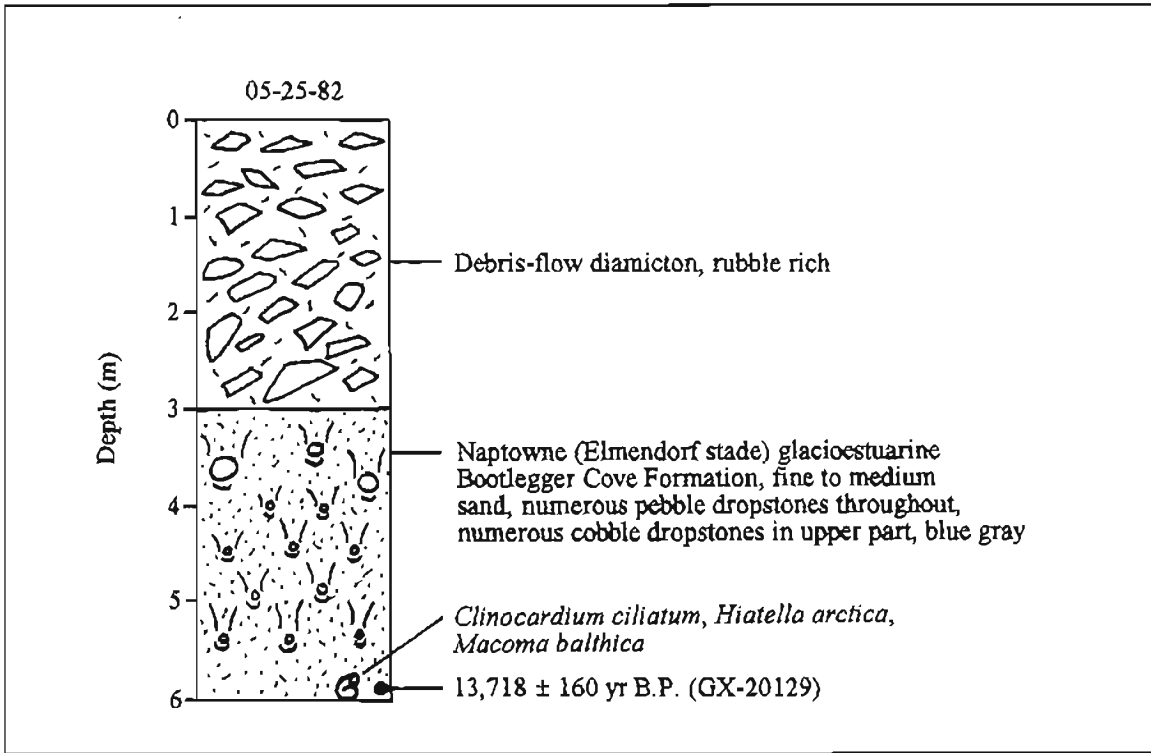
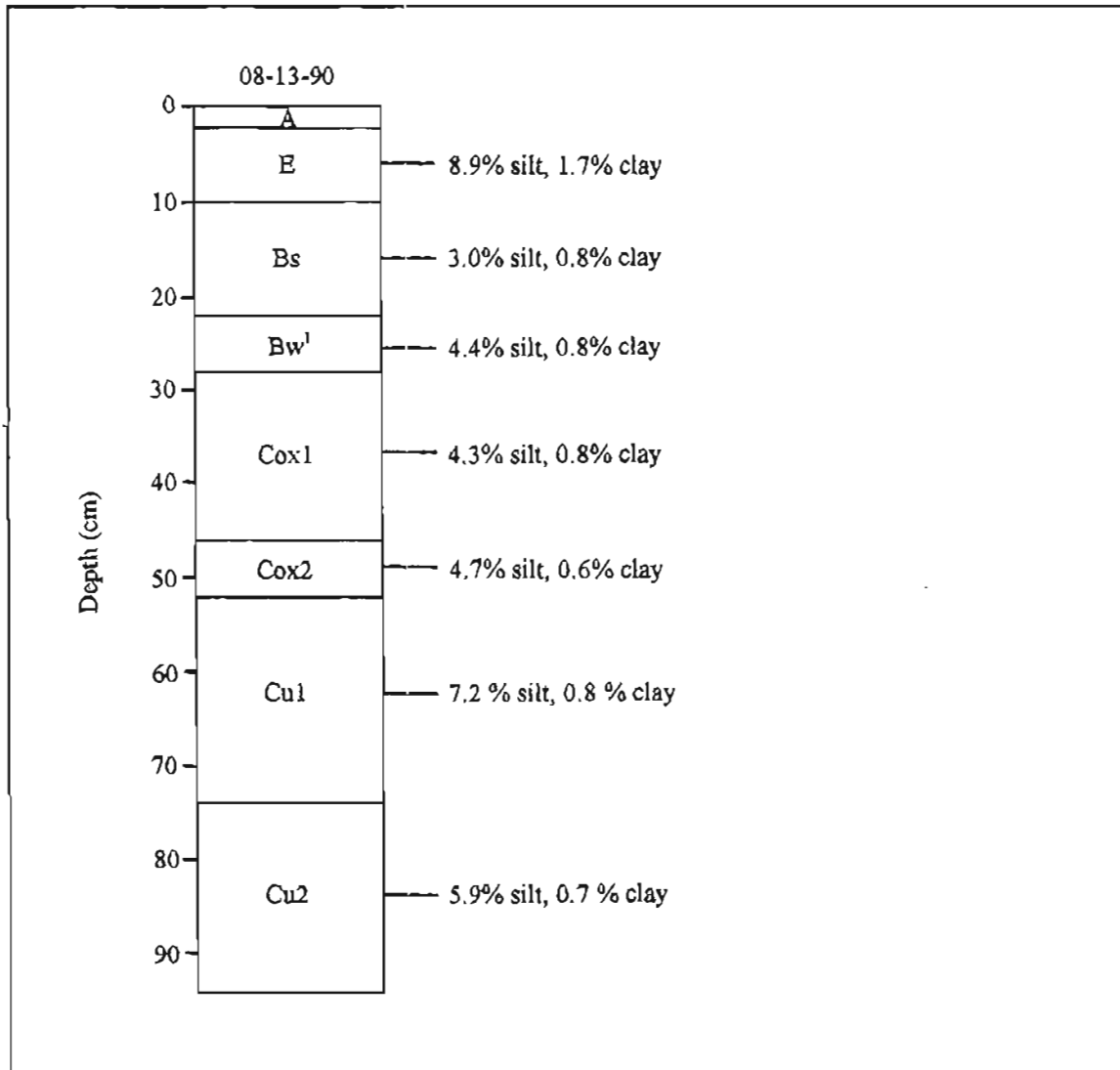


Figure A82. Stratigraphy exposed in section 75 (60°57'14"N, 149°42'16"W), Seward D-8 Quadrangle (SEW-4, sheet 4). Chronologic significance of radiocarbon date given in table 2.



<sup>1</sup> Appears to be mixed Bs and Cox1, perhaps as a transition or by seasonal-frost stirring.

Figure A83. Distribution of silt and clay (calculated as percent of <2-mm fraction) with depth in soil profile S6 on flat crest of Elmendorf-age Bird Creek moraine in Turnagain Arm (60°58'07"N, 149°26'39"W), Seward D-7 NW Quadrangle (SEW-2, sheet 4). Elevation 25 m. Horizons according to Soil Survey Staff (1975), modified by Birkeland and others (1991b) and this study. Horizon O not shown above horizon A. Detailed profile description summarized in table A8.

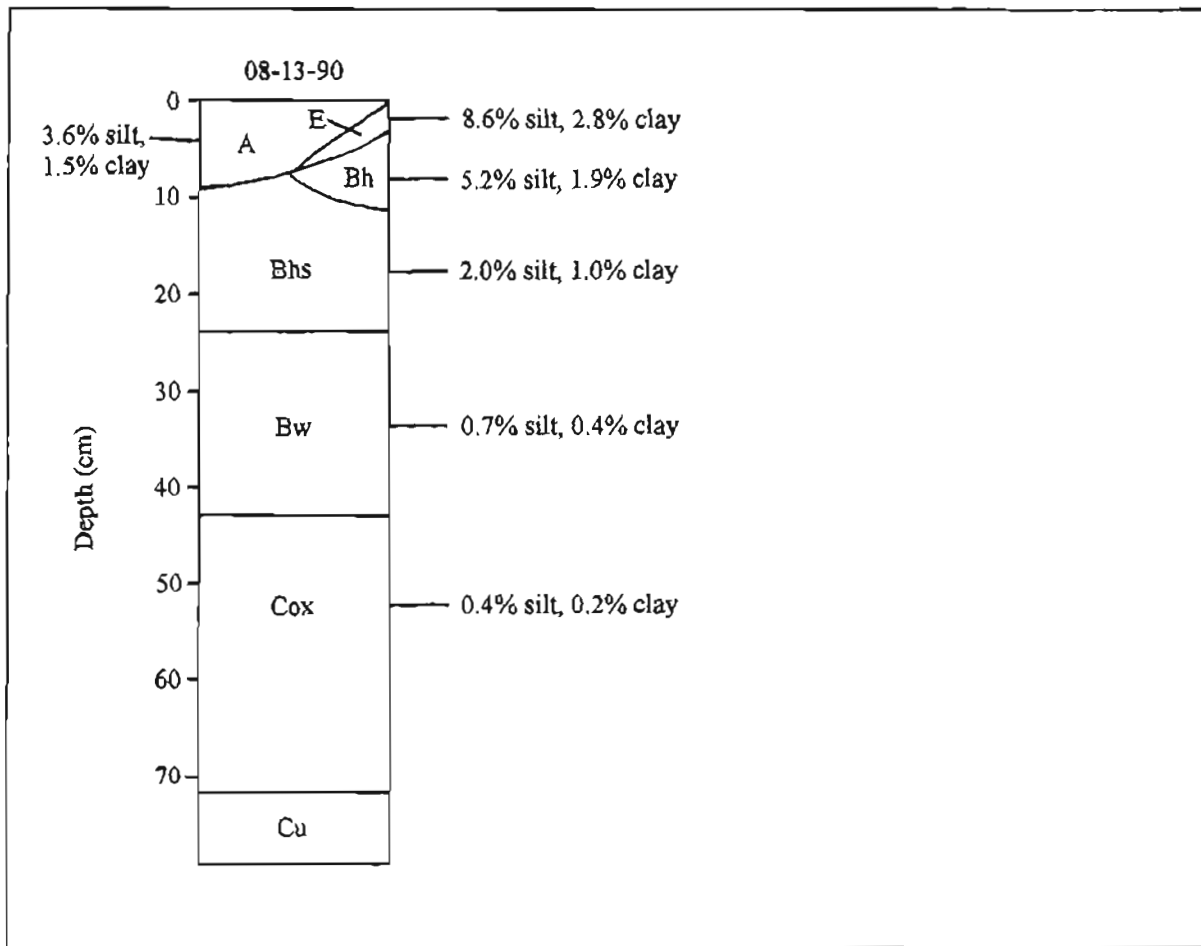


Figure A84. Distribution of silt and clay (calculated as percent of <2-mm fraction) with depth in soil profile S7 on crest of 9,900-yr-old latest-Naptowne moraine in Turnagain Pass (60°47'39"N, 149°13'12"W), southwestern quarter of Seward D-6 Quadrangle (SEW-12, sheet 4). Elevation 297 m. Horizons according to Soil Survey Staff (1975), modified by Birkeland and others (1991b) and this study. Horizon O not shown above horizon A. Detailed profile description summarized in table A9.

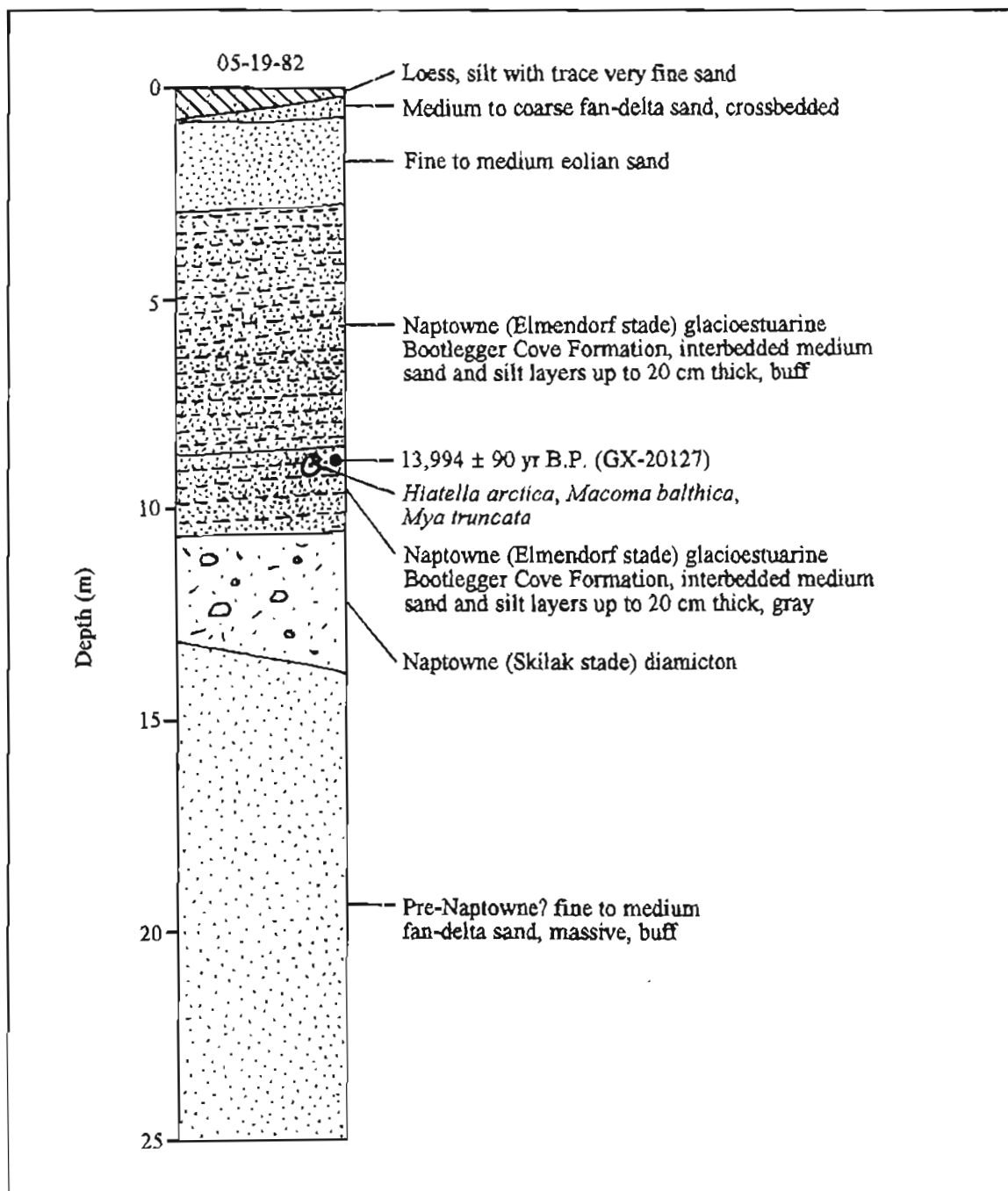


Figure A85. Stratigraphy exposed in section 76 (61°14'49"N, 150°01'43"W), Tyonek A-1 NE Quadrangle (TYO-8, sheet 5). Chronologic significance of radiocarbon date given in table 2.

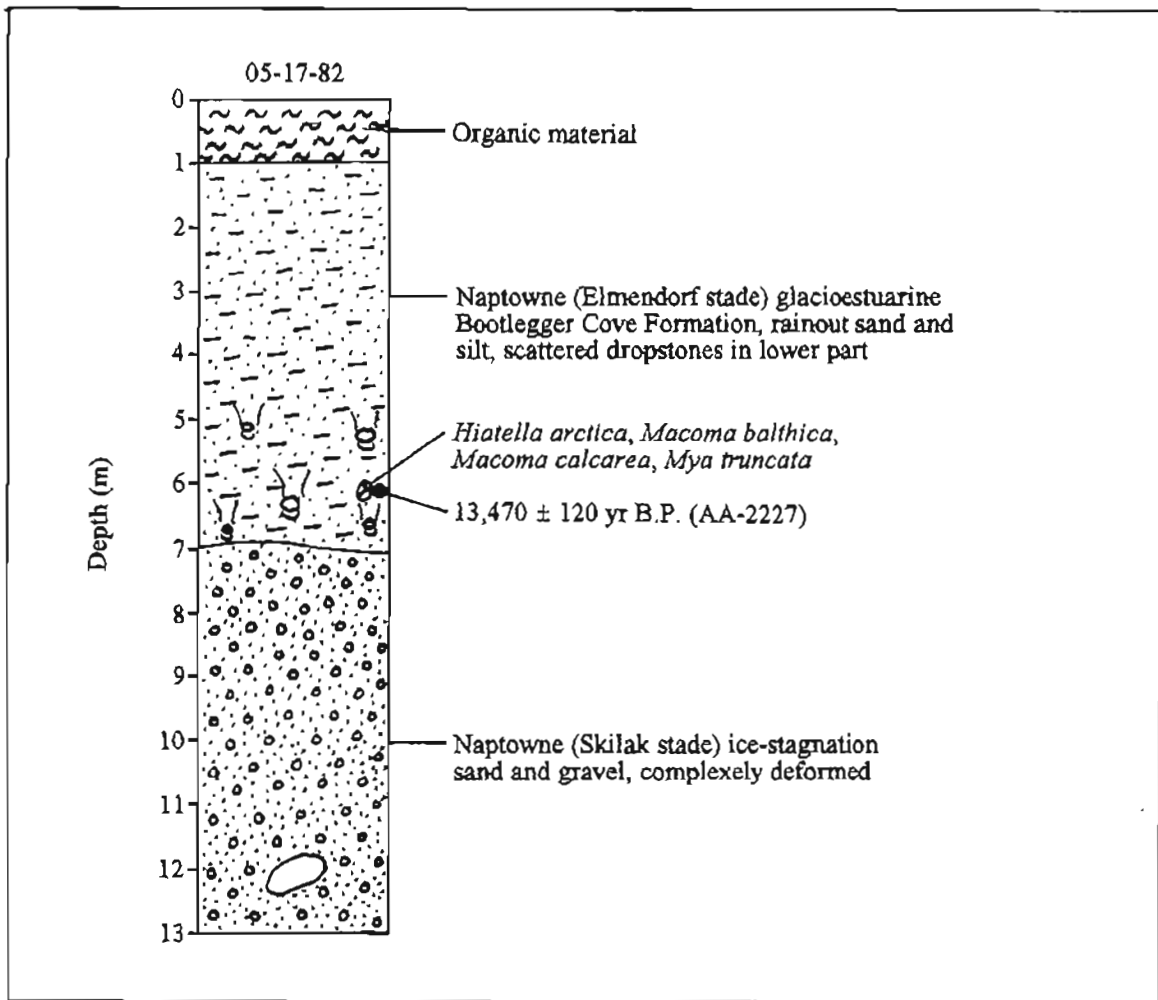


Figure A86. Stratigraphy exposed in section 77 (61°14'36"N, 150°00'25"W), Tyonek A-1 NE Quadrangle (TYO-9, sheet 5). Chronologic significance of radiocarbon date given in table 2.

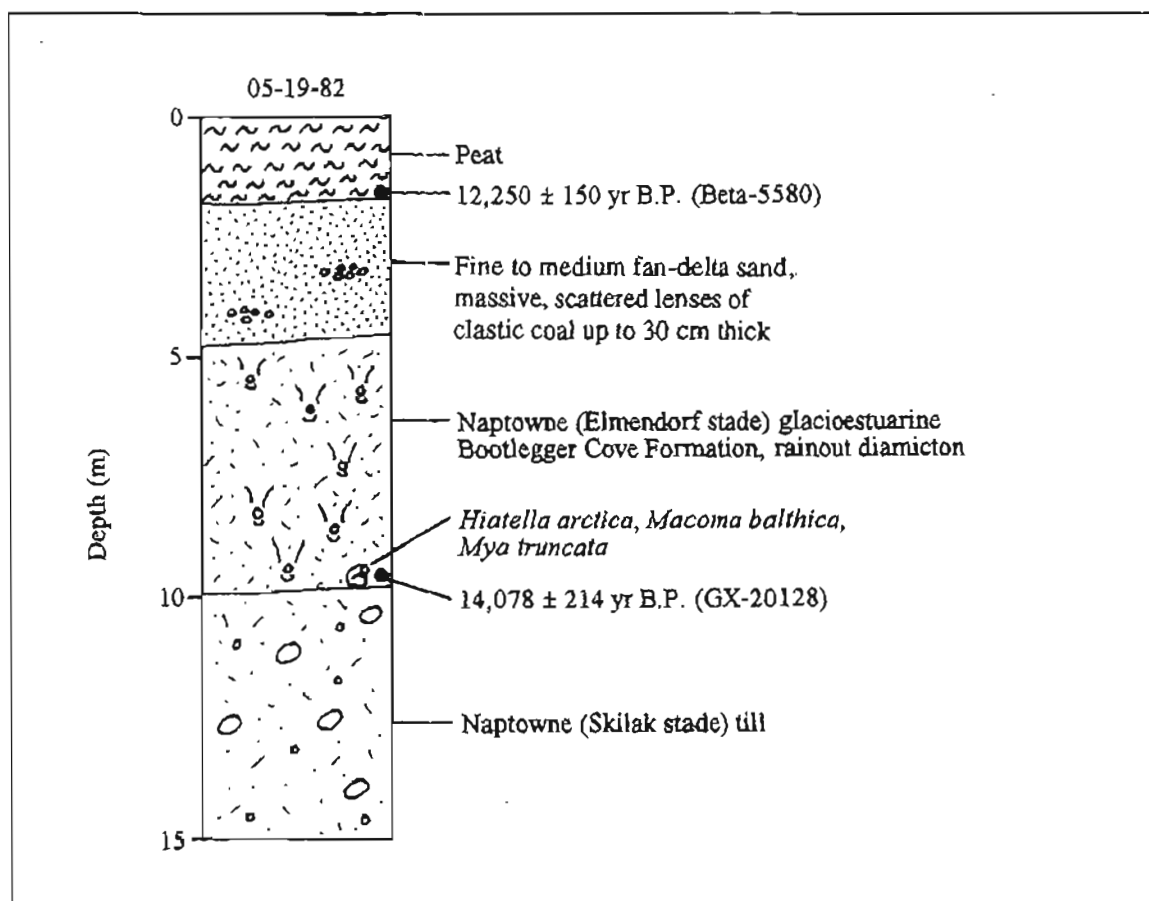


Figure A87. Stratigraphy exposed in section 78 (61°14'32"N, 150°00'07"W), Tyonek A-1 NE Quadrangle (TYO-10, sheet 5). Chronologic significance of radiocarbon date given in table 2.

## **APPENDIX B**

Multivariate analysis of magnetic susceptibility and pebble compositions of till samples from the Cook Inlet region.

## Rationale

The last major glaciation in the Cook Inlet trough was complicated by glacial advances from several upland sources. Our model of the Naptowne glaciation evolved primarily from the study of landform distribution and interrelations and from stratigraphic evidence. To test its validity, we collected 107 till samples and 92 collections of till pebbles to provide the basic data for an evaluation that is independent of the evidence on which our model is built. We reasoned that the magnetic susceptibility of the fine fractions of the till samples (table 15) and the compositions of the till stones (table 16) reflect rock types in the source areas of the glaciers that deposited the tills. Many of these samples came from tills that have known sources because they are located at the mouths of glaciated valleys or in moraines with distributions that clearly indicate they came from a given source. However, many of the samples came from the central lowlands, where topography is complex and till source is questionable, and we hoped that this experiment would ultimately provide us with new information to fine tune our proposed glaciation model.

Realizing that our data set is probably not large enough to be conclusive for an area so large and complex, we asked Dan Hawkins to develop through multivariate analysis an appropriate numerical scheme that will accurately predict sources of tills in the Cook Inlet region. However, if proven reliable, even to a limited degree, the numerical routine could provide the basis for future sampling and testing efforts that are diagnostic. Multivariate programs that were initially considered for testing include CHAID (a program of automatic interaction detection through classification and regression trees), MDA (multiple discriminant analysis), and AIM (abductory inference mechanism). Also considered was a logistic regression program (LOGIT or PROBIT), but Hawkins (oral commun., 1995) did not believe that the results would differ significantly from the CHAID results. This appendix summarizes the results of the tests conducted by Hawkins (written commun., 1995).

### CHAID analysis of the paired-data set

CHAID formulates algorithms for partitioning a given data set into mutually exclusive subsets that best characterize the dependent variables and assigns the statistical significance of these rules. The strengths of this program are: (a) it does not favor one type of independent variable, (b) it does not favor simple partitioning rules, and (c) it does not limit the values assigned to variables with multiple categories (Biggs and others, 1991). The data set that was partitioned by CHAID consists of 10 independent variables, including magnetic-susceptibility measurements of six size fractions of till matrix (ranging from coarse silt to very coarse sand) and counts of four compositional

classes of till pebbles. These independent variables were tested as predictors of the till source (dependent variable), of which there are six sources identified by the proposed model of glaciation in the Cook Inlet region (Reger and Pinney, 1995). Among the 107 till samples and the 92 pebble collections, both magnetic-susceptibility and pebble samples were collected at 85 localities.

CHAID analysis began by initially dividing the data set into two groups. The first group consisted of 54 paired samples that are confidently predicted by the proposed glaciation model to be derived from given sources because they were collected from unambiguous locations. A second group of paired samples ( $n = 31$ ) of questionable derivation came from locations where the likelihood is high that the samples include sediments from more than one source. The group of samples representing proposed known sources was next randomly split in half to form a training or analysis subset (table B1), which CHAID then used to develop two decision trees that incorporate algorithms to predict the source of each paired sample at the 99- and 95-percent confidence levels (table B2).

Predictions of till sources by the proposed glaciation model were matched by CHAID predictions in a significant number of samples at both the 99- and 95-percent confidence levels (table B3). However, the level of correspondence is different in each of the three subsets evaluated.

### Matching predictions (99-percent confidence level)

In the training subset, all 27 CHAID predictions matched the sources predicted by the proposed model (table B4A). However, of three possible matching choices, unambiguous assignments were made only for the five samples from the west side of Cook Inlet. Samples from Matanuska Valley ( $n = 4$ ), Chugach Mountains ( $n = 5$ ), and Kenai Mountains ( $n = 8$ ) were all categorized as the more likely of two possible matching choices. There was a less clear response for samples from Talkeetna Mountains ( $n = 3$ ) and Turnagain Arm ( $n = 2$ ), which were

**Table B1.** *Composition of CHAID training subset of samples representing known till sources predicted by the proposed glaciation model in the Cook Inlet region*

<u>Model source</u>	<u>Number of samples</u>	<u>Percent</u>
Talkeetna Mountains	3	11.1
Matanuska Valley	4	14.8
Chugach Mountains	5	18.5
Turnagain Arm	2	7.4
Kenai Mountains	8	29.6
West side of Cook Inlet	5	18.5
<b>TOTAL</b>	<b>27</b>	<b>99.9</b>

**Table B16.** Matching of till sources predicted by the proposed glaciation model in the Cook Inlet region and sources predicted by CHAID at the 99-percent confidence level in two data subsets, based on the metasediment-pebble content of 85 pebble collections**A. Known-source subset**

Source area predicted by proposed glaciation model	One CHAID match of two possible choices <sup>a</sup>		One CHAID match of three possible choices <sup>a</sup>			No matching prediction	Total
	More likely choice	Less likely choice	Most likely choice	Middle choice	Least likely choice		
Taikeetna Mountains	---	---	---	3 (100.0 %)	---	---	3 (100.0 %)
Matanuska Valley	3 (60.0%)	---	---	---	2 (40.0 %)	---	5 (100.0%)
Chugach Mountains	---	1 (16.7 %)	4 (66.7%)	---	1 (16.7%)	---	6 (100.1 %)
Turnagain Arm	---	---	---	2 (100.0 %)	---	---	2 (100.0 %)
Kenai Mountains	---	---	17 (89.5 %)	2 (10.5 %)	---	---	19 (100.0 %)
West side of Cook Inlet	2 (8.7 %)	4 (17.4 %)	16 (69.6 %)	---	1 (4.3 %)	---	23 (100.0 %)
<b>TOTAL</b>	<b>5 (8.6 %)</b>	<b>5 (8.6 %)</b>	<b>37 (63.8 %)</b>	<b>7 (12.1 %)</b>	<b>4 (6.9 %)</b>	<b>0 (0.0 %)</b>	<b>58 (100.0 %)</b>

<sup>a</sup>Based on group compositions in table B14.**B. Questionable-source subset**

Source area predicted by proposed glaciation model	One CHAID match of two possible choices <sup>a</sup>		One CHAID match of three possible choices <sup>a</sup>			No matching prediction	Total
	More likely choice	Less likely choice	Most likely choice	Middle choice	Least likely choice		
Matanuska Valley "interlobate area"	7 (100.0 %)	---	---	---	---	---	7 (100.0 %)
Kenai Mountains?	---	---	1 (33.3 %)	2 (66.7 %)	---	---	3 (100.0 %)
West side of Cook Inlet?	16 (64.0 %)	4 (16.0 %)	1 (4.0 %)	2 (8.0 %)	1 (4.0 %)	1 (4.0 %)	25 (100.0 %)
<b>TOTAL</b>	<b>23 (65.7 %)</b>	<b>4 (11.4 %)</b>	<b>2 (5.7 %)</b>	<b>4 (11.4 %)</b>	<b>1 (2.9 %)</b>	<b>1 (2.9 %)</b>	<b>35 (100.0 %)</b>

<sup>a</sup>Based on group compositions in table B14.

**Table B15.** Comparison of till sources predicted by the proposed glaciation model in the Cook Inlet region and sources predicted by CHAID at the 99-percent confidence level, based on percent of metasediment till pebbles

Pebble collection	Till source predicted by proposed glaciation model <sup>a,b</sup>	Till source predicted by CHAID <sup>b</sup>
P1	5	5,4,3 <sup>c</sup>
P2	5	5,4,3
P3	5	5,4,3
P4	5	5,4,3
P5	5	5,4,3
P6	5	5,4,3
P7	5	5,4,3
P8	5	5,4,3
P9	5?	5,4,3
P10	5	3,5,6 <sup>d</sup>
P11	5?	3,5,6
P12	6?	6,3 <sup>e</sup>
P13	6?	6,3
P14	6?	3,5,6
P15	6?	3,5,6
P16	5?	3,5,6
P17	5	5,4,3
P18	5	5,4,3
P19	5	5,4,3
P20	5	5,4,3
P21	5	5,4,3
P22	6	6,3
P23	5	5,4,3
P24	6	2,6 <sup>f</sup>
P25	5	5,4,3
P26	6	6,1,2 <sup>g</sup>
P27	5	3,5,6
P28	6	2,6
P29	6	6,3
P30	6	6,1,2
P31	6	6,1,2
P32	6	2,6
P33	2?	2,6
P34	1	6,1,2
P35	1	6,1,2
P36	1	6,1,2
P37	2	2,6
P38	2	2,6
P39	2	6,1,2
P40	2	2,6
P41	2?	2,6
P42	2?	2,6
P43	2?	2,6
P44	2?	2,6
P45	2?	2,6
P46	3	3,5,6
P47	3	3,5,6
P48	3	5,4,3
P49	3	3,5,6
P50	3	3,5,6
P51	3	6,3

Pebble collection	Till source predicted by proposed glaciation model <sup>a,b</sup>	Till source predicted by CHAID <sup>b</sup>
P52	4	5,4,3
P53	4	5,4,3
P54	6?	5,4,3
P55	6?	6,3
P56	6?	3,5,6
P57	6?	6,3
P58	6?	6,3
P59	6?	6,3
P60	6?	2,6
P61	6?	6,1,2
P62	6?	6,3
P63	6?	2,6
P64	6?	6,3
P65	6?	6,3
P66	6?	6,3
P67	6?	6,3
P68	6?	2,6
P69	6?	6,3
P70	6?	2,6
P71	5	5,4,3
P72	6	6,1,2
P73	6	2,6
P74	6?	6,3
P75	6?	6,3
P76	6?	6,3
P77	6?	6,3
P78	2?	2,6
P79	6	6,1,2
P80	6	6,1,2
P81	6	6,1,2
P83	6	2,6
P84	6	6,1,2
P85	6	6,1,2
P86	6	6,1,2
P87	6	6,1,2
P88	6	6,1,2
P89	6	6,1,2
P90	6	6,1,2
P91	6	6,1,2
P92	6	6,1,2
P93	5	5,4,3

<sup>a</sup>Includes both known and questionable till sources.  
<sup>b</sup>1 = Talkeetna Mountains, 2 = Matanuska Valley, 2? = Matanuska Valley "interlobate area," 3 = Chugach Mountains, 4 = Turnagain Arm, 5 = Kenai Mountains, 6 = west side of Cook Inlet.  
<sup>c</sup>The number combination 5,4,3 means that the predicted source is 85.7 percent likely to be 5, 9.5 percent likely to be 4, and 4.8 percent likely to be 3, based on group composition in the selected subset (table B14).  
<sup>d</sup>The number combination 3,5,6 means that the predicted source is 44.4 percent likely to be 3, 33.3 percent likely to be 5, and 22.2 percent likely to be 6, based on group composition in the selected subset (table B14).  
<sup>e</sup>The number pair 6,3 means that the predicted source is 94.4 percent likely to be 6, based on group composition in the selected subset (table B14).  
<sup>f</sup>The number pair 2,6 means that the predicted source is 52.6 percent likely to be 2, based on group composition in the selected subset (table B14).  
<sup>g</sup>The number combination 6,1,2 means that the predicted source is 77.8 percent likely to be 6, 16.7 percent likely to be 1, and 5.6 percent likely to be 2, based on group composition in the selected subset (table B14).

**Table B13.** *Composition of pebble-count subset analyzed by CHAID*

Model till source	Number of samples	Percent
Talkeetna Mountains	3	3.5
Matanuska Valley	11	12.9
Chugach Mountains	6	7.1
Turnagain Arm	2	2.4
Kenai Mountains	21	24.7
West side of Cook Inlet	42	49.4
<b>TOTAL</b>	<b>85</b>	<b>100.0</b>

incorporated during development of the model. For this purpose, the set of magnetic-susceptibility and pebble-lithology data from tills in the eastern and northern Cook Inlet region was evaluated as a predictor of till source areas by four multivariate-analysis techniques. This data set was successfully partitioned to indicate six different till sources. The best partitioning was accomplished by CHAID, which established algorithms to classify source

areas at the 99- and 95-percent confidence levels. Parameters chosen by CHAID as significant predictors include magnetic susceptibility of coarse- and very fine sand fractions of the till matrix and contents of metasediment and plutonic pebbles.

These recommendations were reinforced by the three other analyses. Although our MDA was flawed because its multivariate requirements are violated by the small data set, it clearly demonstrated the importance of metasediment and plutonic pebbles as source indicators. Limiting CHAID analysis to pebble lithologies also demonstrated the importance of metasediment pebbles. Analysis using AIM, although inconclusive, identified three significant parameters as magnetic susceptibility of the very fine sand fraction and the contents of metasediment and plutonic pebbles.

Disparities between predictions of sources by the proposed model and predictions by CHAID and MDA are most obvious and consistent in subsets of samples related by the model to Kenai Mountains and the Aleutian Range west of Cook Inlet. The magnitude of disparity is directly related to the lack of confidence in model assignments. These relations indicate that the proposed glaciation model should be reexamined, particularly in areas where samples of questionable derivation are concentrated.

**Table B14.** *Partitioning rules developed by CHAID from pebble-count subset (n = 85) to predict till sources in the Cook Inlet region at the 99-percent confidence level*

Rule	Content of metasediment pebbles (%) <sup>a</sup>	Till source predicted by CHAID <sup>b</sup>	Group composition (%)
1	0 - 53	6	77.8
		1	16.7
		2	5.6
2	53 - 74.1	2	52.6
		6	47.4
3	74.1 - 90.3	6	94.4
		3	5.6
4	90.3 - 94.5	3	44.4
		5	33.3
		6	22.2
5	94.5 - 100	5	85.7
		4	9.5
		3	4.8

<sup>a</sup>Percent values refer to counts of metasediment pebbles normalized to 100 percent relative to four categories of lithology in each of the 85 pebble collections.

<sup>b</sup>1 = Talkeetna Mountains, 2 = Matanuska Valley, 3 = Chugach Mountains, 4 = Turnagain Arm, 5 = Kenai Mountains, 6 = west side of Cook Inlet.

**Table B12.** Distribution of mismatches of till sources predicted by the proposed glaciation model in the Cook Inlet region and sources predicted by multiple discrimination analysis (MDA) of 92 pebble collections in two subsets

<b>A. Known-source subset</b>							
Till source predicted by proposed model	Mismatched MDA prediction						Total
	Talkeetna Mountains	Matanuska Valley	Chugach Mountains	Turnagain Arm	Kenai Mountains	West side	
Talkeetna Mountains	---	---	---	---	---	---	0 (100.0 %)
Matanuska Valley	---	---	---	---	---	---	0 (100.0 %)
Chugach Mountains	---	---	---	1 (100.0 %)	---	---	1 (100.0 %)
Turnagain Arm	---	---	---	---	---	---	0 (100.0 %)
Kenai Mountains	---	1 (7.1 %)	3 (21.4 %)	10 (71.4 %)	---	---	14 (99.9 %)
West side of Cook Inlet	6 (54.5)	4 (36.4 %)	1 (9.1 %)	---	---	---	1 (100.0 %)
<b>TOTAL</b>	<b>6</b> (12.0 %)	<b>5</b> (30.0 %)	<b>4</b> (32 %)	<b>11</b> (24.0 %)	<b>0</b> (0.0 %)	<b>0</b> (0.0 %)	<b>26</b> (100.0 %)
<b>B. Questionable-source subset</b>							
Till source predicted by proposed model	Mismatched MDA prediction						Total
	Talkeetna Mountains	Matanuska Valley	Chugach Mountains	Turnagain Arm	Kenai Mountains	West side	
Matanuska Valley "interlobate area"	---	---	---	---	---	1 (100.0 %)	1 (100.0 %)
Kenai Mountains?	---	1 (50.0 %)	---	1 (50.0 %)	---	---	2 (100.0 %)
West side of Cook Inlet?	2 (9.5 %)	7 (33.3 %)	12 (57.1 %)	---	---	---	21 (99.9 %)
<b>TOTAL</b>	<b>2</b> (8.3 %)	<b>8</b> (33.3 %)	<b>12</b> (50.0 %)	<b>1</b> (4.2 %)	<b>0</b> (0.0 %)	<b>1</b> (4.2 %)	<b>24</b> (100.0 %)

this classification method compared to CHAID analysis of magnetic susceptibility and pebble lithology. Apparent confirmation of the proposed glaciation model by overwhelming agreement of source predictions (84 of 85 samples) should be tempered with caution because the number of possibly matching categories (five) greatly exceeds the single mismatch category.

#### AIM analysis

AIM is an artificial intelligence program that uses networks of interconnected nodes, each of which performs a simple computation (Lewinson, 1993). In abductive networks, these computations differ considerably among network nodes, and elaborate mathematical operations are possible. This technique searches for hidden relationships in data sets by building elaborate models that mimic the

data sets. In complex sets of multiple independent and dependent variables, AIM automatically programs network solutions to minimize differences between expected and derived outputs. Through graphic displays, significant variables are identified.

AIM could not produce a decision rule that successfully partitions our data set and identifies discrete sources of tills in the Cook Inlet region. However, it did identify three factors as significant for partitioning: (a) 4- $\phi$  magnetic susceptibility, (b) metasediment-pebble content, and (c) plutonic-pebble content. Thus, it supports the results of CHAID analysis of the paired-data set.

#### Summary

The purpose of this multivariate analysis was to test the proposed glaciation model using evidence that was not

**Table B11.** *Matching of till sources predicted by the proposed glaciation model in the Cook Inlet region and sources predicted by multiple discriminant analysis (MDA) of 92 pebble collections in two subsets*

<b>A. Known-source subset</b>			
Source predicted by proposed model	Matching MDA predictions	Mismatched MDA predictions	Total
Talkeetna Mountains	3 (100.0 %)	---	3 (100.0 %)
Matanuska Valley	4 (100.0 %)	---	4 (100.0 %)
Chugach Mountains	5 (83.3 %)	2 (16.7 %)	6 (100.0 %)
Turnagain Arm	2 (100.0 %)	---	2 (100.0 %)
Kenai Mountains	5 (26.3 %)	14 (73.7 %)	19 (100.0 %)
West side of Cook Inlet	10 (47.6 %)	11 (52.4 %)	21 (100.0 %)
<b>TOTAL</b>	<b>29</b> <b>(54.4 %)</b>	<b>26</b> <b>(45.6 %)</b>	<b>55</b> <b>(100.0 %)</b>
<b>B. Questionable-source subset</b>			
Source predicted by proposed model	Matching MDA predictions	Mismatched MDA predictions	Total
Matanuska Valley "interlobate area" "interlobate area"	6 (85.7 %)	1 (14.3 %)	7 (100.0 %)
Kenai Mountains?	1 (33.3 %)	2 (66.7 %)	3 (100.0 %)
West side of Cook Inlet?	6 (22.2 %)	21 (77.8 %)	27 (100.0 %)
<b>TOTAL</b>	<b>11</b> <b>(29.7 %)</b>	<b>26</b> <b>(70.3 %)</b>	<b>37</b> <b>(100.0 %)</b>

the four lithologies included in the pebble-count data. This appraisal was limited to the 85 pebble collections in the set of paired data that was originally evaluated by CHAID (table B13). Using five algorithms, CHAID produced a decision tree that partitions the pebble-count data set and discriminates all six source areas at the 99-percent confidence level (table B14). Among the four classes of lithology, metasediment content was judged the only characteristic to be a significant predictor of till sources in the eastern and northern Cook Inlet region.

Comparison of CHAID classifications of paired samples (magnetic susceptibility and pebble counts) and strictly lithologic data indicates that source areas are less clearly differentiated using only lithologic data. Instead of identifying one clear choice or two possibly matching choices of source area as it did with the paired samples (table B3), CHAID used lithologic data to identify either two or three choices of source for every sample (table B15).

In the known-source subset ( $n = 58$ ), there were no predictions where model and CHAID sources disagree, provided that all five possible matching choices are included (table B16A). The most frequently selected CHAID match was in the category of most likely of three possible matching choices (37 of 58 samples). The four other options were chosen about equally.

In the questionable-source subset ( $n = 35$ ), only one sample, which the model attributed to the west side of Cook Inlet, was not matched by one of five possibly matching CHAID choices (table B16B). The dominant choice among the possibly matching choices was in the category of more likely of two possible matching choices (23 of 35 samples).

In summary, CHAID analysis of pebble data supports the MDA conclusion that metasediment pebble content is a significant indicator of till source in the eastern and northern Cook Inlet region. However, limiting CHAID analysis only to pebble lithology blunted the sensitivity of

**Table B10.** Comparison of till sources predicted by proposed glaciation model and sources predicted by multiple discrimination analysis (MDA), based on percent of metasediment, plutonic, and quartz pebbles

Pebble collection	Till source predicted by proposed glaciation model <sup>a,b</sup>	Till source predicted by MDA <sup>b</sup>	Pebble collection	Till source predicted by proposed glaciation model <sup>a,b</sup>	Till source predicted by MDA <sup>b</sup>
P1	5	5	P49	3	3
P2	5	4	P50	3	3
P3	5	4	P51	3	3
P4	5	2	P52	4	4
P5	5	4	P53	4	4
P6	5	4	P54	6?	3
P7	5	4	P55	6?	2
P8	5	4	P56	6?	3
P9	5?	5	P57	6?	3
P10	5	4	P58	6?	3
P11	5?	2	P59	6?	3
P12	6?	3	P60	6?	6
P13	6?	6	P61	6?	6
P14	6?	3	P62	6?	2
P15	6?	3	P63	6?	6
P16	5?	4	P64	6?	2
P17	5	5	P65	6?	2
P18	5	5	P66	6?	3
P19	5	4	P67	6?	3
P20	5	4	P68	6?	2
P21	5	3	P69	6?	2
P22	6	3	P70	6?	3
P23	5	3	P71	5	4
P24	6	6	P72	6	6
P25	5	5	P73	6	6
P26	6	6	P74	6?	2
P27	5	3	P75	6?	3
P28	6	6	P76	6?	2
P29	6	6	P77	6?	2
P30	6	2	P78	2?	2
P31	6	2	P79	6	6
P32	6	2	P80	6	1
P33	2?	2	P81	6	1
P34	1	1	P83	6	2
P35	1	1	P84	6	6
P36	1	1	P85	6	1
P37	2	2	P86	6	1
P38	2	2	P87	6	1
P39	2	2	P88	6	6
P40	2	2	P89	6	6
P41	2?	2	P90	6	6
P42	2?	2	P91	6	1
P43	2?	6	P92	6	6
P44	2?	2	P93	5	5
P45	2?	2			
P46	3	3			
P47	3	3			
P48	3	4			

<sup>a</sup>Includes known and questionable sources.  
<sup>b</sup>1 = Talkeetna Mountains, 2 = Matanuska Valley, 2? = Matanuska Valley "interlobate area," 3 = Chugach Mountains, 4 = Turnagain Arm, 5 = Kenai Mountains, 6 = west side of Cook Inlet.



**Table B8.** Number of pebble collections in two subsets related to till sources predicted by the proposed glaciation model in the Cook Inlet region

A. Known-source subset		
Model source	Number of samples	Percent
Talkeetna Mountains	3	5.2
Matanuska Valley	4	7.0
Chugach Mountains	6	10.5
Turnagain Arm	2	3.5
Kenai Mountains	19	33.3
West side of Cook Inlet	23	40.4
<b>TOTAL</b>	<b>57</b>	<b>99.9</b>

B. Questionable-source subset		
Model source	Number of samples	Percent
Matanuska Valley "interlobate area"	7	20.0
Kenai Mountains?	3	8.6
West side of Cook Inlet?	25	71.4
<b>TOTAL</b>	<b>35</b>	<b>100.0</b>

In the MDA, discriminant (D) scores, which were produced by six linear discriminant functions that incorporate the percentages of quartz, plutonic, and metasediment pebbles in a pebble collection, are used to predict six corresponding glacier sources as proposed by our model (table B9). For a given pebble collection, the largest discriminant score is the basis for assigning the sample to a particular source. In cases where D scores are close, further calculations can produce more definitive discriminant probabilities, but these calculations are beyond the scope of the present study. MDA algorithms improve our ability to predict source areas 34.8 percent over totally random selection procedures.

MDA indicates that percentages of both metasediment and plutonic pebbles are highly significant (F-probability

= 0.0000) as predictors of till sources, and quartz content is less significant (F-probability = 0.0104). Metasediment-pebble content (F-value = 12.76) is a slightly better indicator than plutonic-pebble content (F-value = 10.33). Combined metasediment and plutonic percentages account for about 70 percent of the within-group variance in the data set. These relationships are clarified when the three parameters are plotted in a ternary diagram (fig. B1). The concentration of data points along the M-P side of the triangle demonstrates the obvious dominance of metasediment and plutonic contents as classifiers of each pebble collection. Relative to these parameters, quartz-pebble content is quite insignificant.

Table B10 compares till sources predicted by the proposed glaciation model and sources predicted by MDA. Of the 92 MDA predictions made, only 42 (45.7 percent) correspond to sources identified by the proposed model (table B11).

MDA matches

In the subset of till samples (n = 55) confidently related to source areas in the proposed model, 29 (54.4 percent) of the MDA predictions matched modeled predictions (table B11A). There was complete agreement for samples from Talkeetna Mountains (n = 3), Matanuska Valley (n = 4), and Turnagain Arm (n = 2). Of six samples modeled to come from Chugach Mountains, five were assigned by MDA to that source. MDA was less successful in matching model predictions of till samples from Kenai Mountains (five of 19 samples) and the west side of Cook Inlet (10 of 21 samples).

In the subset of till samples (n = 35) questionably related to sources in the proposed model, only 11 MDA predictions matched modeled sources (table B11B). Of these, the greatest coincidence exists for samples from the Matanuska Valley "interlobate area" (six of seven samples). Only one of three samples was assigned by MDA to the Kenai Mountains, and only six of 27 samples were related to the west side of Cook Inlet.

**Table B9.** Linear discriminant functions produced by multiple discriminant analysis of 92 pebble collections to predict till sources in the Cook Inlet region

Source area	Linear discriminant function*
Talkeetna Mountains	$D_{21} = 1.77X_1 + 0.73X_2 + 0.48X_3 - 32.35$
Matanuska Valley	$D_{22} = 1.57X_1 + 0.58X_2 + 0.46X_3 - 24.36$
Chugach Mountains	$D_{23} = 0.36X_1 + 0.51X_2 + 0.50X_3 - 24.46$
Turnagain Arm	$D_{24} = -0.06X_1 + 0.50X_2 + 0.51X_3 - 25.66$
Kenai Mountains	$D_{25} = 0.36X_1 + 0.51X_2 + 0.51X_3 - 25.02$
West side of Cook Inlet	$D_{26} = 1.30X_1 + 0.51X_2 + 0.41X_3 - 18.70$

\* $X_1$  = percent of quartz pebbles,  $X_2$  = percent of plutonic pebbles,  $X_3$  = percent of metasediment pebbles.

**Table B7.** *Distribution of mismatches of till sources predicted by the proposed glaciation model in the Cook Inlet region and sources predicted by CHAID at the 95-percent confidence level in two data subsets*

A. Known-source subset										
Model source <sup>a</sup>	CHAID mismatch <sup>a</sup>									Total
	1	1,2	1,5	2	3	3,4	4	4,5	6	
5	---	---	---	---	2 (28.6%)	---	4 (57.1%)	---	1 (14.3%)	7 (100.0%)
6	1 (8.3%)	2 (16.7%)	3 (25.0%)	2 (16.7%)	---	3 (25.0%)	---	1 (8.3%)	---	12 (100.0%)
<b>TOTAL</b>	<b>1</b> (5.3%)	<b>2</b> (10.5%)	<b>3</b> (15.8%)	<b>2</b> (10.5%)	<b>2</b> (10.5%)	<b>3</b> (15.8%)	<b>4</b> (21.1%)	<b>1</b> (5.3%)	<b>1</b> (5.3%)	<b>19</b> (100.1%)

<sup>a</sup>1 = Talkeetna Mountains, 2 = Matanuska Valley, 3 = Chugach Mountains, 4 = Turnagain Arm, 5 = Kenai Mountains, 6 = west side of Cook Inlet.

B. Questionable-source subset										
Model source <sup>a</sup>	CHAID mismatch <sup>a</sup>									Total
	1	1,2	1,5	2	3	3,4	4	4,5	6	
2?	---	---	4 (80.0%)	---	---	---	---	---	1 (20.0%)	5 (100.0%)
6	---	2 (9.1%)	3 (13.6%)	---	1 (4.5%)	15 (68.2%)	---	1 (4.5%)	---	22 (99.9%)
<b>TOTAL</b>	<b>0</b> (0.0%)	<b>2</b> (7.4%)	<b>7</b> (25.9%)	<b>0</b> (0.0%)	<b>1</b> (3.7%)	<b>15</b> (55.6%)	<b>0</b> (0.0%)	<b>1</b> (3.7%)	<b>1</b> (3.7%)	<b>27</b> (100.0%)

<sup>a</sup>1 = Talkeetna Mountains, 2 = Matanuska Valley, 2? = Matanuska Valley "interlobate area," 3 = Chugach Mountains, 4 = Turnagain Arm, 5 = Kenai Mountains, 6 = west side of Cook Inlet.

**Table B6.** Distribution of mismatches of till sources predicted by the proposed glaciation model in the Cook Inlet region and sources predicted by CHAID at the 99-percent confidence level in two data subsets

A. Known-source subset						
Model source <sup>a</sup>	1,2	1,5	CHAID mismatch <sup>a</sup>		6	Total
			3,4	4,5		
5	---	---	3 (75.0 %)	---	1 (25.0 %)	4 (100.0 %)
6	5 (41.7 %)	3 (25.0 %)	3 (25.0 %)	1 (8.3 %)	---	12 (100.0 %)
<b>TOTAL</b>	<b>5 (31.2 %)</b>	<b>3 (18.8 %)</b>	<b>6 (37.5 %)</b>	<b>1 (6.3 %)</b>	<b>1 (6.3 %)</b>	<b>16 (100.1 %)</b>

<sup>a</sup>1 = Talkeetna Mountains, 2 = Matanuska Valley, 3 = Chugach Mountains, 4 = Turnagain Arm, 5 = Kenai Mountains, 6 = west side of Cook Inlet.

B. Questionable-source subset						
Model source <sup>a</sup>	1,2	1,5	CHAID mismatch <sup>a</sup>		6	Total
			3,4	4,5		
2?	---	4 (80.0 %)	---	---	1 (20.0 %)	5 (100.0 %)
6?	2 (9.1 %)	3 (13.6 %)	15 (68.2 %)	2 (9.1 %)	---	22 (100.0 %)
<b>TOTAL</b>	<b>2 (7.4 %)</b>	<b>7 (25.9 %)</b>	<b>15 (55.6 %)</b>	<b>2 (7.4 %)</b>	<b>1 (3.7 %)</b>	<b>27 (100.0 %)</b>

<sup>a</sup>1 = Talkeetna Mountains, 2 = Matanuska Valley, 2? = Matanuska Valley "interlobate area," 3 = Chugach Mountains, 4 = Turnagain Arm, 5 = Kenai Mountains, 6 = west side of Cook Inlet.

### Multiple discriminant analysis

For a set of data consisting of several independent and dependent variables, multiple discriminant analysis (MDA) develops a series of classification rules (algorithms) that maximizes the between-group variance and minimizes the within-group variance (Hair and others, 1995). Basic requirements of this procedure are: (a) there must be a large number of observations ( $\geq 20$ ) for each subset and (b) the number of observations must be about equal in every subset. Normally, in MDA each data set is randomly divided into two groups: (a) the analysis sample, which is used to develop the prediction or classification algorithms and (b) the verification or holdout sample, which is used to test the discriminant functions. Ideally, the sizes of both samples should be equal.

Once again, our data set initially incorporated 10 independent variables, including six classes of magnetic-susceptibility measurements (107 samples) and four classes of pebble lithologies ( $n=92$ ), which we wanted to evaluate as indicators of the six glacier source areas (dependent variables) that are predicted by our proposed glaciation model. Because of the small number of samples, the entire data set was used as an analysis sample from

which the classification rules were developed. The lack of a separate verification sample against which the partitioning algorithms could be tested does not necessarily invalidate the results, but means that the results are less reliable than they seem to be (Hair and others, 1995, p. 196).

In an initial phase, stepwise MDA successfully partitioned the full set and clearly identified pebble lithologies as the important indicator of former glacier sources. In contrast to the CHAID results, MDA rejected magnetic susceptibility as an important parameter. Therefore, during subsequent steps, only pebble-count data were analyzed.

The set of pebble-count data consists of nine small subsets that were identified with different degrees of confidence by the proposed model (table B8). In sample subsets "known" by the model to be derived from six sources, the degrees of freedom vary from one to 22. In sample subsets questionably assigned by the model to given sources, the degrees of freedom range from two to 24. Therefore, small sample size and lack of an equal number of samples in each subset are serious impediments for MDA, but we hoped that this approach, even if flawed, would support the results of the CHAID analysis and provide valuable insights about our proposed model of glaciation in the Cook Inlet region.

matched and almost all of these (seven samples) were single choices (table B5B). Of 11 samples "known" by the proposed model to come from Kenai Mountains, seven (63.6 percent) were assigned by CHAID to other sources and, of 15 samples predicted by the model to contain lithologies of the Aleutian Range west of Cook Inlet, 12 (80.0 percent) were assigned to other sources.

In the subset representing till samples of questionable derivation in the proposed model, two samples each from the Matanuska Valley "interlobate area" and Kenai Mountains? were related by CHAID to the appropriate sources as the more likely of two possibly corresponding choices (table B5C). Of 31 samples in this subset, 27 (87.1 percent) of the CHAID predictions did not match sources identified by the proposed glaciation model. Especially notable is the lack of agreement for all 22 samples predicted by the model to originate west of Cook Inlet.

#### CHAID mismatches (99-percent confidence level)

Of 16 samples in the known-source subset that were classified by CHAID differently than the proposed glaciation model, there is a wide range of mismatches (table B6A). Of four till samples "known" to be derived from Kenai Mountains, three samples were attributed to either Chugach Mountains or Turnagain Arm and one sample was attributed to the west side of Cook Inlet. Among 12 samples from moraines confidently predicted by the proposed model to be built by glaciers flowing southeastward from the Aleutian Range, five (41.7 percent) were assigned by CHAID to either Talkeetna Mountains or Matanuska Valley, three (25.0 percent) were classified as either Talkeetna Mountains or Kenai Mountains samples, three (25.0 percent) were attributed to either Chugach Mountains or Turnagain Arm, and one sample (8.3 percent) was predicted by CHAID to come from either Turnagain Arm or Kenai Mountains.

Of five samples in the questionable-source subset proposed by the model to come from Matanuska Valley "interlobate area," four samples were assigned by CHAID to either Talkeetna Mountains or Kenai Mountains and one sample was attributed to the west side of Cook Inlet (table B6B). Among 22 samples questionably assigned by the proposed model to the west side of Cook Inlet, 15 samples (68.2 percent) were classified by CHAID as samples from either Chugach Mountains or Turnagain Arm, three samples (25.9 percent) were assigned to either Talkeetna Mountains or Kenai Mountains, two samples (9.1 percent) were classified as either Talkeetna Mountains or Matanuska Valley samples, and two samples were attributed to either Turnagain Arm or Kenai Mountains.

#### CHAID mismatches (95-percent confidence level)

As expected, at the 95-percent confidence level, there

are more differences in assignments of till sources by the proposed glaciation model and by CHAID than at the 99-percent confidence level (table B7).

In the subset of samples confidently assigned by the model to the Kenai Mountains, CHAID unambiguously assigned four to Turnagain Arm, two to Chugach Mountains, and one to the Aleutian Range west of Cook Inlet (table B7A). CHAID was less forceful in its assignments of 12 till samples modeled to be derived from the west side of Cook Inlet. Only two samples were unambiguously attributed to Matanuska Valley and one sample was clearly assigned to Chugach Mountains. Among the other nine samples, three each were assigned to either Talkeetna Mountains or Kenai Mountains and either Chugach Mountains or Turnagain Arm, two were classified as samples from either Talkeetna Mountains or Matanuska Valley, and one was attributed to either Turnagain Arm or Kenai Mountains.

In the subset of till samples questionably related to glacial sources by the model, among five samples from the Matanuska Valley "interlobate area," CHAID unambiguously classified one as a till from the west side of Cook Inlet and assigned the other four samples to either Talkeetna Mountains or Kenai Mountains (table B7B). Of 22 till samples tentatively related to the west side of Cook Inlet by the proposed glaciation model, only one sample was clearly assigned by CHAID to the Chugach Mountains. More ambiguous assignments were made for 15 samples to either Chugach Mountains or Turnagain Arm, three samples to either Talkeetna Mountains or Kenai Mountains, two samples to either Talkeetna Mountains or Matanuska Valley, and one sample to either Turnagain Arm or Kenai Mountains.

#### Summary of CHAID analysis

Differences in predictions by the proposed glaciation model and by CHAID correspond to our confidence in the proposed model. Partitioning was perfect in the training subset ( $n = 27$ ), in which the origin of the samples is unambiguous in the proposed model. Clearly, the training subset is statistically significant. Fewer CHAID predictions matched model sources in the equally large split of samples ( $n = 27$ ) that are slightly less confidently attributed to given sources in the model. The greatest disparity between model and CHAID sources is present in the subset ( $n = 31$ ) of questionable samples. In all three subsets, disparities between predictions of till source by the proposed model and by CHAID most notably involved samples attributed by the model to Kenai Mountains and the west side of Cook Inlet. These consistent trends indicate that the proposed model should be reexamined. Sample size is apparently not a factor influencing CHAID performances with the three subsets.

**Table B5.** Matching of model sources and CHAID predictions of till sources in the Cook Inlet region at the 95-percent confidence level in three data subsets

A. Training subset (sources known)					
Source area	Single matching prediction	One CHAID match of two possible choices <sup>a</sup>		No matching prediction	Total
		More likely choice	Less likely choice		
Talkeetna Mountains	2 (66.7 %)	---	1 (33.3 %)	---	3 (100.0 %)
Matanuska Valley	4 (100.0 %)	---	---	---	4 (100.0 %)
Chugach Mountains	5 (100.0 %)	---	---	---	5 (100.0 %)
Turnagain Arm	1 (50.0 %)	---	1 (50.0 %)	---	2 (100.0 %)
Kenai Mountains	6 (75.0 %)	2 (25.0 %)	---	---	8 (100.0 %)
West side of Cook Inlet	5 (100.0 %)	---	---	---	5 (100.0 %)
<b>TOTAL</b>	<b>23</b> <b>(85.2 %)</b>	<b>2</b> <b>(7.4 %)</b>	<b>2</b> <b>(7.4 %)</b>	<b>0</b> <b>(0.0 %)</b>	<b>27</b> <b>(100.0 %)</b>

<sup>a</sup>Based on compositions of test groups in table B2B.

B. Known-source subset					
Source area	Single matching prediction	One CHAID match of two possible choices <sup>a</sup>		No matching prediction	Total
		More likely choice	Less likely choice		
Talkeetna Mountains	---	---	---	---	0 (100.0 %)
Matanuska Valley	---	---	---	---	0 (100.0 %)
Chugach Mountains	1 (100.0 %)	---	---	---	1 (100.0 %)
Turnagain Arm	---	---	---	---	0 (100.0 %)
Kenai Mountains	3 (27.3 %)	1 (9.1 %)	---	7 (63.6 %)	11 (100.0 %)
West side of Cook Inlet	3 (20.0 %)	---	---	12 (80.0 %)	15 (100.0 %)
<b>TOTAL</b>	<b>7</b> <b>(25.9 %)</b>	<b>1</b> <b>(3.7 %)</b>	<b>0</b> <b>(0.0 %)</b>	<b>19</b> <b>(70.4 %)</b>	<b>27</b> <b>(100.0 %)</b>

<sup>a</sup>Based on compositions of test groups in table B2B.

C. Questionable-source subset					
Source area	Single matching prediction	One CHAID match of two possible choices <sup>a</sup>		No matching prediction	Total
		More likely choice	Less likely choice		
Matanuska Valley "interlobate area"	---	2 (28.6%)	---	5 (71.4%)	7 (100.0%)
Kenai Mountains?	---	2 (100.0%)	---	---	2 (100.0%)
West side of Cook Inlet?	---	---	---	22 (100.0%)	22 (100.0%)
<b>TOTAL</b>	<b>0</b> <b>(0.0 %)</b>	<b>4</b> <b>(12.9 %)</b>	<b>0</b> <b>(0.0 %)</b>	<b>27</b> <b>(87.1 %)</b>	<b>31</b> <b>(100.0 %)</b>

<sup>a</sup>Based on composition of test groups in table B2B.

**Table B4. Matching of model sources and CHAID predictions of till sources in the Cook Inlet region at the 99-percent confidence level in three data subsets****A. Training subset (sources known)**

<u>Model source area</u>	<u>Single matching prediction</u>	<u>One CHAID match of two possible choices*</u>		<u>No matching prediction</u>	<u>Total</u>
		<u>More likely choice</u>	<u>Less likely choice</u>		
Talkeetna Mountains	---	---	3 (100.0 %)	---	3 (100.0 %)
Matanuska Valley	---	4 (100.0 %)	---	---	4 (100.0 %)
Chugach Mountains	---	5 (100.0 %)	---	---	5 (100.0 %)
Turnagain Arm	---	---	2 (100.0 %)	---	2 (100.0 %)
Kenai Mountains	---	8 (100.0 %)	---	---	8 (100.0 %)
West side of Cook Inlet	5 (100.0 %)	---	---	---	5 (100.0 %)
<b>TOTAL</b>	<b>5</b> <b>(18.5 %)</b>	<b>17</b> <b>(63.0 %)</b>	<b>5</b> <b>(18.5 %)</b>	<b>0</b> <b>(0.0 %)</b>	<b>27</b> <b>(100.0 %)</b>

\*Based on compositions of test groups in table B2A.

**B. Known-source subset**

<u>Model source area</u>	<u>Single matching prediction</u>	<u>One CHAID match of two possible choices*</u>		<u>No matching prediction</u>	<u>Total</u>
		<u>More likely choice</u>	<u>Less likely choice</u>		
Talkeetna Mountains	---	---	---	---	0 (100.0 %)
Matanuska Valley	---	---	---	---	0 (100.0 %)
Chugach Mountains	---	1 (100.0 %)	---	---	1 (100.0 %)
Turnagain Arm	---	---	---	---	0 (100.0 %)
Kenai Mountains	---	7 (63.6 %)	---	4 (36.4 %)	11 (100.0 %)
West side of Cook Inlet	3 (20.0 %)	---	---	12 (80.0 %)	15 (100.0 %)
<b>TOTAL</b>	<b>3</b> <b>(11.1 %)</b>	<b>8</b> <b>(29.6 %)</b>	<b>0</b> <b>(0.0 %)</b>	<b>16</b> <b>(59.3 %)</b>	<b>27</b> <b>(100.0 %)</b>

\*Based on compositions of test groups in table B2A.

**C. Questionable-sources subset**

<u>Model source area</u>	<u>Single matching prediction</u>	<u>One CHAID match of two possible choices*</u>		<u>No matching prediction</u>	<u>Total</u>
		<u>More likely choice</u>	<u>Less likely choice</u>		
Matanuska Valley "interlobate area"	---	2 (28.6 %)	---	5 (71.4 %)	7 (100.0 %)
Kenai Mountains?	---	2 (100.0 %)	---	---	2 (100.0 %)
West side?	---	---	---	22 (100.0 %)	22 (100.0 %)
<b>TOTAL</b>	<b>0</b> <b>(0.0 %)</b>	<b>4</b> <b>(12.9 %)</b>	<b>0</b> <b>(0.0 %)</b>	<b>27</b> <b>(87.1 %)</b>	<b>31</b> <b>(100.0 %)</b>

\*Based on compositions of test groups in table B2A.

Table B3. (Continued)

Magnetic-susceptibility sample	Pebble collection	Till source predicted by proposed model <sup>a,b</sup>	Till source predicted by CHAID <sup>b</sup>	
			99-percent confidence level	95-percent confidence level
M75	P56	6?	2,1	2,1
M76	P57	6?	3,4	3,4
M77	P58	6?	3,4	3,4
M78	P59	6?	3,4	3,4
M79	P60	6?	3,4	3,4
M80	P61	6?	5,1	5,1
M81	P62	6?	3,4	3,4
M82	P63	6?	3,4	3,4
M83	P64	6?	3,4	3,4
M84	P65	6?	3,4	3,4
M85	P66	6?	3,4	3,4
M86	P67	6?	3,4	3,4
M87	P68	6?	5,1	5,1
M88	P69	6?	3,4	3,4
M89	P70	6?	3,4	3,4
M90	P71	5	5,1	5,1
M91	P72	6	5,1	5,1
M92	P73	6	5,1	5,1
M93	P74	6?	3,4	3,4
M94	P75	6?	3,4	3,4
M95	P76	6?	5,1	5,1
M96	P77	6?	2,1	2,1
M97	P78	2?	6	6
M98	P79	6	2,1	1
M101*	P83*	6	6	6
M102	P84	6	6	6
M103*	P85*	6	6	6
M104	P86	6	6	6
M105	P87	6	2,1	2,1
M106*	P88*	6	6	6
M107*	P89*	6	6	6
M108	P90	6	6	6
M109*	P91*	6	6	6
M2	P93	5	5,4	5

<sup>a</sup>Includes both known and questionable till sources.

<sup>b</sup>1 = Talkeetna Mountains, 2 = Matanuska Valley, 2? = Matanuska Valley "interlobate area," 3 = Chugach Mountains, 4 = Turnagain Arm, 5 = Kenai Mountains, 6 = west side of Cook Inlet.

<sup>c</sup>The numerical pair 5,4 means that the predicted source is 85.7 percent likely to be 5, based on group composition in the selected subset (table B2).

<sup>d</sup>The numerical pair 3,4 means that the predicted source is 83.3 percent likely to be 3, based on group composition in the selected subset (table B2).

<sup>e</sup>The numerical pair 5,1 means that the predicted source is 66.7 percent likely to be 5, based on group composition in the selected subset (table B2).

<sup>f</sup>The numerical pair 2,1 means that the predicted source is 66.7 percent likely to be 2, based on group composition in the selected subset (table B2).

samples predicted by the proposed model to have been deposited by the Trading Bay lobe that spread southeastward across Cook Inlet were assigned by CHAID to other sources.

#### Matching predictions (95-percent confidence level)

In the training subset, all 27 model predictions were once again matched by CHAID predictions (table B5A). Clear matching assignments were made to all six source

areas for 23 of 27 samples (85.2 percent). Two samples, comprising one quarter of the samples predicted by the model to be of Kenai Mountains derivation, were confirmed by CHAID as the more likely of two possibly matching choices. One sample each from Talkeetna Mountains and Turnagain Arm according to the proposed model were assigned there by CHAID as the less likely of two possibly matching choices.

In the subset representing the other half of the known samples ( $n = 27$ ), only eight of 27 predictions (29.6 percent)

**Table B3.** Comparison of till sources predicted by the proposed glaciation model and sources predicted by CHAID, based on magnetic-susceptibility measurements of 0- $\Phi$  and 4- $\Phi$  fractions and percent of metasediment and plutonic pebbles. Sample numbers followed by an asterisk (\*) are part of the training subset ( $n = 27$ )

Magnetic-susceptibility sample	Pebble collection	Till source predicted by proposed model <sup>a,b</sup>	Till source predicted by CHAID <sup>b</sup>	
			99-percent confidence level	95-percent confidence level
M1*	P1*	5	5,4 <sup>c</sup>	5
M5*	P2*	5	5,4	5
M7	P3	5	5,4	4
M8	P4	5	5,4	5
M10	P5	5	3,4 <sup>d</sup>	3
M13*	P6*	5	5,4	5
M16*	P7*	5	5,4	5
M18	P8	5	5,4	4
M20	P9	5?	5,4	5,4
M22	P10	5	5,4	4
M23	P11	5?	5,4	5,4
M25	P12	6?	5,4	5,4
M26	P14	6?	5,4	3
M29*	P17*	5	5,4	5
M30	P18	5	5,4	5
M31*	P19*	5	5,4	5
M32	P20	5	3,4	4
M35*	P21*	5	5,1 <sup>e</sup>	5,1
M37	P22	6	5,1	5,1
M38	P23	5	3,4	3
M40	P24	6	3,4	3,4
M41	P25	5	6	6
M42	P26	6	3,4	3,4
M43*	P27*	5	5,1	5,1
M44	P28	6	3,4	3,4
M46	P29	6	2,1 <sup>f</sup>	2,1
M47	P30	6	2,1	2
M48	P31	6	2,1	2
M49	P32	6	5,4	5,4
M52	P33	2?	3,4	3,4
M53*	P34*	1	5,1	5,1
M54*	P35*	1	2,1	1
M55*	P36*	1	2,1	1
M56*	P37*	2	2,1	2
M57*	P38*	2	2,1	2
M58*	P39*	2	2,1	2
M59*	P40*	2	2,1	2
M60	P41	2?	5,1	5,1
M61	P42	2?	5,1	5,1
M62	P43	2?	5,1	5,1
M63	P44	2?	5,1	5,1
M64	P45	2?	3,4	3,4
M65	P46	3	3,4	3
M66*	P47*	3	3,4	3
M67*	P48*	3	3,4	3
M68*	P49*	3	3,4	3
M69*	P50*	3	3,4	3
M70*	P51*	3	3,4	3
M71*	P52*	4	5,4	4
M72*	P53*	4	3,4	3,4
M74	P55	6?	3,4	3,4

**Table B2.** Partitioning rules for predicting till sources in the Cook Inlet region at the 99- and 95-percent confidence levels, based on CHAID analysis of a training subset (n = 27) of samples assigned by the proposed glaciation model to various source areas

**A. 99-percent confidence level for groupings**

Rule	0- $\Phi$ magnetic-susceptibility range <sup>a</sup>	Till source predicted by CHAID <sup>b</sup>	Group composition (%)
1	1.1 - 2.2	5	85.7
		4	14.3
2	2.2 - 7.9	3	83.3
		4	16.7
3	7.9 - 15.0	5	66.7
		1	33.3
4	15.0 - 23.6	2	66.7
		1	33.3
5	23.6	6	100.0

<sup>a</sup>Passes 0- $\Phi$  screen and retained on 1- $\Phi$  screen (coarse sand).

<sup>b</sup>1 = Talkeetna Mountains, 2 = Matanuska Valley, 3 = Chugach Mountains, 4 = Turnagain Arm, 5 = Kenai Mountains, 6 = west side of Cook Inlet.

**B. 95-percent confidence level for groupings**

Rule	0- $\Phi$ magnetic-susceptibility range <sup>a</sup>	4- $\Phi$ magnetic susceptibility range <sup>b</sup>	Metasediment pebbles (%)	Plutonic pebbles (%)	Till source predicted by CHAID <sup>c</sup>	Group composition (%)
1	1.1 - 2.2	1.7 - 4.1	---	---	5	100.0
2	1.1 - 2.2	4.1 - 7.2	---	---	4	100.0
3	2.2 - 7.9	---	90.1 - 97.3	---	3	100.0
4	2.2 - 7.9	---	99.4 - 100.0	---	4	100.0
5	7.9 - 15.0	---	---	---	5	66.7
					1	33.3
6	15.0 - 23.6	---	---	21.0 - 48.5	2	100.0
7	15.0 - 23.6	---	---	48.5 - 82.4	1	100.0
8	23.6 - 75.7	---	---	---	6	100.0

<sup>a</sup>Passes 0- $\Phi$  screen and retained on 1- $\Phi$  screen (coarse sand).

<sup>b</sup>Passes 4- $\Phi$  screen and retained on 5- $\Phi$  screen (very fine sand).

<sup>c</sup>1 = Talkeetna Mountains, 2 = Matanuska Valley, 3 = Chugach Mountains, 4 = Turnagain Arm, 5 = Kenai Mountains, 6 = west side of Cook Inlet.

categorized as the less likely of two possibly matching choices.

In the subset representing the other split of the known-source samples (n = 27), single clear assignments were made only for three samples from the west side of Cook Inlet (table B4B). Samples from Chugach Mountains (n = 1) and Kenai Mountains (n = 7) were confirmed as the more likely of two possibly matching choices. There were no CHAID matches for four samples that the proposed glaciation model predicted came from Kenai Mountains and 12 till samples that the model assigned to the west side of Cook Inlet.

In the subset representing till samples of questionable

derivation according to the proposed model, there were no single clear assignments of source area (table B4C). Two samples collected in the transition zone between till deposited by Matanuska Valley ice and till deposited by ice from Chugach Mountains (herein termed the Matanuska Valley "interlobate area") were assigned by CHAID to either source as the more likely of two possibly matching choices. Two till samples that the model questionably assigned to Kenai Mountains were also assigned there by CHAID as the more likely of two possibly matching choices. Five samples from the Matanuska Valley "interlobate area" were not assigned by CHAID to either the Matanuska Valley or Chugach Mountains, and 22 till